VOLUME 35 OCTOBER 1957 NUMBER 10

Canadian Journal of Chemistry

Published by THE NATIONAL RESEARCH COUNCIL

OTTAWA CANADA

CANADIAN JOURNAL OF CHEMISTRY

(*Formerly Section B, Canadian Journal of Research*)

Under the authority of the Chairman of the Committee of the Privy Council on Scientific and Industrial Research, the National Research Council issues THE CANADIAN JOURNAL OF CHEMISTRY and five other journals devoted to the publication, in English or French, of the results of original scientific research. Matters of general policy concerning these journals are the responsibility of a joint Editorial Board consisting of: members representing the National Research Council of Canada; the Editors of the Journals; and members representing the Royal Society of Canada and four other scientific societies.

The Chemical Institute of Canada has chosen the Canadian Journal of Chemistry as its medium of publication for scientific papers.

Manuscripts for publication should be submitted to Dr. Léo Marion, Editor-in-Chief, Canadian Journal of Chemistry, National Research Council, Ottawa 2, Canada.
(For instructions on preparation of copy, see **Notes to Contributors** (inside back cover).)

Proof, correspondence concerning proof, and orders for reprints should be sent to the Manager, Editorial Office (Research Journals), Division of Administration and Awards, National Research Council, Ottawa 2, Canada.

Subscriptions, renewals, requests for single or back numbers, and all remittances should be sent to Division of Administration and Awards, National Research Council, Ottawa 2, Canada. Remittances should be made payable to the Receiver General of Canada, credit National Research Council.

The journals published, frequency of publication, and prices are:

Canadian Journal of Biochemistry and Physiology	Monthly	$3.00 a year
Canadian Journal of Botany	Bimonthly	$4.00 a year
Canadian Journal of Chemistry	Monthly	$5.00 a year
Canadian Journal of Microbiology	Bimonthly	$3.00 a year
Canadian Journal of Physics	Monthly	$4.00 a year
Canadian Journal of Zoology	Bimonthly	$3.00 a year

The price of single numbers of all journals is 75 cents.

REFERENCES—CANADIAN JOURNAL OF CHEMISTRY

This is to announce a change from the present system of citing references. Beginning in January 1958, references will be numbered and listed in the order of first citation in the text, not in alphabetical order by authors' names. Authors are requested to follow the new system in all manuscripts submitted henceforth.

Canadian Journal of Chemistry

Issued by THE NATIONAL RESEARCH COUNCIL OF CANADA

VOLUME 35 OCTOBER 1957 NUMBER 10

THE CONFIGURATION OF GLYCOSIDIC LINKAGES IN OLIGOSACCHARIDES

V. THE SUCROSE LINKAGE IN RAFFINOSE AND STACHYOSE[1]

A. K. MITRA[2] AND A. S. PERLIN

ABSTRACT

A direct chemical proof is provided for the occurrence of the sucrose linkage in raffinose and stachyose by isolation of sucrose, after selective removal of D-galactose units. The procedure used takes advantage of the fact that the D-galactopyranosyl residues contain a *cis*-α-glycol group which, in contrast to the *trans* glycol group of the other sugar residues, is rapidly attacked by ethanolic periodate. The resulting dialdehyde is alkali-labile and preferentially hydrolyzed with dilute base, the alkali-stable sucrose unit being released intact.

Raffinose and stachyose are regarded as derivatives of sucrose (I, R = OH) because the glycosidic union between the D-glucose and D-fructose units in each of the three sugars is considered to be identical. Accordingly, raffinose may be described as 6-*O*-α-D-galactopyranosyl-sucrose (I, R = II) and stachyose as *O*-α-D-galactopyranosyl-(1 → 6)-*O*-α-D-galactopyranosyl-(1 → 6)-sucrose (I, R = III), in which the 6-position of sucrose refers to carbon-6 of the D-glucose unit. The chemistry of these and related compounds has been comprehensively reviewed recently by French (8) and Wickstrom (22), and evidence cited from a variety of sources leaves little doubt as to the correctness of structure II and III. Direct proof for the occurrence of the sucrose linkage in raffinose and stachyose has been furnished by the isolation of sucrose after treatment of the oligosaccharides with α-D-galactopyranosidases (3, 9, 16). These enzyme preparations have been impure, however, and required hydrolysis periods of several days. In view of the low yields of sucrose actually obtained under such unfavorable circumstances, French states (8) "If the assumption is permitted that the sucrose and raffinose formed are not artifacts but are genuine hydrolysis products of stachyose, this work provides strong confirmation for the presence of sucrose (and raffinose) units in stachyose." An alternative proof, free from this qualification, is presented in the current paper, which describes the isolation of sucrose from raffinose and stachyose by purely chemical means.

The D-galactopyranose units of raffinose and stachyose contain a *cis*-α-glycol group and therefore should be attacked by glycol-cleaving oxidants more readily than the D-glucopyranose and D-fructofuranose units, which contain only *trans*-α-glycol groups (4, 20). Treatment of the compounds with a limited amount of oxidant would thus be expected to introduce a dialdehyde unit mainly into the D-galactose residues to yield, for example, (I, R = IV) from raffinose. The glycosidic linkage adjacent to such a dialde-

[1]*Manuscript received June 6, 1957.*
Contribution from the National Research Council of Canada, Prairie Regional Laboratory, Saskatoon, Saskatchewan.
Issued as N.R.C. No. 4443 and Paper No. 246 on the Uses of Plant Products.
[2]*National Research Council of Canada Postdoctorate Fellow, 1956–57.*

hyde is readily cleaved by hot phenylhydrazine acetate (1). However, the acidity of this reagent makes it unattractive for use in the presence of the easily-hydrolyzed sucrose linkage. Alternatively, dialdehydes of this type are known to be alkali-labile (12) whereas

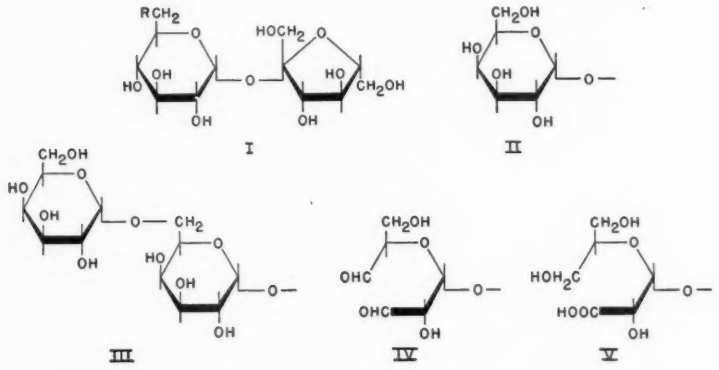

the sucrose linkage is not hydrolyzed by base, circumstances which should favor the liberation of intact sucrose residues.

Accordingly, raffinose and stachyose were oxidized, respectively, with 2 and 3 moles of sodium *meta*periodate in aqueous ethanol, a reagent which attacks *cis* glycol groups much more readily than *trans* glycols (6) (see also "Experimental" section). Sucrose was then obtained by treating each of the reaction products with hot aqueous sodium carbonate, the sugar being separated from other products by the use of ion-exchange resins and charcoal chromatography (21). Preliminary experiments showed that lead tetraacetate in acetic acid (4) also preferentially oxidized D-galactose units, and alkaline degradation of the product obtained from raffinose afforded sucrose. However, lead tetraacetate promoted relatively more oxidation of the sucrose moiety in raffinose than did periodate in aqueous ethanol, and was therefore less suited than the latter reagent to the present study.

The yields of sucrose obtained by partial oxidation of raffinose and stachyose with the periodate reagent were about 20 and 40%, respectively. These yields do not necessarily represent maximum values attainable by the method described, for no rigorous attempt was made to discover optimum conditions for the oxidation and degradation steps. Some oxidation of the sucrose moiety itself in raffinose and stachyose most probably occurs under the conditions used with a consequent lowering of the yield of sucrose obtainable. This is suggested by the fact that sucrose is oxidized at a rate moderately rapid when compared with the rates for raffinose and stachyose ("Experimental" section), it being assumed that the sucrose units in the latter oligosaccharides are attacked approximately as readily as is free sucrose. Further loss of sucrose may be attributable to incomplete degradation by alkali of the partially oxidized oligosaccharides. Thus, in addition to sucrose, acidic products are obtained which contain both D-glucose and D-fructose units. Such acids could arise by an internal Cannizzaro reaction, e.g. IV, giving rise to the hydroxy acid (V), without scission of the glycosidic linkage, by analogy with the action of alkali on the dialdehyde derived from methyl-α-L-rhamnopyranoside (10), and some other dialdehydes prepared by glycol-cleavage (14, 17).

The present work furnishes an instance, in addition to those described previously

(2, 11, 19), of the efficacy of glycol-cleavage oxidation as a tool for preferential degradation of selected units in oligosaccharides.

EXPERIMENTAL

Paper chromatography was carried out using Whatman No. 1 paper, and benzene–butanol–pyridine–water (1:5:4:3) (5) as solvent. Urea oxalate (13) was used to detect fructose and fructose-containing oligosaccharides on chromatograms, and ammoniacal silver nitrate (18) as a general developing spray.

Solutions were concentrated *in vacuo* at 40° C.

Rates of Oxidation of Sucrose, Raffinose, Stachyose, and Related Glycosides by Ethanolic Periodate

In a typical experiment, sucrose (34.4 mg.) was dissolved in 50% ethanol (10 ml.). To this solution was added a solution of sodium *meta*periodate (110 mg.) in 50% ethanol (10 ml.). At chosen intervals, aliquots of the reaction mixture were withdrawn and the periodate content of each was estimated by the arsenite method (7). Reactions were carried out at 0° C. and 25° C. In all experiments the molar ratio of sugar to oxidant was 1 to 5, and estimations were made during early stages of the reaction when a large excess of oxidant was present. Results, expressed as moles periodate/mole sugar, are given below for the following sugars: sucrose (S), raffinose (R), stachyose (ST), methyl-α-D-galactopyranoside (GA), methyl-α-D-glucopyranoside (GL).

Time, min.	Temperature 0° C.			Temperature 25° C.		
	S	R	ST	S	GA	GL
15	0.13	—	—	0.38	0.91	0.24
30	0.31	0.94	1.40	0.66	1.00	0.43
60	0.72	1.30	2.10	1.24	1.30	0.80
100	—	1.85	2.80	—	—	—

Sucrose by Partial Degradation of Raffinose

Crystalline raffinose pentahydrate (5.0 g.), dissolved in 5 ml. of water, was taken up in 500 ml. of cold 50% alcohol. Sodium *meta*periodate (4.0 g.; 2.2 molar equivalents) in a minimum volume of water was added to the raffinose solution at 0° C. After 18 hours at 0° C. the reaction mixture was carefully neutralized to a phenolphthalein end point with hot strontium hydroxide solution (15). The precipitate was removed by filtration and the filtrate was concentrated giving an amorphous solid, weight 4.4 g.

The oxidation product was dissolved in water (250 ml.), sodium carbonate (4.5 g.) added, and the solution heated on the steam bath for 3 hours. After deionization with Amberlites IR-120 and -4B the solution was concentrated to give a sirup. From a chromatographic examination the sirup appeared to contain sucrose and a lesser quantity of fructose. The material corresponding to sucrose was hydrolyzed by invertase giving two products which travelled on a paper chromatogram at the same rate as D-glucose and D-fructose respectively. Chromatography on charcoal–celite (1:1) (21) afforded sucrose (0.55 g.; 19% yield) which, after one recrystallization from methanol, had m.p. 185–186° C., undepressed on admixture with an authentic specimen; $[\alpha]_D$ +66.5° (*c*, 0.72, water); the X-ray diffraction pattern of the compound was identical with that of sucrose. Calculated for $C_{12}H_{22}O_{11}$: C, 42.10%; H, 6.43%. Found: C, 41.98%; H, 6.44%. By treatment with hot acetic anhydride – sodium acetate, a derivative was obtained;

melting point and mixed melting point with authentic sucrose octaacetate, 85–86° C.

In one experiment, the solution obtained after treatment with hot sodium carbonate was deionized with Amberlite IR-120 only. An acidic product was obtained which, together with the sucrose present, gave fructose and glucose in approximately equal quantities upon acid hydrolysis.

Partial Oxidation of Raffinose with Lead Tetraacetate

Raffinose pentahydrate (1.02 g.), dissolved in water (2 ml.), was taken up in acetic acid (75 ml.). Lead tetraacetate (1.60 g.) in acetic acid (50 ml.) was added to the sugar solution. After 18 hours' reaction time the calculated amount of oxalic acid in acetic acid was added, the lead oxalate was filtered off, and the solution was concentrated to a sirup; weight 0.75 g. The product was treated with sodium carbonate followed by ion-exchange resins, affording a sirupy product which, according to paper chromatography, contained sucrose, fructose, and raffinose. A portion of the sucrose was isolated by charcoal chromatography and characterized by its infrared absorption spectrum.

Isolation of Stachyose

The procedure was a composite of several methods described by French (8).

Powdered defatted soybean meal (1000 g.) was extracted for 15 minutes in a Waring blendor with hot 70% ethanol; the solids were separated off by filtration and were washed with hot 70% alcohol. The combined extract and washings were concentrated, taken up in water, and treated with Amberlites IR-120 and -4B, giving a clear, colorless solution which was concentrated to a small volume, filtered, and concentrated to a sirup. The latter, taken up in acetic acid containing butanol (9), deposited a semisolid product which was collected and again dissolved in acetic acid – butanol, the operation being repeated to give finally a heavy, colorless sirup. Addition of an aqueous solution of this sirup to cold alcohol caused precipitation of a powdery material (25 g.) which contained sucrose, raffinose, stachyose, and a higher oligosaccharide (paper chromatogram). The stachyose (8.2 g.) was isolated by separation of the mixture on a charcoal–celite (1:1) column (21), being eluted with 15% alcohol. Crystallized from aqueous ethanol the compound had m.p. 151–152° C., undepressed by admixture with an authentic specimen; the X-ray diffraction pattern was identical with that of stachyose.

Sucrose by Partial Degradation of Stachyose

Crystalline stachyose (1.50 g.) was treated with sodium *meta*periodate (1.3 g.; 3.0 molar equivalents) in 50% alcohol at 0° C. as described above for oxidation of raffinose. The oxidation product was treated with hot sodium carbonate as described above also giving a crude product which contained (paper chromatogram) small quantities of fructose and raffinose in addition to sucrose. The sucrose (weight 0.30 g.; 39% yield) was isolated by charcoal chromatography and after one recrystallization had melting point and mixed melting point with authentic sucrose, 185–186° C., $[\alpha]_D$ +66.0° (*c*, 0.7, water); the X-ray diffraction pattern was identical with that of sucrose. Calculated for $C_{12}H_{22}O_{11}$: C, 42.10%; H, 6.43%. Found: C, 42.33%; H, 6.48%.

ACKNOWLEDGMENTS

The authors express their gratitude to Dr. J. H. Pazur for a sample of stachyose. They also thank Mr. J. A. Baignee for carbon and hydrogen microdeterminations, Mr. J. W. L. C. Christ for technical assistance, Miss A. Epp for preparation of infrared spectra, and Mr. T. M. Mallard for preparation of X-ray diffraction patterns.

REFERENCES

1. BARRY, V. C. Nature, **152**, 537 (1943).
2. CHARLSON, A. J. and PERLIN, A. S. Can. J. Chem. **34**, 1200 (1956).
3. COURTOIS, J. E., ANAGNOSTOPOULOS, C., and PETELA, F. Bull. soc. chim. biol. **35**, 731 (1953).
4. CRIEGEE, R. Ber. **64**, 260 (1931).
5. DE WHALLEY, H. C. S., ALBON, N., and GROSS, D. Analyst, **76**, 293 (1951).
6. FLEURY, P., COURTOIS, J. E., and BIEDER, A. Bull. soc. chim. **19**, 118 (1952).
7. FLEURY, P. and LANGE, J. J. pharm. chim. **17**, 196 (1933).
8. FRENCH, D. Advances in carbohydrate chemistry. Vol. 9. Academic Press, Inc., New York. 1954. p. 149.
9. FRENCH, D., WILD, G. M., and JAMES, W. J. J. Am. Chem. Soc. **75**, 3664 (1953).
10. FRY, E. M., WILSON, E. J., JR., and HUDSON, C. S. J. Am. Chem. Soc. **64**, 872 (1942).
11. GORIN, P. A. J. and PERLIN, A. S. Can. J. Chem. **35**, 262 (1957).
12. HEAD, F. S. J. Textile Inst. **38**, T389 (1947).
13. HIRST, E. L., MCGILVRAY, D. I., and PERCIVAL, E. G. V. J. Chem. Soc. 1297 (1950).
14. HOFREITER, B. T., ALEXANDER, B. H., and WOLFF, I. A. Anal. Chem. **27**, 1930 (1955).
15. JACKSON, E. L. and HUDSON, C. S. J. Am. Chem. Soc. **59**, 994 (1937).
16. NEUBERG, C. Biochem. Z. **3**, 519 (1907).
17. PACSU, E. Textile Research J. **15**, 354 (1945).
18. PARTRIDGE, S. M. Nature, **158**, 270 (1946).
19. PERLIN, A. S. and LANSDOWN, A. R. Can. J. Chem. **34**, 451 (1956).
20. PRICE, C. C. and KNELL, M. J. Am. Chem. Soc. **64**, 552 (1942).
21. WHISTLER, R. L. and DURSO, D. F. J. Am. Chem. Soc. **72**, 677 (1950).
22. WICKSTROM, A. Medd. Norsk Farm. Selskap, **18**, 129 (1956).

STUDIES IN THE WAGNER–MEERWEIN REARRANGEMENT. PART II[1]

F. A. L. Anet and P. M. G. Bavin[2]

ABSTRACT

Dibenz[*b,f*]oxepin and its 10-methyl derivative have been prepared by ring expansion of suitable xanthene derivatives. 2-Fluorophenanthrene was synthesized from 2-fluorofluorene.

In Part I of this series (1) we described the Wagner–Meerwein rearrangement accompanying formolysis of 9-alkyl-9-fluorenylmethyl tosylates. We now report extension of these studies to other systems.

Reduction of xanthene-9-carboxylic acid with lithium aluminum hydride gave the alcohol, which was dehydrated with phosphorus pentoxide in xylene. Rearrangement took place and the product obtained was identified as dibenz[*b,f*]oxepin (I), which has been prepared recently by Manske and Ledingham (16) by an unambiguous method.

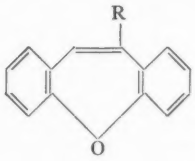

I, R = H
II, R = CH_3

9-Hydroxymethyl-9-methylxanthene was prepared by methylation of methylxanthene-9-carboxylate and subsequent reduction with lithium aluminum hydride. Tosylation followed by formolysis gave 10-methyldibenz[*b.f*]oxepin (II). This ring expansion is similar to that which occurs when 9,10-dihydro-9-anthranylmethyl tosylate undergoes acetolysis to dibenzocycloheptatriene (21). Apart from the parent compound already mentioned the only known derivatives of dibenz[*b.f*]oxepin are a compound related to the alkaloid cularine (15) and 3,4,6-trimethoxy[*b,f*]oxepin 10-carboxylic acid (19).

The ultraviolet spectra of I, II, and methyl 9-methylxanthene-9-carboxylate are shown in Fig. 1. It is interesting that there is a hypsochromic shift on methylation of the dibenzoxepin. Such hypsochromic shifts, except in cases of steric inhibition of resonance, occur only in certain non-alternant systems such as azulene, which has its longest wavelength absorption band at longer wavelength than either 1-methyl- or 5-methyl-azulene (18).

Dehydration of 9-ethylxanthydrol with formic acid did not give the oxepin but most probably 9-ethylidenexanthene, which was, however, not fully characterized (see Experimental).

Formylation of 2-fluorofluorene and reaction with alkaline formaldehyde gave 2-fluoro-9-hydroxymethylfluorene, which, with polyphosphoric acid at 160°, underwent a Wagner–Meerwein rearrangement to give 2-fluorophenanthrene.

It has been reported (20) that 2,2-diphenylpropanol gave *trans*-α-methylstilbene when distilled from phosphorus pentoxide. We prepared the tosylate of this alcohol, required for kinetic studies, and found that it gave the same stilbene on formolysis.

[1]*Manuscript received June 13, 1957.*
Contribution from the Department of Chemistry, University of Ottawa, Ottawa, Ontario.
[2]*National Research Council Postdoctorate Fellow, 1954–1956. Present address: Chemistry Department, The Ohio State University, Columbus 10, Ohio, U.S.A.*

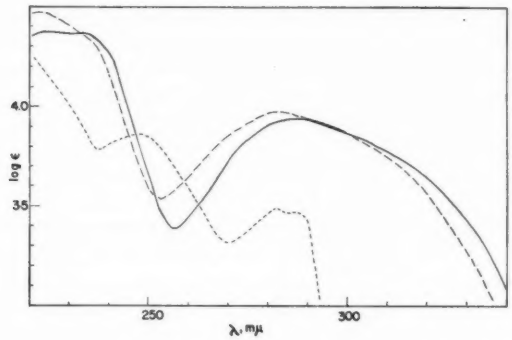

FIG. 1. Absorption spectrum of dibenz[*b,f*]oxepin ———, 10-methyldibenz[*b,f*]oxepin – – – –, methyl 9-methylxanthene-9-carboxylate - - - - -.

EXPERIMENTAL

The ultraviolet spectra were measured in methanol solution with a Beckman DK-2 Recording Spectrophotometer.

9-Xanthylmethanol

Xanthene-9-carboxylic acid (0.2 g., Fluka A.G., m.p. 222–226°) was reduced with an excess of ethereal lithium aluminum hydride. After it had been allowed to stand for two hours the excess reagent was decomposed with wet ether and enough water added to coagulate the precipitate. The ether layer was decanted from the inorganic solids and evaporated to a small volume. Addition of pentane caused the alcohol (0.1 g.) to crystallize. It was recrystallized from ether–pentane, m.p. 68°. Found: C, 79.14; H, 5.74. Calc. for $C_{14}H_{12}O_2$: C, 79.22; H, 5.70%.

Dibenz[b,f]oxepin (I)

9-Xanthylmethanol (0.05 g.), phosphorus pentoxide (1 g.), and xylene (10 ml.) were boiled under reflux for 10 minutes. Water was added and the xylene solution separated, dried, and evaporated. When the residue was recrystallized several times from a small volume of methanol, colorless plates were obtained, m.p. 109–110°, undepressed by mixture with authentic dibenz[*b,f*]oxepin, kindly given by Dr. R. H. F. Manske.

Methyl 9-Methylxanthene-9-carboxylate

Xanthene-9-carboxylic acid was esterified with methanol saturated with dry hydrogen chloride. The product crystallized from methanol or hexane as prisms (91%), m.p. 85° (lit. m.p. 85–86° (10)).

The preceding ester (0.05 mole) was alkylated in ether – liquid ammonia, using sodamide (0.15 mole) and methyl iodide (0.2 mole). The product was crystallized twice from methanol or hexane to give colorless prisms (71%), m.p. 95–96° (lit. m.p. 96–97° (11)). Attempted methylation under the conditions used for methyl fluorene-9-carboxylate failed (cf. 1).

Hydrolysis of a portion of the product with potassium hydroxide in warm 50% aqueous ethanol and crystallization from heptane gave 9-methylxanthene-9-carboxylic acid as colorless needles, m.p. 204–206° (lit. m.p. 205–206° (11)). Neutralization equivalent: found, 238; calculated, 240.

9-Hydroxymethyl-9-methylxanthene Tosylate

The preceding 9-methyl ester was reduced with ethereal lithium aluminum hydride, giving 9-hydroxymethyl-9-methylxanthene in 94% yield. One crystallization from hexane gave colorless prisms, m.p. 77–78°. Esterification with tosyl chloride in pyridine gave the tosylate, which crystallized from benzene–hexane as rectangular tablets, m.p. 152–153° with decomposition, raised to 154° by a further crystallization. Yield: 81%. Found: C, 68.9; H, 5.5. Calc. for $C_{21}H_{20}O_4S$: C, 68.5; H, 5.5%.

10-Methyldibenz[b,f]oxepin (II)

The preceding tosylate (0.5 g.) was boiled for a few minutes with formic acid (10 ml.) and then poured into water. The product was isolated with chloroform and crystallized from methanol, giving clusters of needles (0.22 g.), m.p. 57–58.5°. Found: C, 86.35; H, 5.89%. Calc. for $C_{15}H_{12}O$: C, 86.51; H, 5.81%.

Oxidation of the product (0.1 g.) with sodium dichromate in acetic acid gave only a trace of an acidic product. Xanthone could not be isolated.

The product (0.02 g.) in acetone (20 ml.) containing potassium permanganate (0.1 g.) was heated under reflux for 2 hours. The solution was decolorized with sodium bisulphite solution and the acetone evaporated. The crystals (m.p. 150–180°) which separated were collected and dissolved in *N* NaOH (2 ml.). Iodine was added until no more iodoform precipitated and then the filtered solution was acidified. Colorless prisms separated, m.p. 225–228°, undepressed by admixture with an authentic sample of diphenyl ether 2,2-dicarboxylic acid, m.p. 229–230° (lit. m.p. 231° (16)).

9-Ethylidenexanthene

9-Ethylxanthydrol was prepared as described in the literature (12) except that most of the ether was replaced by benzene to increase the solubility of the xanthone. The product (3 g.) was boiled with formic acid (20 ml.) for half an hour. The neutral fraction was isolated and purified by passage of a hexane solution through a column of activated alumina. Evaporation of the eluant gave 9-ethylidenexanthene as a slightly yellow oil with a green fluorescence. It failed to crystallize and did not form crystalline adducts with picric acid or trinitrobenzene. That it was 9-ethylidenexanthene was shown by the following: it was very rapidly oxidized by sodium dichromate in hot acetic acid, giving xanthone in almost quantitative yield, identified by melting point and mixed melting point. The ultraviolet spectrum was very similar to that of xanthone. It rapidly adsorbed 1.1 moles of hydrogen when reduced in ethanol with 10% palladium on charcoal as catalyst. The reduction product was a colorless non-fluorescent oil having a typical xanthene ultraviolet spectrum and, as expected for 9-ethylxanthene, it was oxidized by sodium dichromate in hot acetic acid very slowly.

1,1-Diphenylpropionic Acid

A solution of sodamide (0.1 mole) in liquid ammonia was added to a well-stirred solution of methyl diphenylacetate (0.1 mole) in a mixture of ether and liquid ammonia. After half an hour, methyl iodide (0.11 mole) was added dropwise and stirring continued for half an hour more. These additions were repeated twice more with 0.05 mole quantities. The product was isolated in the usual way to give an oil (methyl 1,1-diphenylpropionate has not been reported crystalline (14)) which was hydrolyzed as described for methyl 9-*t*-butylfluorene-9-carboxylate (1). Crystallization from benzene–hexane gave 1,1-diphenylpropionic acid as prisms (55%), m.p. 172–174° (lit. m.p. 172–174° (4)). Neutralization equivalent: found, 224; calculated, 226.

The anilide was prepared from the acid chloride and aniline. It crystallized from toluene–heptane as fine white needles, m.p. 117°.

2,2-Diphenylpropyl Tosylate

The preceding acid was reduced by boiling with ethereal lithium aluminum hydride for 24 hours. The product, isolated in the usual way, failed to crystallize. (2,2-Diphenylpropanol has not been reported crystalline (20).) Esterification with tosyl chloride in pyridine gave the crystalline tosylate, which formed small needles from benzene–hexane, m.p. 74°. Yield: 89% based on the acid. Found: C, 72.6; H, 6.3. Calc. for $C_{22}H_{22}O_3S$: C, 72.2; H, 6.1%.

Trans-α-methylstilbene

The preceding tosylate was boiled for a few minutes with formic acid. Crystallization of the neutral product from methanol gave lustrous plates, m.p. 81–82° (77%) (lit. m.p. 81–82° (13)). The ultraviolet spectrum was identical with the reported (13).

2-Fluorophenanthrene

2-Nitrofluorene (8) was reduced with ethanolic hydrazine and Raney nickel,[3] giving 2-aminofluorene in almost quantitative yield. This procedure is very much more convenient than that reported in Organic Syntheses (8). The preparation of 2-fluorofluorene has been described previously (7). 2-Fluorofluorene-trinitrobenzene adduct formed yellow needles from methanol, m.p. 95°. Found: C, 57.58; H, 3.17; N, 10.63. Calc. for $C_{19}H_{12}N_3O_6F$: C, 57.43; H, 3.05; N, 10.58%. 2-Fluoro-9-fluorenylmethanol was prepared from 2-fluorofluorene as described for the parent compound, 9-fluorenylmethanol (9). It crystallized from heptane as colorless microprisms, m.p. 94° (57%). Found: C, 78.55; H, 5.29. Calc. for $C_{14}H_{11}OF$: C, 78.49; H, 5.18%.

Dehydration of the carbinol by method A of Part I (1) gave 2-fluorophenanthrene in 64% yield, lustrous plates from methanol, m.p. and mixed m.p. 101–103° (see (5)). 1,3,5-Trinitrobenzene adduct: yellow needles from methanol, m.p. 132°.

REFERENCES

1. ANET, F. A. L. and BAVIN, P. M. G. Can. J. Chem. **34**, 991 (1956).
2. ANET, F. A. L. and BAVIN, P. M. G. Unpublished work.
3. BALCOM, D. and FURST, A. J. Am. Chem. Soc. **75**, 4334 (1953).
4. BATEMAN, D. E. and MARVEL, C. S. J. Am. Chem. Soc. **49**, 2917 (1927).
5. BAVIN, P. M. G. and DEWAR, M. J. S. J. Chem. Soc. 4486 (1955).
6. BAVIN, P. M. G. and DEWAR, M. J. S. Unpublished work.
7. BERGMANN, E., HOFFMANN, H., and WINTER, D. Ber. **66**, 46 (1933).
8. BLATT, A. H. (*Editor*). Organic Syntheses, Collected Volume II. John Wiley and Sons, New York. 1943. p. 447.
9. BURR, J. G. J. Am. Chem. Soc. **73**, 823 (1951).
10. CONANT, J. B. and GARVEY, B. S. J. Am. Chem. Soc. **49**, 2085 (1927).
11. CONANT, J. B. and GARVEY, B. S. J. Am. Chem. Soc. **49**, 2602 (1927).
12. CONANT, J. B., SMALL, L. F., and SLOAN, A. W. J. Am. Chem. Soc. **48**, 1743 (1928).
13. CRAM, D. J. and ELHAFEZ, F. A. A. J. Am. Chem. Soc. **74**, 5828 (1952).
14. DEWAR, M. J. S. and MOLE, T. J. Chem. Soc. 2556 (1956).
15. MANSKE, R. H. F. J. Am. Chem. Soc. **72**, 55 (1950).
16. MANSKE, R. H. F. and LEDINGHAM, A. E. J. Am. Chem. Soc. **72**, 4797 (1950).
17. PIETRA, S. Ann. chim. (Rome), **45**, 850 (1955).
18. PULLMAN, B. and PULLMAN, A. Les théories électroniques de la chimie organique. Masson et Cie, Paris. 1952. p. 449.
19. PSCHORR, R. and KNÖFFLER, G. Ann. **382**, 54 (1911).
20. RAMART, P. and AMAGAT, P. Ann. chim. (Paris), [10], **8**, 292 (1927).
21. RIGAUDY, J. and TARDIEU, P. Compt. rend. **240**, 1347 (1955).

[3]*This method of reduction was first reported by Balcom and Furst (3). It is readily applicable to 1 mole or larger quantities by adding the hydrazine slowly to moderate an otherwise violent reaction. Compounds reduced on this scale include o- and p-bromonitrobenzene, p-nitrophenol, and 2-nitrofluorene (2, 6). Similar reduction of 2,2'-dinitrodiphenyl gave 3,4-benzcinnoline in 94% yield, providing the best preparation of this and similar compounds (2). Palladium on charcoal may replace the Raney nickel (14, 17).*

OXYMERCURATION OF THE METHYLCYCLOHEXENES[1]

W. R. R. Park and George F Wright

ABSTRACT

It has been found that, while hydroxymercuration of 2-methylcyclohexene leads to a single product, 3-methylcyclohexene gives a nonworkable mixture and 4-methylcyclohexene gives both positional and diastereoisomers of which three of the four have been isolated. The ratio of positional isomers is found to be 5:1 in favor of farthest distance of the methyl group from the mercury atom. The conversion of the chloromercuri-hydroxy-methylcyclohexanes to chloromercuri-methoxy-methylcyclohexanes by potassium *tert*-butoxide and dimethyl sulphate has been accomplished. Thus the products of hydroxymercuration have been related configurationally to two of the three products of 4-methylcyclohexene methoxymercuration. Among these products that one is most prevalent in which the mercury is most distant, positionally and configurationally, from the methyl group in the alkene.

Since oxymercuration of a single geometric form of an alkene containing no substituent possessing asymmetry always forms but one diastereomer (15) it has seemed worth while to oxymercurate alkenes in which one substituent contains an asymmetric center. Such an alkene might be expected to form either or both of positional and diastereoisomers. One such alkene has previously been oxymercurated, but in this circumstance the alkene (4, 11, 12), α-terpineol, contains an alcoholic function which may influence the oxymercuration or partake in it. For this reason the absence of diastereoisomers or positional isomers in the oxymercuration of α-terpineol may not define generally the behavior of alkenes containing an asymmetric substituent. Consequently we have chosen to examine simpler types, the methylcyclohexenes.

The hydroxymercuration of 2-methylcyclohexene (I) does not involve the possibility of diastereoisomerism although positional isomers are possible. However, the reaction yields only one compound, which is called* 1-↓-chloromercuri-1-↓-hydroxy-2-↑-methylcyclohexane (II) (where the symbols ↑ and ↓ signify 'upper' and 'lower' positions in a planar cyclohexane structure assumed to be the mean of the several conformational possibilities). This substance may be reduced by sodium amalgam in water to 1-methylcyclohexanol (III).

The oxymercuration of 3-methylcyclohexene (IV) (2) does not proceed so smoothly. No crystalline product can be isolated from the methoxymercuration (all attempts at separation by differences in density and by selective adsorption or ion-exchange techniques have thus far failed) and only a small amount of crystalline product has been segregated from the oily mixture obtained by hydroxymercuration of this alkene. This compound seems to be 1-↓-chloromercuri-2-↓-hydroxy-3-↑-methylcyclohexane (V) since it may be reduced by hydrazine to 2-↑-methyl-↓-cyclohexanol (VI). The latter is identified as its α-naphthylurethane (6). It is evident that either or both of diastereomers and positional isomers may be present in the oxymercuration product, but its intractability makes a decision about isomer type impossible until new techniques of separation are devised.

Although a multiplicity of products has also been obtained from the oxymercurations of 4-methylcyclohexene (VII) the separation has been more successful than that of the previous instance. However, quantitative isolation has not been effected. The crude

[1]*Manuscript received May 13, 1957.*
Contribution from the Department of Chemistry, University of Toronto, Toronto, Ontario.
**The configuration of oxymercurials cannot yet be specified with certainty. The assignment used in this report is based on experimental results of Ref. 8 and the discussion of Ref. 16.*

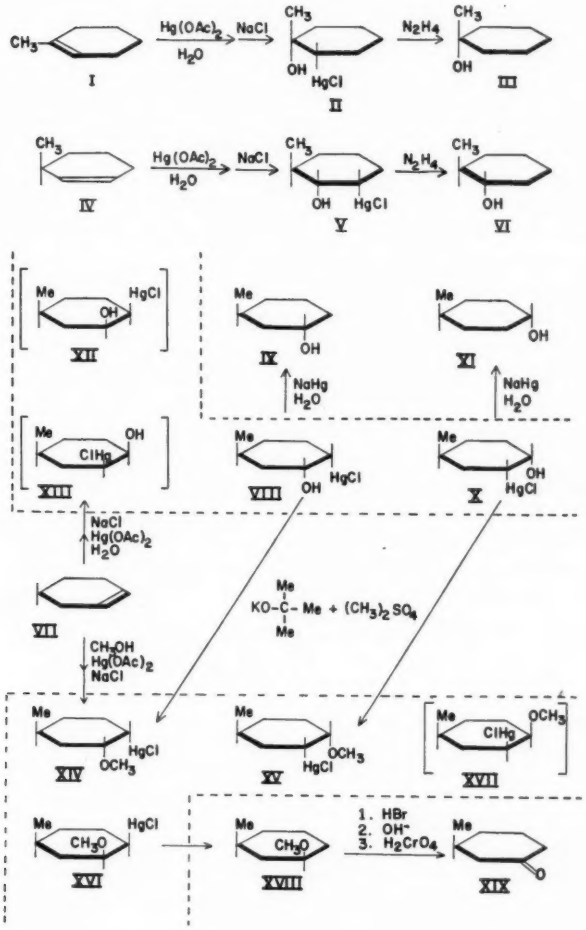

hydroxymercuration product melts at 100–120°, but not more than a 1% yield of 1-↓-chloromercuri-2-↓-hydroxy-4-↑-methylcyclohexane (VIII, m.p. 165°) has been isolated from this mixture. This structure has been demonstrated (assuming apex–apex addition during oxymercuration (8)) by sodium amalgam reduction to 3-↑-methyl-↓-cyclohexanol (IX) (1), identified by refractive index, by conversion to the α-naphthylurethane (m.p. 118°) or the *p*-nitrobenzoate (m.p. 68°), and by assuming that Angyal and Mills' correction of the structures assigned by Macbeth and Mills (7) is valid.

In addition to this component of the hydroxymercuration product of 4-methylcyclohexene, a second isomer, in 0.6% yield, has been isolated from the aqueous saline mother liquors. This substance, m.p. 143°, seems to be the positional isomer 1-↓-chloromercuri-2-↓-hydroxy-5-↑-methylcyclohexane (X) since reduction with sodium amalgam converts it to 4-↑-methyl-↓-cyclohexanol (XI) (1). The melting point – composition diagram of this mercurial (X) with respect to VIII has been determined, and a eutectic temperature of 108° has been found. Since many of the crystal crops obtained during the

separation of VIII melt below this binary eutectic temperature we assume that either or both of the diastereomers XII and XIII also are present in the hydroxymercuration product of 4-methylcyclohexene.

The ratio of the positional isomers 1-chloromercuri-2-hydroxy-4-methylcyclohexane (VIII and XII) versus 1-chloromercuri-2-hydroxy-5-methylcyclohexane (X and XIII) has been determined by sodium amalgam reduction of the entire hydroxymercuration product (aqueous-soluble and insoluble). This mixture of 3- and 4-methylcyclohexanols has been oxidized to the corresponding mixture of 3- and 4-methylcyclohexanones, which are converted to their 2,4-dinitrophenylhydrazones. Chromatographic separation of these derivatives on a bentonite column shows that the ratio of 3-methylcyclohexanone to 4-methylcyclohexanone is 5:1. It may be significant that the preponderant positional isomer is 1-chloromercuri-2-hydroxy-4-methylcyclohexane (VIII and perhaps XII), in which the mercury atom is situated as far as possible from the methyl group.

The products (VIII and X) obtained from 4-methylcyclohexane have been methylated in order, for the first time, to correlate the disposition of addends in hydroxymercuration with that in methoxymercuration; also it was expected that the methylated mercurials would be useful as seeds to induce crystallization of the products from methoxymercuration. The reliability of the methylation technique has been demonstrated with α-1-chloromercuri-2-hydroxycyclohexane (XX) (3). When this compound is treated with potassium *tert*-butoxide, the potassium salt (XXI) is obtained (no precipitation of potassium chloride occurs). Aqueous acidification regenerates XX showing that inversion has not occurred. Alternatively if XXI is treated with dimethyl sulphate a 90% yield of α-1-chloromercuri-2-methoxycyclohexane (XXII) is obtained.

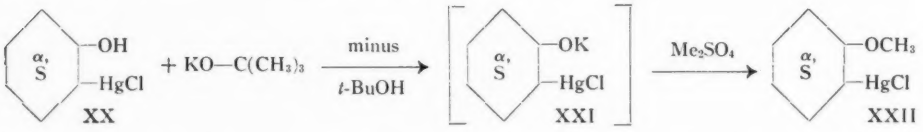

Since inversion is not expected during the methylation step it would seem that configuration of the hydroxymercurial from cyclohexene is identical with that of the methoxymercurial. The same technique has been employed in conversion of the hydroxymercurial (VIII) to 1-↓-chloromercuri-2-↓-methoxy-4-↑-methylcyclohexane (XIV) and of the hydroxymercurial X to 1-↓-chloromercuri-2-↓-methoxy-5-↑-methylcyclohexane (XV).

Three of the four possible isomers have been isolated as pure compounds in small amount from the 94% of crude product, m.p. 53–62°, obtained by methoxymercuration of 4-methylcyclohexane. The isomer obtained in largest amount has been found to be XIV, m.p. 108–109°, the methylation product of 1-↓-chloromercuri-2-↓-hydroxy-4-↑-methylcyclohexane, VIII, which also was found in greatest quantity among the hydroxymercuration products by crystallization. The second product was isolated in 3% yield by fractional precipitation from the mother liquors, and evidently is 1-↑-chloromercuri-2-↑-methoxy-4-↑-methylcyclohexane (XVI), the diastereomer of the first product, XIV. This structure has been demonstrated by sodium amalgam reduction to 1-↑-methoxy-3-↑-methylcyclohexane which has been degraded by ether fission, hydrolysis of the resultant bromide to the alcohol, and oxidation of the latter to 3-methylcyclohexanone (XIX). The third isomer, 1-↓-chloromercuri-2-↓-methoxy-5-↑-methylcyclohexane (XV) was obtained in 0.3% yield by seeding of the rediluted crystallization liquors with the same substance obtained by methylation of the hydroxymercurial, X.

The fourth possible isomer, 1-↑-chloromercuri-2-↑-methoxy-5-↑-methylcyclohexane (XVII), which would be diastereomeric with XV was not isolated, though it is probably present in small amount. However, it would seem that the methoxymercuration which disposes the mercuri group on position 4 with respect to the methyl group is more rapid than that which disposes it on position 3, either from steric or polar influences or both. If this opinion is valid then acceleration of the methoxymercuration ought to accentuate this difference.

This has been found to be the fact. When the accelerator, boron trifluoride etherate, is included in the system, neither of the positional isomers XV or XVII is detectable. Their absence has been demonstrated by treating the entire product through the reaction sequence of reduction, ether fission, hydrolysis, and oxidation (XVI → XIX), whereby only 3-methylcyclohexanone is found. The actual products, XIV and XVI, have been isolated in better yield than obtains in the uncatalyzed reaction. Since none of the fractions encountered during separation of XIV and XVI by crystallization melted below 54°, the eutectic temperature of a mixture of the two, it is reasonable to assign a composition to the crude methoxymercuration product, m.p. 54–74°. Since the melting point of this crude product is depressed by admixture of a small amount of 1-↑-chloromercuri-2-↑-methoxy-4-↑-methylcyclohexane (XVI) it is evident from the temperature–composition diagram that the catalyzed methoxymercuration product of 4-methylcyclohexene comprises about 80% of 1-↓-chloromercuri-2-↓-methoxy-4-↑-methylcyclohexane, XIV. Thus the methoxymercuration, like the hydroxymercuration, yields predominantly the isomer in which the mercuri linkage is farthest removed from the methyl group in 4-methylcyclohexene.

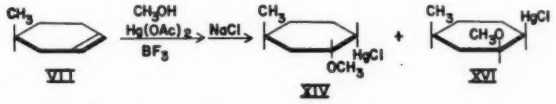

VII XIV XVI

If this tendency toward farthest disposition of the mercuri linkage with respect to the methyl group is a steric one then it must be related to the mercury substituent itself rather than to its acyl substituent. When mercuric benzoate or mercuric stearate is used instead of mercuric acetate in the methoxymercuration of 4-methylcyclohexene and the initial products are converted to the mixture of methoxychloromercurials, the melting point of the crude products is not essentially different from that obtained when mercuric acetate is used.

EXPERIMENTAL*

1-↓-Chloromercuri-2-↓-hydroxy-2-↑-methylcyclohexane (II)

A mixture of 4.8 g. (0.05 mole) of 2-methylcyclohexene (14), b.p. 108.5–109.5° (760 mm.), n_D^{20} 1.4507, with 15.9 g. (0.05 mole) of mercuric acetate dissolved in 125 ml. of water was shaken for 45 minutes, then filtered from mercurous salt into 80 ml. of saturated aqueous sodium chloride. The precipitate, vacuum-dried, weighed 10.8 g. (62%), m.p. 115–118°. Two crystallizations from benzene (4 ml. per g.) left 5.5 g. (51% recovery), m.p. 128.0–129.5°. Calc. for $C_7H_{13}OHgCl$: C, 24.1; H, 3.75. Found: C, 24.2; H, 3.71. Sodium amalgam reduction (described below) gave a 51% yield of 1-methylcyclohexanol, m.p. and m.m.p. 25–26°.

**Melting points have been corrected against reliable standards. X-Ray patterns are recorded as relative intensities [I/I_1] at d spacings in Å using Cu K_α (Ni filtered) radiation, for strongest lines.*

1-↓-Chloromercuri-2-↓-hydroxy-3-↑-methylcyclohexane (*V*)

The 3-methylcyclohexene (b.p. 100.8–101.5° at 760 mm., n_D^{20} 1.4452), 9.6 g. (0.10 mole), was shaken with a solution of 31.8 g. (0.10 mole) of mercuric acetate in 300 ml. of water for 50 minutes, then the whole was poured into 1500 ml. of 4% aqueous sodium chloride. The gummy precipitate (15.3 g., 44%) was filtered off, m.p. 74–80°. We have not yet been able to separate this mixture.

The aqueous liquors, vacuum-evaporated to a volume of 300 ml., yielded 3.40 g. (10%) of product, m.p. 110–115°. After six crystallizations from methanol (5–10 ml. per g.) a pure product, 0.83 g., m.p. 175.0–175.6°, was obtained. Calc. for $C_7H_{13}OHgCl$: C, 24.1; H, 3.75. Found: C, 23.9; H, 3.64.

2-↑-Methyl-↓-cyclohexanol (*VI*)

To a mixture of 0.85 g. (0.0024 mole) of 1-↓-chloromercuri-2-↓-hydroxy-3-↑-methylcyclohexane and 35 g. of 3% sodium amalgam was added 6 ml. of ice-cold water. After 2 days at 0° the system was extracted with four 5-ml. portions of diethyl ether. The extract, water-washed and magnesium sulphate-dried, was distilled, 0.19 g. (68%), b.p. 60–62° (10 mm.). The melting point of the α-naphthylurethane, 158.5–159.5°, was not lowered by mixture with the authentic material.

Preparation and Purification of 4-Methylcyclohexene (*VII*)

A mixture of 171.5 g. of 4-methylcyclohexanol (E.K.) and 90 g. of 85% phosphoric acid was heated in a fractionating still at a rate such that the head temperature did not exceed 105°. When no more would distill the organic layer of the residue was separated, dried with magnesium sulphate, and distilled, b.p. 102–104°, 116 g. (81%). Distillation through a 50-plate column (r.r. 50:1) gave 67% as pure 4-methylcyclohexene, b.p. 103–103.2° (760 mm.), n_D^{20} 1.4420, d_4^{20} 0.800, identical with that reported previously (9).

Hydroxymercuration of 4-Methylcyclohexene

A solution of 159 g. (0.50 mole) of mercuric acetate in 1850 ml. of water was shaken with 48 g. (0.50 mole) of 4-methylcyclohexene for 1 hour, then poured into 5.5 liters of 4% aqueous sodium chloride at 35°. The precipitate was filtered and the aqueous filtrate was vacuum-evaporated, leaving a residue which was water-washed to remove sodium chloride. The remainder (6.6 g., 3.8%), m.p. 68–102°, was crystallized seven times from benzene (10 ml. per g.) leaving 0.96 g. (0.5%) of 1-↓-chloromercuri-2-↓-hydroxy-5-↑-methylcyclohexane (X), m.p. 142–143°. Calc. for $C_7H_{13}OHgCl$: C, 24.1; H, 3.75. Found: C, 24.3; H, 3.84. X-Ray diffraction: [10] 15.63, 13.48, 7.89; [8] 2.82; [7] 6.70, 5.94, 5.37.

The crude saline-insoluble mercurial (134 g., 77%), m.p. 116–129°, was boiled with 1500 ml. of benzene. The cooled mixture was filtered to remove 113 g., m.p. 126–137°. Crystallization from 1300 ml. of benzene raised this melting point to 135–160°. Four more crystallizations from 10:1 benzene:methanol (9 ml. per g.) left 1.9 g. (1.7%) of 1-↓-chloromercuri-2-↓-hydroxy-4-↑-methylcyclohexane (VIII), m.p. 164–164.8°. Calc. for $C_7H_{13}OHgCl$: C, 24.1; H, 3.75. Found: C, 24.0; H, 3.95. X-Ray diffraction: [10] 11.2; [9] 11.9; [8] 9.93; [7] 3.72; [6] 5.43, 4.98, 4.52, 4.17.

The high hydrogen value is typical of analyses of mercurials using the ordinary Pregl micro carbon–hydrogen tube filling. The more precise hydrogen values reported here were obtained by a modification of the tube filling (5).

4-↑-Methyl-↓-cyclohexanol (*XI*)

Sodium amalgam reduction of X as described above gave 85% as 4-↑-methyl-↓-cyclohexanol, b.p. 80–82° (22 mm.). The α-naphthylurethane melted at 158.5–159°.

3-↑-Methyl-↓-cyclohexanol (IX)

A similar reaction with 1-↓-chloromercuri-2-↓-hydroxy-4-↑-methylcyclohexane gave 80% as IX, b.p. 75–77° (18 mm.), n_D^{20} 1.5479. The α-naphthylurethane melted at 116–118°. The *p*-nitrobenzoate melted at 68–69°.

Melting Point – Composition Diagram, Binary System of VIII and X

Weighed portions of VIII and X were dissolved in 0.25 ml. of methanol and vacuum-evaporated, and the melting point was taken. The final mixture, defining the eutectic mixture, was examined in the thaw-point apparatus (10). Both softening point and disappearance of last crystal are recorded.

Mg. VIII	Mg. X	% VIII	Shrink	Melt
5.5	1.7	76	140	149
6.7	0.8	89	151	156
1.6	1.5	52	117	132
1.3	4.7	22	111	130
3.0	3.2	48	117	125
1.3	1.9	41	110	120
1.8	4.5	29	109	118
1.3	2.4	35	109	119
1.711	3.183	34.8	106.5	119.5

Ratio of 1-Chloromercuri-2-hydroxy-4-methylcyclohexanes to 1-Chloromercuri-2-hydroxy-5-methylcyclohexanes Obtained by Hydroxymercuration of 4-Methylcyclohexene

A mixture of 4.2 g. (0.05 mole) of 4-methylcyclohexene and 15.9 g. (0.05 mole) of mercuric acetate in 125 ml. of water was shaken for 80 minutes, then poured into 100 ml. of saturated aqueous sodium chloride. The precipitate (12.4 g., 71%) was combined with 0.33 g. obtained by chloroform extraction of the saline filtrate, and this 0.036 mole was treated in 100 ml. of water for 15 days at 25° with a 2.5% amalgam containing 8.4 g. (0.364 atom) of sodium. The system was extracted with four 15-ml. portions of diethyl ether and this extract, distilled, gave 1.32 g., 0.0115 mole (32%), of 3- and 4-methylcyclohexanols, b.p. 74–76° (15 mm.). This mixture was dissolved in 2.494 g. (0.075 mole) of cold 70% aqueous sulphuric acid and stirred at 0° while a solution of 1.16 g. (0.004 mole) of sodium dichromate in the same amount of sulphuric acid was added during 75 minutes. Subsequently, after 15 minutes at 70°, the cooled system was extracted with four 3-ml. portions of diethyl ether. The extracts, dried and distilled, gave 0.89 g. (69%) of the cyclohexanones, b.p. 59–61° (14 mm.), n_D^{20} 1.4465. This mixture (0.20 g., 0.0018 mole) was treated with 20 ml. of 2,4-dinitrophenylhydrazine reagent (13). The precipitate, 0.39 g. (75%), melted at 99–108°. A solution of 15 mg. in 1 ml. of benzene was placed on a column (18 by 360 mm.) containing 65 g. of tightly-packed Volclay bentonite. This column was eluted (under 500 mm. gauge pressure) first with 300 ml. of 7.5:92.5 diethyl ether – petroleum ether (b.p. 60–70°) and then with 600 ml. of these solvents in 12:88 mixture. The two bands were removed separately and each was eluted with three 50-ml. portions of methanol. The upper band gave 2 mg. of 4-methylcyclohexanone dinitrophenylhydrazone, m.p. 130–132°, while the bottom band gave 10 mg. of 3-methylcyclohexanone, m.p. 143–145°. Both samples were identified by mixture melting point. The ratio of isomers is thus 17:83.

Methylation of α-1-Chloromercuri-2-hydroxycyclohexane

From a 200 ml. modified Claisen flask containing 80 ml. of sulphur-free toluene was

distilled 15 ml. to remove residual water. To the remainder under nitrogen was added 0.59 g. (0.015 atom) of potassium and 10 ml. of dry *tert*-butyl alcohol. After stirring and refluxing had caused the metal to dissolve, the excess of the alcohol was removed by fractional distillation. The remaining suspension was cooled, treated with 1.68 g. (0.005 mole) of α-1-chloromercuri-2-hydroxycyclohexane, and stirred until after 20 minutes the mercurial had dissolved. After 15 minutes the whole was vacuum-distilled for the same time (large ebullition tube containing nitrogen) until 15 ml. of distillate was obtained. The remainder was stirred vigorously for 90 minutes with 1.89 g. (0.015 mole) of dimethyl sulphate. Then 20 ml. of 10% aqueous sodium hydroxide was added and, after 10 minutes of stirring, the toluene was vacuum-distilled. The remainder was filtered, diluted with 90 ml. of 1.5% aqueous sodium chloride, and saturated with carbon dioxide. The α-1-chloromercuri-2-methoxycyclohexane (1.57 g., 90%) melted at 109–112°. After crystallization from 8 ml. of methanol, the remaining 1.1 g. melted at 113.5–115.5° and was identified by mixture melting point.

1-↓-Chloromercuri-2-↓-methoxy-5-↑-methylcyclohexane (*XV*)

A similar methylation of 1-↓-chloromercuri-2-↓-hydroxy-5-↑-methylcyclohexane (X) gave a 77% yield of XV, m.p. 82–88°. Crystallized twice from methanol (80% recovery), it melted at 88–89°. Calc. for $C_8H_{15}OHgCl$: C, 26.4; H, 4.16; Found: C, 26.4; H, 4.32. X-Ray diffraction: [10] 11.70; [9] 5.84, 3.90, 3.49; [7] 3.66, 3.62, 3.25, 2.91.

1-↓-Chloromercuri-2-↓-methoxy-4-↑-methylcyclohexane (*XIV*)

Methylation of 1-↓-chloromercuri-2-↓-hydroxy-4-↑-methylcyclohexane (VIII) by the same procedure gave an 83% yield of XIV, m.p. 100–106°. Crystallization from methanol (3.3 ml. per g., 33% recovery) raised the melting point to 108.0–109.2°. Calc. for $C_8H_{15}OHgCl$: C, 26.4; H, 4.16. Found: C, 26.5; H, 4.39. X-Ray diffraction: [10] 2.40; [9] 13.8, 2.85; [8] 10.97, 10.39; [7] 2.097; [6] 2.47.

Methoxymercuration of 4-Methylcyclohexene

A. Uncatalyzed

A solution of 9.6 g. (0.10 mole) of 4-methylcyclohexene and 31.8 g. (0.10 mole) of mercuric acetate in 250 ml. of methanol was poured into 700 ml. of 2% aqueous sodium chloride after 30 minutes. After 2 hours the precipitate, 34.1 g. (94%), was filtered off, m.p. 53–62°. After 14 crystallizations from methanol the remainder (1.1 g., 3.2%) melted at 108–109°. A mixture melting point with 1-↓-chloromercuri-2-↓-methoxy-4-↑-methylcyclohexane (XIV) was not lowered.

The filtrate from the first methanolic crystallization (80 ml.) was evaporated to a volume of 65 ml. and then cooled at 0° for 3 days. The crystal crop, 3.4 g., m.p. 62–76°, was largely XIV. The filtrate was again evaporated to a volume of 50 ml. and cooled 5 days at 0° while 4.42 g., m.p. 50–60°, separated. Eight crystallizations from methanol (2–5 ml. per g.) left 1.07 g. (m.p. 89°) (2.9%) of 1-↑-chloromercuri-2-↑-methoxy-4-↑-methylcyclohexane (XVI). The X-ray powder pattern of XVI was: [10] 10.16, 3.45, 4.09; [9] 5.18, 5.75; [8] 3.72, 2.55, 3.08; [7] 2.11, 2.52, 3.08, 10.16; [6] 2.81, 2.94. Calc. for $C_8H_{15}OHgCl$: C, 26.4; H, 4.16. Found: C, 26.7; H, 4.12. Electrical polarization in dioxane at 20° is 387 cc.: Calc. R_D is 55.4 so dipole moment is 3.97 D.

The filtrate from the 4.42 g. portion was diluted with methanol to a volume of 120 ml., and chilled to −70°, and a layer of petroleum ether (b.p. 60–70°) was added. When this system was seeded with 1-↓-chloromercuri-2-↓-methoxy-5-↑-methylcyclohexane (XV), precipitation of 0.52 g., m.p. 43–60°, occurred during 3 days. When this crop was

crystallized four times from methanol (3 ml. per g.) there remained 0.10 g. (0.3%) of XV, m.p. 86–88°, identified by mixture melting point.

B. Catalyzed

To a solution of 3.18 g. (0.01 mole) of mercuric acetate in 100 ml. of methanol at 1° was added a solution of 0.96 g. (0.01 mole) of 4-methylcyclohexene and 0.14 g. (0.001 mole) of boron fluoride etherate in 50 ml. of methanol at 1°. After 30 minutes the system was poured into 400 ml. of 1% aqueous sodium chloride solution. After 12 hours the precipitate was filtered, 2.64 g. (73%), m.p. 54–74°.

When this product was submitted to the reactions described below the sole product was the 2,4-dinitrophenylhydrazone of 3-methylcyclohexanone, m.p. 143–145°.

Alternatively the 2.64 g. portion was crystallized six times from methanol (4 ml. per g.), leaving 0.31 g. (12%) of 1-↓-chloromercuri-2-↓-methoxy-4-↑-methylcyclohexane (XIV), m.p. 102–105°. A further crop (0.6 g.) was obtained by evaporation of 3 ml. of methanol from the 10 ml. filtrate from the first crystallization. Further evaporation of 2 ml. from the final 7 ml. filtrate caused separation of 0.27 g., m.p. 68–75°. Crystallization from 2 ml. of methanol gave 0.18 g. (7%) of 1-↑-chloromercuri-2-↑-methoxy-4-↑-methylcyclohexane (XVI), m.p. 84–86°, authenticated by mixture melting point. The crystalline nature of subsequent fractions indicated that not more than these two compounds were present (no fraction melted below 54°).

Thaw Point – Composition Diagram, Binary System of XIV and XVI

The mixtures were prepared by evaporation of solutions of weighed samples in 0.25 ml. of methanol. All determinations were made in the thaw-point apparatus (10). Disappearance of the last crystal in this determination is called the melting point.

Mg. XVI	Mg. XIV	% XVI	Eutectic	M.p.
0.802	2.198	26.7	57.0	94.9
0.749	0.897	45.5	55.5	85.8
1.333	0.329	80.3	54.2	73.8
1.359	0.536	71.8	53.9	56.6
1.586	1.030	60.7	54.8	71.8
1.577	0.858	64.8	54.0	70.2

3-Methylcyclohexanone

A mixture of 1.30 g. (0.0036 mole) of α-1-↑-chloromercuri-2-↑-methoxy-4-↑-methylcyclohexane (XVI), 33 g. of 3% sodium amalgam, and 6 ml. of water reacted at 0° for 1 day and was ether-extracted. After evaporation of the ether the residue (*ca.* 0.5 ml.) with 1.03 g. (0.007 mole) of 40% hydrobromic acid and 10 ml. of acetic acid was heated at 90–100° for 11 hours, then made alkaline with 65 ml. of 15% alkali and boiled under reflux for 8 hours. Ether extraction gave 0.21 g. (52%) of 3-methylcyclohexanol, b.p. 65–70° (13 mm.). This distillate was dissolved in 0.332 g. (0.001 mole) of 30% aqueous sulphuric acid. The solution was stirred at 0° while 0.16 g. (0.0005 mole) of sodium dichromate in the same amount of sulphuric acid was added during 10 minutes. After 25 minutes more at 0° and 20 minutes at 70° the system was cooled and ether-extracted. The extract, water-washed and evaporated, left 0.15 ml., which was treated with 5 ml. of 2,4-dinitrophenylhydrazine reagent (13). The 0.110 g. of precipitate, m.p. 120–130°, was crystallized from 5 ml. of methanol, 0.065 g., m.p. 142–145°. A mixture melting point with an authentic sample was not lowered.

1-↓-Chloromercuri-2-↓-methoxy-2-↑-methylcyclohexane

A solution of 3.18 g. (0.01 mole) of mercuric acetate in 50 ml. of methanol was treated with 0.96 g. (0.01 mole) of 2-methylcyclohexene. After 5 minutes, a test with sodium hydroxide gave no yellow precipitate so the system was poured into 100 ml. of 3% aqueous sodium hydroxide with stirring. The solid chloromercurial (2.17 g., m.p. 79–82°, 75%) was four times crystallized from commercial hexane plus methanol, m.p. 83–84°. Diffraction pattern is [10] 9.82; [9] 4.29; [8] 6.06; [7] 3.26; [6] 6.41; [5] 4.92; [4] 5.64, 5.21; [3] 4.44, 3.65. Electric polarization in dioxane at 20° is 446.7 cc.; calc. R_D 55.0; dipole moment 4.31 D. Anal. calc. for $C_8H_{15}OHgCl$: C, 26.5; H, 4.16. Found: C, 26.1; H, 4.14.

REFERENCES

1. Angyal, S. J. and Mills, J. A. Rev. Pure Appl. Chem. (Australia), **2**, 185 (1952).
2. Berlande, A. Bull soc. chim. **9**, 642 (1942).
3. Brook, A. G. and Wright, G. F. Can. J. Research, B, **28**, 623 (1950).
4. Brook, A. G. and Wright, G. F. To be published.
5. Cross, C. K. and Wright, G. F. Anal. Chem. **26**, 886 (1954).
6. Jackman, L. N., Macbeth, A. K., and Mills, J. A. J. Chem. Soc. 1717 (1949).
7. Macbeth, A. K. and Mills, J. A. J. Chem. Soc. 709 (1945).
8. McNeely, K. H., Rodgman, A., and Wright, G. F. J. Org. Chem. **20**, 714 (1955).
9. Nametkin, S. and Brussow, L. Ber. **56**, 1807 (1923).
10. Rheinboldt, H. and Kircheisen, M. J. prakt. Chem. **113**, 348 (1926).
11. Sand, J. and Singer, F. Ann. **329**, 166 (1903).
12. Sand, J. and Singer, F. Ber. **35**, 3170 (1902).
13. Shriner, R. L. and Fuson, R. C. Identification of organic compounds. 3rd ed. John Wiley & Sons, Inc., New York. 1948. p. 97.
14. Wallach, O. Ann. **359**, 298 (1908).
15. Wright, G. F. J. Am. Chem. Soc. **57**, 1993 (1935).
16. Wright, G. F. Ann. N. Y. Acad. Sci. **65**, 436 (1957).

PREPARATION OF DISTILBENE (1,2,3,4-TETRAPHENYLCYCLOBUTANE)[1]

J. M. MORTON,[2] E. A. FLOOD, AND N. F. H. BRIGHT[3]

ABSTRACT

The reaction between benzyl chloride and potassium amide in liquid ammonia has been shown to yield, in addition to stilbene as the main product, considerable quantities of 1,2,3,4-tetraphenylcyclobutane. The isomer of this compound formed in this reaction is believed to be one that has not been reported previously.

The reaction between alkyl halides and metal amides leads to the formation of ethylenic compounds (5, 6). The reaction between benzyl chloride and potassium amide in liquid ammonia was first worked on by one of the present authors (2). In general it has been found previously that when a solution of potassium amide in liquid ammonia was added to a solution of benzyl chloride, also in liquid ammonia, a white solid precipitate formed. If excess potassium amide was present, a deep reddish purple color developed in the ammonia solution. This color was removed by the addition of excess benzyl chloride or any acid substance such as ammonium chloride. The white solid reaction product, after the liquid ammonia had been allowed to evaporate, was washed with water and dried. It has been reported by all who have worked on this reaction previously that this represents a yield of 95 to 100% stilbene (5, 7).

In the course of the present work it has been found that if the white solid product of the reaction is recrystallized from 95% alcohol, its melting point is higher than that of stilbene (124° C.). After five crystallizations, a material is obtained that is distinctly different from stilbene. This material, consisting of needle-shaped crystals rather than rhombic plates characteristic of stilbene, melts at 149° C. The experimental evidence is that this material is the dimer of stilbene, viz., 1,2,3,4-tetraphenylcyclobutane. The yield of the dimer varies considerably and we have not yet been able to find the most favorable conditions for its formation.

EXPERIMENTAL

1. Materials

The benzyl chloride used was a middle fraction from a vacuum distillation (75.5° to 76.0° C. at 14 mm.) of Eastman α-chlorotoluene. The metallic potassium was Baker and Adams Reagent Grade. The pieces were cut and the surface material removed under heavy mineral oil.

2. Reaction

The process was carried out by preparing a solution of benzyl chloride in liquid ammonia and a separate solution of potassium amide in liquid ammonia and adding one solution to the other with constant stirring over a period of 10–20 minutes. The solution of potassium amide was prepared by adding pieces of potassium metal to liquid ammonia and adding about 0.1 g. of ferric chloride. The deep blue color characteristic of alkali metals in liquid ammonia disappears after the solution had been allowed to stand and the fading out of the blue color was taken as an indication that all the potassium had

[1]*Manuscript received June 6, 1957.*
Contribution from the Division of Pure Chemistry, National Research Council, Ottawa, Canada.
Issued as N.R.C. No. 4452.
[2]*Department of Chemistry, Carleton University, Ottawa.*
[3]*National Research Council Postdoctorate Fellow. Present address: Department of Mines and Technical Surveys, Ottawa.*

been converted to potassium amide. The solutions were then mixed by means of a good stirring and allowed to stand until the ammonia had evaporated. This usually took overnight since the reaction vessel was a vacuum-jacketted pyrex container. The reaction has been carried out in an open system with a slight positive pressure of ammonia and also in a system that could be evacuated and the reaction carried out under anhydrous conditions using ammonia from a cylinder containing sodium and therefore perfectly dry. The reaction appeared to give similar results by both methods. When the benzyl chloride is added to the solution of potassium amide a deep reddish purple color develops in the liquid and this will persist as long as there is excess of potassium amide. Most of the work was done using an excess of potassium amide of 25% and the purple color was marked at the end of the reaction.

3. Crystallization

The reaction products that had become almost free of ammonia by standing overnight were washed repeatedly with large quantities of water and transferred to a Buchner funnel and washed. The material was dried and dissolved in hot 95% alcohol and filtered while hot. This was set aside to crystallize and the crop of crystals separated, dissolved in fresh alcohol, and again crystallized. The fifth crystallization yielded a product that melted at 149.7° C. (corrected). Since the melting point of stilbene is 124° C. this is obviously a different substance. It is difficult to obtain exact figures for the percentage yield of the higher melting material because it is so hard to separate from stilbene. However, in two batches where careful separations by fractional crystallization were made, the percentages of the dimer obtained were 19.5% and 24.7%, based on the weight of benzyl chloride at the start. These are conservative figures since small losses are inevitable.

4. Characterization

Carbon Hydrogen Analysis

Calculated for $(C_7H_6)_x$	Found
C 93.36	C 93.03, 93.07
H 6.64	H 6.87, 6.68
	C 93.56, 93.49
	H 6.64, 6.72

Molecular Weight Determination

	Found	Calculated
Vapor pressure lowering of isopentane	346, 377 } av. 361±10%	360
Lowering freezing point of benzene	357, 323 } av. 340±10%	360

Under similar conditions a sample of pure stilbene gave a molecular weight in benzene of 178 (theoretical = 180). The conclusion is that our material is a dimer of stilbene. Since the compound shows no evidence of unsaturation it must involve a ring structure and it is concluded that it is 1,2,3,4-tetraphenylcyclobutane. An infrared spectrogram was done on a sample of the material using a solution in carbon disulphide. The characteristic absorption bands for monosubstituted benzene rings showed up in two places (a strong band at 695 $cm.^{-1}$ and four bands between 1700 and 2000 $cm.^{-1}$). There was

evidence of a band consistent with tertiary carbon atoms (2920–2940 cm.$^{-1}$) but this could have been due to secondary carbon atoms. There was no evidence of ethylenic linkages or of methyl groups. The literature does not, so far as we know, contain any information on the absorption bands due to four-membered rings, however everything in the infrared spectrogram was consistent with the material being the compound 1,2,3,4-tetraphenylcyclobutane.

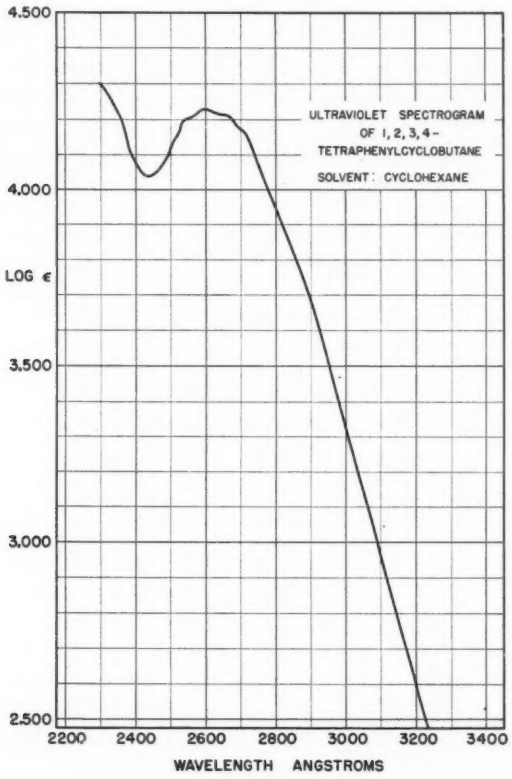

FIG. 1.

Stilbene dimers have been prepared by J. D. Fulton (3) by irradiating stilbamidine (4,4′-diamidinostilbene β-hydroxyethane sulphonate) and two have been found, one melting at 163° C. and another at 149° C. He also prepared the isomer of 1,2,3,4-tetraphenylcyclobutane melting at 163° C. by irradiation of stilbene in benzene solution. The melting point of the distilbene prepared by both methods was the same, 163°, and there was no change in melting point on mixture of the two. Dunitz (1) also showed that the two substances melting at 163° C. were identical by means of X-ray crystallographic analysis. Fulton further showed (3) that the two distilbenes prepared as above showed the same absorption spectra to ultraviolet radiation. His plot of the absorption spectrum for 1,2,3,4-tetraphenylcyclobutane in cyclohexane is very similar to what we have obtained for the material we have produced (see Fig. 1). He found an absorption

band at 2610 Å; our curve also shows an absorption band at 2603 Å. The extinction coefficient that we have found at this maximum of adsorption is 16,900 in cyclohexane. (This is a molar extinction coefficient with concentration in gram moles per liter.) The value seems high when compared with the results of Fulton (3) for his isomer of 1,2,3,4-tetraphenylcyclobutane melting at 163°. The isomer that we believe we have produced is different in melting point and in several other respects and the enhanced absorption at this frequency may be due to a different arrangement of the phenyl groups around the cyclobutane ring, but the significant thing is that the absorption band is in the same position. This leads to the conclusion that we have a compound with similar linkages and of similar structure but since it differs in melting point it is probably a different isomer of 1,2,3,4-tetraphenylcyclobutane. Not only is the melting point different but the X-ray analysis of our product has been found to be different from either of the two isomers previously studied by Fulton and Dunitz (4) and more comprehensively by Dunitz (1). The compound 1,2,3,4-tetraphenylcyclobutane can exist theoretically in four possible isomers (Fig. 2).

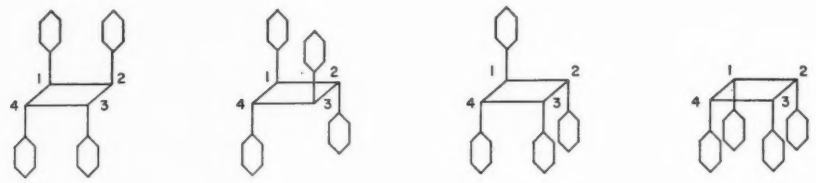

I	II	III	IV
Melting points: 163–164°	149°	?	?

FIG. 2.

The substance represented by formula I has been the subject of a comprehensive X-ray analysis by Dunitz (1). There seems to be no doubt that the isomer melting at 163° has the "chair" structure illustrated; the configuration about 1-2, 3-4 is *cis*-, while about 2-3, 1-4 it is *trans*-. Although no comprehensive study has been made by Dunitz of the isomer melting at 149°, preliminary X-ray examination indicates that it has the structure represented by II above, i.e., with alternate phenyl groups being above and below the cyclobutane ring as one goes round the ring.

Since our isomer was not the same as either I or II as shown by X-ray analysis, the possibilities remaining were III and IV. The structure represented by III seems more probable. This compound is one that has a unique hydrogen atom in the molecule and is therefore particularly suitable for characterization by the method of nuclear magnetic resonance.

Our compound melting at 149° and some material prepared by prolonged irradiation of stilbene in benzene solution to ultraviolet light, purified by recrystallization and melting at 163°, were both examined in 3% benzene solution by the nuclear magnetic resonance method. In the case of our compound melting at 149° there is one band at 3.25 parts per million on the high field side of benzene, with intensity one, and another at 4.0 parts per million at intensity three. The isomer melting at 163° shows a simpler spectrogram with a single band at 2.8 parts per million. These results indicate that our compound melting at 149° is the isomer with three phenyl groups down and one up (III in Fig. 2), since it is

the one isomer with a unique hydrogen atom. In any case, ours can not be the same as the compounds with two up and two down as prepared by Fulton (3).

CONCLUSION

From this study it is concluded that the reaction between benzyl chloride and potassium amide in liquid ammonia yields, in addition to stilbene, fairly substantial amounts of a dimer of stilbene. This dimer is believed to be the isomer of 1,2,3,4-tetraphenylcyclobutane having one phenyl group up and three down with respect to the plane of the cyclobutane ring. This method of preparing this compound is a simple one for producing a compound that is difficult to prepare by any other method.

When a better means of separating the stilbene from the distilbene or a method of analyzing the crude reaction product for distilbene has been found, it is hoped to investigate the optimum conditions for production of distilbene.

ACKNOWLEDGMENTS

The authors wish to express their appreciation to Dr. R. N. Jones and to Mr. R. Lauzon for their help in connection with the infrared spectrogram, and to Dr. W. G. Schneider and Dr. H. J. Bernstein for the examination by the nuclear magnetic resonance method.

REFERENCES

1. DUNITZ, J. D. Acta Cryst. **2**, 1 (1949).
2. FLOOD, E. A. Trans. Roy. Soc. Can. **33**, 180 (1939).
3. FULTON, J. D. Brit. J. Pharmacol. **3**, 75 (1948).
4. FULTON, J. D. and DUNITZ, J. D. Nature, **160**, 161 (1947).
5. HAUSER, C. R., WALLACE, R. B., SKELL, P. S., KANTOR, S. W., and BRODHAG, A. E. J. Am. Chem. Soc. **78**, 1653 (1956).
6. KHARASCH, M. S. and STERNFELD, E. J. Am. Chem. Soc. **61**, 2318 (1939). KHARASCH, M. S., NUDENBERG, W., and STERNFELD, E. J. Am. Chem. Soc. **62**, 2034 (1940). KHARASCH, M. S. and KELIMAN, M. J. Am. Chem. Soc. **65**, 11 (1943). KHARASCH, M. S., NUDENBERG, W., and FIELDS, E. K. J. Am. CHEM. Soc. **66**, 1276 (1944).
7. KHARASCH, M. S., NUDENBERG, W., and FIELDS, E. K. J. Am. Chem. Soc. **66**, 1276 (1944).

THE STRUCTURE OF RHYNCOPHYLLINE[1]

J. C. SEATON[2] AND LÉO MARION

ABSTRACT

It is shown that hydrolysis of rhyncophylline with dilute hydrochloric acid gives rhyncophyllal ($C_{19}H_{24}O_2N_2$), which contains an aldehyde group but no longer contains the methoxyl, the isolated double bond, and the carbomethoxy group originally present in the alkaloid. Rhyncophyllal is reduced by sodium borohydride to the corresponding alcohol, rhyncophyllol, and this is further reduced by lithium aluminum hydride to dihydrodesoxy-rhyncophyllol ($C_{19}H_{28}ON_2$), which shows the properties of an aromatic amine. Reduction of rhyncophyllal by the Wolff-Kishner reaction gives rhyncophyllane ($C_{19}H_{26}ON_2$), which, when dehydrogenated over palladium–charcoal, yields 3,4-diethylpyridine. Direct dehydrogenation of rhyncophyllal produces β-collidine. On the basis of these as well as previously described results a total structure for rhyncophylline is derived.

Rhyncophylline ($C_{22}H_{28}O_4N_2$) is an alkaloid that has been isolated from various species of the rubiaceous genera *Mitragyna* (1, 2) and *Ourouparia* (≡ *Uncaria*) (3). It is a monoacidic tertiary base containing one active hydrogen (Zerewitinow) (2) and two methoxyl groups, one of which is part of a carbomethoxy group (3). When saponified, the alkaloid yields the amorphous amphoteric rhyncophyllic acid ($C_{21}H_{26}O_4N_2$) (2, 3), which is esterified by diazomethane to isorhyncophylline (4). When boiled with acetic anhydride, this isomer is converted to rhyncophylline and its acetyl derivative. Since the acetyl derivative is basic, it must be the neutral nitrogen that is secondary and has been acetylated.

Barger, Dyer, and Sargent (2) distilled rhyncophyllic acid over calcium oxide and obtained a neutral substance, $C_{10}H_9ON$, which they regarded as a methylcarbostyril. This substance has also been obtained from mitraphylline (5) and uncarine-A (6). The product isolated from mitraphylline was readily hydrogenated over palladium to 3-ethyloxindole, and this led to the conclusion that the neutral substance $C_{10}H_9ON$ was 3-vinyloxindole (5). It has been suggested, however, by Wenkert and Reid (7) that the substance might more probably be spiro-3,3-cyclopropyloxindole, and this has been demonstrated to be so by Kondo and Nozoye (8). Hence rhyncophylline must have an oxindole structure.

It has also been suggested that the ultraviolet absorption spectrum of rhyncophylline (λ_{max} 245 mμ, log ε 4.24; 280 mμ, log ε 3.15) resembles that of an oxindole such as gelsemine (λ_{max} 252 mμ, log ε 3.87; 280 mμ, log ε 3.15), and that the enhanced intensity at *ca.* 250 mμ may be due to the effect of the chromophore $CH_3O_2C-\underset{\diagdown}{C}=CHOCH_3$ (9), which is known to be present in corynantheine (10). No chemical evidence had been produced, however, to support this assumption.

We have now obtained evidence which makes it possible to advance a total structure for rhyncophylline. The infrared absorption spectrum of the base in chloroform shows bands at 3415 cm.$^{-1}$ indicative of an NH group, and in nujol mull it contains bands at 1732 and 1708 cm.$^{-1}$ attributable to ester carbonyl and oxindole carbonyl, at 1646 cm.$^{-1}$ probably due to a double bond, and at 1623 and 743 cm.$^{-1}$ attributable to a benzene ring. Hydrogenation of the alkaloid in acetic acid solution, in the presence of perchloric acid and a platinum catalyst, yielded a hexahydro-derivative I (cf. 11). The infrared absorption spectrum of this product lacked the bands at 1623 and 743 cm.$^{-1}$ present in

[1]*Manuscript received June 26, 1957.*
Contribution from the Division of Pure Chemistry, National Research Council, Ottawa, Canada.
Issued as N.R.C. No. 4453.
[2]*National Research Council of Canada Postdoctoral Fellow.*

the spectrum of the alkaloid, thus indicating that the benzene ring had been hydrogenated. The ultraviolet spectrum of hexahydrorhyncophylline still showed intense absorption at 243 mμ and the band at 1646 cm.$^{-1}$ in the infrared was still present. It can be concluded that the double bond in the chromophore, which is the source of the intense absorption in the ultraviolet, is quite resistant to hydrogenation.

Hydrolysis of rhyncophylline with dilute hydrochloric acid gave a crystalline base ($C_{19}H_{24}O_2N_2$) II, which contained no methoxyl group and showed absorption bands in the infrared at 2720 and 1710 cm.$^{-1}$ characteristic of an aldehyde group, besides the split peak due to the oxindole carbonyl. This base, which will be designated rhyncophyllal, gave positive aldehyde reactions with Brady's, Schiff's, and Tollens' reagents. The ultraviolet spectrum of II was almost identical with that of 3,3-dimethyloxindole, and when it was added to the ultraviolet spectrum of hexahydrorhyncophylline I, a spectrum similar to that of rhyncophylline was obtained. The derivation of rhyncophyllal is consistent with the presence in the alkaloid of the grouping $CH_3O_2C—\underset{\diagdown}{C}=CHOCH_3$, since hydrolysis of the ester and enol-ether groups followed by decarboxylation of the resultant β-aldehydocarboxylic acid would give rise to an aldehyde having the empirical formula of rhyncophyllal II. As no absorption occurs at *ca.* 1650 cm.$^{-1}$ in the infrared spectrum of II, the presence of an absorption band in that region of the infrared spectra of the alkaloid and of I must be due to the conjugated enol-ether system. The presence of such a grouping consisting of an enol-ether conjugated with a carbomethoxy group has been established in corynantheine and on hydrolysis this alkaloid gives rise to the aldehyde corynantheal (10).

Reduction of rhyncophyllal II with sodium borohydride gave an alcohol, $C_{19}H_{26}O_2N_2$, which we shall designate rhyncophyllol III, and this was further reduced by lithium aluminum hydride in boiling dioxane to dihydrodesoxy-rhyncophyllol IV ($C_{19}H_{28}ON_2$). This substance, which was also obtained directly from rhyncophyllal by reduction with lithium aluminum hydride, had an infrared spectrum showing no absorption in the carbonyl region, so that the oxindole carbonyl must have been reduced as well as the aldehyde group. 3-Monosubstituted oxindoles form indoles on reduction with lithium aluminum hydride (12) whereas 3,3-disubstituted oxindoles give aromatic amines (13). IV shows all the properties of an aromatic amine and none of an indole. Its ultraviolet absorption spectrum was similar to that of an aromatic amine, both in its shape and in the change that occurred in acid solution. The compound IV coupled with diazotized sulphanilic acid to form an indicator-type dye, whereas rhyncophylline, rhyncophyllal II, and rhyncophyllol IV did not couple. The presence of only one active hydrogen in the alkaloid also suggests a 3,3-disubstituted oxindole since a monosubstituted oxindole contains two active hydrogens (12).

Reduction of rhyncophyllal by the Wolff-Kishner method gave a compound $C_{19}H_{26}ON_2$. This compound, for which the designation rhyncophyllane V is suggested, could not be crystallized, but formed a crystalline picrate. When dehydrogenated with palladium–charcoal, rhyncophyllane produced a good yield of an oil with a pyridine-like odor. The picrate of the oily base melted at 140–141° and was shown by melting point, mixed melting point, and comparison of infrared absorption spectra to be identical with both the picrate of the dehydrogenation product of rotundifoline (2), which has been identified as 3,4-diethylpyridine[3] (11), and with a synthetic sample of 3,4-diethylpyridine picrate. One of the ethyl groups of the dehydrogenation product must have arisen from the

[3]*We are indebted to Dr. B. Witkop for this sample, which he had obtained from Dr. L. J. Sargent.*

reduction of the —CH_2CHO grouping, while the other must have been present as such in the alkaloid.

Palladium–charcoal dehydrogenation of rhyncophyllal II gave a base whose picrate melted at 150°, and proved by comparison with an authentic sample (melting point, mixed melting point, and infrared absorption spectra) to be identical with β-collidine picrate. In rhyncophyllal, therefore, the —CH_2.CHO group must be attached to a piperidine ring in position 4, and consequently the fragment VI must be present in the alkaloid. As well as β-collidine, in the dehydrogenation of rhyncophyllal, there was isolated

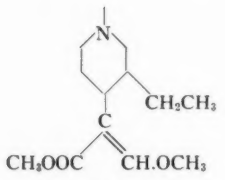

VI

a small quantity of 3-ethyloxindole (identified by comparison with an authentic specimen), which supplied still more evidence of the presence of an oxindole fragment.

The biogenetic derivation of rhyncophylline could be similar to that described by Janot and Goutarel (10) for corynantheine involving dihydroxyphenylalanine, formaldehyde, and tryptophane or their biochemical equivalents. It would differ in that, to obtain rhyncophylline, condensation must take place either in the 3-position of tryptophane, which would later be oxidized in position 2, or in the 3-position of oxindolylalanine. Thus the α-position of the piperidine ring would be linked to the 3-position of the oxindole system giving VII as the structure of the alkaloid.

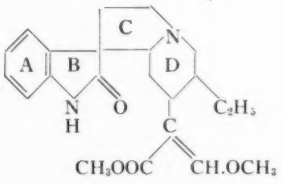

VII

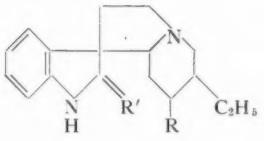

II, R = CH_2CHO R′ = O
III, R = $CH_2.CH_2.OH$ R′ = O
IV, R = CH_2CH_2OH R′ = H_2
V, R = CH_2CH_3 R′ = O

The formation of spiro-3,3-cyclopropyloxindole renders a structure such as VIII possible. Since, however, Kondo and Nozoye (14) have shown that 1-methyl-3-diethylaminoethyloxindole methiodide gives on pyrolysis 1-methyl-spiro-3,3-cyclopropyloxindole, it

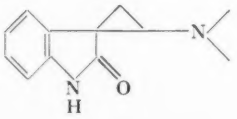

VIII

is not necessary to postulate VIII to explain the formation of the cyclopropyl derivative.

On the basis of structure VII, the structures of the various derivatives derived from rhyncophylline become obvious. Thus rhyncophyllal is represented by formula II, rhyncophyllol by III, dihydrodesoxy-rhyncophyllol by IV, and rhyncophyllane by V. The spirocyclic oxindole and the piperidine ring and its substituents are firmly established chemically. Ring C, however, is derived biogenetically and lacks chemical confirmation.

The reduction of rhyncophylline with lithium aluminum hydride in boiling dioxane gave a complex mixture, but the reaction at 0° produced a base, $C_{21}H_{28}O_3N_2$, which[4] was recovered unchanged from boiling dilute hydrochloric acid. As the infrared absorption spectrum of this base no longer contained the bands at 1735 and 1646 cm.$^{-1}$ present in the spectrum of the alkaloid it is concluded that the carbomethoxy group has been reduced to a primary alcohol and that the double bond has shifted as in formula IX, which is tentatively suggested to represent this base. Further treatment of IX with lithium aluminum hydride gave a fully reduced base which may be X.

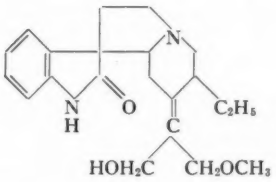

IX

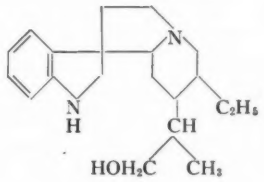

X

Kondo and Nozoye (8) have suggested that uncarine might contain the dihydropyran structure XI, and it is possible that mitraphylline may have the same system. If it be assumed that these alkaloids possess the same 3,3-disubstituted oxindole system as rhyncophylline, then the two alkaloids might well be stereoisomers of the structure XII.

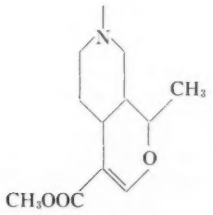

XI

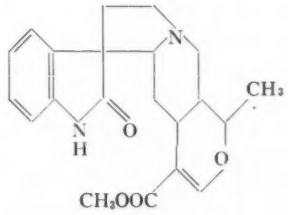

XII

EXPERIMENTAL

The ultraviolet spectra were determined in absolute ethanol, unless otherwise stated, on a Beckman DU spectrophotometer. The infrared absorption spectra were determined on a Perkin–Elmer double beam instrument model 21. The peaks are indicated by a wave number and the percentage absorption (in parentheses). Shoulders are indicated by an S after the wave number. The compounds were dispersed in mulls in nujol unless otherwise mentioned. All melting points were taken on a microscope hot stage and are uncorrected.

[4]*This base was first prepared in this laboratory by Dr. R. Tondeur.*

Hexahydrorhyncophylline (*I*)

Rhyncophylline (164 mg.) was hydrogenated in glacial acetic acid (10 ml.) containing perchloric acid (0.1 ml., 10%) over Adams' catalyst (50 mg.) at 25° C. and 746 mm. Hg; 30.7 ml. of hydrogen were absorbed (calculated for three double bonds 30.3 ml.). The catalyst and solvent were removed and the residue was basified with sodium carbonate solution and extracted with chloroform. The solvent was removed from the dried (Na_2SO_4) extract and the residue crystallized from acetone in colorless prisms (108 mg.) melting at 202–204° C. $[\alpha]_D^{23}$ +27.0° (*c*, 1.08 in ethanol). Calc. for $C_{22}H_{24}O_4N_2$: C, 67.66; H, 8.78; N, 7.17%. Found: C, 67.49; H, 8.90; N, 7.24%. Ultraviolet spectrum: max. at 243 mμ (log ε 4.13); min. at 216 mμ (log ε 3.63). Infrared spectrum: 1705 (91), 1695 S (64), 1650 (50).

Rhyncophyllal (*II*)

Rhyncophylline (260 mg.) was refluxed with 8% hydrochloric acid (50 ml.) for 3 hours. The cooled solution was neutralized with sodium bicarbonate and extracted with ether. The extract was dried (Na_2SO_4) and evaporated leaving the aldehyde, which separated from benzene in fine colorless needles (170 mg.), m.p. 178–179° C. $[\alpha]_D^{23}$ +12.6° (*c*, 2.27 in ethanol). Calc. for $C_{19}H_{24}O_2N_2$: C, 73.04; H, 7.74; N, 8.97%. Found: C, 73.28; H, 7.65; N, 9.00; —OMe, 0.00%.

The aldehyde restored the color to Schiff's reagent and gave a dark precipitate with Tollens' reagent. An amorphous yellow precipitate was formed with Brady's reagent. Ultraviolet spectrum: Shoulder at 280 mμ (log ε 3.18); max. at 252 mμ (log ε 3.89); min. at 228 mμ (log ε 3.52). Infrared spectrum: 2720 (38), 1726 (91), 1710 (79), 1695 S (62), 1625 (54), 735 (51).

The picrate crystallized from ether in pale yellow needles, m.p. 198–199° C. Calc. for $C_{19}H_{24}O_2N_2.C_6H_3O_7N_3$: C, 55.45; H, 5.03. Found: C, 55.28; H, 4.92%.

Rhyncophyllol (*III*)

Sodium borohydride (100 mg.) was added to a solution of rhyncophyllal (100 mg.) in methanol–water (4:1) (5 ml.). After 1 hour at room temperature the solvent was evaporated and the residue extracted with chloroform and the extract was dried (Na_2SO_4) and evaporated. The residue crystallized on cooling and was recrystallized from acetone giving the alcohol III in colorless prisms (87 mg.), m.p. 157° C. $[\alpha]_D^{23}$ +14.0° (*c*, 1.50 in ethanol). Calc. for $C_{19}H_{26}O_2N_2$: C, 72.58; H, 8.34; N, 8.91. Found: C, 72.66; H, 8.13; N, 9.07%. Ultraviolet spectrum: Shoulder at 280 mμ (log ε 3.18); max. at 252 mμ (log ε 3.87); min. at 228 mμ (log ε 3.46). Infrared spectrum: 3250 (64), 1726 (93), 1995 (84), 1625 (64), 745 (62). The picrate crystallized from ethyl acetate in long yellow prisms, m.p. 194–195°. Calc. for $C_{19}H_{26}O_2N_2.C_6H_3O_7N_3$: C, 55.24; H, 5.38. Found: C, 55.5; H, 5.67%.

Dihydrodesoxy-rhyncophyllol (*IV*)

(*a*) Rhyncophyllol (80 mg.) and lithium aluminum hydride (80 mg.) were refluxed in dioxane (10 ml.) in an atmosphere of dry nitrogen for 3 hours. After it was cooled, the excess of lithium aluminum hydride was decomposed with water and the mixture extracted with ether. The extract was washed with water and dried (Na_2SO_4), and the solvent was evaporated leaving the alcohol IV, which crystallized from hexane in long colorless prisms (50 mg.), m.p. 108° C. $[\alpha]_D^{23}$ +92.8° (*c*, 1.73 in ethanol). Calc. for $C_{19}H_{28}ON_2$: C, 75.95; H, 9.39; N, 9.33. Found: C, 76.11; H, 9.29; N, 9.27%.

(*b*) Rhyncophyllal (300 mg.) and lithium aluminum hydride (300 mg.) were refluxed

in dioxane under dry nitrogen for 3 hours. The reaction mixture was worked up as in (*a*) above yielding dihydrodesoxy-rhyncophyllol (150 mg.), m.p. 108° identical with that obtained from rhyncophyllol. Ultraviolet spectrum: max. at 298 mμ (log ε 3.67) and 244 mμ (log ε 4.06); min. at 271 mμ (log ε 3.17) and 224 mμ (log ε 3.75). In normal hydrochloric acid, max. at 262 mμ (log ε 3.4); min. at 235 mμ (log ε 2.67). Infrared spectrum: 3300 (62), 1615 (62), 740 (72).

A few drops of solution of diazotized sulphanilic acid were added to a solution of dihydrodesoxy-rhyncophyllol in hydrochloric acid. A red color formed immediately which became yellow when the solution was made alkaline. The red color returned when acid was added. Neither rhyncophylline, nor rhyncophyllal, nor rhyncophyllol coupled with diazotized sulphanilic acid.

Rhyncophyllane (*V*)

Rhyncophyllal (100 mg.), trimethyleneglycol (2 ml.), and 95% hydrazine (200 mg.) were heated at 150° for 30 minutes. Potassium hydroxide (0.5 g.) was added and the excess of hydrazine evaporated while the temperature was increased to 200°. After 3 hours the mixture was cooled, acidified with dilute hydrochloric acid, and extracted with ether. The aqueous liquid was basified with sodium carbonate, extracted with ether, the extract washed with water and dried (Na_2SO_4). The stiff gum remaining after the solvent had been removed was dissolved in ethanol and a solution of picric acid (100 mg.) in ethanol added. The picrate was collected and recrystallized from ethanol giving yellow needles (80 mg.), m.p. 228–229° decomp. Calc. for $C_{19}H_{26}ON_2.C_6H_3O_7N_3$: C, 56.92; H, 5.54. Found: C, 56.75; H, 5.29%. The base was liberated on a basic resin (Amberlite IRA 400) in methanol and was distilled (air-bath temp. 170–180°) at 0.1 mm. giving a colorless glass (40 mg.). $[\alpha]_D^{23}$ +27.1 (*c*, 3.3 in ethanol). Calc. for $C_{19}H_{26}ON_2$: C, 76.47; H, 8.78; N, 9.39. Found: C, 76.37; H, 8.69; N, 9.67%. Infrared spectrum: 1715 (93), 1626 (63), 750 (61).

Dehydrogenation of Rhyncophyllane

Rhyncophyllane (66 mg.) and palladium–charcoal (80 mg., 30%) were heated under dry nitrogen to 290° during the course of 1 hour. A colorless liquid distillate with a pyridine-like odor was collected and converted into its picrate which crystallized from ethanol in long yellow plates (51 mg.), m.p. 140–141° C., not depressed on admixture with a specimen of 3,4-diethylpyridine picrate obtained by Barger *et al.* (2) from rotundifoline or with a synthetic specimen of 3,4-diethylpyridine picrate. Calc. for $C_9H_{13}N.C_6H_3O_7N_3$: C, 49.45; H, 4.43. Found: C, 49.28; H, 4.27%.

Dehydrogenation of Rhyncophyllal

Rhyncophyllal (75 mg.) and palladium–charcoal (100 mg., 30%) were heated together under dry nitrogen to 290° during the course of 1 hour. The distillate gave two fractions:

(*a*) Boiling below 220° was a colorless liquid with a pyridine-like odor, the picrate of which crystallized from ethanol in yellow plates m.p. 150°, not depressed on admixture with an authentic specimen of β-collidine picrate. Calc. for $C_8H_{11}N.C_6H_3O_7N_3$: C, 48.0; H, 4.03. Found: C, 48.18; H. 3.92%.

The infrared spectrum was identical with that of β-collidine picrate.

(*b*) Boiling higher than 220° was a fraction which crystallized on cooling and recrystallized from hexane in colorless prisms with m.p. 101° not depressed on admixture with an authentic specimen of 3-ethyloxindole. The X-ray powder photograph was identical with that of the synthetic specimen.

Reduction of Rhyncophylline with Lithium Aluminum Hydride at 0° C. (Compound IX)

A solution of rhyncophylline (400 mg.) and lithium aluminum hydride (375 mg.) in tetrahydrofuran (50 cc.) was allowed to stand at 0° for 4 hours. Water (3 ml.) was added and the precipitate filtered off and washed with ether. The combined washings and filtrate were dried (Na_2SO_4), the solvent evaporated, and the crystalline residue was recrystallized from acetone to give IX as colorless prisms (124 mg.), m.p. 189°. $[\alpha]_D^{23}$ +5° (*c*, 1.2 in ethanol). Calc. for $C_{21}H_{28}O_3N_2$: C, 70.76; H, 7.92; N, 7.86. Found: C, 70.93; H, 7.65; N, 8.00%. Ultraviolet spectrum: Shoulder at 280 mμ (log ε 3.18); max. at 252 mμ (log ε 3.87); min. at 228 mμ (log ε 3.46). Infrared spectrum: 3060 (44), 1735 (92), 1710 (85), 1625 (55), 745 (71). In chloroform: 3410 (40), 3180 (23), 1725 (97), 1625 (73).

Acid Hydrolysis of IX

XI (30 mg.) was refluxed with 10% hydrochloric acid (10 ml.) for 4 hours. After it was cooled, the solution was basified with sodium carbonate, extracted with chloroform, and the extract dried (Na_2SO_4). Removal of the solvent yielded a crystalline residue, which, when recrystallized from acetone, gave colorless prisms (20 mg.), m.p. 189° not depressed on admixture with IX.

Reduction of IX with Lithium Aluminum Hydride (Compound X)

IX (50 mg.) and lithium aluminum hydride (50 mg.) were refluxed in boiling dioxane (10 ml.) under dry nitrogen for 3 hours. After it was cooled, the mixture was decomposed with water and extracted with ether. The extract was washed with water and dried (Na_2SO_4) and the solvent removed. The residue crystallized from ether in long colorless prisms (20 mg.), m.p. 174°. Calc. for $C_{20}H_{30}ON_2$: C, 76.39; H, 9.62; N, 8.91. Found: C, 76.37; H, 9.56; N, 8.95%. Ultraviolet spectrum: max. at 296 mμ (log ε 3.56) and 244 mμ (log ε 3.95); min. at 270 mμ (log ε 3.03) and 225 mμ (log ε 3.6). Infrared spectrum: 3480 (36), 3180 (51), 1615 (53), 735 (60).

ACKNOWLEDGMENT

We wish to thank Dr. R. N. Jones and Mr. R. Lauzon of these laboratories for obtaining the infrared absorption spectra.

REFERENCES

1. Raymond-Hamet and Millat, L. Compt. rend. **199**, 587 (1934).
2. Barger, G., Dyer, E., and Sargent, L. J. J. Org. Chem. **4**, 418 (1939).
3. Kondo, H., Tukuda, T., and Tomita, M. J. Pharm. Soc. Japan, **48**, 321 (1928).
4. Kondo, H. and Ikeda, T. J. Pharm. Soc. Japan, **57**, 881 (1937).
5. Cook, J. W., Gailey, R. M., and Loudon, J. D. Chemistry and Industry, 640 (1953).
6. Ikeda, T. J. Pharm. Soc. Japan, **63**, 393 (1943); Chem. Abstr. **44**, 7332 (1950).
7. Wenkert, E. and Reid, T. L. Chemistry and Industry, 1390 (1953).
8. Kondo, H., Nozoye, T., and Tsukamoto, H. Ann. Report ITSUU Lab. Tokyo, **6**, 53 (1955).
9. Kondo, H. and Nozoye, T. Ann. Report ITSUU Lab. Tokyo, **7**, 49 (1956).
10. Janot, M. M. and Goutarel, R. Bull. soc. chim. France [5], **18**, 588 (1951).
11. Badger, G. M., Cook, J. W., and Ongley, P. A. J. Chem. Soc. 867 (1950).
12. Julian, P. L. and Printz, H. C. J. Am. Chem. Soc. **71**, 3206 (1949).
13. Kates, M. and Marion, L. Can. J. Chem. **29**, 37 (1951).
14. Kondo, H. and Nozoye, T. Ann. Report ITSUU Lab. Tokyo, **7**, 44 (1956).

AMIDOMYCIN, A NEW ANTIBIOTIC FROM A STREPTOMYCES SPECIES, CHEMICAL STRUCTURE[1]

L. C. VINING AND W. A. TABER

ABSTRACT

Amidomycin, an antibiotic active primarily against yeast, has been isolated from a *Streptomyces* species. The Compound $C_{40}H_{68}O_{12}N_4$ is neutral, optically active, and shows no unsaturation nor characteristic light absorption maxima. It is composed of 4 moles each of D(−)-valine and D(−)-α-hydroxyisovaleric acid, linked alternately by ester and amide bonds to form a 24-membered ring (I). This structure is assigned from the following observations: on mild alkaline hydrolysis 4 moles of alkali are consumed with formation of a hydroxy acid, $C_{10}H_{19}O_4N$ (II). The latter on distillation gave a crystalline lactone, $C_{10}H_{17}O_3N$, considered to be 3,6-diisopropyl-2,5-diketomorpholine (III), which was hydrolyzed to give 1 mole each of D(−)-valine and D(−)-α-hydroxyisovaleric acid.

Amidomycin is closely related to valinomycin, an antibiotic isolated from *Streptomyces fulvissimus* and shown to be a 24-membered ring compound containing D(−)-valine, D(−)-α-hydroxyisovaleric acid, L(+)-valine, and L(−)-lactic acid. It also resembles the enniatins, produced by certain species of *Fusarium*, but differs from these compounds in the number of units in the ring structure as well as in containing D(−)-valine rather than an N-methyl-L-amino acid.

Amidomycin was isolated from an unidentified *Streptomyces* species (PRL 1642) grown in a soybean meal – cerelose medium. Details of its production, isolation, and biological properties, and a description of the organism are reported in a separate publication (9). The range of antibiotic activity was found to be limited principally to certain yeasts, although germination of the uredospores of wheat stem rust (race 15B) was inhibited at concentrations as low as 0.5 μg. per ml.

Isolation of the active substance was achieved by solvent extraction procedures and colorless needles, m.p. 192° C., were obtained after repeated crystallization from aqueous ethanol or petrol (b.p. 60–80° C.). Examination of this material by paper chromatography in several solvent systems showed the presence of only a single active zone when *Candida albicans* was used as the test organism.

The antibiotic is a stable, neutral compound, readily soluble in most organic solvents, slightly soluble in cold petrol, and insoluble in water. It is optically active and analyses and molecular weight determinations indicated the formula $C_{40}H_{68}O_{12}N_4$. It shows no characteristic absorption maxima in the ultraviolet or visible regions of the spectrum and does not take up hydrogen in the presence of Adams catalyst. The infrared absorption spectrum is shown in Fig. 1A. The band at 1740 cm.$^{-1}$ is assigned to an ester carbonyl; bands at 1650 and 1540 cm.$^{-1}$ to amide I and amide II bands respectively, and at 3300 cm.$^{-1}$ to the NH group of an amide. Isopropyl groups can be recognized by the presence of two peaks at 1395 and 1375 cm.$^{-1}$.

The compound was unchanged by treatment normally used for acid hydrolysis of polypeptides, probably because of poor solubility. After a preliminary hydrolysis in alcoholic acid or alkali and subsequent treatment with concentrated hydrochloric acid, however, amidomycin was completely degraded. Paper chromatography of the product showed only two substances to be present and these were tentatively identified by comparison of R_f values with authentic samples as valine and α-hydroxyisovaleric acid. Methanolic sodium hydroxide under mild conditions hydrolyzed the ester bonds with

[1]*Manuscript received in original form April 18, 1957, and, as revised, June 17, 1957.*
Contribution from the National Research Council of Canada, Prairie Regional Laboratory, Saskatoon, Saskatchewan.
Issued as paper No. 4449.

the consumption of 4 moles of alkali per mole of amidomycin. The product, after acidification, could not be crystallized. Esterification with diazomethane yielded a methyl ester, $C_{11}H_{21}O_4N$, purified by distillation *in vacuo* in an over-all yield of 1.74 moles/mole of amidomycin. The infrared absorption spectrum of this product (Fig. 1B) retained the amide I and amide II bands at 1660 and 1525 cm.$^{-1}$ respectively as well as the isopropyl bands (1395 and 1375 cm.$^{-1}$). In addition a band due to ester carbonyl (1740 cm.$^{-1}$) and a

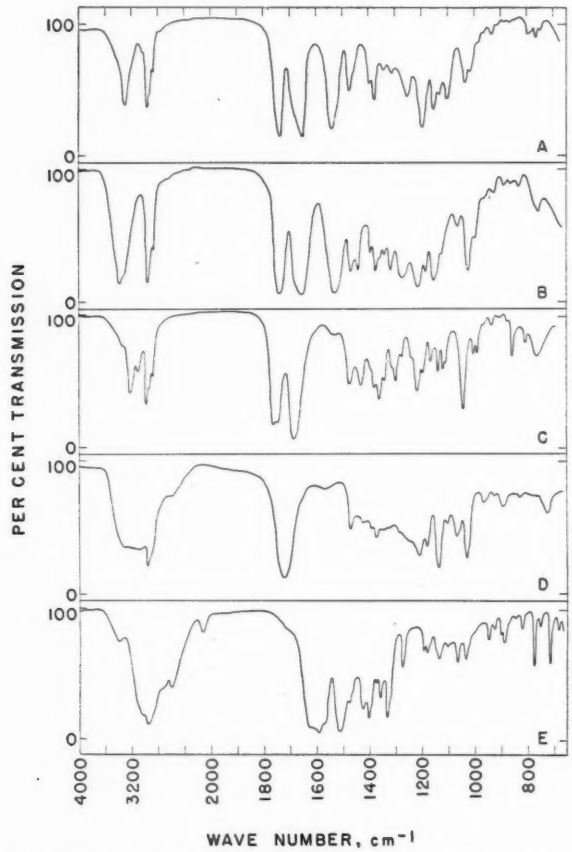

FIG. 1. Infrared spectra of amidomycin and its degradation products (pressed potassium bromide pellet). A—amidomycin; B—D(−)-α-hydroxyisovaleryl-D(−)-valine methyl ester; C—3,6-diisopropyl-2,5-diketomorpholine; D—D(−)-α-hydroxyisovaleric acid; E—D(−)-valine.

broad band centered around 3400 cm.$^{-1}$, which is a result of the combination of NH and OH vibrations, may be recognized. The existence of a free hydroxyl group was confirmed by the preparation of an α-naphthylurethane derivative. An attempt to purify the free hydroxy acid by distillation in high vacuum resulted in the loss of 1 mole of water and formation of a new product, $C_{10}H_{17}O_3N$, which was sublimed and collected as colorless needles, m.p. 153–154° C. Examination of the infrared absorption spectrum confirmed that lactonization of the hydroxy acid had taken place (band at 1760–1740 cm.$^{-1}$) and the appearance of the carbonyl band at 1680 cm.$^{-1}$ and NH band at 3220 cm.$^{-1}$,

which is indicative of a lactam grouping, was consistent with the formation of a ring compound (Fig. 1C).

The lactone, when subjected to vigorous acid hydrolysis, yielded approximately 1 mole each of a mixture of two acids. One of these, extracted from the hydrolyzate with ether and purified by high vacuum sublimation, was a water soluble, crystalline, optically-active substance, m.p. 67–68° C. Analyses and neutralization equivalent determinations indicating a formula $C_5H_{10}O_3$, the positive test for an α-hydroxy acid given with ferric chloride, and the presence of bands at 1390 and 1373 cm.$^{-1}$, characteristic of isopropyl groups in the infrared absorption spectrum (Fig. 1D), suggested that it might be D(−)-α-hydroxyisovaleric acid. This was confirmed by comparison with an authentic sample prepared from D(−)-valine by the method of Fischer and Scheibler (6). The *p*-phenylphenacyl esters of the two samples were also identical.

The aqueous acid hydrolyzate, after removal of the hydroxy acid by extraction with ether, was evaporated to dryness and examined by paper chromatography in a number of solvent systems. A single ninhydrin positive substance was found to be present, corresponding in R_f value with valine. The free amino acid was precipitated from an ethanolic solution of the hydrochloride by neutralization with ammonia and recrystallized from aqueous ethanol. Its optical rotation, melting point, infrared absorption spectrum (Fig. 1E) were identical with those of D(−)-valine. The 2,4-dinitrophenyl derivatives of the two samples were also identical.

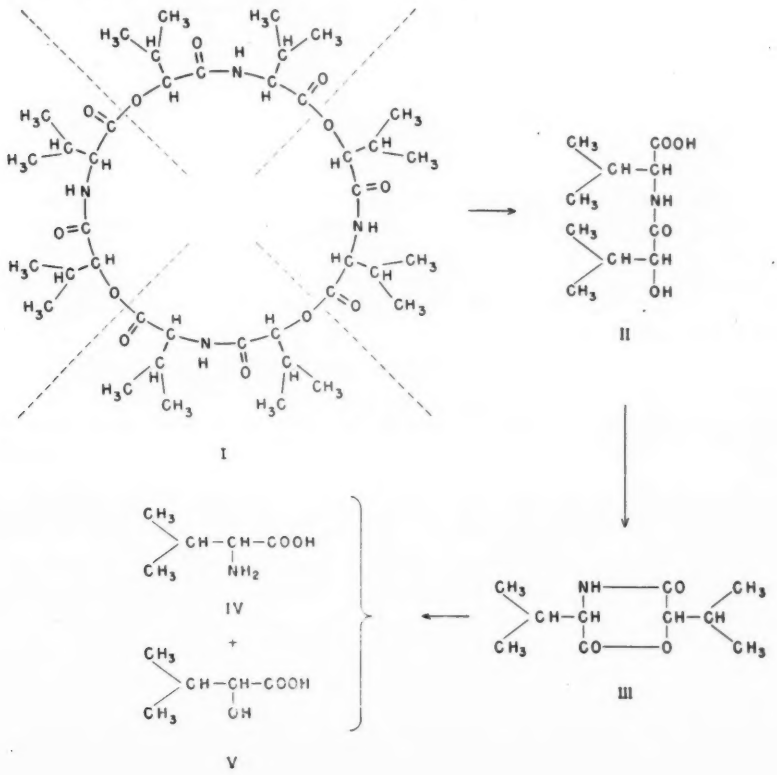

These results are consistent with the cyclic structure I, for amidomycin, in which 4 moles each of D(−)-α-hydroxyisovaleric acid and D(−)-valine are linked alternately by ester and amide bonds. Alkaline hydrolysis results in a selective cleavage of the four ester bonds to give 4 moles of the hydroxy acid, II, which lactonizes on heating to III. Acid hydrolysis of the lactone yields 1 mole each of D(−)-α-hydroxyisovaleric acid (V) and D(−)-valine (IV).

Brockmann and Geeren (1) have recently reported the isolation from *Streptomyces fulvissimus* of an antibacterial antibiotic valinomycin with an analogous structure (IX). Whereas in amidomycin the basic unit D-α-hydroxyisovaleryl-D-valine is repeated four times in the ring, valinomycin is believed to contain only two units of D-α-hydroxyisovaleryl-D-valine, separated from each other in the cyclic chain by two units of a second type, L-lactyl-L-valine. The relationship between the two antibiotics is apparent, and it now seems likely that other structures of the same general type will be found among the products of *Streptomyces* metabolism.

The isolation from *Streptomyces* species of substances with these structures is also of interest in view of the production by certain species of *Fusarium* of the closely related enniatins (VI, VII, VIII). These have been shown by Plattner and Nager (7) to be 12-

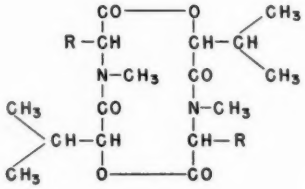

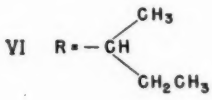

VI

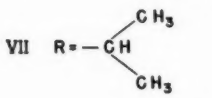

VII

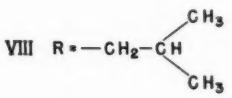

VIII

membered cyclic molecules containing 2 moles of D(−)-α-hydroxyisovaleric acid together with 2 moles of a N-methyl-L(+)-amino acid. In enniatin A, the latter is N-methyl-L(+)- isoleucine; enniatin B contains N-methyl-L(+)- valine, and the presence of a third compound, enniatin C, containing N-methyl-L(+)- leucine was suggested by their results. The strains of *Fusarium* that were used always produced mixtures of these three antibiotics, but the relative proportions of each varied considerably for different strains. Separation of the enniatin mixtures was difficult to achieve except in those instances where one component was produced in overwhelming proportion, and this fact may have been responsible for the isolation by Cook and co-workers (3) from several *Fusarium* species of a series of such compounds which differed somewhat in melting point, analyses, and optical rotation, but gave rise to the same degradation products. Plattner and Nager

(7) have examined one of these products and found in the acid hydrolyzate four ninhydrin reacting compounds, three of which were identical with those in the different enniatins.

The formation by two taxonomically distinct organisms, *Streptomyces* and *Fusarium*, of compounds with such a close structural relationship suggests that compounds of this type are common products of microorganisms, and may be of some importance in their metabolism.

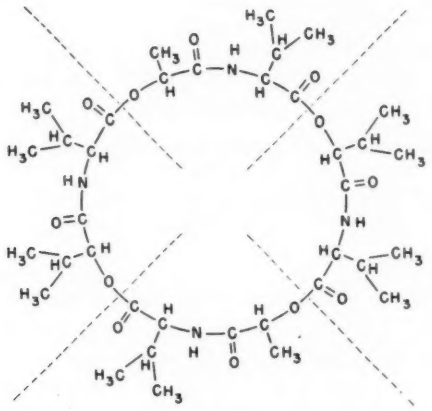

IX

EXPERIMENTAL

Amidomycin

Amidomycin was obtained pure by repeated crystallization from aqueous ethanol or petrol as colorless needles, m.p. 192° C. $[\alpha]_D^{26°}$ +19.2° (c = 1.2 in ethanol). Calculated for $C_{40}H_{68}O_{12}N_4$: C, 60.28; H, 8.60; N, 7.03; 6C-Me, 32.4%; mol. wt., 797. Found in samples dried at 25° C. over phosphorus pentoxide for 72 hours *in vacuo*: C, 59.86, 60.57; H, 8.59, 8.65; N, 7.05, 7.07; C-Me, 31.7%. The molecular weight was determined by the Rast method in camphor. Found: 812, 799, 787. By isothermal distillation in acetone (2) values of 765 and 792 were obtained.

A sample in ethanol was treated with hydrogen under atmospheric pressure at room temperature using Adams catalyst. No uptake of hydrogen was observed over a period of 2 hours.

Acid Hydrolysis of Amidomycin

A sample (109 mg.) was heated at 100° C. in a sealed tube with 20% (w/v) HCl (5 ml.) for 5 days. The undissolved material was filtered off, washed with water, and dried (98 mg.), m.p. 192° C., undepressed on admixture with amidomycin. The filtrate gave a negative ninhydrin test.

A second sample heated in concentrated HCl at 130° C. for 24 hours was also recovered unchanged.

A sample (10 mg.) was heated under reflux in a mixture of ethanol (2.5 ml.) and 20% (w/v) HCl (1 ml.) for 24 hours. The solution was evaporated to dryness *in vacuo*, transferred to a sealed tube, and heated for a further 24 hours at 100° C. with 20% (w/v) HCl. After again being evaporated to dryness *in vacuo*, the product was redissolved in

water (1 ml.) and paper chromatographed by the circular method using as the solvent system a mixture of *t*-butanol, ammonia (*d*, 0.880), and water (20:1:4). When developed with a 2,6-dichlorobenzenoneindophenol indicator spray a single pink zone appeared at R_f 0.56 identical with that of an authentic sample of α-hydroxyisovaleric acid. When ninhydrin was used and the treated paper heated briefly to 100–120° two zones appeared. The first, a dark blue zone at R_f 0.56, again corresponded to α-hydroxyisovaleric acid. The second, a purple zone at R_f 0.42, was found to be indistinguishable from that of an authentic sample of valine.

Alkaline Hydrolysis of Amidomycin

Amidomycin (26.5 mg.) was dissolved in 0.02 *N* 80% (v/v) aqueous methanolic NaOH (25 ml.) at 40° C. Aliquots (5 ml.) were removed at intervals and titrated potentiometrically against 0.1 *N* HCl. The results are given below:

Time (hours)	1½	3½	6	12
Moles of NaOH consumed per mole amidomycin	3.80	4.34	4.52	4.84

A larger sample (200 mg.) was then treated with 0.02 *N* 80% (v/v) aqueous methanolic NaOH (200 ml.) at 40° C. After 3 hours the solution was diluted with an equal volume of water, concentrated *in vacuo* at 40° C. to half volume, and extracted twice with ether (50 ml.). It was then acidified with *N* HCl (5 ml.) and re-extracted three times with ether (50 ml.). The acid–ether extracts were combined, dried over $MgSO_4$, and evaporated to dryness *in vacuo*.

The residual gum was strongly acidic (effervescence with $NaHCO_3$). It could not be induced to crystallize.

Methyl Ester of Alkaline Degradation Product

The product obtained above was redissolved in ether (25 ml.) and treated with an excess of ethereal diazomethane (25 ml., containing approximately 5 moles). After 2 hours at 4° C., the ether was removed *in vacuo* and the residual oil distilled at 10^{-2} mm. It was obtained as a single fraction at a block temperature of 60–70° C. and was a colorless viscous oil (201 mg., over-all yield = 1.74%) $[\alpha]_D^{25°}+24°$ (c = 1.38 in chloroform). Calculated for $C_{11}H_{21}O_4N$: C, 57.12; H, 9.15; N, 6.57%; mol. wt., 231.3. Found: C, 57.10; H, 9.08; N, 6.55%; mol. wt. (by isothermal distillation in acetone), 244.

The infrared absorption spectrum is shown in Fig. 1B.

α-Naphthylurethane Derivative

The methyl ester obtained above (66 mg.) was heated for 10 minutes on a steam bath with α-naphthylisocyanate (50 mg.). The product was crystallized twice from aqueous ethanol, then twice from petrol (b.p. 60–80° C.) to give colorless needles, m.p. 142° C. $[\alpha]_D^{25°}$ +5.8° (c = 0.35 in ethanol). Calculated for $C_{22}H_{28}O_5N_2$: C, 65.98; H, 7.05; N, 7.00%. Found in a sample dried over phosphorus pentoxide for 24 hours at 25° C.: C, 65.79; H, 7.02; N, 6.97%.

Lactonization of Alkaline Degradation Product

The product obtained from alkaline hydrolysis of amidomycin (234 mg.) under the conditions described above was heated at 10^{-2} mm. At a block temperature of 75° C., a crystalline sublimate began to form, and sublimation continued for 8 hours, during which the block temperature rose to 110° C. The product (224 mg., over-all yield = 96%),

m.p. 153–154° C. $[\alpha]_D^{25°}$ +116.9° (c = 0.74 in ethanol), was recrystallized from an ether–petrol mixture as colorless needles, unchanged in melting point and rotation. Calculated for $C_{10}H_{17}O_3N$: C, 60.28; H, 8.60; N, 7.03%; mol. wt., 199.2. Found in a freshly sublimed sample: C, 60.36; H, 8.65; N, 7.06%; mol. wt. (by isothermal distillation in acetone), 212.

The infrared absorption spectrum is shown in Fig. 1C.

Acid Hydrolysis of Lactone

(*a*) *Isolation and Identification of* D(−)-*α-Hydroxyisovaleric Acid*

The lactone (100 mg.) was heated at 100° C. in a sealed tube for 16 hours with 20% (w/v) HCl (5 ml.). The solution was diluted with 3 volumes of water and extracted four times with an equal volume of ether. The ether extracts were combined, dried over anhydrous $MgSO_4$, and evaporated to dryness. The residue was distilled at 10^{-2} mm. and a block temperature of 60° C. A single fraction was collected (49 mg. = 83% yield), which crystallized on standing as colorless needles, m.p. 64–67° C., raised to 67–68° C. after two further sublimations. The pure substance had $[\alpha]_D^{25°}$ −19.1° (c = 0.89 in chloroform), was water soluble, and gave a yellow color with dilute ferric chloride solution. Calculated for $C_5H_{10}O_3$: C, 50.83; H, 8.53%; neutralization equivalent, 118.1. Found in a freshly distilled sample: C, 50.99; H, 8.51%; neutralization equivalent by potentiometric titration with NaOH, 116.

A sample of D(−)-α-hydroxyisovaleric acid was prepared from D(−)-valine by deamination with nitrous acid (6) and purified by repeated sublimation, m.p. 67–68° C., undepressed on admixture with a sample of the hydroxy acid from amidomycin. The optical rotation, $[\alpha]_D^{25°}$ −19.3° (c = 0.90 in chloroform), and infrared absorption spectra (Fig. 1D) of the two samples were identical.

Preparation of p-phenylphenacyl esters.—The *p*-phenylphenacyl ester of the natural α-hydroxy acid was prepared according to the method described by Drake and Bronitsky (4). It was repeatedly crystallized from 50% aqueous ethanol to constant m.p. 109–110.5° C. The melting point was not depressed on admixture with a sample of the *p*-phenylphenacyl ester of authentic D(−)-α-hydroxyisovaleric acid prepared in a similar manner. Calculated for $C_{19}H_{20}O_4$: C, 73.06; H, 6.45%. Found in a sample dried over phosphorus pentoxide for 18 hours at 25° C. and 10^{-2} mm.: C, 73.34; H, 6.46%.

(*b*) *Isolation and Identification of* D(−)-*Valine*

The aqueous acid hydrolyzate, after extraction with ether, was evaporated to dryness *in vacuo* then three times successively redissolved in water and re-evaporated. The residue was dissolved in ethanol (25 cc.) and treated with concentrated NH_4OH until slightly alkaline. After 12 hours ot 0° C., the crystalline precipitate was collected and washed thoroughly with warm ethanol (48 mg. = 83% yield). It was recrystallized from aqueous ethanol to constant m.p. (sealed tube) 293–294° C. (decomp.); $[\alpha]_D^{25°}$ +30° (c = 1.2 in 6 *N* hydrochloric acid). Calculated for $C_5H_{11}O_2N$: C, 51.25; H, 9.46; N, 11.84%. Found in a sample dried over phosphorus pentoxide for 48 hours at 80° C. and 10^{-2} mm.: C, 51.32; H, 9.45; N, 11.90%.

A sample of D(−)-valine was prepared by resolution of DL-valine (5), m.p. (sealed tube) 293° C. (decomp.), undepressed with the amino acid from amidomycin. The optical rotation and infrared absorption spectra (Fig. 1E) of the two samples were also identical.

A sample of the hydrolyzate was examined by paper chromatography in the solvent systems: *sec*-butanol (3) 0.3% aqueous ammonia (1); water-saturated phenol; water-saturated benzyl alcohol. The chromatogram after development with ninhydrin always showed only a single purple spot with an R_f value identical with that of authentic valine.

Preparation of 2,4-dinitrophenyl derivative.—A 2,4-dinitrophenyl derivative of the amino acid from amidomycin was prepared by the method of Sanger (8). Yellow needles, m.p. 134–135° C., after repeated crystallization from ether–petrol (b.p. 60–80° C.), were obtained. Calculated for $C_{11}H_{13}O_6N_3$: C, 46.65; H, 4.62; N, 14.84%. Found in a sample dried at 80° C. for 48 hours over phosphorus pentoxide at 10^{-2} mm.: C, 46.66; H, 4.67; N, 14.78%.

2,4-Dinitrophenyl-D(−)-valine prepared similarly had a m.p. 136° C. A mixture of the two derivatives melted at 134–135° C.

ACKNOWLEDGMENTS

The authors wish to express their gratitude to Mr. J. A. Baignee for the analyses, Miss A. Epp for the infrared spectra, and Miss M. J. A. Gates for valuable technical assistance.

REFERENCES

1. BROCKMAN, H. and GEEREN, H. Ann. **603**, 216 (1957).
2. CHILDS, C. E. Anal. Chem. **26**, 1963 (1954).
3. COOK, A. H., COX, S. F., and FARMER, T. H. J. Chem. Soc. 1022 (1949).
4. DRAKE, N. L. and BRONITSKY, J. J. Am. Chem. Soc. **52**, 3715 (1930).
5. FISCHER, E. Chem. Ber. **39**, 2320 (1906).
6. FISCHER, E. and SCHEIBLER, H. Chem. Ber. **41**, 2894 (1908).
7. PLATTNER, P. A. and NAGER, U. Helv. Chim. Acta, **31**, 665, 2192, 2203 (1948).
8. SANGER, F. Biochem. J. **394**, 507 (1945).
9. TABER, W. A. and VINING, L. C. To be published.

VAPOR ABSORPTION SPECTRA AND OSCILLATOR STRENGTHS OF NAPHTHALENE, ANTHRACENE, AND PYRENE[1]

J. FERGUSON,[2] L. W. REEVES,[3] AND W. G. SCHNEIDER

ABSTRACT

Vapor absorption spectra have been measured for naphthalene, anthracene, and pyrene using a modified Beckman DU Spectrometer. Vapor concentrations were determined using published vapor pressure data, and oscillator strengths were computed for a total of five transitions in the three molecules. It was found that the vapor oscillator strengths are considerably lower than in solution by a factor greater than that predicted by classical theory. An absorption region at about 41,000 cm.$^{-1}$ in anthracene is tentatively assigned as the $^1B_{2u}{}^+$ state calculated by Pariser to lie at 42,400 cm.$^{-1}$.

INTRODUCTION

Although the electronic energy levels of aromatic molecules have been studied rather extensively both experimentally and theoretically, data relating to absorption intensities in the vapor are lacking. Nearly all measurements of absorption intensity have been made in solution and it is assumed that in every case the solvent modifies this intensity only slightly so that theoretical intensities can be compared with solution intensities directly, at least for allowed transitions. This assumption is derived from the classical theory of Chako (5) and is substantiated by the work of Almasy and Laemmel (1) on diphenyl. However, it was felt that this assumption should be investigated by a measurement of the vapor absorption spectra of a number of aromatic compounds of interest. We have therefore investigated the absorption spectra of naphthalene, anthracene, and pyrene and used published vapor pressure data to determine the vapor concentrations; finally calculating the oscillator strengths of a total of five electronic transitions in these molecules. Information about the intensity of distribution throughout each band system which is of theoretical interest (2) was also obtained.

EXPERIMENTAL

Research grade anthracene, naphthalene, and pyrene were further purified by chromatography using the method of Sangster (14). The spectra were taken in a silica cell, length 20 cm., containing a small quantity (a few milligrams) of the purified crystals. The cell was first pumped out to a residual pressure of 10^{-6} mm. Hg, then a small amount of argon was admitted (approximately $\frac{1}{2}$ cm. Hg) before the sidearm of the cell was sealed off. This added argon enabled thermal equilibrium to be achieved more quickly.

The sealed cell was mounted rigidly in a small air thermostat fitted with appropriate silica windows. A heating element covering most of the floor of the thermostat was used and with the aid of natural convection within the lagged space a temperature variation of $\pm 0.3°$ C. could be achieved by using a contact thermometer and relay box. This temperature was measured in contact with the cell by means of a mercury in glass thermometer. No condensation on the windows was detected when the cell was cooled from the highest to the lowest temperature used in any experiment. Spectra were taken after 20 minutes at the chosen temperature. The spectra of anthracene were reproduced with different loadings of the cell.

[1]*Manuscript received May 9, 1957.*
Contribution from the Division of Pure Chemistry, National Research Council, Ottawa, Canada.
Issued as N.R.C. No. 4458.
[2]*N.R.C. Postdoctorate Fellow, now at Chemistry Department, University of British Columbia, Vancouver, B.C.*
[3]*N.R.C. Postdoctorate Fellow, now at Mellon Institute, University of Pittsburgh, Pa.*

The absorption spectra were measured with a modified Beckman DU Spectrophotometer made semiautomatic by use of a constant speed motor, a Photovolt Photometer No. 520M, and a Varian G10 recorder, details of which will be published at a later date. Recorder tracings of the light transmission at each temperature were compared with tracings of the blank cell in order to compute optical densities. For anthracene and pyrene these blank runs were taken with the cell at room temperature where the vapor pressures are too low to record absorption by these compounds. The blank determinations for the naphthalene spectrum were obtained by carefully removing, cleaning, and replacing the cell without changing the optical arrangement. The stability of the light source, a xenon high pressure a-c. arc (Osram XBO-162), was checked by taking a number of blank runs before and after the absorption spectra were recorded.

RESULTS

Fig. 1 shows the vapor absorption spectrum of naphthalene in the region of the second transition. The extinction coefficients have been computed with the vapor pressure data of Bradley and Cleasby (4) (extrapolated) and Sears and Hopke (15), for the temperature 313° K., where the two sets of data agree. The oscillator strength was computed from the well-known relation

$$f = 4.31 \times 10^{-9} \int \epsilon \, d\bar{\nu}.$$

When f is oscillator strength, ϵ is molar extinction coefficient, and $\bar{\nu}$ is frequency in cm.$^{-1}$.

Table IA contains this quantity computed from two sets of vapor pressure data.

Fig. 2 shows the vapor absorption spectrum of anthracene in the region of the first transition where extinction coefficients have been computed from the vapor pressure data of Sears and Hopke, and in Table IB the oscillator strength of this transition is calculated from three sets of vapor pressure data. Similarly Fig. 3 shows the extinction coefficient of the second transition in this compound from the vapor data of Sears and Hopke; the variation of the oscillator strength with the same vapor pressure data used above is shown in Table IC.

Fig. 4 shows the vapor absorption spectrum of pyrene in the region of the second transition (pyrene has a weaker absorption region lying at slightly longer wavelengths) and Table ID contains the oscillator strength of this transition computed from the data of Bradley and Cleasby. Fig. 5 shows most of the absorption spectrum of the third transition and Table IE contains the oscillator strength computed up to the cutoff in Fig. 5 from the vapor pressure data of Bradley and Cleasby.

Table II summarizes the values of the oscillator strengths in the vapor and also compares them with solution values computed from absorption spectra kindly provided by Dr. R. N. Jones.*

DISCUSSION

The computation of the oscillator strength in each of the absorption transitions depends critically on the published vapor pressure data. The various studies of the vapor pressure of naphthalene show marked discrepancies in the range of our measurements (25–40° C.). The measurements of Sears and Hopke (14) made in our range agree (within 6%) with those of two other determinations (17, 3). In spite of the fact that there seems to be some curvature in the Antoine equation near 20° C. in all of these results, we feel that they have the advantage of applying directly to our range of temperatures. The extrapolated results of Bradley and Cleasby (4) are lower, and while they might be less suspect from

J. Am. Chem. Soc. **67**, 2127 (1945); *Can. J. Chem.* **34**, 1017 (1956). *We are indebted to Dr. Jones for loaning us the originals.*

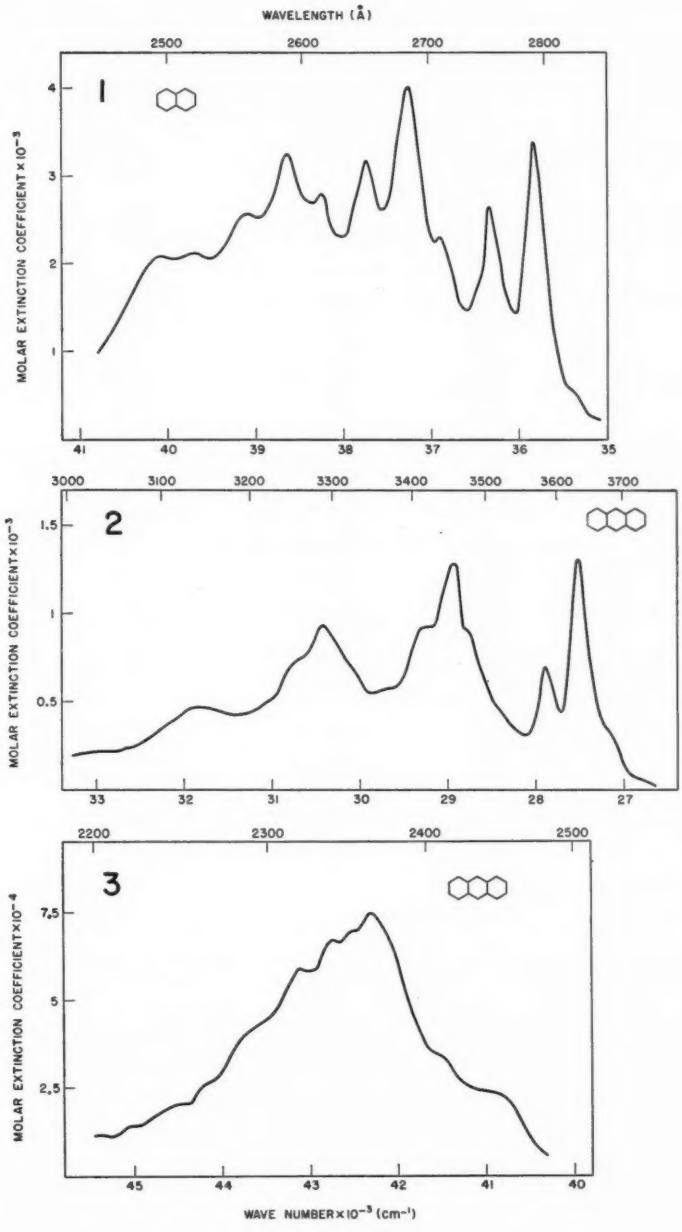

FIG. 1. Naphthalene absorption spectrum, second transition.
FIG. 2. Anthracene absorption spectrum, first transition.
FIG. 3. Anthracene absorption spectrum, second transition.

TABLE I

TEMPERATURE, CONCENTRATION, AND OSCILLATOR STRENGTH

Source of vapor pressure data	Temperature, $T°$ K.	Concentration, moles/liter	Oscillator strength, f	Average f
		A. Second naphthalene transition		
Bradley and Cleasby (6.7°–20.7° C.)	298.7	$5.47^{*}\times10^{-6}$	0.063	
	302.2	7.51*	0.068	0.062
	313.2	22.2*	0.055	
Sears and Hopke (19°–35° C.)	298.7	7.26×10^{-6}	0.047	
	302.2	11.5	0.044	0.049
	313.2	22.2*	0.055	
		B. First anthracene transition		
Bradley and Cleasby (65°–80° C.)	422.7	$10.27^{*}\times10^{-5}$	0.012	
	414.7	5.74*	0.014	0.013
	409.7	3.96*	0.014	
	402.2	2.22*	0.013	
Sears and Hopke (105°–125° C.)	422.7	$7.77^{*}\times10^{-5}$	0.016	
	414.7	4.43*	0.018	0.017
	409.7	3.09*	0.018	
	402.2	1.77*	0.016	
Nita, Seki, and Mornatau (72°–100° C.)	422.7	$5.31^{*}\times10^{-5}$	0.023	
	414.7	3.09*	0.026	0.024
	409.7	2.18*	0.025	
	402.2	1.26*	0.023	
		C. Second anthracene transition		
Bradley and Cleasby (65°–80° C.)	364.2	$8.38^{*}\times10^{-7}$	0.74	
	358.7	4.94*	0.86	0.80
Sears and Hopke (105°–125° C.)	364.2	$7.75^{*}\times10^{-7}$	0.80	0.85
	358.7	4.63*	0.91	
Nita, Seki, and Mornatau (72°–100° C.)	364.2	5.86×10^{-7}	1.10	
	358.7	3.56	1.20	1.15
		D. Second pyrene transition		
Bradley and Cleasby (72°–85° C.)	390.9	$4.46^{*}\times10^{-6}$	0.107	
	384.7	2.75*	0.101	0.102
	379.7	1.88*	0.098	
		E. Third pyrene transition		
Bradley and Cleasby (72°–85° C.)	390.9	$4.46^{*}\times10^{-6}$	0.118†	
	384.7	2.75*	0.128†	0.117
	379.7	1.88*	0.104†	

**Denotes extrapolation of vapor pressure data.*
†*To cut-off.*

the point of view of impurity, they were made in a region where measurements are more difficult.

Two determinations of anthracene vapor pressure are in fairly good agreement (4, 15) but a third set (10) of results indicates a lower vapor pressure. Both the effusion method of Bradley and Cleasby (4) and the modified Rodebush gauge used by Sears and Hopke (15) appear to be reliable and the results agree with the less accurate determination by Stevens (16) using the intensity of the fluorescence as a measure of the concentration. There seems no reason why the effusion method used by Nita, Seki, and Mornatau (10) should be less accurate so concentrations calculated from these data were also used to compute the oscillator strengths.

Pyrene vapor pressures were measured by Bradley and Cleasby (4), and there has been an extrapolation of their results for the purpose of the present work. The concentrations computed for pyrene are therefore less reliable than for the others but still indicate considerable intensification of the absorption intensity from vapor to solution.

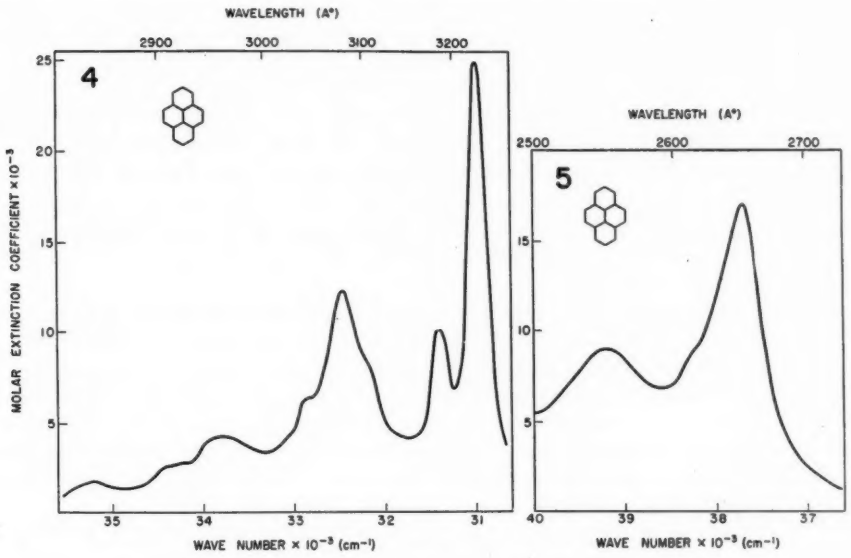

FIG. 4. Pyrene absorption spectrum, second transition.
FIG. 5. Pyrene absorption spectrum, third transition.

TABLE II

COMPARISON OF OSCILLATOR STRENGTHS IN VAPOR AND SOLUTION

Compound		Vapor		Solution
		Range of f	Average f	f
Naphthalene	2nd transition	0.049–0.062	0.055	0.11_5
Anthracene	1st transition	0.013–0.024	0.018	0.11_5
	2nd transition	0.80 –1.15	0.93	1.56
Pyrene	2nd transition	0.098–0.107	0.10	0.30_0
	3rd transition (to cutoff)	0.104–0.128	0.12	0.26_5

The question "Does ultraviolet absorption intensity increase in solution?" was asked and answered by Jacobs and Platt (8) for isoprene, *cis*-, and *trans*-piperylenes. They concluded that the correction factor is close to unity, a result previously obtained by Pickett and co-workers (12) for cyclopentadiene and cyclohexadiene. Almasy and Laemmel (1) have extensively investigated the absorption spectrum of diphenyl using a photographic technique and have found a correction factor of 1.32, and more recently Price and Hammond (13) have found both an increase and a decrease over solution intensities for two transitions of benzene in the vacuum ultraviolet. As can be seen from Table II our results for naphthalene, anthracene, and pyrene show a marked intensification of absorption intensity in solution. Although there are variations in the vapor pressures measured by different authors these are relatively small and cannot account consistently, no matter how they are arranged, for the large changes observed between the absorption intensity of the vapor and the solution of these substances.

Although there is a lack of published data concerning solvent intensification in aromatic hydrocarbon spectra some interesting results reported by Herrington and Kynaston (7)

have established that the effect of the solvent is not simple and varies from molecule to molecule and also depends on the electronic transition in the molecule. These workers have reported the difference in molar extinction coefficient between cyclohexane and alcoholic solutions and between 1 *N* LiCl and alcoholic solutions for a number of aromatic molecules. Of most interest to the present discussion is the difference in the behavior of the 2600 Å and 3800 Å region of the anthracene spectrum. The former shows a marked intensification in going from alcohol to cyclohexane while the latter does not change much; both systems, however, are more intense in 1 *N* LiCl than in alcohol. As can be seen from Table II we also find a considerable difference between the 2600 Å and 3800 Å systems of anthracene, but in this case the solvent intensification is much greater for the 3800 Å system.

In view of the results of Herrington and Kynaston and those quoted in this paper there appears to be an obvious need for an investigation of solvent induced intensity changes. With intensity changes as large as those recorded above, the transition from unperturbed gas molecule to solvent perturbed molecule could be followed with the aid of pressure techniques similar to those developed by Robin and Vodar (18). These authors have noted an increase in the absorption coefficient of phenanthrene dissolved in compressed N_2 and H_2, but have worked at very high pressures; intensity changes should become apparent at much lower pressures.

It is interesting to make a comparison between theory and experiment. Theory has aimed at increasing the accuracy of calculating transition energies and the recent work of Pariser (11) is evidence of this. However, calculated intensities differ considerably from experimental intensities and Table III summarizes the more recent theoretical values

TABLE III

THEORETICAL OSCILLATOR STRENGTHS OF THEORETICAL *f*

Molecule	Pariser (11)	Moffitt (9)	Ham and Ruedenberg (6)
Naphthalene II	0.256	0.38 0.11*	0.11
Anthracene I	0.386	0.37 0.11*	0.27
Anthracene II	3.23	4.8 1.45*	3.09
Pyrene II			0.012
Pyrene III			1.53

*"*Normalized*" *with respect to benzene.*

of *f*. As can be seen from a comparison between Tables III and Table II, agreement is poor, particularly for pyrene. In connection with the theoretical work of Pariser (11) it is interesting to examine more closely the vapor absorption spectrum of anthracene (Fig. 3) in the region corresponding to the 2600 Å system in solution. It is unlikely, in view of the shape of the absorption band in solution, that the low intensity region at about 41,000 cm.$^{-1}$ belongs to the more intense part of the absorption and more likely corresponds to a separate absorption transition. Pariser has calculated that a $^1B_{2u}{}^+$ state should lie 2000 cm.$^{-1}$ below the $^1B_{3u}{}^+$ state calculated at 44,400 cm.$^{-1}$ and it is possible that the absorption in the region around 41,000 cm.$^{-1}$ corresponds to the former. This would explain the marked difference in the shape of the absorption curve in solution because both transitions would probably react differently to solvent perturbation.

Four of the five transitions studied have very similar red shifts in going from vapor to

solution, amounting to about 1000 cm.$^{-1}$. The intense 2600 Å system of anthracene, however, shifts to low energies by as much as 3000 cm.$^{-1}$ depending on the solvent.

REFERENCES

1. ALMASY, F. and LAEMMEL, H. Helv. Chim. Acta, **33,** 2092 (1950).
2. ALTMANN, S. L. Proc. Phys. Soc., A, **63,** 1234 (1950).
3. BARKER, J. T. Z. physik. Chem. **71,** 235 (1910).
4. BRADLEY, R. S. and CLEASBY, T. G. J. Chem. Soc. 1690 (1953).
5. CHAKO, N. Q. J. Chem. Phys. **2,** 644 (1934).
6. HAM, N. S. and RUEDENBERG, K. J. Chem. Phys. **25,** 13 (1956).
7. HERRINGTON, E. F. G. and KYNASTON, W. J. Chem Soc. 3137, 3143 (1952).
8. JACOBS, L. E. and PLATT, J. R. J. Chem. Phys. **16,** 1137 (1948).
9. MOFFITT, W. J. Chem. Phys. **22,** 320 (1954).
10. NITA, J., SEKI, S., and MORNATAU, M. J. Chem. Soc. Japan, **71,** 430 (1950).
11. PARISER, R. J. Chem. Phys. **24,** 250 (1956).
12. PICKETT, L. W., PADDOCK, E., and SACKTER, E. J. Am. Chem. Soc. **63,** 1073 (1941). PICKETT, L. W. and HENRI, V. J. Chem. Phys. **7,** 439 (1939).
13. PRICE, W. C. and HAMMOND, V. J. Trans. Faraday Soc. **51,** 605 (1955).
14. SANGSTER, R. C. and IRVINE, J. W. J. Chem. Phys. **24,** 670 (1956).
15. SEARS, G. W. and HOPKE, E. R. J. Am. Chem. Soc. **71,** 1633 (1949).
16. STEVENS, B. J. Chem. Soc. 2943 (1953).
17. SWAN, T. H. and MACK, E. J. Am. Chem. Soc. **47,** 2112 (1925).
18. VODAR, B. and ROBIN, S. J. Chem. Phys. **16,** 996 (1948); **18,** 1413 (1950).

HEATS OF ACTIVATION IN ELECTRODE PROCESSES

THE ELECTROCHEMICAL DESORPTION MECHANISM OF THE DISCHARGE OF HYDROXONIUM IONS[1]

B. E. CONWAY AND J. O'M. BOCKRIS

ABSTRACT

Quasi-quantitative potential energy profile diagrams are estimated for the electrochemical desorption reaction $H_{aq.}^{+}+H_{ads.}+e_0^{-} \rightarrow H_2$ of the electrolytic hydrogen evolution reaction at Ni, Cu, W, and Hg. The calculated heats of activation for this reaction increase with increasing heat of adsorption of H on the metal, the converse of the situation found for the simple proton discharge reaction $H_{aq.}^{+}+e_0^{-} \rightarrow H_{ads.}$. The direction of the trend of calculated $\Delta H^{\ddagger}$ values for electrochemical desorption, with heat of adsorption of H, is in agreement with the observed dependence of exchange currents on heat of adsorption for a series of transition metals. For systems where stoichiometric number data cannot be obtained, the calculations allow distinction between rate-determining proton transfer and electrochemical desorption reactions. The experimental groups of values for the H/D separation factor are interpreted.

I. INTRODUCTION

Three rate determining steps in the hydrogen evolution reaction (h.e.r.) from aqueous acid solutions are (4, 5, 6): $H_3O^{+}+e_0^{-} \rightarrow H_{ads.}$(A); $H_3O^{+}+H_{ads.}+e_0^{-} \rightarrow H_2$ (B)*; and $H_{ads.}+H_{ads.} \rightarrow H_2$ (C). Criteria for a given rate determining step have been proposed in terms of Tafel slopes and stoichiometric numbers (5), but A and B can give the same b values ($2.303(2RT/F)$), although their stoichiometric numbers (ν) differ. Sometimes ν is not determinable, so that a further criterion must be available. Conway and Bockris have pointed out (9, 10) that the direction of dependence of i_0 upon heat of adsorption of H at various metals should be different for reactions A and B since the heat of adsorption of H will appear in the expression for the potential energy of the state after the transition state in reaction A, but in the potential energy of the state *before* the transition state in B. The consequences of this concept are evaluated here quasi-quantitatively for reaction B. Previously it has been assumed, without proof (19), that the rates of reactions A and B will be affected in the *same* way by changes of heats of adsorption of H. This is shown to be theoretically invalid and in disagreement with experiment.

II. POTENTIAL ENERGY DIAGRAM CALCULATIONS

Inherent in potential energy surface calculations by the Eyring–Polanyi semiempirical method (17) is the difficulty of assigning the correct proportion of coulombic and dispersion interaction energy. For electrode processes involving transitions between *ions* and molecules the usual assumptions of the contribution of coulombic energy are likely to be inapplicable. However, for reaction A in the h.e.r. and some others (18), e.g. that between alkali metals and alkyl halides (16, 21), use of a cross section of the potential energy surface (the potential energy profile) assuming a linear reaction co-ordinate gives reasonable agreement with experiment (32, 11).

The configuration in the model to be considered (III*a*) is one in which the OH bond

[1]*Manuscript received May 28, 1957.*
Contribution from the Department of Chemistry, University of Ottawa, Ottawa, Ontario, and John Harrison Laboratory of Chemistry, University of Pennsylvania, Philadelphia, Pa.

**The generally accepted term for mechanism B is the "electrochemical" mechanism, although this is hardly a logical name because A is no less "electrochemical". "Proton discharge" and "Electrochemical desorption" (to distinguish from desorption by means of the chemical reaction H+H) might be logical terms. The name "Horiuti-Volmer" mechanism, recently used by some German authors (19, 35), has little logical support because the mechanism was originated by Kobosew and Nekrassow (24), and not contributed by Volmer.*

containing the reacting proton in the H_3O^+ ion adsorbed in the Helmholtz layer at an electrode is in line with the H atom adsorbed on the metal M, i.e., the O—H^+ and M—H bonds are collinear. For the four atom reaction (viz. O, H^+, H, and M in the present case), the other two OH bonds in the H_3O^+ ion are unchanged in the reaction since H_2O is a product of the reaction of H_3O^+ with MH, and are hence not specially considered as a part of the reacting system (cf. 18, p. 139). The coplanar configuration of four reacting atoms has been shown (18, pp. 90, 91) to give minimum heat of activation. Since the reaction will proceed predominantly via the path of minimum heat of activation, calculations will be made for a collinear configuration of H_3O^+—MH, whereupon use of the potential energy profile is valid.

The absolute evaluation of a theoretical heat of activation by this approach is subject to considerable error, an analysis of which (32) has been made for A. However, such calculations allow accurate (± 1 kcal.) evaluations of the effect of *change* of some variable (e.g., heat of adsorption) upon the heat of activation for an electrode process, and thus permit mechanism-determining comparisons with experiment.

III. THE ELECTROCHEMICAL MECHANISM OF THE HYDROGEN EVOLUTION REACTION

Preliminary calculations of the potential energy curves for this reaction were first made by Conway (12) for Ag.

(*a*) *Model*

Two orientations of the H_3O^+ ion at the surface are possible. At Hg (26) the orientation of an adsorbed film of H_2O is as shown in Fig. 1*a* and interaction of one pair of the non-bonding 2*p* electrons in H_2O with the metal can occur; for the water molecule adsorbed on an electrode in solution the second pair of the non-bonding 2*p* electrons of O in the H_2O molecule is directed towards the bulk of the solution and probably takes part in a hydrogen bond with the H of an adjacent H_2O molecule in the bulk (Fig. 1*a*). The creation of an H_3O^+ ion at the metal–solution interface is not through the diffusion of such an ion from the bulk of the solution to the electrode, but by means of the switchback proton transfer mechanism involving H_3O^+ ions and adjacent H_2O molecules (13), the final step being the transfer of a proton from an H_3O^+ ion in the penultimate layer of H_2O molecules in the bulk to a water molecule adsorbed on the electrode (Figs. 1*a* and 1*b*). If the energy gained in reorienting the H_3O^+ dipole by the electric field to the position in Fig. 1*c* is greater than the energy lost in breaking the MO bond in Fig. 1*b* and reorienting the H bonds between the adsorbed H_3O^+ ion and its neighboring H_2O molecules, then the configuration in Fig. 1*c* will be preferred to that of Fig. 1*b*. However, the proton X in both Figs. 1*b* and 1*c* is still in the same position relative to the adsorbed H atom Y and the O atom in the H_3O^+ ion.

H atoms are probably adsorbed (7) interstitially in holes on the metal surface, where they interact with three metal atoms instead of only the one. The position of the adsorbed H atom in the metal with respect to the three M atoms is determined* by the MH equilibrium internuclear separation* (20).

At the commencement of proton transfer from H_3O^+ to MH, the proton is localized at X (Figs. 1*b* and 1*c*) (at other times its location in the H_3O^+ ion cannot be defined

**The applicability of the spectroscopic* MH *separations is not an important factor since activation of the proton in* H_3O^+ *is the principal process considered (see p. 1133), whilst the position of the adsorbed* H *atom remains constant (18, p. 93). The calculations involve a knowledge of the* M—H *bond strength but not a detailed evaluation of the dependence of this energy upon* M—H *distance.*

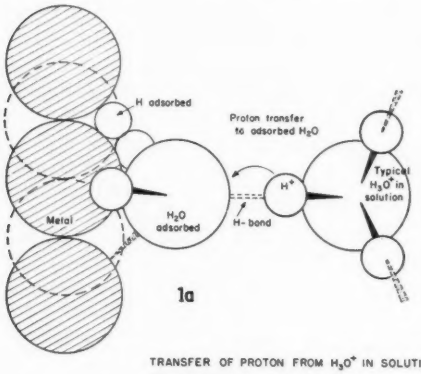

TRANSFER OF PROTON FROM H_3O^+ IN SOLUTION TO ADSORBED H_2O WITH ADSORBED H AT INTERSTITIAL SITE.

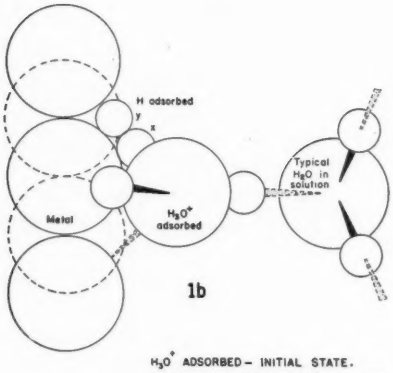

H_3O^+ ADSORBED – INITIAL STATE.
ADSORBED H AT INTERSTITIAL SITE.
PROTON X REACTS WITH ADSORBED H ATOM Y.

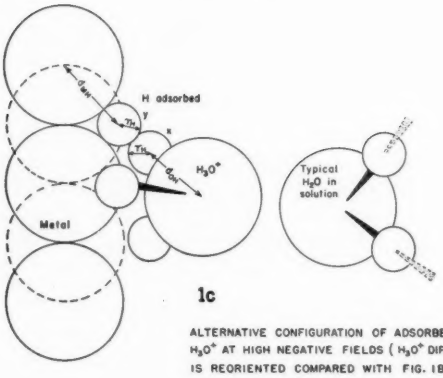

ALTERNATIVE CONFIGURATION OF ADSORBED H_3O^+ AT HIGH NEGATIVE FIELDS (H_3O^+ DIPOLE IS REORIENTED COMPARED WITH FIG. 1B.) REACTION OCCURS BY PROTON X REACTING WITH ADSORBED H, Y.

Fig. 1.

owing to resonance (13)). The H_3O^+ ion has its O atom in contact with the metal and one of its H atoms (at its mean position of vibration) in contact with the adsorbed H atom (at its mean position of vibration). The OH bond distance in H_3O^+ is taken as 1.05 Å (23); MH distances are as discussed.

The internuclear separation of the reacting proton and H atom in the initial state depends upon the effective radii for these entities. That chosen for H arises as follows: (i) From the ionic radius of NH_4^+; this is 1.48 Å (36); the N—H bond distance is 1.0 Å (30) and $r_H = r_{NH_4^+} - d_{NH} = 0.48$ Å. (ii) From the critical volume of CH_4; $V_c = 98.77$ cm.^{3} g. mole^{-1} (29), i.e., $r_{CH_4} = 1.69$ Å and $d_{CH} = 1.07$ Å (30) so that $r_H = 0.62$ Å. (iii) For NH_3, $V_c = 72.02$ cm.^{3} g. mole^{-1} (29) and $d_{NH} = 1.0$ Å (30) so that $r_H = 0.50$ Å. (iv) For H_2, $V_c = 69.7$ cm.^{3} g. mole^{-1} (29) and $d_{HH} = 0.74$ Å (20), i.e., $r_H = 1.06$ Å. (v) For H_2O, $V_c = 55.5$ cm.^{3} g. mole^{-1} (29) and $d_{OH} = 0.96$ Å (30), i.e., $r_H = 0.44$ Å. (vi) The first Bohr radius for the electron of an H atom is 0.53 Å. The mean value of r_H is then 0.60 ± 0.12 Å. The effective (time average) radius of the proton in H_3O^+ follows from the model recently discussed by Conway *et al.* (13) as 0.4 Å. If an H atom in H_3O^+ spends one-third of its time effectively as a proton (of negligible radius), its time average radius would be approximately $2/3\, r_H$, i.e., 0.4 Å, in agreement with the value of Conway *et al.* The H—H^+ internuclear separation, d_{HH^+}, in the initial state is hence

[1] $$d_{HH^+} = r_H + r_{H^+\ (\text{effective})} = 1.0 \text{ Å}.$$

The final state consists of an H_2 molecule in its ground state adsorbed on the metal electrode. It follows from Fig. 1*b* and 1*c* that the H_2 molecule in the final state is oriented as shown in Fig. 2, i.e. with one of its H atoms nearer the interior of the metal

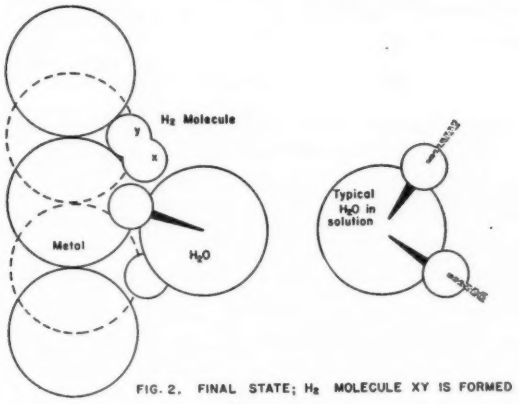

FIG. 2. FINAL STATE; H_2 MOLECULE XY IS FORMED

Fig. 2.

than the other. The equilibrium internuclear separation of H atoms in this state will be that in the H_2 molecule, i.e. 0.74 Å (20).

(*b*) *Free Energy of Activation*

The four relevant states are: (i) *The initial state*: H_3O^+ in the bulk of the solution at unit activity; the metal surface saturated* with H atoms; and electrons in the metal.

**This assumes that the Tafel b value of 2.303(2RT/F) for the electrochemical reaction applies down to the reversible potential, and not the slope 2.303(2RT/3F), which corresponds to a sparsely covered surface (5).*

TABLE I

ESTIMATES OF THE RADIUS OF THE H ATOM

Method	Calculated radius of r_H in Å	
From radius of NH_4^+	0.48	
From critical vol. of CH_4	0.62	
From critical vol. of NH_3	0.50	Mean value =
From critical vol. of H_2O	0.44	0.60 ± 0.12 Å
From critical vol. of H_2	1.06	
From 1st Bohr radius of H	0.53	

The standard state is for 25° C. and 1 gram-ion of H_3O^+ l.$^{-1}$ in the bulk and the following surface concentrations of H atoms, corresponding to saturation at each of the metals Hg, Ni, Cu, and W examined: Hg: 1.0×10^{15}; Ni: 1.6×10^{15}; Cu: 1.5×10^{15}; W: 1.3×10^{15} atoms cm.$^{-2}$; one extra electron is in the metal for each H_3O^+ ion about to be discharged in the Helmholtz layer. The above figures for surface concentration of H atoms are derived by calculating the number of interstitial positions per cm.^{2} between groups of 3 coplanar atoms of the metal. H atoms are then assumed to reside at these positions on the surface (cf. 7) as stated on p. 1125 and shown diagrammatically in Figs. 1*a* and 1*b*. (ii) *The double-layer state*: H_3O^+ adsorbed at the electrode in the Helmholtz layer at unit surface activity (1 gram-ion cm.$^{-2}$). H atoms adsorbed at the electrode and electrons in the metal as in (i). (iii) *The activated state*: the activated complex (at unit surface activity, 1 mole of activated complex cm.$^{-2}$) between H_3O^+ and an H atom and electrons as in (i) except that the electron is now partially withdrawn from the metal. (iv) The H_2 molecule (ground state) physically adsorbed at the electrode and near the H_2O molecule from which one of its atoms was derived. The standard state is 1 mole cm.$^{-2}$ of adsorbed H_2 at 25° C.

The condition for equilibrium of B in state (i) is:

$$[2] \qquad (\bar{\mu})_{H^+} + (\bar{\mu})_e + (\mu)_{H\ ads.} = \mu_{H_2},$$

where $(\bar{\mu})_{H^+}$ is the electrochemical potential of the H_3O^+ ions, $(\bar{\mu})_e$ that of the electron in the metal, $(\mu)_{H\ ads.}$ the chemical potential of adsorbed H, and μ_{H_2} the chemical potential of H_2 in the gas phase, respectively, the values referring to the equilibrium condition of B at 25° C. Writing [2] in terms of the standard electrochemical and chemical potentials gives

$$[3] \qquad (\bar{\mu}^\circ)_{H^+} + RT \ln a_{H^+} + (\bar{\mu})_e + (\mu^\circ)_{H\ ads.} + RT \ln a_{H\ ads.} = (\mu^\circ)_{H_2} + RT \ln p_{H_2}.$$

Let ϕ_{metal} and $\phi_{soln.}$ be the inner potentials* of the metal and solution phases respectively, then, expressing electrochemical potential terms as chemical and electrical potentials terms, [3] becomes

$$[4] \qquad (\mu^\circ)_{H^+} + RT \ln a_{H^+} + \phi_{soln.} F + (\mu)_e - \phi_{metal} F + (\mu^\circ)_{H\ ads.} + RT \ln a_{H\ ads.} = (\mu^\circ)_{H_2} + RT \ln p_{H_2}.$$

We then write the Galvani potential difference, $\phi_{metal} - \phi_{soln.}$, between the metal and solution phases as $V + V'$, where V is the coulombic and V' the surface potential contribution to $\phi_{metal} - \phi_{soln.}$ (cf. 32). Equation [4] can then be written as

$$[5] \qquad (\mu^\circ)' - VF + RT \ln a_{H^+} + (\mu^\circ)_{H\ ads.} + RT \ln a_{H\ ads.} = (\mu^\circ)_{H_2} + RT \ln p_{H_2},$$

**That is, the potential inside the phase beyond any region where surface potential differences are existent; for original definition, see Lange (25).*

where

[6] $$(\mu^\circ)' = (\mu^\circ)_{H^+} + (\mu)_e - V'F.$$

For $p_{H_2} = 1$ atm., and the condition of surface saturation assumed as the standard state for adsorbed H, [5] becomes

[7] $$(\mu^\circ)' - VF + RT \ln a_{H^+} + (\mu^\circ)_{H\ ads.} = 0,$$

taking the conventional chemical potential of H_2 at 1 atm. as equal to zero; this procedure is valid since only the correct *relative* position of the initial and final state potential energy curves is required for the evaluation of heats of activation, and the arbitrary value of $(\mu^\circ)_{H_2} = 0$ is involved in determining the position of *both* initial *and* final state curves in the same way.

Let us call $(\bar{\mu}^\circ)_1$ the standard electrochemical potential of state (i); then [7] becomes

[8] $$(\bar{\mu}^\circ)_1 = (\mu^\circ)_1 = -RT \ln (a_{H^+})_{max.},$$

at the potential of zero charge on the metal surface (i.e. the electrocapillary maximum (e.c.m.) potential) where $V = 0$, if $(\mu^\circ)_1 = (\mu^\circ)' + (\mu^\circ)_{H\ ads.}$ and $(a_{H^+})_{max.}$ is the activity of hydrogen ions required for reaction B to proceed reversibly at the electrocapillary maximum potential.

The standard electrochemical potential of state (ii) is given by

[9] $$(\bar{\mu}^\circ)_2 = (\mu^\circ)_1 - (V - \phi_2)F,$$

where ϕ_2 is the mean electric potential of the ions in the outer Helmholtz layer taken with respect to the potential in the bulk of the solution; $\phi_2 = 0$ at the e.c.m. in the absence of specific adsorption.

For the final state, (iv), the condition for equilibrium of adsorbed H_2 molecules and molecules in the gas phase is

[10] $$(\mu^\circ)_4 + RT \ln (a_{H_2M}) = (\mu^\circ)_{H_2} + RT \ln p_{H_2}$$

and at 1 atm. pressure of H_2

[11] $$(\mu^\circ)_4 = -RT \ln (a_{H_2M}); \quad [p_{H_2} = 1 \text{ atm.}].$$

From the above expressions for $(\bar{\mu}^\circ)_1$, $(\bar{\mu}^\circ)_2$, and $(\mu^\circ)_4$, the heat contents of these states can be calculated from the known respective standard entropies (see below). The position of the zero point energies of the Morse functions of the initial and final states on the ordinate axis of the potential energy diagram can then be fixed at these respective heat content values and the heat of activation derived from the point of intersection of the Morse curves.

IV. EVALUATION OF THE POTENTIAL ENERGY DIAGRAMS

(*i*) *Initial State*

To obtain $(\mu^\circ)_1$ from [8], a_{H^+} (e.c.m.) is required, and must be the activity of H^+ ions which gives an electrode the potential of the e.c.m., on the assumption that the free energy change controlling the potential is the one corresponding to the reaction

$$H_3O^+ + H_{ads.} + e_0^- \rightleftarrows H_2 + H_2O. \qquad (B)$$

It is therefore necessary to know the standard potential of this hypothetical equilibrium, compared with that corresponding to the reaction

$$2H_3O^+ + 2e_0^- \rightleftarrows H_2 + 2H_2O. \qquad (D)$$

For B at equilibrium in the standard states of unit activity of H_3O^+ ions in solution, $p_{H_2} = 1$ atm., and surface saturation by adsorbed H,

$$[12] \qquad (\Delta\mu^\circ)_B = (\mu^\circ)_{H_2} + (\mu^\circ)_{H_2O} - (\mu^\circ)_e - (\mu^\circ)_{MH\ ads.} - (\mu^\circ)_{H_3O^+} = -e_B^\circ F,$$

and for D at equilibrium in the standard states of unit activity of H_3O^+ ions in solution and $p_{H_2} = 1$ atm.,

$$[13] \qquad (\Delta\mu^\circ)_D = (\mu^\circ)_{H_2} + 2(\mu^\circ)_{H_2O} - 2(\mu^\circ)_e - 2(\mu^\circ)_{H_3O^+} = -2e_D^\circ F,$$

where e_B° and e_D° are the standard potentials for the reactions B and D. Then, by multiplying [12] by two and subtracting the result from [13] is obtained

$$[14] \qquad (e_B^\circ - e_D^\circ)F = (\mu^\circ)_{H\ ads.} - \tfrac{1}{2}(\mu^\circ)_{H_2},$$

which is equal to $e_B^\circ F$ since, conventionally, $e_D^\circ F = 0$. The activity of H_3O^+ ions required for reaction B to be in equilibrium at the e.c.m. potential of the metal is given from

$$[15] \qquad e_{e.c.m.} = e_B^\circ + (RT/F) \ln (a_{H^+})_{max.},$$

where $e_{e.c.m.}$ is the potential of the e.c.m. of the metal. Now

$$(\mu^\circ)_1 = -RT \ln (a_{H^+})_{max.},$$

so that

$$(\mu^\circ)_1 = (e_B^\circ - e_{e.c.m.})F$$

$$[16] \qquad = (\mu^\circ)_{H\ ads.} - \tfrac{1}{2}\mu^\circ_{H_2} - e_{e.c.m.}F \quad \text{(from [14])}.$$

We require ΔH_1 for the reaction

$$H_2 \rightarrow H_3O^+ + MH_{ads.} + e_0^-, \qquad (B')$$

which is the heat content of the state $H_3O^+ + e_0^- + MH_{ads.}$ with respect to that of H_2 taken as zero. This is given from $(\mu^\circ)_1$ using [16], as

$$[17] \qquad \Delta H_1 = (\mu^\circ)_1 + T(\Delta S^\circ)_1 = (\mu^\circ)_{H\ ads.} - \tfrac{1}{2}\mu^\circ_{H_2} - e_{e.c.m.}F + T(\Delta S^\circ)_1$$

where ΔS°_1 is the standard entropy change in the reaction B'. ΔH_1 is then given by

$$[18] \qquad \Delta H_1 = H^\circ_{H\ ads.} - TS^\circ_{H\ ads.} - \tfrac{1}{2}H^\circ_{H_2} + \tfrac{1}{2}TS^\circ_{H_2} - e_{e.c.m.}F + TS^\circ_{H^+aq.} + TS^\circ_{H\ ads.} + TS^\circ e - TS^\circ_{H_2},$$

where the subscripts indicate the species to which the respective thermodynamic quantities refer. In [18] the term $H^\circ_{H\ ads.}$ is the heat content of adsorbed H referred to molecular H_2, and is equal to the heat of adsorption measured experimentally per half mole of H_2, i.e., $H^\circ_{H\ ads.} = \frac{1}{2}(D^\circ)_{H_2} + \Delta H_{H\ ads.}$, where $(D^\circ)_{H_2}$ is the heat of dissociation of H_2 and is equal to 51.7 kcal. mole^{-1} (3) and $\Delta H_{H\ ads.}$ has the values: Ni: -67.2; Cu: -63.4; W: -75, and Hg: -57 kcal. mole^{-1} (2, 33). $S^\circ_{H_2}$ is 31.2 cal. °C.$^{-1}$ mole^{-1} (3); S°_e = 3.28 cal. °C.$^{-1}$ mole^{-1} (27)† and $S^\circ_{H^+aq.}$ is -4.6 cal. °C.$^{-1}$ mole^{-1} (10). The e.c.m. potentials required for evaluation of ΔH_1 by [18] are Ni: -0.06; Cu: -0.18;* W: -0.18;* and Hg: -0.19 v. (24) with respect to the NH_2 electrode.

The following values of ΔH_1 at 25° C. are then calculated from [18] using the above data: Ni: -19.1; Cu: -12.5; W: -24.0; and Hg: -5.9 kcal. mole^{-1} and these are

Interpolated using the relation between known e.c.m. potentials and the electronic work functions (31).
†*This value is obtained neglecting the small entropy of mixing of electrons with the lattice.*

the heat contents of the initial states for each metal, i.e., these values determine the height of the minimum of the initial state potential energy curves when the zero point energy of the state is known (see p. 1134).

(*ii*) *The Double Layer State*

In the absence of specific adsorption and at the e.c.m. potential, the ions in the layer next to the electrode do not differ in potential energy from those in the bulk, i.e., $\Delta H_2 = \Delta H_1$, where ΔH_2 is the heat content change in formation of the state (ii) from H_2. The variation of ΔH_2 with displacement of the transferring proton from its equilibrium position in H_3O^+ is thus needed and follows from consideration of the following cycle which leads to the initial state of B.

[19] $\frac{1}{2}H_2(p_{H_2} = 1 \text{ at.}) \rightarrow H(p_H = 1 \text{ at.}), \quad \Delta H = 51.7 \text{ kcal. mole}^{-1}$

[20] $H(p_H = 1 \text{ at.}) \rightarrow H^+_{gas} + e_0^-, \quad \Delta H = I_H = 313 \text{ kcal. mole}^{-1}$

[21] $e_0^- + M_{H \text{ ads.}} \rightarrow e_0^- M_{H \text{ ads.}}, \quad \Delta H = -\phi_{MH \text{ ads.}}$

[22] $H^+_{gas} \rightarrow H^+_{aq.}, \quad \Delta H = \Delta H_{s(H^+)} = -263 \pm 13 \text{ kcal. mole}^{-1}$ (32, 14, 11)

[23] $\frac{1}{2}H_2 + M \rightarrow M_{H \text{ ads.}}, \quad \Delta H = \Delta H_{H \text{ ads.}} + \frac{1}{2}(D^\circ)_{H_2}$

where $\Delta H_{s(H^+)}$ is the heat of hydration of the proton, $\Delta H_{H \text{ ads.}}$ is the heat of adsorption of H at the metal, $\phi_{MH \text{ ads.}}$ is the electronic work function of the H-covered metal (34). Values of $\phi_{MH \text{ ads.}}$ are known for Al, Tl, Ag, Au, and Pt. A plot (34) of the *change* of ϕ_M from its value for a clean metal surface to its value ($\phi_{MH \text{ ads.}}$) when the surface is covered with adsorbed hydrogen is a linear function of ϕ_M for Al, Tl, Ag, Au, and Pt and thus enables $\phi_{MH \text{ ads.}} - \phi_M$ to be obtained for Ni, Cu, W, and Hg, considered above, by interpolation in the plot of $\phi_{MH \text{ ads.}} - \phi_M$ at known values of ϕ_M of these metals. The values of $\phi_{MH \text{ ads.}}$ can then be obtained and are as follows:
Ni: 3.85; Cu: 3.70; W: 3.70; Hg: 3.75 ev. $\Delta H_{s(H^+)}$, the heat of solvation of the proton, is -263 ± 13 kcal. mole^{-1} (14).

The variation of $\Delta H_{s(H^+)}$ with displacement of the proton is calculated from a Morse function in the usual way (32, 11), using Morse constants a and r_e discussed previously (32, 11). $\Delta H_{H \text{ ads.}}$ is also distance dependent and its value as a function of displacement of H from the metal is calculated similarly using the date of Table II. Values for 'a' for the Morse function for $\Delta H_{H \text{ ads.}}$ are calculated from

[24] $$a = \pi \nu_e \sqrt{\frac{2m^*}{\Delta H_{H \text{ ads.}}}},$$

TABLE II

MOLECULAR CONSTANTS FOR MH MOLECULES

Hydride	ω_e, cm.$^{-1}$	$\nu_e \times 10^{-13}$, sec.$^{-1}$	$\Delta H_{H \text{ ads.}}$, kcal.g-atom^{-1}	r_e, Å	m^*
NiH	1927	5.781	67	1.474	0.9911
HgH	1387	4.163	57	1.740	0.9952
CuH	1940	5.820	68.0	1.463	0.9922
FeH	(1930)	5.790	68.5	1.476	0.9902
AgH	1760	5.280	57.8	1.617	0.9988
WH	?		75	?	0.9942

NOTE: *Values of $\Delta H_{H \text{ ads.}}$ are for zero coverage. They do not diminish rapidly until near saturation, when the values for different metals probably have the same relative order as those at low coverage.*

where ν_e is the vibrational frequency in the ground state of MH and m^* the reduced mass of MH; ν_e values are obtained from spectroscopic values of the corresponding wave number ω_e (20).

Values of ΔH_1 may be calculated from the cycle [19] to [23] and it is of interest to compare the values obtained with those by the procedure where allowance for the surface potential is made.* From [19] to [23], $\Delta H_1 = +3$ (Ni), $+4.6$ (Cu), -7.0 (W), and $+9.5$ (Hg). The mean difference of these values from those calculated from [8] is 0.69 ± 0.03 volt.*

Two other interactions contribute to the energy of state (ii) as a function of displacement of the proton. Firstly, the H atom previously discharged by the simple discharge process on to a vacant site on the metal, and now forming part of the initial state for the electrochemical discharge process, will suffer a repulsive interaction with the H_3O^+ ion about to undergo discharge by the electrochemical mechanism in the same way that the discharged H atom in the simple discharge reaction suffers repulsive interaction with an H_2O molecule from which it was transferred. Since the repulsive interaction with H_3O^+ is likely to be very similar to that with H_2O the applicability of the repulsive function (1) used previously (32, 11) for the H—H_2O interaction is assumed. Secondly, the MH in the initial state has a dipole moment and there will therefore be a contribution to the energy of the initial state due to the interaction of the H_3O^+ ion and the MH dipole. This has been calculated for various displacements of the proton in H_3O^+ by classical electrostatic theory in the cases of NiH, HgH, and WH for which MH surface dipole moments are available (28). The ion–MH dipole contribution to the potential energy of the initial state is of the order of 5 kcal. mole^{-1}.

(*iii*) *Final State*

The heat content of the final state is that of an H_2 molecule physically adsorbed at the electrode amongst adsorbed H atoms and H_2O molecules. Heats of physical adsorption of small rare gas molecules are approximately -3 kcal. mole^{-1} (8) with respect to the molecules in the gas phase and this value probably applies to ± 1 kcal. also to molecular H_2 at each of the metals. With reference to H_2 in the gas phase, the heat content of state (iv) is then $H_4 = -3.0$ kcal. mole^{-1}.

V. CONSTRUCTION OF THE POTENTIAL ENERGY DIAGRAMS

The energy of the double-layer state (i.e., the state from which activation and transfer of the proton occurs) must be described as a function of the distance between H in $MH_{ads.}$ and H in H_3O^+ during the reaction, and the energy of the final state as a function of the H—H internuclear separation in H_2. Since the co-ordinates of two particles (viz. the H^+ in H_3O^+ and the H atom in $MH_{ads.}$) are involved in the potential energy curves, it is convenient for the construction of a planar potential energy cross section diagram to plot the energy of the system as a function of the H—H separation. This is carried out as follows:

Double-layer State

The center of the H_3O^+ ion (Fig. 1*b* or 1*c*) is at a distance $r_{OH} + r_{H^+(H_3O^+)} + r_H$ (where

**The first method (pp. 1130–1131) for obtaining ΔH_1 gives the value of this quantity corresponding to the minimum of the potential energy curve for the initial state, and makes allowance for the surface potential. The second method makes no allowance for the surface potential, but enables calculation to be made of the dependence of ΔH_1 on distance. The value from this second method for ΔH_1 at the equilibrium internuclear separation should differ from that of the first method by a quantity equal to the Faraday multiplied by the surface potential difference at the electrode–solution interface. Values of ΔH_1 obtained by the first method must be used to fix the height of the minimum of the initial state potential energy curve.*

r_{OH} is the OH bond distance in H_3O^+ (1.05 Å) and r_{H^+} (H_3O^+) is the effective radius of the proton in H_3O^+) from the center of the adsorbed H atom (Fig. 1*c*). With respect to H_2 in the gas phase, the heat content of $H_{ads.}$ is $R+\Delta H_{H\ ads.}+51.7$, where R is the repulsive interaction between H in MH and H_3O^+ (see p. 1132); $\Delta H_{H\ ads.}$ and R vary as indicated in section IV, (ii), with the displacement of H from its equilibrium separation

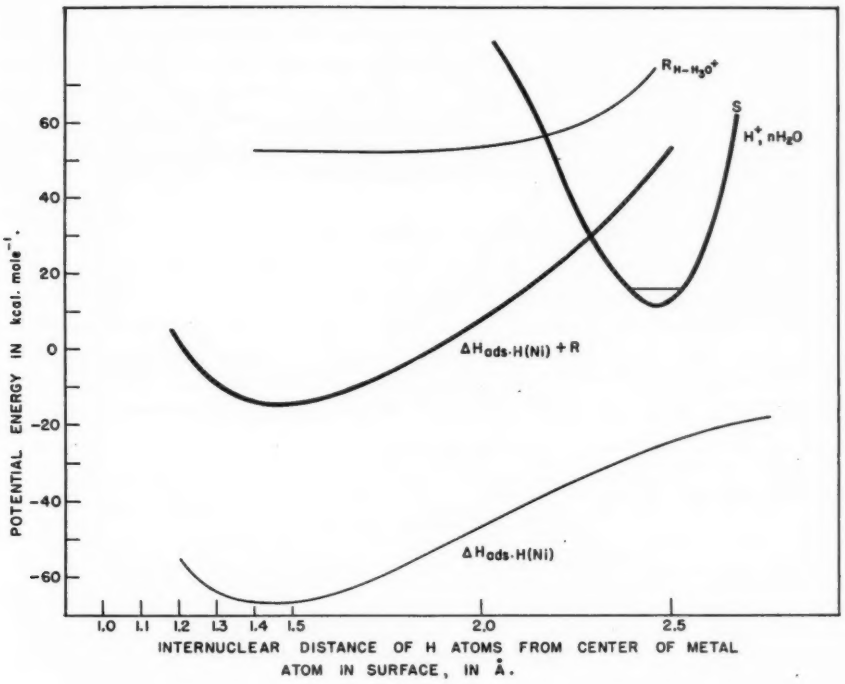

Fig. 3.

from the metal. The heat content of the H_3O^+ ion plus an electron in the metal with respect to that of H_2 is determined by $I_H-\phi_{MH\ ads.}+\Delta H_{s(H^+)}+51.7$. The heat content curves for $R+\Delta H_{H\ ads.}+51.7$ and $I-\phi_{MH\ ads.}+\Delta H_{s(H^+)}+51.7$ are plotted in Fig. 3 with their minima at a separation of 1.0 Å ($= r_H+r_{H^+(H_3O^+)}$). The heat content of the initial state can then be obtained from this diagram as the algebraic sum of the heat contents of $H_{ads.}$ and H^+ in H_3O^+ as a function of position of the two H particles with respect to each other, at a series of displacements of the proton towards the adsorbed H on the metal.* The results of such a computation are given in Fig. 4.

Final State

The heat content, H_4, of the final state with respect to H_2 in the gas phase at 1 atm. pressure is -3 kcal. mole^{-1}, and depends on the H—H separation, r, according to

$$[25] \qquad (H_4)_r = (H_4)_{r_e} + D^\circ_{HH}(1-e^{-a(r-r_e)})^2,$$

**A similar procedure has been adopted in other cases by Hirschfelder, Eyring, and Topley (22) to examine the main features of the potential energy surface (18, p. 93).*

where the constants (20) are $D°_{HH}$ = 109 kcal. mole^{-1} (including the zero point energy of 6.2 kcal. mole^{-1}); $a = 1.963\times10^{8}$, calculated from $D°_{HH}$ and the vibrational frequency ν_e, of the ground state, 1.32×10^{14} sec.$^{-1}$; and $r_e = 0.75\times10^{-8}$ cm. (20).

The potential energy profile diagram used for estimation of the heats of activation is then obtained by plotting the potential energy of the initial and final states as a function of H—H separation; the H_3O^+—MH dipole interaction is included in the initial state potential energy curve, which has its minimum situated at a position d_{HH} = 1.0 Å on the abscissa axis. The final state has its minimum at d_{HH} = 0.75 Å. The *heat of activation* then follows approximately* as the difference of the heat content of the activated state (point of intersection of curves of states (i) and (iv)) and that of the ground level of the initial state. This latter quantity is obtainable from the potential energy curve for the initial state if the sum of the zero point energies of H_3O^+ and MH is added to the minimum of the energy of the initial state curve. The zero point energies are calculated from:

$$E_0 = \tfrac{1}{2}h\nu_{0,\text{MH ads.}} + \tfrac{1}{2}h\nu_{0,\text{OH in } H_3O^+},$$

where $\nu_{0,\text{MH ads.}}$ is the lowest vibrational frequency of $MH_{ads.}$ and $\nu_{0,\text{OH in } H_3O^+}$ is the lowest vibrational frequency of the OH bond in H_3O^+.

Potential energy profile diagrams for reaction B at Ni, Cu, W, and Hg are plotted in Fig. 4. It is shown that the heat of activation $\Delta H°^{\ddagger}$ of the electrochemical discharge of H_3O^+ increases as the heat of adsorption of H increases, an effect *opposite to that for the simple proton discharge reaction* A and in agreement with experiment (9, 10).

TABLE III

VALUES OF THE MINIMUM HEATS OF ACTIVATION FOR THE "ELECTROCHEMICAL" DISCHARGE REACTION $H_3O^+ + MH_{ads.} + e_0^- \rightarrow H_2$ CALCULATED FROM POTENTIAL ENERGY PROFILE DIAGRAMS

Metal	$\Delta H°^{\ddagger}$, kcal. mole^{-1}, calculated	$\Delta H°^{\ddagger}$, kcal. mole^{-1}, experimental
W	16.0	—
Ni	11.5	7–16 depending on HCl concentration
Cu	6.5	10–11 depending on HCl concentration
Hg	2.0	21 (simple discharge step rate-determining)

The theory concerning the increase of the heat of activation of the electrochemical desorption mechanism with heat of adsorption confirmed here quantitatively for four metals is perfectly general, and independent of the uncertainties of the rough numerical estimates reported above. Hence, for a series of metals on which the Tafel slopes in the h.e.r. are near to $2.303(2RT/F)$ (characteristic of either slow discharge or electrochemical desorption as rate determining steps), a regular decrease of exchange current densities with increase of heat of adsorption indicates rate determining $H^+_{aq.} + H_{ads.} + e_0^- \rightarrow H_2$, and this becomes a new and important method by which such a distinction can be made (cf. 9, 10), and of particular importance when the determination of the stoichiometric number is not possible.

VI. THE ELECTROLYTIC SEPARATION FACTOR, (S), OF H AND D

Absolute calculation† of this quantity provides an appropriate application of these calculations because the major uncertainties in the estimates of the molecular parameters

*The resonance energy of the activated complex has not been specially calculated here. By analogy to other proton transfer reactions (13) its value will be approximately 2–3 kcal. mole^{-1} for the metals considered.

†Conway, B. E. In course of publication.

are not effective. Calculations of S for rate determining simple proton discharge (5) indicate an S of about 1.4, in fair agreement with that observed experimentally on mercury. For rate determining proton discharge, S depends mainly upon the difference of the difference in zero point energies of the H_3O^+ and the D^+H_2O ions, and those of $H_{ads.}$ and $D_{ads.}$ which tend to compensate each other. In rate determining electrochemical desorption, these differences in zero point energies are additive in the initial state,

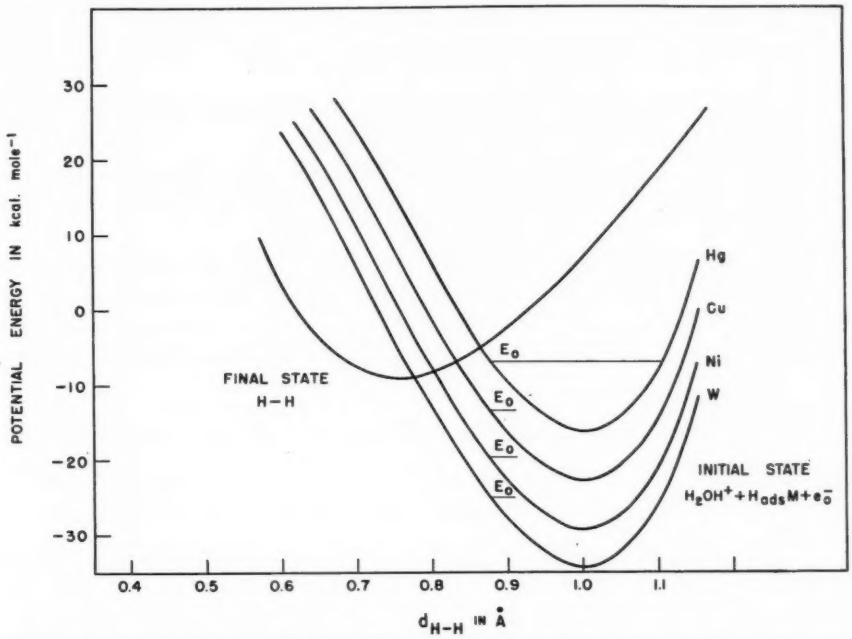

Fig. 4. Potential energy profile diagram for the electrochemical desorption reaction at Hg, Cu, Ni, and W.

indicating a greater value of S. It is noteworthy that on those metals on which there is now every indication that (in acid solution) the rate of the electrolytic hydrogen evolution reaction is controlled by the electrochemical desorption reaction, S is two to three times greater than that on Hg (where simple proton discharge is rate determining).

REFERENCES

1. Amdur, G. J. Chem. Phys. **17**, 844 (1949).
2. Beeck, O. Advances in Catalysis, **2**, 151 (1950).
3. Bichowsky, F. R. and Rossini, F. D. Thermochemistry of chemical substances. Reinhold Publishing Corporation, New York, N.Y. 1936.
4. Bockris, J. O'M. Chem. Revs. **43**, 525 (1948).
5. Bockris, J. O'M. Modern aspects of electrochemistry. Academic Press Inc., New York, N.Y. 1954. Chap. 4.
6. Bockris, J. O'M. and Potter, E. C. J. Electrochem. Soc. **99**, 169 (1952).
7. Boudart, M. J. Am. Chem. Soc. **72**, 1040 (1950).
8. Brunauer, S. Adsorption of gases on solids. Vol. I. Princeton University Press. 1949.
9. Conway, B. E. and Bockris, J. O'M. Nature, **178**, 488 (1956).
10. Conway, B. E. and Bockris, J. O'M. J. Chem. Phys. **26**, 532 (1957).
11. Conway, B. E., Bockris, J. O'M., and Lovrocek, B. Compt. rend. C.I.T.C.E. 207 (1955).
12. Conway, B. E. Ph.D. Thesis, London. (1949), pp. 276–324.
13. Conway, B. E., Bockris, J. O'M., and Linton, H. J. Chem. Phys. **24**, 834 (1956).

14. CONWAY, B. E. and BOCKRIS, J. O'M. Modern aspects of electrochemistry. Academic Press Inc., New York, N.Y. 1954. Chap. 2.
15. ELEY, D. D. Discussions Faraday Soc. **8**, 34 (1950).
16. EVANS, M. G. and POLANYI, M. Trans. Faraday Soc. **34**, 11 (1938).
17. EYRING, H. and POLANYI, M. Z. physik. Chem. (Leipzig), **B12**, 229 (1931).
18. GLASSTONE, S., LAIDLER, K. J., and EYRING, H. The theory of rate processes. McGraw-Hill Book Company, Inc., New York and London. 1941.
19. GERISCHER, H. and MEHL, W. Z. Elektrochem. **59**, 1049 (1955); Angew. Chem. **68**, 20 (1956).
20. HERZBERG, G. Spectra of diatomic molecules. D. Van Nostrand Co., Inc., New York. 1950.
21. HINSHELWOOD, C. N., LAIDLER, K. J., and TIMM, E. W. J. Chem. Soc. 848 (1938).
22. HIRSCHFELDER, J., EYRING, H., and TOPLEY, B. J. Chem. Phys. **4**, 170 (1946).
23. HUND, M. Z. Physik, **32**, 1 (1925).
24. KOBOSEW, N. I. and NEKRASSOV, I. Z. Elektrochem. **36**, 529 (1930).
25. LANGE, E. Wien-Harms Handbuch exp. Phys. **12** (12), 267 (1933).
26. LAW, J. T. Thesis, London (1954); BOCKRIS and LAW, in press.
27. LEWIS, G. N. and RANDALL, M. Thermodynamics of chemical substances. McGraw-Hill Book Company, Inc., New York and London. 1923. p. 458.
28. MIGNOLET, J. C. P. Discussions Faraday Soc. **8**, 105 (1950).
29. MOELWYN-HUGHES, E. A. Physical chemistry. Cambridge University Press. 1947.
30. PAULING, L. Nature of the chemical bond. Cornell University Press., Ithaca 1948.
31. PARSONS, R. Modern aspects of electrochemistry. Academic Press Inc., New York. 1954. Chap. 3.
32. PARSONS, R. and BOCKRIS, J. O'M. Trans. Faraday Soc. **47**, 914 (1951).
33. STEVENSON, D. P. J. Chem. Phys. **23**, 203 (1955).
34. SUHRMANN, W. J. and CSESCH, K. Z. physik. Chem. (Leipzig), **28B**, 215 (1935).
35. VETTER, K. Z. Elektrochem. **59**, 435 (1955).
36. WELLS, A. F. Structural inorganic chemistry. Oxford University Press, London. 1945.

THE PHOTOLYSIS OF KETENE AT LOW TEMPERATURES[1]

W. G. PATERSON[2] AND H. GESSER

ABSTRACT

The photochemical decomposition of ketene at 2700 Å has been investigated at −78° C. The quantum yield of carbon monoxide is two, indicating that the recombination of methylene radicals does not occur at this low temperature.

INTRODUCTION

The primary photochemical process at 2700 Å is now (4, 5, 6) accepted as

$$CH_2CO+h\nu \rightarrow CH_2+CO. \qquad [1$$

At room temperature and above, the quantum yield of CO is about two (5, 6), indicating that the reaction

$$CH_2+CH_2CO \rightarrow C_2H_4+CO \qquad [2]$$

is of major importance. Some polymerization by methylene radicals also occurs as shown by the consistent value of 2.2 for $R_{CO}/R_{C_2H_4}$ (where R refers to the rate of formation) at 25° C. which increases at higher temperatures (1, 4).

If the recombination reaction

$$CH_2+CH_2 \rightarrow C_2H_4 \qquad [3]$$

occurs, the quantum yield for CO would have a value between one and two and the following relation would be expected to hold:

$$k_2/k_3^{\frac{1}{2}} = 1.414I_a^{\frac{1}{2}}(\phi_{CO}-1)/\{[CH_2CO](2-\phi_{CO})^{\frac{1}{2}}\}.$$

Recent work at −40° C. (4) seemed to indicate that the recombination of methylene radicals is of no importance. It was decided to obtain more direct evidence regarding the possibility of such a recombination reaction at lower temperatures.

EXPERIMENTAL

Ketene was prepared by the pyrolysis of acetic anhydride at 500° C. (2). It was degassed repeatedly at the temperature of liquid oxygen, and distilled from a trap at −125° C. into a bulb where it was stored in liquid nitrogen.

The photolysis was performed in a mercury-free apparatus identical to that of Gesser, Mullhaupt, and Griffiths (3). The source of radiation was a Hanovia S-500 medium pressure mercury arc. The light was collimated with a quartz lens and a stop. The almost parallel beam filled the cell. The volume of the cell and connecting tubing was 260 cm.[3] The low temperatures were obtained by acetone – dry ice mixtures. The radiation was filtered with a Corning glass filter No. 9863 (3 mm.), $NiSO_4.6H_2O$ (319 g./liter in water, 4.7 cm.) and 2,7-dimethyl-3,6-diazacycloheptadiene-1,6 perchlorate (127.5 mg./250 ml. in water, 1 cm.). This filter combination has a transmission from about 2450 to about 2950 Å with a maximum at 2700 Å (6).

Ketene at room temperature was used as an internal actinometer (5, 6); the quantum

[1]*Manuscript received July 2, 1957.*
Contribution from the Department of Chemistry, University of Manitoba, Winnipeg, Manitoba. Grateful acknowledgment is made to the National Research Council of Canada for financial assistance.
[2]*Holder of a National Research Council Bursary. Present address: Department of Chemistry, McGill University, Montreal, Quebec.*

yield of CO being two. The light intensity and any variation during an experiment was determined by a General Electric GL 935 phototube and a multiple deflection galvanometer.

RESULTS AND DISCUSSION

Assuming ϕ_{CO} to be two, it was possible to calculate a phototube–galvanometer circuit constant β where $I_0 = \beta i$ (I_0 is the incident intensity in quanta/cm.^{3} sec. and i is the current in amperes). At 25° C. and ketene concentrations of 1.50, 1.79, and 1.74×10^{18} molecules/cm.^{3}, the values 3.79, 3.73, and 3.68×10^{18} quanta/cm.^{3} sec. amp., respectively, were obtained for β.

Preliminary experiments gave a consistent value of 2.21 for the ratio $R_{CO}/R_{C_2H_4}$. The maximum extent of decomposition was 0.2%.

The results are recorded in Table I and indicate that the quantum yield of CO is the same (two), within experimental error, as that at 25° C.

TABLE I

QUANTUM YIELD OF KETENE PHOTOLYSIS

Temperature = −78° C. Illuminated volume = 130 cm.^{3}

$[CH_2CO]$, molecules/cm.^{3}, $\times 10^{-18}$	R_{CO}, molecules/cm.^{3} sec., $\times 10^{-13}$	ϕ_{CO}
1.66	0.280	2.24
2.08	0.334	2.07
2.58	0.366	1.85
1.27*	0.196	1.88
2.28	0.149	1.96
		Mean 2.00±0.13

*Temperature = −91° C.

The results suggest that reaction [3] does not occur to any notable extent and that reaction [2] has a very low activation energy. It must also be concluded that at this wavelength (2700 Å) and low temperature, the primary dissociation of ketene does not involve an excited state.

REFERENCES

1. CHANMUGAM, J. and BURTON, M. J. Am. Chem. Soc. **78**, 509 (1956).
2. FISHER, G. J., MACLEAN, A. F., and SCHNIZER, A. W. J. Org. Chem. **18**, 1055 (1953).
3. GESSER, H., MULLHAUPT, J. T., and GRIFFITHS, J. E. J. Am. Chem. Soc. (In press).
4. GESSER, H. and STEACIE, E. W. R. Can. J. Chem. **34**, 113 (1956).
5. HOLROYD, R. A. and NOYES, W. A., Jr. J. Am. Chem. Soc. **78**, 4831 (1956).
6. STRACHAN, A. N. and NOYES, W. A., Jr. J. Am. Chem. Soc. **76**, 3258 (1954).

VOLTAIC CELLS IN FUSED SALTS

PART I. THE SILVER – SILVER CHLORIDE, COBALT – COBALTOUS CHLORIDE SYSTEM[1]

S. N. FLENGAS[2] AND T. R. INGRAHAM[3]

ABSTRACT

A reversible silver – silver chloride reference electrode for use in melts at high temperatures has been developed. It was found that the solution of silver chloride in an equimolar mixture of KCl–NaCl melt is ideal for the range of concentrations studied, i.e. 1.0×10^{-3} to 6.0×10^{-2} mole fraction of AgCl.

The electromotive force of the voltaic cell

$$\mathrm{Co} \;\Big|\; \begin{matrix}\mathrm{CoCl_2}\,(x_2)\\ \mathrm{KCl\text{–}NaCl\ (1/1\ mole)}\end{matrix} \;\Big\|\; \begin{matrix}\mathrm{AgCl}\,(x_1)\\ \mathrm{KCl\text{–}NaCl\ (1/1\ mole)}\end{matrix} \;\Big|\; \mathrm{Ag},$$

in which the half-cell to the right contains the above-mentioned reference electrode, was measured as a function of $CoCl_2$ concentration. The applicability of the Nernst equation to this system was established. Deviation from ideality was observed in the case of the solution of $CoCl_2$ in the melt solvent, and this was attributed to the formation of a complex. The dissociation constant of this complex was calculated as 4.50×10^{-2} at 710° C.

The effect of temperature on the electromotive force of this cell was also measured, and the heat of the cell reaction in the presence of solvent ($Co + 2AgCl \rightarrow CoCl_2 + 2Ag$) was calculated from the data as 22.8 ± 1.3 kcal.

The thermodynamic significance of the standard electrode potential of the Co–Ag voltaic cell, derived experimentally as 0.324 volt, is discussed briefly.

INTRODUCTION

The electrochemistry of ionic discharge at electrodes in aqueous solutions has been well worked out over a period of years, and extensive tabulations of experimental electrode potentials based on the hydrogen scale are available.

On the other hand, recent metallurgical studies on electrowinning in molten salts have emphasized the almost complete lack of experimental data on the reversible discharge potentials of ions in media such as molten alkali and alkali earth chlorides, and their mixtures, particularly at high temperature.

Almost all the available data in this field, including the pioneer work of Lorenz (9), consist of values for the decomposition potentials of electrolytic cells containing molten salt electrolytes, and electromotive forces of concentration cells with (1, 5) and without (10, 11, 12, 13, 16) transference.

The few attempts which have been made to measure the electrode potential of metals in solutions of their ions in molten salts have been restricted to rather low temperature melts, and were only partly successful owing to the difficulty of constructing a reversible reference electrode which would be both simple to handle and stable.

This paper is the first in a series which will describe experiments done at the Mines Branch to establish an electrochemical series in melts under equilibrium conditions, and to calculate the related thermodynamic data from electromotive force measurements on voltaic cells. As an initial step, a reversible electrode for high temperatures has been developed and used to determine the potentials of a cobalt – cobaltous chloride half-cell under varying conditions of concentrations and temperature.

[1]*Manuscript received May 28, 1957.*

Contribution from the Extractive Metallurgy Section, Department of Mines and Technical Surveys, Ottawa, Canada. Published with the permission of the Director, Mines Branch, Department of Mines and Technical Surveys, Ottawa.

[2]*N.R.C. Postdoctorate Fellow assigned to the Mines Branch, Department of Mines and Technical Surveys, Ottawa.*

[3]*Head, Extractive Metallurgy Section, Mineral Dressing and Process Metallurgy Division, Mines Branch, Ottawa.*

In subsequent publications in this series, similar data will be reported for other metals.

A. THE DEVELOPMENT OF A HIGH TEMPERATURE Ag–AgCl REFERENCE ELECTRODE

Several types of reference electrodes for use in fused systems have been introduced recently (2, 3, 4, 14, 15). Senderoff and Brenner (14) have described an Ag–AgCl reference electrode constructed in pyrex glass, in which free diffusion and mixing of the solutions were hindered by means of a coarse asbestos plug. This cell, however, was not completely free from the effects of diffusion and it introduced into the measurements an unknown boundary potential. Delimarski *et al.* (3, 4) used half-cells of the type

$$\text{Na} \;\Big|\; \begin{matrix}\text{amalgamated with Hg}\\ \text{or other metals}\end{matrix} \;\Big\|\; \text{Na–glass diaphragm} \;\Big\|\; \text{Na melt}$$

and measured the electrode potentials of several metals.

A modification of this electrode is that introduced recently by Bockris *et al.* (2), in which the sodium amalgam was replaced by an Ag–AgCl (KCl, LiCl) electrode. Unfortunately, by the nature of its construction, the use of this type of reference electrode is confined to low temperatures. Furthermore, electrodes of this type are not amenable to an exact thermodynamic treatment and, hence, cannot be used in establishing the equilibria in chemical reactions taking place in an electrolytic cell, except in the case of concentration cells.

Experimental

In the present investigation, as the result of studying a number of different cell designs, the following type of reference electrode was adopted:

$$\text{Ag} \;\Big|\; \begin{matrix}\text{AgCl } (x)\\ \text{KCl–NaCl (1/1 mole)}\end{matrix} \;\Big\|\; \text{Asbestos fiber}$$

The half-cell was constructed from silica tubing and is essentially a modification of a low temperature reference electrode developed by Flengas and Rideal (5) for measuring the electromotive forces of concentration cells in fused alkali nitrate melts. The design of the half-cell is shown in Fig. 1 *a*. Very pure silver foil (99.999%) was spot-welded to a platinum wire for the electrical contact and, before use, it was cleaned with acetone and inserted in the molten solution of AgCl in 1/1 mole KCl–NaCl in the half-cell. To prepare this solution, Analar grade salts KCl and NaCl were used. AgCl was prepared from the corresponding nitrate salt. The mole fraction (x) of AgCl in the reference half-cell, unless otherwise stated, was 6.103×10^{-2} (which corresponds to about 1 mole of AgCl per 1000 g. of KCl–NaCl mixture).

The metallic silver electrode, apart from being completely immersed in the melt, did not require any special protection from air, since it is known that Ag_2O decomposes at 300° C. and, therefore, this metal at high temperature always presents a clean surface (8).

Electrical contact between the solutions in the standard cell and the indicator electrode was made through an asbestos fiber sealed into the end of the side-arm tube of the reference. To obtain a good seal between the asbestos and silica, the silica tubing was first drawn down to about 3 mm. I.D. and then the asbestos fiber, taken from an asbestos rope, was inserted and heated until all organic matter contained in it had been burned. The narrow part of the tube was then heated in a hydrogen flame, care being taken to avoid fusion of the asbestos with the silica. This was feasible only when the asbestos fiber was hanging in the center of the tubing and was not in contact with the walls.

Finally, when the silica was uniformly pliable, the flame was withdrawn and the sides of the tube were pressed into contact with the asbestos fiber, using platinum-foil-covered pliers.

It was found that a half-cell reference having about 1.5 cm. of asbestos sealed into the end of the silica side-arm could be used for several weeks with the potential remaining constant within 1 mv. A 10,000 ohm resistor was connected in series with the electrode to ensure that during operation only very small currents could be drawn through the cell, thus preventing changes in concentration.

The applicability of the Nernst equation to the Ag–AgCl(x) system, and the reversibility of the system, were first investigated by measuring the electromotive forces of the following concentration cells:

Ag	AgCl ($x_1 = 1.1\times10^{-3}$)	Asbestos fiber	AgCl (x_2)	Ag
(−)	KCl–NaCl (1/1 mole)		KCl–NaCl (1/1 mole)	(+)

As written above, the half-cell to the left was the reference electrode as described previously, and the half-cell to the right contained the indicator electrode, which in this case was a long silver wire spot-welded to a platinum wire lead. The container for the solution of the indicator electrode consisted of a 250 ml. silica beaker placed in a tubular electric furnace. The entire apparatus is shown in Fig. 1. During a run, oxygen-free

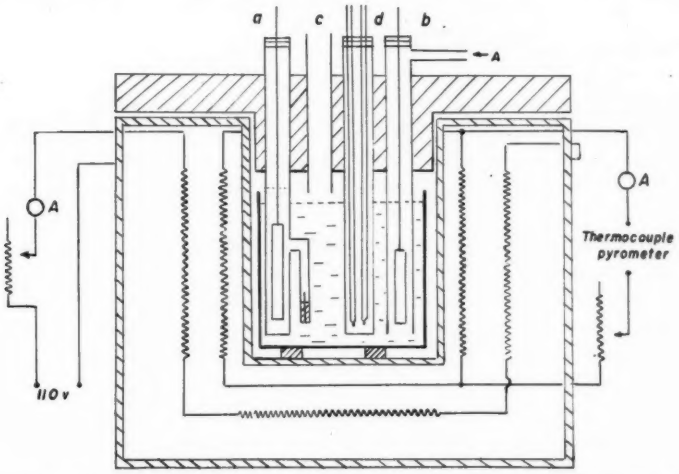

FIG. 1. Apparatus diagram. *a*—Silver – silver chloride reference electrode. *b*—Indicator electrode (Ag or Co). *c*—Feeding tube. *d*—Temperature control and temperature measuring thermocouples.

argon was preheated and bubbled into the melt through the indicator electrode, both to provide stirring of the solution and to prevent the development of temperature gradients within the melt.

The tubular electric furnace used in these experiments was heavily insulated with successive layers of insulation brick and vermiculite. The furnace was heated by two series of elements. The current through the outer cylindrical elements was regulated by means of a variable transformer. The current through the inner elements was controlled with both a variable transformer and a thermocouple pyrometer controller. This method of heating improved the temperature control within the furnace and increased the

durability of the elements. Temperature control within ±3° C. at 1000° C. was achieved. The temperature of the melt was measured separately with a calibrated Pt – Pt 13% Rh thermocouple. During the measurements, the reference and indicator electrodes and the two thermocouples (enclosed in silica tubing) were immersed in the melt to ensure that all were at the same temperature.

When not in use, the reference half-cell was cleaned by dipping in pure molten alkali chlorides and was stored at operating temperature inside the furnace. Its potential was checked occasionally against a similar reference electrode which had been freshly prepared.

All potential measurements were made with a Leeds & Northrup Type K potentiometer which, in the range 0–1.6 volts, had a precision of 0.00001 volt.

Results

Solutions of different concentrations of AgCl in the chloride melt solvent were prepared, and the potential of the indicator electrode was measured against the reference at a temperature of 700° C. The results of these experiments are shown in Fig. 2 *a*, from which it is evident that the relationship between $\log(x_2/x_1)$ (where x_1 and x_2 are respectively the mole fractions of AgCl in the reference and indicator electrodes) and the electromotive force is linear, as required from theory. The slope of the line in the figure is 0.192. The slope calculated from the Nernst equation

$$[1] \qquad E_{\text{cell}} = (2.303RT/\mathcal{F})\log(x_2/x_1),$$

where $R = 1.987$ cal. deg.$^{-1}$ mole^{-1},

$\mathcal{F} = 23{,}060$ cal./abs. volt gram equivalent,

and $T = 973.2°$ K.,

is 0.193. The excellent agreement between the theoretical and experimental values indicates that there is no change in the activity coefficient for AgCl in this medium for the range of concentrations considered in the experiment, i.e. from 1.10×10^{-3} to 6.35×10^{-2} mole fraction.

The effect of temperature on the electromotive force of a concentration cell was determined for temperatures between 650° and 950° C., and the results are given in Fig. 2 *b*. The relationship between temperature and electromotive force is linear with a slope of 3.60×10^{-4} volt/degree, which is in excellent agreement with the theoretical slope of 3.495×10^{-4} volt/degree.

To test the reversibility of the Ag–AgCl electrode, two similar half-cells with different AgCl concentrations were short-circuited for a period of 5 minutes and their potentials then measured against a third reference. The observed changes in potential before and after short-circuiting were of the order of 0.5–1 mv., which could be attributed to temperature gradients within the cells or to small changes in concentration during the short-circuiting. This is in good agreement with the results obtained by Senderoff and Brenner in a similar test of their reference electrode (14).

To study the possible formation of complexes between silver chloride and the alkali chloride melt solvent, the electromotive force of a concentration cell in which the reference electrode contained only pure molten silver chloride was measured.

Ag	AgCl (x)	Asbestos fiber	AgCl	Ag
(−)	KCl–NaCl (1/1 mole)			(+)

The electromotive force of this cell should be a function of both the individual electrode potentials (E_e) and the liquid junction potential (E_L),

$$[2] \qquad E_{\text{cell}} = E_e + E_L.$$

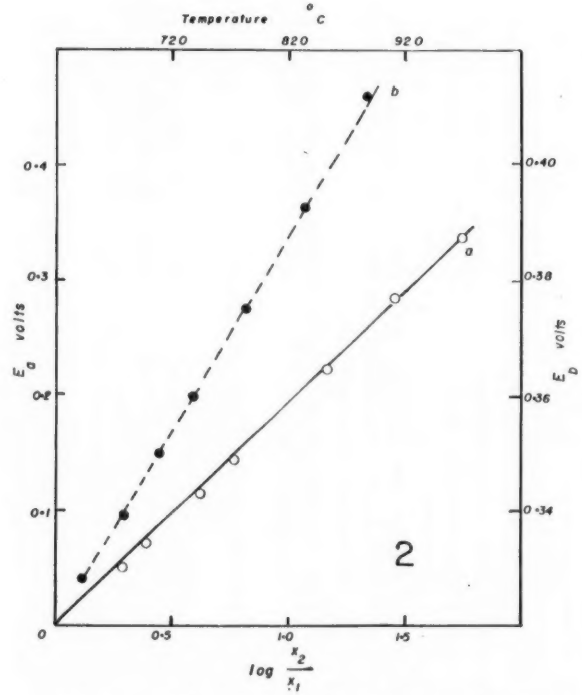

FIG. 2. *a*—Electromotive forces (E_a) of a silver – silver chloride concentration cell as a logarithmic function of silver chloride concentrations at a constant temperature of 700° C. The mole fraction of silver chloride in the reference electrode is 1.10×10^{-3}.

b—Electromotive forces (E_b) of the same cell as above as a function of temperature at constant silver chloride concentrations ($x_1 = 1.10\times10^{-3}$ and $x_2 = 6.35\times10^{-2}$ mole fraction).

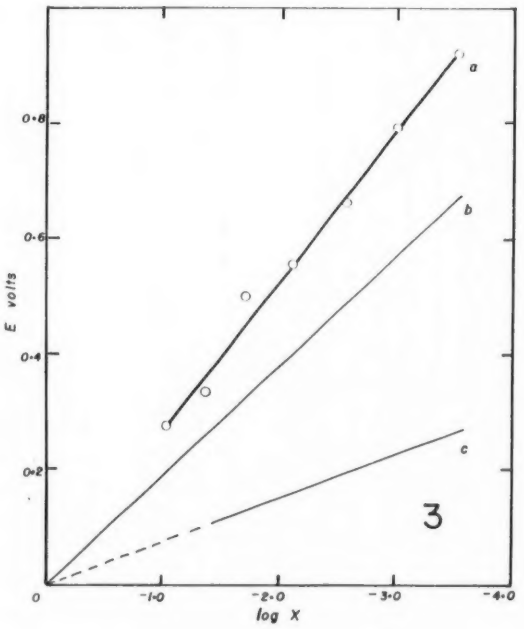

FIG. 3. Electromotive forces of the cell:

$$\mathrm{Ag}\ \Big|\ \begin{matrix}\mathrm{AgCl}\ (x)\\ \mathrm{KCl\text{-}NaCl}\\ (1/1\ \mathrm{mole})\end{matrix}\ \Big\|\ \mathrm{AgCl}\ \Big|\ \mathrm{Ag}$$

as a logarithmic function of silver chloride concentration. *a*—Experimental results. *b*—Calculated values. *c*—Liquid junction potentials (*a*–*b*).

In the case of complex formation, where K is the dissociation constant of the complex $AgCl_n^{(n-1)-}$ the electrode potential is given by the equation

$$[3] \qquad E_e = (2.303RT/\mathcal{F})\log(1/x)+(2.303RT/\mathcal{F})\log(f_s/K.f_c),$$

where f_s and f_c are respectively the activity coefficients of the simple and complex ions. The liquid junction potential is given by an equation of the general form (6)

$$[4] \qquad E_L = \frac{-2.303RT}{\mathcal{F}}\int_{c_1}^{c_2}\sum_i t_i\, d\log(x_i f_i),$$

where x_i is the mole fraction of the ith molecular species,
f_i is the corresponding activity coefficient,
and t_i is the transference number.
By a combination of equations [2], [3], and [4], an expression of the following form is obtained:

$$[5] \qquad \left[E_{cell} - \frac{2.303RT}{\mathcal{F}}\log\frac{1}{x}\right] = \frac{-2.303RT}{\mathcal{F}}\int_{c_1}^{c_2}\sum_i t_i\, d\log x_i - \frac{2.303RT}{\mathcal{F}}\left[\int_{c_1}^{c_2}\sum_i t_i\, d\log f_i - \log\frac{f_s}{Kf_c}\right].$$

Since this equation is linear with respect to $[E_{cell}-(2.303RT/\mathcal{F})\log(1/x)]$ and $\log x$, it follows that a plot of these quantities should be a straight line with an intercept equal to the second parenthetical term of equation [5].

Experimental results plotted in Fig. 3 *c* show that this relationship is linear, as expected. However, when the straight line is extrapolated to unity mole fraction ($\log = 0$), it passes through the origin, thus indicating that no complex is formed between the AgCl and the solvent. Based on this observation, the activity coefficient of AgCl in the melt for this range of concentrations can then be considered as unity. From equation [5], it is seen that the slope of the straight line is a function of several factors which are at present unknown and could not be resolved in the present investigation.

From Fig. 3 *c*, it is possible to derive an empirical relationship for the potential of a reference half-cell using AgCl diluted with KCl–NaCl, against a reference using pure AgCl at 700° C.:

$$[6] \qquad E_L = 0.075\log x.$$

From the experimental results above, it follows that the Ag|AgCl electrode, as constructed, is both reversible and thermodynamically predictable. The absence of complex formation between AgCl and the solvent indicates that it can be used to study the formation of other complexes in melts.

B. ELECTROMOTIVE FORCE MEASUREMENTS ON A SILVER – SILVER CHLORIDE, COBALT – COBALTOUS CHLORIDE VOLTAIC CELL

Having established the reversibility and reproducibility of the silver – silver chloride reference electrode, the electromotive force of the following voltaic cell was measured as a function of cobaltous chloride concentration and temperature:

Co	$CoCl_2$ (x_2)		Asbestos fiber	AgCl (x_1)	Ag
(−)	KCl–NaCl (1/1 mole)	‖		KCl–NaCl (1/1 mole)	(+)

The half-cell to the right is the reference electrode, the half-cell to the left is the indicator electrode, and x_1 and x_2 are respectively the mole fractions of silver chloride and cobaltous chloride in the two solutions. Voltaic cells of this type are practically free of liquid junction potential, owing to the presence of a great excess of the same melt solvent on both sides of the junction.

The design of the indicator electrode was similar to that described for silver in section A. A clean block of cobalt metal (99.9% pure), connected to a platinum wire lead, was inserted in the silica tubing of the indicator half-cell. The electrode was immersed in the molten electrolyte in the cell under a protective stream of oxygen-free argon; when electromotive force measurements were to be made the argon flow was interrupted, because the voltages were unsteady when the gas was bubbling through the electrolyte.

Results

The electromotive force of the silver – silver chloride, cobalt – cobaltous chloride voltaic cell was measured at 710° C. at different cobaltous chloride concentrations. Anhydrous cobaltous chloride was pelletized and added as required to the melt in the cell through a silica feeding pipe leading over the surface of the melt. The results of these measurements are shown in Table I.

TABLE I

ELECTROMOTIVE FORCES OF A COBALT–SILVER VOLTAIC CELL AS A FUNCTION OF COBALTOUS CHLORIDE CONCENTRATION

Mole fraction of AgCl (x_1)	Mole fraction of CoCl (x_2)	E_{cell} (volts)
6.103×10^{-2}	7.60×10^{-4}	0.3935
6.103×10^{-2}	1.80×10^{-3}	0.3560
6.103×10^{-2}	3.90×10^{-3}	0.3242
6.103×10^{-2}	8.40×10^{-3}	0.2894
6.103×10^{-2}	2.05×10^{-2}	0.2511
6.103×10^{-2}	3.97×10^{-2}	0.2206
6.103×10^{-2}	5.07×10^{-2}	0.2054
6.103×10^{-2}	6.12×10^{-2}	0.1950

The over-all cell reaction in an ideal solution would be

$$Co + 2AgCl = CoCl_2 + 2Ag$$

and the cell voltage can be expressed by the Nernst equation in the form:

[7] $$E_{cell} = (E^\circ_{Co} - E^\circ_{Ag}) - (2.303RT/2\mathcal{F})\log(x_2/x_1^2),$$

where E°_{Co} and E°_{Ag} are respectively the standard electrode potentials of the half-cells Co| $CoCl_2$ and Ag | AgCl, under the conditions of the experiment.

From equation [7], it follows that the relationship between E_{cell} and $\log(x_2/x_1)$ should be linear, and that when x_1 and x_2 are chosen so that the log term of this equation becomes zero, then

$$E_{cell} = E^\circ_{Co} - E^\circ_{Ag}.$$

When the electromotive force of the cell is plotted against $\log(x_2/x_1^2)$, as calculated from the experimental data given in Table I, the results can be represented by a straight line which deviates from linearity at values higher than 4×10^{-2} mole fraction of $CoCl_2$. This is shown in Fig. 4, from which it is found that

$$E^\circ_{Co} - E^\circ_{Ag} = 0.324 \text{ volt.}$$

The accuracy of this value is difficult to establish, but in duplicate experiments it was observed that the value could be reproduced within 0.002 volt. The slope of the linear part of the plot is 0.103 volt, which agrees well with 0.0975 volt calculated from equation [7] for a two-electron electrode process.

The major part of the curve, which is linear, indicates that the activity coefficient of $CoCl_2$ is essentially constant, although small deviations occur at higher mole fractions.

The effect of temperature change on the electromotive force of this voltaic cell was also investigated. The results of these measurements for a temperature range between 650° and 850° C. are shown in Table II.

TABLE II

THE EFFECT OF TEMPERATURE ON THE ELECTROMOTIVE FORCE OF THE CELL Co | $CoCl_2$ in KCl–NaCl || AgCl in KCl–NaCl | Ag, for AgCl and $CoCl_2$ mole fractions of 6.10×10^{-2} and 6.12×10^{-2}, respectively

T, ° K.	E_{cell}, experimental (volts)	$E^\circ_{Co}-E^\circ_{Ag}$, calculated (volts)
On heating		
925	0.2194	0.3309
947	0.2100	0.3243
949	0.2113	0.3262
983	0.1950	0.3129
1003	0.1873	0.3083
1028	0.1797	0.3037
1049	0.1732	0.2996
1070	0.1669	0.2958
1097	0.1543	0.2912
1119	0.1540	0.2884
On cooling		
1090	0.1668	0.2981
1081	0.1688	0.2989
1050	0.1792	0.3057
1012	0.1910	0.3126
984	0.1983	0.3170
961	0.2008	0.3169

Included in the table are $E^\circ_{Co}-E^\circ_{Ag}$ values calculated from the experimental results using equation [7]. From these data, using the equations

$$\Delta F^\circ = -nE^\circ\mathcal{F}, \qquad [8]$$

$$\Delta F^\circ = -2.303\,RT\log K \qquad [9]$$

it was possible to calculate, for various temperatures, the effective equilibrium constant for the reaction

$$Co + 2AgCl \rightarrow CoCl_2 + 2Ag.$$

This equilibrium constant is understood to include any effects on the reaction due to the presence of the melt solvent. The results of these calculations are shown in Fig. 5, where $\log K$ is plotted against the reciprocal of the absolute temperature. It is seen that the curve is linear over this temperature range, i.e. 650° to 850° C. In Fig. 5, the best straight line was calculated from the experimental results applying the least squares method. The average deviation of $\log K$ from the experimental values is only ±0.027.

The heat of the reaction taking place in the cell, which is the difference between the

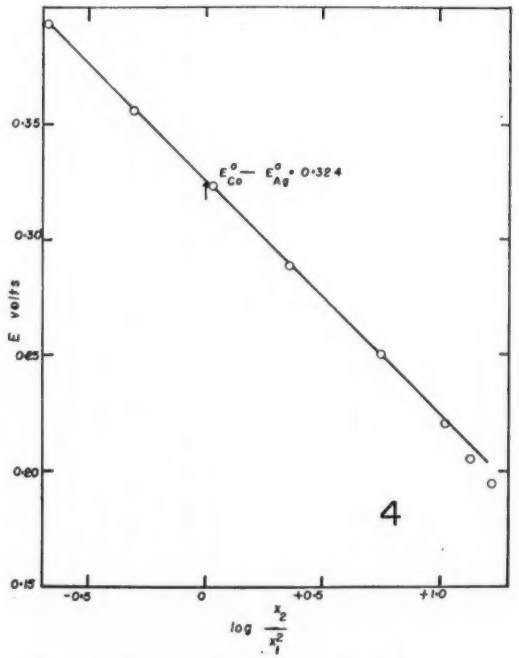

FIG. 4. Electromotive forces of the cell:

$$\mathrm{Co} \;\Big|\; \begin{matrix} \mathrm{CoCl_2}\,(x_2) \\ \mathrm{KCl\text{-}NaCl} \\ (1/1\ \mathrm{mole}) \end{matrix} \;\Big\|\; \begin{matrix} \mathrm{AgCl}\,(x_1 = 6.1\times10^{-2}) \\ \mathrm{KCl\text{-}NaCl} \\ (1/1\ \mathrm{mole}) \end{matrix} \;\Big|\; \mathrm{Ag}$$

as a function of $\log (x_2/x_1^2)$, at a constant temperature of 710° C.

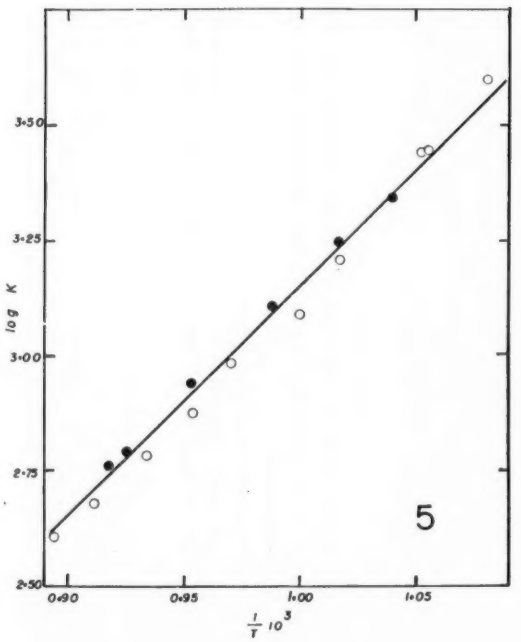

FIG. 5. The variation of log K with the reciprocal of temperature for the system:

$$\mathrm{Co} \;\Big|\; \begin{matrix} \mathrm{CoCl_2}\,(x_2 = 6.12\times10^{-2}) \\ \mathrm{KCl\text{-}NaCl}\,(1/1\ \mathrm{mole}) \end{matrix} \;\Big\|\; \begin{matrix} \mathrm{AgCl}\,(x_1 = 6.10\times10^{-2}) \\ \mathrm{KCl\text{-}NaCl}\,(1/1\ \mathrm{mole}) \end{matrix} \;\Big|\; \mathrm{Ag}$$

○ With increasing temperature. ● With decreasing temperature.

heats of formation of cobaltous chloride and silver chloride in the melt, can be calculated with the aid of the van't Hoff equation,

$$[10] \qquad d \ln K/dT = \Delta H_r/RT^2.$$

The heat of reaction thus obtained from the slope of the straight line in Fig. 5 is:

$$\Delta H_r = -22.8 \pm 1.3 \text{ kcal.}$$

DISCUSSION

In the foregoing experimental work, a standard electrode potential for cobalt was calculated for the conditions of the experiments. The exact thermodynamic significance of this potential will now be discussed.

By definition, the standard electrode potential of a voltaic cell is given by the algebraic sum of the standard single electrode potentials of the two constituent half-cells. This in turn is defined as the potential of the electrode when the species involved in the electrode process are at unit activity.

When dealing with molten salt solutions, it will be realized that the fundamental method of expressing concentrations is by mole fractions. This implies that a mole fraction of unity represents the pure solute without solvent. Thus, in the case of the Co–Ag voltaic cell, the standard electrode potential is defined as the electromotive force of the cell

$$\text{Co} \mid \text{CoCl}_2 \ (x_2 = 1) \parallel \text{AgCl} \ (x_1 = 1) \mid \text{Ag}.$$

Because of the unknown boundary potential, the experimentally measured electromotive force would not represent the standard electrode potential. However, the standard potential can be calculated from the theoretical data of Hamer, Malmberg, and Rubin (7), as

$$E^\circ_{Co} - E^\circ_{Ag} = 0.193 \text{ volt at } 710^\circ \text{ C.}$$

A comparison of the theoretical value calculated above with that obtained in these experiments (0.324 volt) is of interest because of the indicated lack of ideality in molten salt solutions. Since the AgCl–KCl–NaCl system was shown earlier in this paper to be ideal, the deviation must be attributed to a non-ideality in the $CoCl_2$–KCl–NaCl system, and may represent either a difference in activity or a tendency to complex formation with the solvent, or both. From available data, these effects cannot be differentiated and, in any case, they could be expressed entirely as a complexing tendency.

On the assumption of complex formation, it is possible to calculate the dissociation constant of the cobaltous chloride complex ion in the molten alkali chloride solvent by application of equations [8] and [9]. In this calculation, E° of equation [8] was replaced by the difference between the experimental and theoretical standard electrode potentials. This difference is -0.131 volt, and the resulting dissociation constant is 4.5×10^{-2}, which indicates a weak complex.

REFERENCES

1. Blickslayer, H. J. Rec. trav. chim. **46,** 305 (1927).
2. Bockris, J. O'M., Hills, G., Inman, D., and Young, L. J. Sci. Instr. **33,** 438 (1956).
3. Delimarski, Yu. Zhur. Obshcheĭ Khim. **26,** 2968 (1956).
4. Delimarski, Yu. Zhur. Fiz. Khim. **29,** 28 (1955).
5. Flengas, S. and Rideal, E. Proc. Roy. Soc. A, **233,** 443 (1956).
6. Glasstone, S. Introduction to electrochemistry. D. Van Nostrand Company, Inc., New York. 1951. p. 211.
7. Hamer, W., Malmberg, M., and Rubin, B. J. Electrochem. Soc. **103,** 8 (1956).

8. LEWIS, G. Z. Phys. Chem. **52,** 310 (1905).
9. LORENZ, R. and KAUFLER, F. Die Elektrolyse Geschmolzener Selze. Verlag von Johann Ambrosius Bartz, Leipzig. 1909.
10. SALSTROM, E. and HILDEBRAND, J. J. Am. Chem. Soc. **52,** 4641 (1930).
11. SALSTROM, E. J. Am. Chem. Soc. **53,** 1794 (1931).
12. SALSTROM, E. and HILDEBRAND, J. J. Am. Chem. Soc. **54,** 4257 (1932).
13. SALSTROM, E., KEW, T., and POWELL, T. J. Am. Chem. Soc. **58,** 1848 (1936).
14. SENDEROFF, S. and BRENNER, A. J. Electrochem. Soc. **101,** 31 (1954).
15. VERDIECK, R. and Yntema, L. J. Phys. Chem. **46,** 344 (1942).
16. WACHTER, A. and HILDEBRAND, J. J. Am. Chem. Soc. **52,** 4655 (1930).

A DETERMINATION OF THE SURFACE FREE ENERGY OF SODIUM CHLORIDE[1]

F. VAN ZEGGEREN[2] AND G. C. BENSON

ABSTRACT

The surface free energy for the interface between crystalline sodium chloride and a saturated alcoholic solution was determined from the solubility of sodium chloride in absolute ethyl alcohol as a function of the particle size of the salt. At 298° K. a value of 171 ergs/cm.^{2} was found. A general discussion of the validity of the Ostwald equation, which relates solubility and particle size, is presented.

I. INTRODUCTION

The solubility of a solid in a liquid depends upon its particle size. The relationship governing this dependence was derived for spherical particles by Ostwald (11) and applied only to non-ionic materials. Jones (8) gave an extension of Ostwald's theory for ionic compounds and derived a general formula for the case where the solid is only partly dissociated after dissolving in the liquid. Dundon and Mack (5) pointed out that Jones' rather complicated expression could be approximated quite well by the equation

$$[1] \qquad i(RT/M)\ln(c_F/c_B) = 2\gamma/\rho r,$$

where c_F and c_B are the concentrations of solutions saturated with respect to fine particles of radius r and bulk material respectively. The differential surface Gibbs free energy γ, which will be referred to as the surface free energy in this paper, is the derivative of the Gibbs free energy ($G = E - TS + pV$) of the solid with respect to its area A at constant temperature T, pressure p, and number of moles n, i.e.

$$[2] \qquad \gamma = (\partial G/\partial A)_{T,p,n}.$$

It is important to note that γ is a function of the particular interface and thus depends on the nature of the medium surrounding the solid. The other quantities in Eq. [1] are R, the gas constant, M, the molecular weight of the material, ρ, its density, and i, the van't Hoff factor

$$[3] \qquad i = 1 + \alpha(\nu - 1),$$

where α is the fraction of the molecules of the material which dissociate upon solution and ν is the number of ions produced by the dissociation of one molecule.

Few measurements of surface free energies based on the use of Eq. [1] have been carried out to date. Dundon and Mack (5) and Dundon (4) obtained values of the surface free energies of $CaSO_4.2H_2O$, $BaSO_4$, $SrSO_4$, CaF_2, PbF_2, PbI_2, and Ag_2CrO_4. In each case the finely divided salt was added to an aqueous solution saturated with respect to bulk material and the increase in solubility determined from conductivity measurements. However, they examined only one fine sample of each salt and thus did not establish the linear relation between $\ln(c_F/c_B)$ and $1/r$. Also their use of Eq. [1] involved the assumption that the particles were spherical in shape.

[1]*Manuscript received June 20, 1957.*
Contribution from the Division of Pure Chemistry, National Research Council, Ottawa, Canada.
Issued as N.R.C. No. 4466.
[2]*National Research Council Postdoctorate Fellow 1955–56. Present address: Central Research Laboratory, Canadian Industries Limited, McMasterville, Quebec.*

In Section II of the present paper a generalized form of the Ostwald equation is derived. This is followed in Section III by a description of a new experimental investigation of the solubility of sodium chloride in absolute alcohol as a function of the particle size of the salt; the new data are used to obtain a value of the surface free energy of this compound. The validity of the method in the light of certain criticisms of Eq. [1] is considered in Section IV and the significance of the result for the surface free energy in relation to other experimental and theoretical data is discussed in the last section.

II. DERIVATION OF THE FUNDAMENTAL EQUATION

The change in the energy E of a one-component system is expressed in terms of changes in the entropy S, volume V, and number of moles n of substance X by the equation

$$dE = TdS - pdV + \mu dn, \tag{4}$$

where μ is the chemical potential. In this equation it is assumed that surface effects are negligible. A simple extension of Eq. [4], when the system possesses an appreciable surface area A, is the addition of another work term γdA giving

$$dE = TdS - pdV + \gamma dA + \mu dn. \tag{5}$$

Next suppose that the system remains isomorphic, i.e. the shape is preserved when its size is changed. In this case A and V are not independent variables since

$$A = qV^{2/3}, \tag{6}$$

where q is a constant for a given shape and Eq. [5] becomes

$$dE = TdS - (p - \tfrac{2}{3}\gamma\rho\mathscr{A})dV + \mu dn. \tag{7}$$

The symbol $\mathscr{A}$ is used to represent the specific surface (i.e. the area per unit mass). It can be readily shown that the conditions for equilibrium between the present system and another (external) phase which contains X as a component are equality of the temperature in the two phases, equality of the chemical potential of X in the two phases, and a pressure p_{ext} in the external phase such that

$$p_{ext} = p - \tfrac{2}{3}\gamma\rho\mathscr{A}. \tag{8}$$

For a spherical shape (radius r) this last equation becomes

$$p_{ext} = p - 2\gamma/r \tag{9}$$

and in the case of a cube (edge l)

$$p_{ext} = p - 4\gamma/l. \tag{10}$$

Eq. [9] is the well-known formula for the pressure difference across the surface of a liquid drop. Application of Eqs. [5] and [8] to a solid assumes that it is possible to use, as a first approximation, a single or average value of γ for the various parts of the surface and that it is meaningful to consider the pressure within the solid to be homogeneous.

We now consider the difference in chemical potential of two isomorphic particles F and B differing in size but having the same temperature and value of the external pressure. In general

$$d\mu = \left(\frac{\partial\mu}{\partial T}\right)_{p,A,n} dT + \left(\frac{\partial\mu}{\partial p}\right)_{T,A,n} dp + \left(\frac{\partial\mu}{\partial A}\right)_{T,p,n} dA + \left(\frac{\partial\mu}{\partial n}\right)_{T,p,A} dn. \tag{11}$$

By applying Euler's theorem for homogeneous functions to γ and to μ it can be shown that the last two terms of the above equation vanish on the basis of the usual assumption that

$$[12] \qquad (\partial\gamma/\partial A)_{T,p,n} = 0.$$

Thus for constant temperature Eq. [11] becomes

$$[13] \qquad d\mu = (\partial\mu/\partial p)_{T,A,n}\, dp = (\partial V/\partial n)_{T,p,A}\, dp = \bar{V}dp,$$

where $\bar{V}$ is the molar volume. In obtaining the approximation on the right side of Eq. [13], $(\partial\gamma/\partial p)_{T,A,n}$ has been neglected. Assuming the compressibility of the solid is small, Eq. [13] can be integrated to give

$$[14] \qquad \mu_F - \mu_B = \bar{V}\Delta p = \bar{V}\tfrac{2}{3}\gamma\rho[\mathscr{A}_F - \mathscr{A}_B.$$

In the case where B is bulk material the specific surface $\mathscr{A}_B$ is negligibly small and

$$[15] \qquad \mu_F - \mu_B = \tfrac{2}{3}\, M\gamma\mathscr{A}_F.$$

Finally, suppose that there are two solutions containing substance X in some suitable solvent at the same temperature T, the same pressure p_{ext}, and at concentrations such that particle F can exist in equilibrium with one solution and particle B with the other. Then

$$[16] \qquad \mu_F - \mu_B = \Delta\mu_{soln} = RT\ln(a_F/a_B),$$

where a_F and a_B are the activities of X in the two solutions. Combining Eqs. [15] and [16] leads to the fundamental formula

$$[17] \qquad \tfrac{2}{3}\gamma\mathscr{A}_F = (RT/M)\ln(a_F/a_B).$$

This result is quite general and holds regardless of the extent of dissociation of X into ions upon solution. It thus contains Dundon and Mack's formula as a particular case.

Another special form of Eq. [17] is required for application to the data to be described in the next section. This is obtained by assuming that X is completely dissociated in the solution and that each molecule produces ν_i ions of species i, where

$$[18] \qquad \nu = \sum_i \nu_i.$$

The activity a can then be expressed in terms of the molar concentration c and the stoichiometric mean ionic molar activity coefficient $y_\pm$ by the relation

$$[19] \qquad a = c^\nu\, y_\pm^{\,\nu} \prod_i \nu_i^{\nu_i}.$$

Substituting this formula for a_F and a_B in Eq. [17] gives the result

$$[20] \qquad \tfrac{2}{3}\gamma\mathscr{A}_F = (\nu RT/M)\ln[(cy_\pm)_F/(cy_\pm)_B].$$

III. CONDUCTIVITY MEASUREMENTS

The increase in solubility when finely divided sodium chloride was added to a normally saturated solution of this salt in absolute alcohol was determined by measuring the increase in conductivity of the solution (13). Samples of finely divided salt with different specific surface areas were prepared by electrostatic precipitation of a sodium chloride smoke (16). Surface areas were determined by the BET method using nitrogen at 77° K.

The conductance measurements were made with an a-c. bridge built from standard components around a Leeds and Northrup Campbell-Shackelton shielded ratio box (1) with a Wagner earth connection. A frequency of 1000 cycles per second was used and the bridge balance point was detected with an oscilloscope (7) using a phase shift circuit (10) which facilitated the separation of the resistive and capacitative components. All measurements were made in a pyrex glass conductivity cell with platinum electrodes which was thermostated in a small oil bath at 25.00±0.02° C.

A saturated solution was prepared by adding coarse salt to water-free ethyl alcohol and leaving the solution in contact with excess solid for 24 hours at 25° C. At the end of this time the conductivity of this solution was measured at intervals of 2 minutes for about one-half hour. After a constant value was established, about 500 mg. of a fine salt sample was added to the solution. The resistance decreased rapidly and a minimum value was reached after a period of about one hour. Then, owing to recrystallization of the fine particles, the resistance started to increase but the latter process went very slowly and in fact took several hours before any appreciable increment could be determined. The minimum value of the resistance was taken to correspond with the saturated solution in equilibrium with the fine material added. In calculating the specific conductivity, the observed resistance was corrected for the capacity of the solution and the specific conductance of the alcohol.

A calibration graph was constructed from measurements of the specific conductivities of solutions just below the normal saturation point. It was found that a plot of specific conductivity against the square root of the concentration relative to a selected standard concentration gave a straight line and this was extrapolated to concentrations above the saturation point. This procedure had the advantage that it was unnecessary to know the absolute value of the concentration of any of the solutions. Using the conductivities of the solutions in equilibrium with coarse and fine salt, the root of the concentrations relative to that of the standard solution could be read from the graph and the concentration ratio c_F/c_B readily obtained. Values of this ratio for a number of salt samples with different specific surfaces are given in Table I.

TABLE I

Area $\mathscr{A}_F$ in m.²/g.	Concentration ratio c_F/c_B
1.2	1.0000
1.2	1.0030
3.8	1.0128
8.2	1.0189
11.6	1.0206
14.2	1.0157
15.9	1.0248
26.7	1.0517
30.6	1.0357
35.9	1.0461
42.5	1.0671

Assuming that NaCl is completely dissociated in ethyl alcohol, Eq. [20] with $\nu = 2$ and $T = 298.16°$ K. leads to the formula

$$\log_{10}(c_F/c_B) = 3.4135\times10^{-6}\,\gamma\mathscr{A}_F, \qquad [21]$$

where γ is expressed in ergs/cm.², $\mathscr{A}_F$ in m.²/g., and the ratio of the activity coefficients has been set equal to unity. In Fig. 1 $\log_{10}(c_F/c_B)$ is plotted as a function of the specific

area $\mathscr{A}_F$. The correlation obtained is approximately linear. The slope of the least square line through the points gives a value of $\gamma = 171$ ergs/cm.^{2} for the surface free energy with a probable error of about 12 ergs/cm.^{2} Since the {100} face is the one occurring for sodium chloride under normal conditions, the result obtained for γ should be associated with the interface between a {100} surface of the crystal and a saturated alcoholic solution at

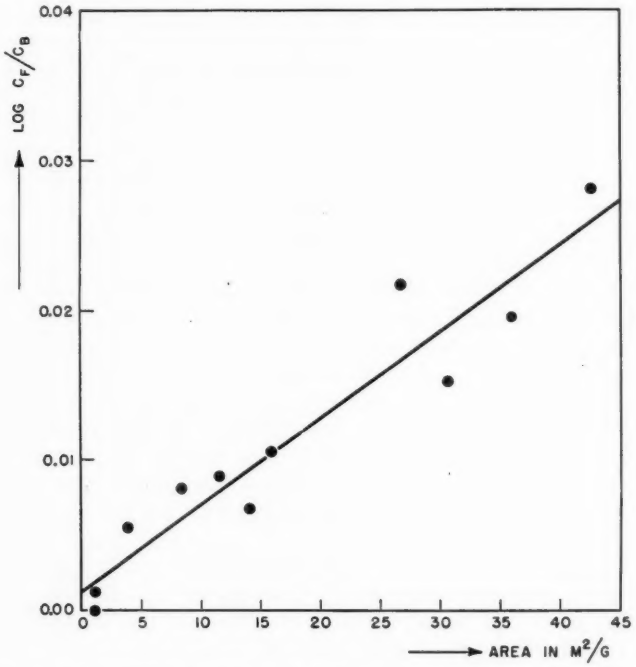

FIG. 1. Log $_{10}(c_F/c_B)$ plotted as a function of the specific surface $\mathscr{A}_F$ in m.^{2}/g. The slope of the least square line gives a value $\gamma = 171$ ergs/cm.^{2} for the surface free energy.

298° K. The fact that the least square line in Fig. 1 does not pass through the origin is not significant since the intercept 0.0013 has a probable error of 0.0009.

IV. CRITIQUE OF THE METHOD

The formula for the solubility of a solid particle in a liquid, Eq. [1], has been the subject of severe criticism. Harbury (6) stated that this equation is unsuitable even as a first approximation for determining the surface free energy. The points which led to this conclusion will be reconsidered here and their relevance to the present investigation assessed.

(*a*) According to Harbury it is not permissible to consider the transformation accompanying crystal breakdown by solution in the same way as for example the transition between an amorphous solid and a liquid. We believe this criticism is more applicable to non-equilibrium aspects of the problem such as the rate of the solution process and that the final equilibrium state can be treated by ordinary thermodynamics.

(*b*) For very small particles the surface free energy and the density will change with the size of the particles and in the case of particles containing only a few molecules the concept

of surface free energy needs clarification. The largest specific surface (42.5 m.²/g.) used in the present work corresponds to particles with an average cube edge larger than 650 Å. A particle of this size still contains about 10^7 molecules of sodium chloride and it is not likely that the values of γ or ρ will differ appreciably from their values for bulk material.

(*c*) In the case of highly soluble compounds the values for the saturation concentrations for coarse and fine salt will be high and the dissolved material will, according to Harbury, no longer follow the ideal osmotic law. However, our Eq. [20] has been derived in terms of activities and the only assumption needed to obtain Eq. [21] was that the activity coefficients, which vary only slowly with the concentration, were nearly equal in the two solutions. In justification of this it may be noted that the concentration of a saturated solution of sodium chloride in alcohol at 25° C. is quite small (about 0.01 *N*) and that the increases in concentration due to the particle size effect were always less than 7%.

(*d*) Both Harbury and Jones (8) have stated that departure from a spherical shape might give marked changes in the concentration ratio. In our own derivation it was shown that a similar relation is valid for any particular shape provided that the shape remains the same for changes in size. Sodium chloride is a very favorable case since it has a strong tendency to crystallize in cubes with faces all of the same {100} type.

(*e*) Harbury has noted that there are a great many difficulties inherent in the preparation of small particles suitable for this type of work. Impurities and defects are often introduced in the course of such preparation. In the present case a study (16) of the purity of sodium chloride produced by electrostatic precipitation has shown that it is possible to reduce such contamination to a negligible amount. Harbury also suggested the possibility of preferential adsorption of ions which might cause a larger stability of small particles in the presence of big ones. However, provided factors like the surface free energy and surface roughness are the same for small and big particles the reasons for this preference are lost.

Finally there are the problems of producing uniform surfaces free from structural effects and of ensuring a single size of crystal in a sample rather than a distribution of sizes. As pointed out in (*d*) sodium chloride crystals generally are cubic and involve only one type of face, but at any finite temperature there will always be some surface structure present owing to thermal fluctuations. However, provided the individual faces still involve a fairly considerable number of ions this structure will on the average be the same for all faces in thermal equilibrium. The work of Benson, Schreiber, and van Zeggeren (3) offers some evidence in support of this view. These authors determined the surface enthalpy of sodium chloride by measuring the difference in the heat of solution of coarse and fine salt. The results indicated that to a good approximation the surfaces of the small crystals can be considered as uniform in the sense that the surface contribution to the heat of solution varies linearly with the specific surface of the fine material. The question of the distribution of particle sizes is of greater importance in the surface free energy determination than in the surface enthalpy investigation. Undoubtedly the samples of fine salt contain a distribution of particle sizes. The scatter of the points in Fig. 1 is larger than estimates of the experimental error and may arise from this source. Nevertheless the fact that there is a roughly linear relation in Fig. 1 can be interpreted as indicating that the distribution must be fairly sharp.

V. DISCUSSION

From the considerations (*a*) to (*e*) outlined above it appears that use of the Ostwald type of equation is justified under the present circumstances and that the value of $\gamma = 171$

ergs/cm.^{2} obtained should be a reasonable approximation to the surface free energy of the interface. There are no data available in the literature for a direct comparison with this value. At absolute zero and for moderate pressures the surface free energy is the same as the surface enthalpy and the surface energy. As a general rule the surface free energy decreases and the surface enthalpy increases as the temperature is raised.

Shuttleworth (12) and also van Zeggeren and Benson (15) have calculated a value of about 189 ergs/cm.^{2} at 0° K. for the surface energy of a {100} face of an undistorted sodium chloride crystal using the classical theory of ionic crystals. Estimates of distortion corrections based on calculations by Benson, Schreiber, and Patterson (2) lower this to about 112 ergs/cm.^{2} (cf. Ref. 14). Recently van Zeggeren and Benson (14) computed the surface energy of sodium chloride using a simplified quantum mechanical model in which terms corresponding to van der Waals interactions were neglected and no distortion was permitted. The result 187 ergs/cm.^{2} at 0° K. would probably be increased by inclusion of of the higher interaction terms and decreased by distortion effects. It is difficult to estimate the final result but judging from classical calculations the two corrections (+88 ergs/cm.^{2} and −77 ergs/cm.^{2}) cancel within about 10%.

Assuming that the forces between ions of the crystal play the major role in determining the magnitude of the interfacial free energy, our value for the crystal-solution interface may be taken as an approximation to the surface free energy of the solid alone. It then appears that the corrected value for the classical theoretical treatment is too low or that our experimental value is too high. The quantum mechanical result may be consistent with our measurements but this conclusion is not clear-cut because of the use of classical corrections. In connection with the surface enthalpy (3) it was also found that the value predicted by classical theory was lower than the experimental one.

It is interesting to combine our result for the surface free energy with the value 276 ergs/cm.^{2} obtained by Benson, Schreiber, and van Zeggeren (3) for the surface enthalpy, again neglecting the difference in the type of interface. The value of the surface entropy obtained in this way is 0.35 erg/cm.^{2}/deg. at 298° K. The magnitude of this result seems reasonable in view of the value 0.28 erg/cm.^{2}/deg. reported by Jura and Garland (9) for magnesium oxide at 298° K.

ACKNOWLEDGMENTS

We wish to express our thanks to Dr. P. Balk and Dr. E. A. Flood for helpful discussions of the application of thermodynamics to surface problems.

REFERENCES

1. Behr, L. and Williams, A. J. Proc. Inst. Radio. Engrs. **20**, 969 (1932).
2. Benson, G. C., Schreiber, H. P., and Patterson, D. Can. J. Phys. **34**, 265 (1956).
3. Benson, G. C., Schreiber, H. P., and van Zeggeren, F. Can. J. Chem. **34**, 1553 (1956).
4. Dundon, M. L. J. Am. Chem. Soc. **45**, 2658 (1923).
5. Dundon, M. L. and Mack, E. J. Am. Chem. Soc. **45**, 2479 (1923).
6. Harbury, L. J. Phys. Chem. **50**, 190 (1946).
7. Jones, G., Mysels, K. J., and Juda, W. J. Am. Chem. Soc. **62**, 2919 (1940).
8. Jones, W. J. Z. physik. Chem. **82**, 448 (1913).
9. Jura, G. and Garland, C. W. J. Am. Chem. Soc. **74**, 6033 (1952).
10. Lamson, H. W. Rev. Sci. Instr. **9**, 272 (1938).
11. Ostwald, W. Z. physik. Chem. **34**, 495 (1900).
12. Shuttleworth, R. Proc. Phys. Soc. (London), A, **62**, 167 (1949).
13. van Zeggeren, F. Surface energies of alkali halides. Thesis, Amsterdam. 1956.
14. van Zeggeren, F. and Benson, G. C. Can. J. Phys. **34**, 985 (1956).
15. van Zeggeren, F. and Benson, G. C. J. Chem. Phys. **26**, 1077 (1957).
16. van Zeggeren, F., Schreiber, H. P., and Benson, G. C. Can. J. Chem. **34**, 1591 (1956).

ON THE PROTON MAGNETIC RESONANCE SHIFT DUE TO HYDROGEN BONDING[1]

G. J. KORINEK[2] AND W. G. SCHNEIDER

ABSTRACT

In order to investigate further the nature of the proton resonance shifts accompanying hydrogen bonding, and their relation to the properties of the hydrogen bond, the resonance shift of the acceptor molecule chloroform, interacting in turn with a variety of donor molecules, was measured. The donor liquids chosen were $(Et)_3N$, $(Et)_2O$, PrF, $(Me)_2CO$, and EtCN. These are all virtually non-associated in the pure state and may be expected to form simple 1:1 hydrogen-bonded complexes with chloroform, whose existence was confirmed by measuring the binary freezing-point phase diagrams. The difference between the proton shift of chloroform at infinite dilution in each of the donor solvents and at infinite dilution in inert hydrocarbon solvents was taken as the "association" shift representing the difference between chloroform in the hydrogen bonded complex and unassociated chloroform. These shifts correlate well with the expected hydrogen bond strengths in each system and the relative donor strength of the individual solvent molecules. The proton resonance technique appears as a promising method for measuring these properties.

INTRODUCTION

Proton magnetic resonance measurements provide a fruitful method of studying hydrogen bonding as well as other types of molecular interactions. The possibility of applying such measurements for this purpose was generally recognized following the observation by Arnold and Packard (1) that the chemical shift of the proton of the OH group in ethyl alcohol was temperature dependent. An increase in temperature caused the proton signal to shift to higher magnetic field; the signals of the CH_2 and CH_3 groups were virtually unaffected by temperature. It was also observed that solvent dilution of the alcohol had an effect similar to raising the temperature. This behavior was attributed by Liddel and Ramsey (6) to molecular association (hydrogen bonding). Since this involves the hydrogen of the OH group, this hydrogen will experience a different electronic shielding in the associated and unassociated state. More recently, several investigators (3, 4, 10, 11) have studied the molecular interactions of a number of systems by proton resonance measurements. Solvent dilution generally provides a more convenient method of dissociating the interacting molecules than raising the temperature. The dilution shift of the proton signals involved in the interaction is surprisingly large, and is measurable even for rather weak interactions, which may not be detectable by other methods presently available.

The results to date indicate that on hydrogen bonding the signal of the proton in the bond is shifted to lower field relative to its position for the dissociated molecule. (An exception to this may occur when the donor molecule contains an aromatic ring (10).) The nature of the changes in the electron environment of the proton accompanying association, which are responsible for the low-field shift, is not yet well understood. A complete interpretation of these results may in fact have to await a better understanding of the hydrogen bond itself.

The magnitude of the proton resonance shift to low field due to hydrogen bonding may be expected to be proportional to the strength of the bond. If a proportionality of this kind can be demonstrated, the usefulness of the NMR technique for studying hydrogen bonding would be considerably extended. On the other hand a lack of correspondence of

[1]*Manuscript received June 20, 1957.*
Contribution from the Division of Pure Chemistry, National Research Council, Ottawa, Canada.
Issued as N.R.C. No. 4465.
[2]*National Research Council Postdoctorate Fellow.*

the association shift with hydrogen bond strength could conceivably result from anomalous induced paramagnetic effects, arising either in the acceptor or in the donor molecule, when association occurs in the presence of a magnetic field. Such effects may be expected to be highly specific and characteristic of individual molecules.

In order to investigate these questions it was desired to measure the proton resonance shift of an H–X acceptor group interacting in turn with a series of molecules of different donor strengths. In this way hydrogen bonds of different strengths can be formed which can then be correlated with the proton resonance shifts measured under comparable conditions. Ideally the H–X probe molecule should itself be non-associating in the pure state, since otherwise addition of a second substance irrespective of its donor strength will give rise to a dilution shift. For the present work, chloroform was chosen as the acceptor molecule and, although it is weakly self-associating, this can be readily corrected for. The donor molecules, which may be represented by the formula R_xD, where D is the donor atom or group, must likewise be non-associating in the pure state. The molecules $(C_2H_5)_3N$, $(C_2H_5)_2O$, C_3H_7F, $(CH_3)_2CO$, and C_2H_5CN satisfactorily meet this condition and were chosen for the present work. The first three of these contain the atoms N, O, and F, each with approximately sp^3 lone pair donor orbitals with varying donor strength. The O atom in acetone may be regarded as having an sp^2 donor orbital and the N atom in propionitrile a donor orbital approaching an sp hybrid. The advantage of choosing systems of this type is that when they are combined with the chloroform acceptor only dimeric species of the type $R_xD \ldots H–X$ are formed and chain association or the formation of polymeric species is largely avoided.

Direct measurements of hydrogen bond strengths are unfortunately lacking and at present there is no accepted method for obtaining reliable data of this kind. The measured proton resonance shifts of the chloroform hydrogen in each system were correlated with the relative hydrogen bond strengths predicted from theoretical considerations and also, where available, with infrared spectral measurements. Finally, in order to confirm that the expected 1:1 hydrogen-bonded complexes with chloroform actually occur, the binary freezing-point phase diagrams were measured for the systems studied.

EXPERIMENTAL

Reagent grade chloroform was fractionally distilled; the fraction boiling at 61.3±0.2° C. was used in the experiments. Similar purifications were used for triethylamine (b.p. 89.2±0.2° C.) and propionitrile (b.p. 97.0±0.2° C.). We are indebted to the Du Pont Company (Wilmington, Delaware) for supplying us with research samples of ethyl and propyl fluoride. All other chemicals used were of research grade.

The proton resonance measurements were made with a stabilized Varian V-4300 NMR spectrometer, operating at a fixed frequency of 40 Mc./s. Glass sample tubes of 5 mm. o.d. were used, except at low chloroform concentrations where sample tubes of 12 mm. o.d. were used. Sample spinning was employed in all measurements. A sealed capillary containing water was added to the sample tube to provide an external reference signal. Signal separations (in cycles per second) were measured by the side-band technique in the usual way (1). In order that the results of the different solutions can be compared, bulk diamagnetic susceptibility corrections were applied to the measured shifts as described previously (10). Values of the volume susceptibilities used are collected in Table I.

In the case of propyl fluoride the internal standard (methyl signal of the propyl group) was used. In the propionitrile system both external and internal standards were used because of the uncertainty connected with the value for the diamagnetic susceptibility

of propionitrile. The values of the chemical shift at infinite dilution of chloroform differed by 3 c./s. using the two mentioned standards. The value based on the internal standard was used.

TABLE I

VOLUME SUSCEPTIBILITY DATA (c.g.s.m.)

	$\times 10^6$		$\times 10^6$
Water	−0.720	*n*-Hexane	−0.586
Chloroform	−0.731	Triethylamine	−0.636
Cyclohexane	−0.631	Diethyl ether	−0.547
Cyclopentane	−0.661	Propionitrile	−0.551

RESULTS

The self-association of chloroform was found in earlier measurements (10) to give rise to a shift of the proton signal amounting to ~11 c./s. on dilution in cyclohexane. This dilution shift is to high field, which corresponds to the formation of monomeric or unassociated chloroform molecules. Because of the importance of correcting for this dilution shift in the present work, further measurements of the chloroform dilution shift were carried out. The inert solvents cyclohexane, *n*-hexane, and cyclopentane were used for the dilution experiments. The results are shown in Fig. 1 (upper curve) where the dilution shifts are plotted in c./s. relative to the position of the chloroform proton signal in pure liquid chloroform. The latter was measured relative to an external water reference

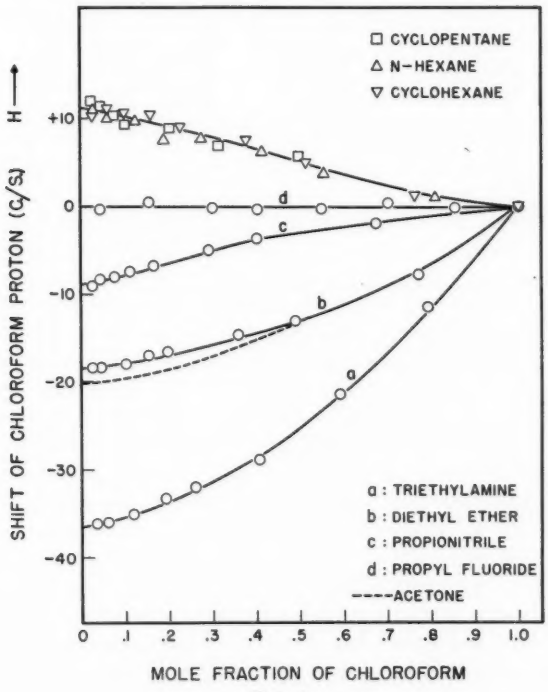

FIG. 1.

signal in a separate experiment. The extrapolated infinite dilution shifts in cyclohexane, *n*-hexane, and cyclopentane were 11.5, 12.0, and 12.5 c./s. respectively, which are all within the estimated experimental error of ±1.0 c./s. The average value of 12.0 c./s. was taken as representing the self-association of chloroform at room temperature.

The shifts of the chloroform proton signal as a function of concentration in triethylamine, diethyl ether, propionitrile, and propyl fluoride are also shown in Fig. 1 relative to the position of the chloroform signal in pure liquid chloroform. Corrections for differences in the volume susceptibilities of the solutions have been applied. The acetone–chloroform system has been previously measured by Huggins, Pimentel, and Shoolery (4). Their measurements are shown as a dotted curve in Fig. 1. These authors have also measured chloroform proton resonance shifts in the triethylamine–chloroform system. The present measurements agree to within the experimental error.

The difference between the infinite dilution shift of chloroform in the inert hydrocarbon solvents and the infinite dilution shift in a given donor liquid represents the actual shift between unassociated chloroform and that of chloroform complexed with the donor molecule. These shifts are listed in Table II, column 2, for the respective donor mole-

TABLE II

SUMMARY OF CHLOROFORM SOLUTION DATA

Donor liquid	Infinite dilution proton resonance shift[a] (c./s.)	Ionization potential[b] (ev.)	Lone pair dipole (12) (e.s.u.)×10^{18}	Infrared data (5)	
				C–D frequency shift ($cm.^{-1}$)	Half-band width ($cm.^{-1}$)
Triethylamine	48.0	9.0	3.25	84	42
Acetone	32.4 (4)	9.69	3.03	0	16
Diethyl ether	30.5	9.54	2.78	10	15
Propionitrile	22.0	11.9	3.74	—	—
Propyl fluoride	13.0	(12)	2.44	—	—

[a]*Corrected for differences in diamagnetic susceptibility and self-association of chloroform. Operating frequency 40 Mc./s.*

[b]*The values of the ionization potentials are those of Morrison and Nicholson (7), Price (9), and Watanabe (13).*

cules. From these values, as well as from the actual dilution curves shown in Fig. 1, it is evident that propyl fluoride has approximately the same donor strength as chloroform itself, but that all the remaining donor liquids are more basic.

Fig. 2 shows the binary freezing-point diagram for three chloroform systems. The measurement procedure was described previously (2). Triethylamine, acetone, and diethyl ether each clearly show the anticipated 1:1 complexes with chloroform. In the diethyl ether system, however, additional weak complexes are indicated. Melting points and eutectic temperatures are summarized in Table III. The chloroform–propionitrile system given in a previous publication (8) likewise shows a well-defined 1:1 molecular compound. Measurement of the freezing-point diagram of the system chloroform – propyl fluoride was attempted, but this turned out to be rather unsatisfactory. Considerable difficulty was experienced because of pronounced supercooling. Moreover, because of the large difference in melting points of the two components, it would be extremely difficult to detect a 1:1 compound, particularly since this may be expected to be very weak. Since, however, the donor property of fluorine has not been amply demonstrated, it was decided to measure the f.p. diagram of the system ethyl fluoride – hydrogen chloride. Here the freezing points of the two components are more favorable and hydrogen chloride is a stronger acceptor than chloroform. The results are shown in Fig. 3. The anticipated 1:1

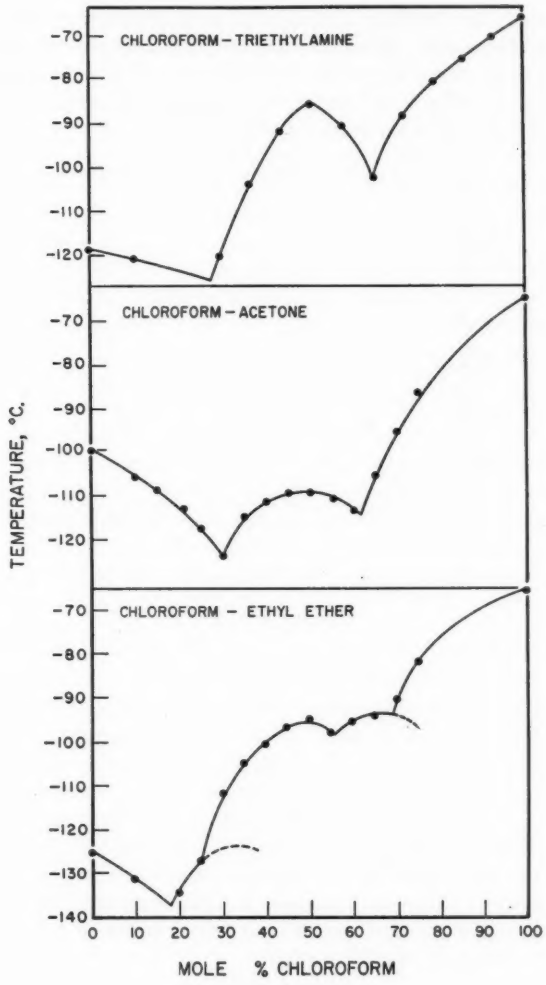

FIG. 2.

TABLE III

	Eutectics		Compounds	
	Composition, mole % chloroform	M.p., °C.	Composition, mole % chloroform	M.p., °C.
Triethylamine	72.5	−126	50	− 85
Acetone	70.0	−123	50	−109
Ethyl ether	81.5	−137.5	33	− 93
			50	− 95
Propionitrile	79.0	−108.0	50	− 90.5
Ethyl fluoride	75.0*	−176	50*	−171.5
			66*	−171.0

**Mole* % HCl.

complex is confirmed. By analogy a similar though perhaps weaker complex may be expected with chloroform, since although chloroform is a weaker acceptor than hydrogen chloride, this is partially offset by the greater tendency of hydrogen chloride to associate with itself (see Ref. 8). The ethyl fluoride – hydrogen chloride system also exhibits a second molecular compound of composition 1:2.

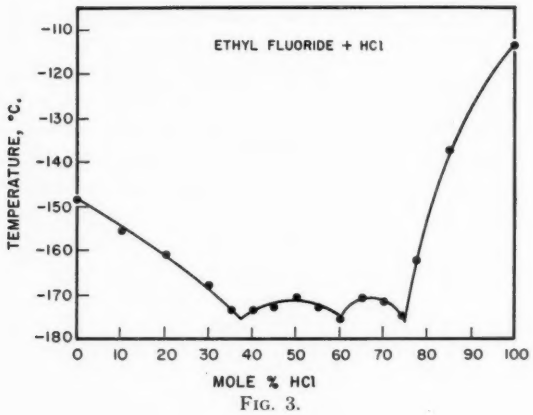

FIG. 3.

DISCUSSION

The results shown in Fig. 1 indicate a high field shift of the chloroform proton resonance signal on dilution in inert solvents. This is consistent with the assumption that the chloroform proton experiences a somewhat smaller diamagnetic shielding in the associated state. However, addition to chloroform of the donor solvents triethylamine, ether, acetone, propionitrile, and propyl fluoride, each of which is a stronger donor than chloroform itself, causes a shift of the proton signal to low field. In the complexes formed with these solvents, the proton shielding of the chloroform is still further reduced in the order triethylamine > acetone > ether > propionitrile > propyl fluoride. This order is numerically represented by the chloroform proton resonance shifts extrapolated to infinite dilution for each system (Table II, column 2). Alternatively, these numbers may be regarded as the relative shifts at room temperature* between the chloroform complex in each system and unassociated chloroform.

The measured association shifts (infinite dilution shifts) are approximately of the correct relative order of magnitude to parallel the expected hydrogen bond strengths in these systems. Since actual measurements of the latter are not available, a quantitative comparison is not possible. Further support for this conclusion may, however, be found by a comparison with other properties. Since a common acceptor molecule was used, the relative hydrogen bond strengths may be expected to depend directly on the donor strength of the second component. The ionization potential may usually be regarded as a good indication of donor strength of molecules of this kind. These are listed in the third column of Table II. A satisfactory correlation with the measured association shifts is evident. A second indication of donor strength is the charge distribution of the lone pair orbital of the donor atom. This can be estimated for various degrees of hybridization if a dipole approximation is assumed (12). The lone pair dipoles calculated in this manner

**These shifts are, of course, temperature dependent and will be larger at lower temperature.*

for each of the donor atoms are shown in column 4 of Table II. Except for the case of propionitrile, a reasonable correlation with the measured proton shifts is again evident, although the inadequacy of a dipole representation of the lone pair charge distribution must be borne in mind. The discrepancy presented by propionitrile has been discussed previously (8). Evidently the lone pair orbital of the N atom in this molecule is more *s*-like, as in the nitrogen molecule, and does not approximate an *sp* hybrid orbital.

Infrared absorption measurements have been carried out by Huggins and Pimentel (5) for dilute solutions of deuterated chloroform in the solvents triethylamine, acetone, and ether. The band intensity as approximated by the half-band width and the frequency shift of C–D stretching mode of $CDCl_3$ in the three solvents are shown in Table II. Pimentel and co-workers (4, 5) have pointed out the inadequacy of the measured frequency shift to give an indication of the hydrogen bonding interactions in these systems, and suggest that a more reliable measure of this is provided by the band intensity. A convenient indication of band intensity is the half-band width. The latter can be seen to give a rather satisfactory correlation with the measured proton resonance shifts, but unfortunately data for only three of the systems studied are available.

On the basis of the results shown in Table II the conclusion that the proton resonance shifts provide a measure of the relative hydrogen bond strengths in these systems appears justified. There is no evidence of anomalous magnetic effects accompanying association and the observed shifts may be regarded simply as due to a perturbation of the diamagnetic shielding of the proton when it is part of a hydrogen bond. Although electrostatic interaction and polarization effects undoubtedly play a part, the nature of the perturbation remains to be satisfactorily explained.

ACKNOWLEDGMENT

We wish to acknowledge the assistance of Mr. Yves Lupien in carrying out the freezing-point measurements in these systems.

REFERENCES

1. Arnold, J. T. and Packard, M. G. J. Chem. Phys. **19,** 1608 (1951).
2. Cook, D., Lupien, Y., and Schneider, W. G. Can. J. Chem. **34,** 957 (1956).
3. Gutowsky, H. S. and Saika, A. J. Chem. Phys. **21,** 1688 (1953).
4. Huggins, C. M., Pimentel, G. C., and Shoolery, J. N. J. Chem. Phys. **23,** 1244 (1955); J. Phys. Chem. **60,** 1311 (1956).
5. Huggins, C. M. and Pimentel, G. C. J. Chem. Phys. **23,** 896 (1955).
6. Lidell, V. and Ramsey, N. F. J. Chem. Phys. **19,** 1608 (1951).
7. Morrison, J. D. and Nicholson, A. J. C. J. Chem. Phys. **20,** 1021 (1952).
8. Murray, F. E. and Schneider, W. G. Can. J. Chem. **33,** 797 (1955).
9. Price, W. C. Chem. Revs. **41,** 257 (1947).
10. Reeves, L. W. and Schneider, W. G. Can. J. Chem. **35,** 251 (1957).
11. Reid, C. J. Chem. Phys. **25,** 790 (1956).
12. Schneider, W. G. J. Chem Phys. **23,** 26 (1955).
13. Watanabe, K. J. Chem. Phys. **26,** 542 (1957).

ATTEMPTED LOCATION OF THE SUBSTITUENT IN CELLULOSE XANTHATE BY NEW METHODS[1]

AMIYA K. SANYAL,[2] E. L. FALCONER,[3] D. L. VINCENT,[4] AND C. B. PURVES

ABSTRACT

Cellulose sodium xanthate of degree of substitution (D.S.) about 0.4 was methylated in 91% to 96% yield by methyl iodide in ether or benzene to the corresponding white *S*-methyl xanthate. This *S*-methyl xanthate was partly hydrolyzed, less than 40% of the substituent being incidentally lost, and the hydrolyzate was chromatographed on paper. About 20% of glucose was recovered together with two substances recognized as characteristic hydrolytic products of glucose 6-*S*-methyl xanthate. The procedure was not quantitative for xanthate groups in the primary alcohol positions of cellulose, and was too drastic to yield information about the less stable groups in the secondary positions.

The acetylation of the above cellulose *S*-methyl xanthate with acetic anhydride and pyridine led to a near-white, fibrous, fully acetylated product with unaltered xanthate substitution. Repeated attempts to remove the *S*-methyl xanthate groups by reaction with heavy metals or their salts, or with sodium chlorite, resulted in the simultaneous removal of about the same number of acetyl groups.

INTRODUCTION

Standard textbooks (12, 13, 32) describe in adequate detail the combination of alkali cellulose with carbon disulphide to form a crude cellulose sodium xanthate, the solution of which in excess alkali produces the viscose for the rayon and cellophane industries. The physical instability of viscose, revealed by the phenomenon of "ripening", probably reflects a redistribution of xanthate groups over the cellulose macromolecules, as well as a progressive decrease in their total number. These factors not only make it difficult to isolate the cellulose xanthate in a reproducible way so that observations made at different times by different workers can be confidently compared, but also limit very greatly the methods available to study the distribution of xanthate groups in a given sample. Analogy rather than experiment led in 1930 to the suggestion that the sixth positions in the anhydroglucose units of cellulose were substituted preferentially (33), in 1945 to the suggestion that the second, sixth, and third positions of the same glucose residues reacted in that order (23), while in 1952 the secondary hydroxyl groups were supposed to be favored initially, and the sixth or primary positions toward the end of the xanthation (30).

The work of Lieser (25) furnished the first direct approach to the problem of locating the substituents in cellulose xanthate. Lieser found that when a suspension of the dry sodium salt in cold methanol or ethanol was treated with 65 molar equivalents of nitrosomethylurethane for 4 to 5 hours the cellulose acquired a methoxyl content corresponding to the original xanthate substitution. Since samples of unsubstituted cellulose were methylated only slightly by the diazomethane from nitrosomethylurethane, Lieser assumed that the methylation replaced the sodium xanthate group selectively and quantitatively by a methyl ether group. When, however, Vincent and Purves (44)

$$\text{Cell—O—CSSNa} \xrightarrow{CH_2N_2} \text{Cell OCH}_3$$

[1]*Manuscript received June 28, 1957.*
Contribution from the Wood Chemistry Division, Pulp and Paper Research Institute of Canada, and from the Division of Industrial and Cellulose Chemistry, McGill University, Montreal, Que. Abstracted from Ph.D. theses submitted to the University by D. L. V. in March, 1953, by A. K. S. in August, 1953, and by E. L. F. in April, 1956.
[2]*Present address: 12/1/4 Monoharpukur Road, Calcutta-26, India.*
[3]*Present address: Central Research Laboratory, Canadian Industries Limited, McMasterville, Que.*
[4]*Present address: National Research Council of Canada, Atlantic Regional Laboratory, Halifax, N.S.*

attempted to prepare crystalline octadecyl methyl ether from crystalline octadecyl sodium xanthate by the same method, a nearly quantitative yield of crystalline octadecyl *S*-methyl xanthate resulted. Benzyl sodium xanthate reacted in the same way. These

$$C_{18}H_{37}OCSSNa \longrightarrow C_{18}H_{37}OCSSCH_3$$

observations at once cast doubt upon the validity of Lieser's assumption, and suggested that the initial product in his experiments was cellulose *S*-methyl xanthate.

If such was the case, then the alkalinity of the system would gradually saponify the *S*-methyl xanthate ester (44), and cellulose would be regenerated in a highly accessible form. Several workers (10, 34, 35, 41) showed that an excess of diazomethane was capable of methylating moist cellulose to an extent that increased with the accessibility of the sample, and methoxyl substitutions as high as 0.9 (OCH_3, 16%) were attained. It was thus most probable that cellulose regenerated in Lieser's experiments was methylated at random by diazomethane from the excess nitrosomethylurethane, the conditions being such that the residual amount of alkali present caused the process to cease near the expected methoxyl content. Moreover, there was no good evidence that the final *O*-methylcellulose was free of *S*-methyl xanthate groups, because the only sample definitely reported as free of sulphur (26) had been purified by extraction with alcohol, water, and by a bleach with very dilute aqueous chlorine dioxide. The great efficiency of this bleach in removing *S*-methyl xanthate groups from cellulose is demonstrated in the experimental portion of this article. If Lieser's methylcelluloses retained some *S*-methyl xanthate groups, then the slight response of the latter to the Kirpal–Bühn methoxyl estimation (44) he used would render the observed methoxyl content, and the derived D.S., somewhat too high.

Although Lieser's method was adopted in several later researches, his assumption that nitrosomethylurethane did in fact replace sodium xanthate by methyl ether groups was apparently not checked by demonstrating the absence of sulphur in the products. Chen, Montonna, and Grove (4) stressed their observation that the cellulose sodium xanthate had to contain no free alkali if overmethylation was to be avoided; although Noguchi (31) claimed satisfactory results with free diazomethane, Kuriyama and his colleagues (20, 21) considered that the use of this reagent, or of nitrosomethylurea, in place of nitrosomethylurethane could cause excessive methylation. The assignments of structure to the resulting *O*-methylcelluloses were not concordant. One sample of D.S. about 0.5 was thought to be substituted mainly in the 2-position (25), although isomers might have been present (28); this substitution was dominant in samples of D.S. 0.5 or less to the exclusion of substitution in the 3- and 6-positions, but more highly methylated products had increasing amounts of 2,3-substituents (22); the 2- and 2,6-positions were preferred and 2,3,6-trisubstitution was not found (31); finally, one *O*-methylcellulose studied in detail had D.S. 0.27, 0.21, and 0.24 in positions 2, 3, and 6, respectively, with perhaps a trace of disubstitution (4). In all cases it seemed probable that these *O*-methylcelluloses were derived from regenerated cellulose, and did not necessarily correspond in structure to the parent cellulose xanthate. The preponderance of substitution in the 2-position might be expected from other studies (11, 32, 46) of the partial methylation of cellulose in alkaline media.

In order to avoid the uncertainties encountered by Lieser and later workers in elucidating the structure of cellulose xanthate, it seemed desirable first to convert the sodium salt to a more stable derivative, and the *S*-methyl xanthate ester came into consideration. As Lieser and later workers (36, 44) noted, the xanthate esters of simple alcohols and

sugar derivatives possessed considerable stability toward hydrolysis with aqueous acid, and differed markedly in this respect from the sodium salts. Lilienfeld (29) attempted to prepare the cellulose ester by adding dimethyl sulphate or methyl iodide directly to viscose, but the analytical data reported were inadequate. Lieser (24) found that the isolated sodium salt was partly dexanthated by dimethyl sulphate, but reacted rapidly with methyl iodide in aqueous alcohol to produce a nearly ash-free substance whose thiomethyl and sulphur contents were only about 25% and 65% respectively, of the calculated values. Some dexanthation obviously occurred, and if methoxylation was absent, the apparent "methyl" content must be attributed to the highly incomplete response of the *S*-methyl xanthate group to the Kirpal–Bühn estimation (44) for alkoxyl. The methylation of a cellulose sodium xanthate by dimethyl sulphate, heterogeneously in pyridine, and homogeneously in aqueous solution, was reported by Aleksandru and Rogovin (1) to give products with the expected content of *S*-methyl groups as determined by sulphur analyses and by a micro-modification of the Zeisel determination of methoxyl groups. Overmethylation almost certainly occurred in this case also. Methylxanthyl chloride, $ClCSSCH_3$, was thought (9) to condense selectively with the primary hydroxyl groups in cellulose to yield the 6-*S*-methyl xanthate.

In the present research, cellulose xanthate *S*-methyl esters were readily prepared in 91 to 96% yield by condensing the corresponding sodium salts with methyl iodide in a non-hydroxylic solvent. The slight loss in yield and the slight change in xanthate D.S. (Table I, columns 1 and 2) were attributed to the presence in the sodium salts of sodium acetate or other impurities which were removed when the *S*-methyl xanthates were purified by extraction with water. There was no reason to suppose that wandering of xanthate groups occurred during the methylation, and their distribution in the cellulose was assumed to be unchanged. No significant number of unsubstituted hydroxyl groups were methylated, because the acetylation of the *S*-methyl xanthates increased the sum of the acetyl and xanthate substitutions to the theoretical value of 3.00 (right-hand column).

As expected (1, 44), the *S*-methyl xanthate group in the cellulose derivative was not stable to the periodate ion and reduced almost three molar equivalents within 2 days at room temperature. Hence the number of unsubstituted 2,3-glycol groups could not be determined in the customary way by oxidation with periodate. Fifteen attempts were made to degrade cellulose *S*-methyl xanthate of D.S. about 0.4 to the corresponding glucose derivatives without loss of xanthate groups. Degradations in methanolic hydrogen chloride at temperatures up to 160°, and in 43% hydrochloric acid at 0°, gave black liquors containing products from which 40 to 90% of the xanthate ester groups had been removed. Unlike cellulose itself, the *S*-methyl xanthate dissolved readily in concentrated (37%) hydrochloric acid at room temperature, and this was the most promising method of degradation found. There appeared to be no satisfactory way to follow the progress of the hydrolysis, which in the best experiments was stopped by trial and error when about 20% of glucose had been formed and less than 40% of the xanthate ester groups had decomposed. Care was taken to avoid dexanthation during the isolation of the product, which amounted to 65% by weight of a brittle, yellow gum.

When this gum was examined by paper chromatography, it produced spots which had moved only slightly from the starting line and were attributed to incompletely hydrolyzed material. In addition to an intense spot for glucose, there were others at R_f 0.56 and 0.70 which were traced to a fraction extractable from the gum in 4.5% yield by acetone. These R_f values coincided with those of control spots given by the

TABLE I

CONVERSION OF CELLULOSE SODIUM XANTHATE TO *S*-METHYL ESTER AND ACETATE

Cellulose Na xanthate D.S.	*S*-Methyl ester D.S.	Acetylated[a] *S*-methyl xanthate		
		Xanthate D.S.	Acetyl D.S.	Total D.S.
0.43	0.45	—	—	—
0.42	0.37	—	—	—
0.37	0.41	0.40	2.59	2.99
0.25	0.29	—	—	—
0.39	0.41	0.41	2.61	3.02[b]
		0.41	2.61	3.02
0.34	0.34	0.35	2.66	3.01
0.15	0.12	—	—	—
0.12	0.10	—	—	—

[a] *A 10-g. sample heated at 100° for 24 hours with 250 ml. of acetic anhydride and 400 ml. of pyridine.*
[b] *Duplicate acetylations.*

substances formed when glucose 6-*S*-methyl xanthate (R_f 0.84) was drastically treated with acid. The substances yielding the two spots were isolated by paper chromatography on a larger scale, and the one of R_f 0.70 had a sulphur content close to the expected value. Although glucose 6-*S*-methyl xanthate was not isolated as such, the results showed that some of the substituents of the original cellulose xanthate occupied sixth or primary alcohol positions. Aleksandru and Rogovin (1) arrived at the same conclusion by observing that their cellulose *S*-methyl xanthate condensed with less than 1 mole of triphenylmethyl chloride per anhydroglucose unit. No spot corresponding to glucose 3-*S*-methyl xanthate appeared on the present chromatograms, and none was expected, because this substance and also the 2,3-derivative were too readily hydrolyzed by acids (36). The same reason discouraged an attempt to prepare a control sample of glucose 2-*S*-methyl xanthate from the corresponding acetylated methyl-α-glucopyranoside (47).

The hydrolysis of cellulose *S*-methyl xanthate to the corresponding glucose derivatives thus proved to be of very limited value in elucidating structure, because it was inapplicable to substituents in the 2- and 3-positions and was non-quantitative for those in position 6. The stability of the *S*-methyl xanthate group during acetylation (27, 44, 47), however, revealed the possibility of completely acetylating cellulose *S*-methyl xanthate, removing the xanthate without disturbing the acetyl substitution, and locating the vacant hydroxyl groups in the resulting cellulose acetate by standard methods. Conditions were eventually found in which pyridine and acetic anhydride gave 90 to 95% yields of products whose xanthate substitution accurately reflected that of the parent substance, and whose total substitution was 3.0 within the analytical error (Table I). The attempts to remove the *S*-methyl xanthate groups from this product in a selective way included heating solutions in moist acetone or dioxane under reflux with silver carbonate, mercuric acetate, or Raney nickel, but the formation of inorganic sulphide could not be detected. Although lead acetate was without apparent effect even in boiling 97% acetic acid, solutions of silver acetate or mercuric acetate, or suspensions of Raney nickel, in the same solvent at 100° all produced dexanthation. Unfortunately, deacetylation was also substantial (Table II, column 5), a wandering of acetyl groups was probable, and dexanthations with metallic agents were abandoned.

Chlorine dioxide or sodium chlorite was used to oxidize various thio compounds (39),

TABLE II

ATTEMPTED DEXANTHATIONS OF CELLULOSE *S*-METHYL XANTHATE ACETATE

Reagent	S, %	Acetyl, %	Xanthate D.S.	Acetyl D.S.
None	8.4	36.8	0.40	2.59
Zn in 97% AcOH[a]	2.1	37.7	0.09	2.38
$Pb(OAc)_2$–Zn[b]	0.7	35.6	0.03	2.07
	1.3	27.9	0.05	1.47
None	8.5	36.4	0.41	2.61
$Hg(OAc)_2$[c]	4.2	36.1	0.18	2.30
$NaClO_2$[d]	2.9	37.3	0.12	2.36
$NaClO_2$[e]	2.6	37.7	0.11	2.38
$NaClO_2$[f]	3.0	37.2	0.13	2.35
$NaClO_2$[g]	0.5	37.3	0.02	2.24

[a]*Sample, 0.5 g., and 4.4 g. of zinc dust in 100 ml. of 97% acetic acid boiled under reflux for 3 hours; then a further 4.2 g. of zinc dust added and heating continued for further 90 minutes. Yield 73% of theory.*

[b]*Sample, 1.4 g., lead acetate, 2 g., and zinc dust, 5 g., in boiling 97% acetic acid for 10 hours, a further 5 g. of zinc being added at intervals. The analyses quoted were for portions of products soluble and almost insoluble in glacial acetic acid. Yields 25% and 50%, respectively. The gas evolved was exclusively hydrogen sulphide.*

[c]*Sample, 0.5 g., and mercuric acetate, 2 g., boiled under reflux in 50 ml. of 97% acetic acid for 30 minutes. Yield 95%.*

[d]*Sample, 1 g., dissolved in 75 ml. of acetone and 15 ml. of acetic acid; then 5 ml. of 10% aqueous sodium chlorite added. Isolation after 15 minutes. Subsequent experiments were for 1 hour.*

[e]*Sulphate sulphur recovered in liquors was 3.95% of weight of original sample, or 46% of original sulphur.*

[f]*Acetone – acetic acid ratio increased to 40 : 1.*

[g]*Acetone – acetic acid reduced to 1 : 6.*

sulphites (18), sulphur (43), sulphur leuco dyes (45), thio groups in wool (6, 37, 38), and the use of chlorite for reducing the sulphur content of cellulose regenerated from viscose was patented (42). These reports suggested that the above reagents might eliminate the *S*-methyl xanthate group, and experiments with suspensions of cellulose *S*-methyl xanthate showed that such was the case. The reaction was swift and exothermic with either oxidant; approximately 1 mole of chlorine dioxide was reduced per *S*-methyl xanthate group, and approximately 1 mole of sulphuric acid was liberated. The second sulphur atom in the xanthate group was oxidized in an undetermined way. A residual sulphur content of about 1% was stubbornly retained by the cellulose.

When fully acetylated cellulose *S*-methyl xanthate in acetone – acetic acid solution was dexanthated at pH 5 with 10% aqueous sodium chlorite, it was easy to reduce the sulphur content of the resulting cellulose acetate to 2 to 3% (Table II), but a reduction to about 0.5% sulphur required 90% acetic acid (last experiment). No conditions were found in which the sulphur could be completely eliminated, and its state of chemical combination, either with the cellulose or as a tenaciously adsorbed impurity, was not ascertained. Moreover, the removal of *S*-methyl xanthate groups by chlorite was always accompanied by the removal of approximately the same number of acetyl groups. This disadvantage rendered the method unsuitable for the purpose in view, and attempts at dexanthation with sodium chlorite were discontinued.

EXPERIMENTAL

Materials and Analytical Methods

A published procedure (4) was followed in preparing alkali cellulose from dewaxed cotton linters and 18% sodium hydroxide, the press weight ratio being 3.4 to 3.7. Shred-

ding was carried out with tweezers, and aging was for 60 to 65 hours at room temperature. After the xanthation, the product was dissolved in ice-cold 4% sodium hydroxide and was reprecipitated by a large excess of ice-cold methanol. The crude cellulose sodium xanthate was steeped for 15 minutes in cold methanol containing 4% of glacial acetic acid before being solvent-exchanged through cold methanol into ether or benzene. Found for a typical sample (after thorough drying): S, 11.9, 11.8; Na, 4.6, 4.7%. Calc. for cellulose sodium xanthate of D.S. 0.37: S, 11.8; Na, 4.2%. Hence some of the excess sodium salt was retained after the extraction with methanol – acetic acid. Precipitation into methanol–isopropanol–acetone (1:1:1) gave an acid-washed product of lower D.S.

Sodium was determined as sulphated ash (14) and sulphur either by the Carius (5), the Parr bomb (8), or the alkaline hypobromite (7) procedure. The determination of xanthate in salts by the sodium zincate (2) method gave results that were usually too high, and the hypobromite method (7) responded to only about one-half of the sulphur in xanthate *S*-methyl esters. The methyl group in these esters could not be determined as methyl iodide by standard methods of determining methoxyl groups, and previous observations to the same effect (36, 44) were confirmed. Acetyl groups in acetylated cellulose *S*-methyl xanthates were determined by saponification in 1 *N* ethanolic potassium hydroxide followed by acidification and isolation of the acetic acid by steam distillation (5); omission of the steam distillation, as in the Kunz and Hudson (19) procedure, gave indefinite results.

Cellulose S-Methyl Xanthate

Since cellulose sodium xanthate did not esterify readily when thoroughly dried, samples were used soon after their preparation and while still wet with ether or benzene. A suspension of the sodium salt in 10 to 15 parts of one or other of these liquids was mixed with a 20-fold excess of redistilled methyl iodide. The container was stoppered and was kept for 6 days in the dark at room temperature, during which time the color of the suspended material changed from light yellow to white. The product was solvent-exchanged into methanol and was then washed with water and 50% aqueous methanol until the washings were free of iodide ion. After being washed again with ether, the cellulose *S*-methyl xanthate was dried *in vacuo* over phosphorus pentoxide at room temperature. The yield was 91 to 96% of theory. Found: S, 13.2, 13.4; ash, 0.0%. Calc. for cellulose *S*-methyl xanthate, D.S. 0.414 (base mol. wt. 199); S, 13.3; ash, 0.0%. One sample with S, 12.2%, was kept for 8 months in the dark at room temperature without change in its appearance or sulphur content. Found: S, 12.4, 12.1%.

Cellulose *S*-methyl xanthate of D.S. 0.4 or less was a snow white, fibrous substance that was insoluble in all liquids tried with the exception of 4% sodium hydroxide. The xanthate ester slowly dissolved at room temperature in the alkali to yield a clear yellow viscous solution smelling of mercaptan. After a few hours the progress of the decomposition caused the deposition of a less highly xanthated cellulose.

Oxidations of Cellulose S-Methyl Xanthate

(*a*) *With Periodate*

A 0.064 *M* solution of trisodium paraperiodate, $Na_3H_2IO_6$, was buffered to pH 4.0 with acetic acid. Ten 100-mg. samples of the *S*-methyl xanthate, D.S. 0.45, were each suspended in a 50-ml. aliquot of the periodate solution, and the suspensions were kept in the dark and at room temperature in stoppered flasks. A blank was also prepared. At various times thereafter, one of the suspensions was filtered on sintered glass, and filtrate and washings were neutralized with sodium bicarbonate. The unreduced periodate was

estimated by adding 6 ml. of 10% potassium iodide, and titrating with 0.072 *M* sodium arsenite. The amount consumed was found by difference from the blank. This amount was 1.7, 1.83, 1.99, 2.12, and 2.29 moles per anhydroglucose unit after 1, 2, 3, 4, and 8 days, respectively. Since cellulose itself would utilize about 1 mole, about 1.2 moles was consumed by the 0.45 mole of *S*-methyl xanthate group, which was thus unstable to the oxidant.

(*b*) *With Aqueous Chlorine Dioxide*

Six accurately weighed 0.2-g. samples of cellulose *S*-methyl xanthate, D.S. 0.335, were mixed in separate glass-stoppered flasks with 2 ml. aliquots of a 1 *M* sodium acetate – 1 *M* acetic acid buffer. The flasks were kept at 20°, and 25 ml. of 0.02 *M* (0.1 *N*) aqueous chlorine dioxide (17) was added with shaking to each. At various times thereafter, an excess of potassium iodide and acetic acid was added to five of the flasks and the liberated iodine was titrated with 0.05 *N* sodium thiosulphate. The assumption that chlorine dioxide had only 2 effective oxidizing equivalents per mole (17) led to the conclusion that 1.03, 1.23, 1.17, 1.27, and 1.41 moles per *S*-methyl xanthate group had been consumed after 0.25, 0.5, 1.0, 3.0, and 5.0 hours, respectively. A further 10 ml. of 0.02 *M* chlorine dioxide was added after about 5 hours to the sixth sample, which reduced 2.04 moles after a total time of 20 hours.

In a larger scale experiment, 30 ml. of 1.3 *N* chlorine dioxide in 50% acetic acid buffered with 0.5 g. of crystalline sodium acetate was stirred with 1 g. of the cellulose *S*-methyl xanthate. A vigorous exothermic reaction ensued, and after 24 hours at room temperature the white fibers were recovered on a filter, washed well with water and ethanol, and dried *in vacuo* over phosphorus pentoxide. Yield: 0.85 g. Found: S, 0.74, 0.82%. Calc. for cellulose *S*-methyl xanthate of D.S. 0.02: S, 0.78%.

(*c*) *With Aqueous Sodium Chlorite*

A 0.5-g. sample, D.S. 0.335, was stirred for 10 hours with 25 ml. of water containing 1 g. of crystalline sodium acetate and 5 ml. of glacial acetic acid, while 5 ml. of 10% aqueous sodium chlorite was slowly added. Reaction was swift, and the white fibrous product retained only 0.67% of sulphur (residual xanthate, D.S. 0.02). The sulphate ion contained in the oxidation liquors was determined by precipitation with barium chloride and accounted for a sulphur content of 6.5% in the cellulose *S*-methyl xanthate. Since the sample had S 11.2% (D.S. 0.335), almost half of the original sulphur had not been oxidized to sulphate ion. This half was probably present as methylsulphonic acid.

Hydrolysis of Cellulose S-Methyl Xanthate

(*a*) A 1-g. sample of D.S. 0.45 soon dissolved in 50 ml. of 37% hydrochloric acid at room temperature, the clear solution being red in color after 2 hours and purple after 3 hours. At the latter time the dilution of a 1 ml. aliquot with 1 ml. of water caused the separation of a precipitate, but after 5 hours the solution remained clear when diluted with an equal volume of water. Six days later the slightly turbid, orange solution was clarified with a little adsorbent carbon and the clear, faintly pink filtrate was diluted to 200 ml. The optical rotation, observed in a 4 dm. tube, was 0.40°, and 30 hours later was 0.36°. These values were almost within the limits of observational error and afforded no guide to the progress of the hydrolysis. Interference of the *S*-methyl xanthate group, or of its decomposition products, with the Shaffer–Hartmann–Somogyi (40) alkaline copper reagent caused the failure of attempts to follow the increase in the reducing power of the hydrolyzate.

Since neutralization with silver carbonate rapidly caused dexanthation, the hydrolyzate was freed from hydrochloric acid by shaking at room temperature with basic

lead carbonate followed by filtration, the passage of hydrogen sulphide, and neutralization with sodium bicarbonate. The filtrate was then deionized by passage through columns of Amberlite IR-120 cation-exchange and Amberlite IR-4B anion-exchange resins and was evaporated to dryness *in vacuo* at less than 50°. A considerable amount of the product was lost with the inorganic residues. The residual, brittle yellow solid weighed 0.62 g. (64.5%). Found: S, 8.8, 8.8, 9.0%. Since the original cellulose *S*-methyl xanthate contained 14.3% of sulphur, about 38% of the substituent had been decomposed.

An aqueous solution containing 0.5 to 1.0 mg. of the residual solid was then placed as a spot on the starting line of an 18×3 inch strip of Whatman No. 1 chromatograph paper, and spots of glucose and crude glucose 3-*S*-methyl xanthate (36) were used as controls. The chromatogram was developed for 12 to 23 hours by the descending method with *n*-butanol saturated with water, aniline phthalate being the spray (15, 16). Brown spots developed during drying at 105° for 15 minutes. One very faint spot had R_f 0.025, a strong spot with R_f 0.11 coincided with that for glucose and was removed by fermentation, two faint spots appeared of R_f 0.19 and 0.37, and two stronger ones of R_f 0.55 and 0.73. There was no sign of the spot of R_f 0.68 given by the 3-glucose *S*-methyl xanthate solution. These R_f values varied slightly but systematically with the equipment used. To determine the amount of glucose present (15), the segments of paper containing the proper spots from three 2-mg. samples were extracted with water in a micro-Soxhlet apparatus, and blank pieces of paper of the same area were similarly extracted. When the Shaffer–Hartmann–Somogyi (40) copper reducing values were corrected by those of the blanks (about 0.02 mg.) they corresponded to 0.44, 0.42, and 0.44 mg. of glucose. Thus only 22% of the original cellulose *S*-methyl xanthate was recovered as glucose, and the hydrolysis had therefore been incomplete.

(*b*) The hydrolysis of a 2-g. sample of a cellulose *S*-methyl xanthate, D.S. 0.41 (S, 13.3%), in 37% hydrochloric acid was carried out as in (*a*), but after 2 hours one-half (50 ml.) of the solution was diluted with an equal volume of water. A small precipitate was removed, and the clear filtrate was kept for 8 days at room temperature and in the dark. The other half of the original solution was diluted in the same way after 3 hours, was kept for 8 days, and was denoted as the 3-hour sample. After removal of hydrochloric acid and deionization, the filtrate from the 2-hour sample was concentrated *in vacuo* at 30° to 5 ml., and was then diluted with 50 ml. of absolute ethanol. The precipitate was rejected, and the filtrate was evaporated to yield a residue (A), 0.56 g., which was extracted with acetone. Evaporation of the extract left 45 mg. of a semisolid gum (B).

When the gum B was chromatographed on paper with products from a drastic hydrolysis of crystalline 1,2;3,5-di-*O*-methylene glucose 6-*S*-methyl xanthate (36) as a control, both chromatograms had identical spots at R_f 0.56 and R_f 0.70. The residue A yielded the same two spots together with that of glucose. In order to isolate the product of R_f 0.70, 34 mg. of the gum B was dissolved in 3 ml. of acetone and chromatographed on paper. Extraction of the appropriate strips of paper with absolute methanol yielded 16 mg. of a dry solid. Found: S, 9.9, 8.7%. The product of R_f 0.70 chromatographed from the hydrolyzate of the *bis*-methylene glucose 6-*S*-methyl xanthate was found (36) to have S, 9.2%. In the same way, the 3-hour sample mentioned above yielded a substance of R_f 0.70 (found: S, 9.2%) although it contained more glucose. Neither sample appeared to contain glucose 6-*S*-methyl xanthate (R_f 0.84; S, 23.7%) as such.

Acetylation of Cellulose S-Methyl Xanthate

A 1-liter flask, equipped with a reflux condenser and a mechanical stirrer with mercury seal, was used to heat a mixture of cellulose *S*-methyl xanthate (D.S. 0.41), 10 g., acetic

anhydride, 150 ml., and pyridine, 240 ml., on the steam bath. The mixture changed to a highly viscous, red-brown gel within 90 minutes. After 12 hours, when the viscosity had decreased markedly, a further 100 ml. of acetic anhydride and 160 ml. of pyridine were added, and the heating was continued for another 12 hours. A few swollen, undissolved lumps were removed by filtration through "extra-coarse" sintered glass before the dark brown liquid was poured with vigorous stirring into 3 liters of ice and water. The precipitate of short, brown fibers was washed with water and alcohol and was reprecipitated from acetone solution into ethanol. Drying was *in vacuo* over phosphorus pentoxide. Found: S, 8.5, 8.5; CH_3CO, 36.3, 36.5%. Calc. for cellulose substituted with 0.41 methyl xanthate and 2.61 acetyl groups: S, 8.5; CH_3CO, 36.4%. When based on this analysis, the yield of 14.6 g. was 94% of theory. The near-white, fibrous substance was soluble in acetone, acetic acid, and dioxane.

The heating was restricted in a similar experiment to 7 hours at 98°, and the product had D.S. 0.41 and 2.54 for *S*-methyl xanthate and acetyl groups, respectively. The total D.S. was much less than 3 when the heating was at 67° for 9 hours. Cellulose *S*-methyl xanthate, 1 g., lost no xanthate groups when acetylated for 5 days at room temperature with 50 ml. of acetic anhydride containing 0.5 ml. of concentrated sulphuric acid, or 0.5 g. of anhydrous zinc chloride. Acetylation was not quite complete in the first case and did not occur in the second.

Dexanthations of Acetylated Cellulose S-Methyl Xanthate

(*a*) *With Zinc*

In an experiment similar to the first described in Table II, footnote *a*, a slow current of nitrogen was bubbled through the reaction mixture to carry the evolved gases through an absorption train (3). The first adsorption tubes, which contained a 10% solution of cadmium sulphate in 1% hydrochloric acid, accumulated the yellow precipitate of cadmium sulphide characteristic of hydrogen sulphide. The 5% aqueous mercuric cyanide in the next tubes remained clear, and mercaptans were therefore absent; organic sulphides were also absent, because no change was apparent in the last tube filled with 5% aqueous mercuric chloride.

(*b*) *With Sodium Chlorite*

A solution of 1 g. of acetylated cellulose *S*-methyl xanthate, xanthate D.S. 0.35, and acetyl D.S., 2.66, in 15 ml. of acetone was mixed with an equal volume of acetic acid. The solution became cloudy and yellow-green as 5 ml. of 10% aqueous sodium chlorite was slowly added with vigorous stirring; the temperature increased slightly and a small amount of inorganic material separated. After it had been left for 3 hours at room temperature, the solution was poured into water, and the precipitate of very short white fibers was dried *in vacuo* at 40°. Found: S, 2.48, 2.48; acetyl, 38.5, 38.5%. Calc. for cellulose substituted with 0.11 methyl xanthate and 2.46 acetyl groups: S, 2.47; acetyl, 38.5%. Yield: 0.89 g., or quantitative on the basis of the analysis.

The product was precipitated from acetone solution by ethanol, and was reoxidized with aqueous sodium chlorite, without significant change in its composition. A similar, partly dexanthated sample, of methyl xanthate D.S. 0.13 and acetyl D.S. 2.35, was acetylated with pyridine – acetic anhydride in the way already described. The product had D.S. 0.09 and 2.75, respectively. Found: S, 2.0, 2.1; acetyl, 41.3, 41.5%.

ACKNOWLEDGMENTS

Three of the authors (D. L. V., A. K. S., and E. L. F.) thank the Spruce Falls Power and

Paper Company, Limited, the American Viscose Corporation, the Visking Corporation, the National Research Council of Canada, and the Pulp and Paper Research Institute of Canada for Studentships, Fellowships, and summer stipends awarded to them during the research.

REFERENCES

1. ALEKSANDRU, L. and ROGOVIN, Z. J. Gen. Chem. U.S.S.R. **23**, 1259, 1263 (1953); Chem. Abstr. **47**, 12802 (1953).
2. BARTHELEMY, H. L. and WILLIAMS, L. Ind. Eng. Chem. Anal. Ed. **17**, 624 (1945).
3. BERGSTRÖM, H. and TROBECK, K. G. Svensk Papperstidn. **42**, 554 (1939).
4. CHEN, C. Y., MONTONNA, R. E., and GROVE, C. S., Jr. Tappi, **34**, 420 (1951).
5. CLARK, E. P. Semimicro quantitative organic analysis. Academic Press Inc., New York, N.Y. 1943.
6. DAS, D. B. and SPEAKMAN, J. B. J. Soc. Dyers and Colourists, **66**, 583 (1950); Chem. Abstr. **45**, 1349 (1951).
7. DORÉE, C. Methods of cellulose chemistry. 2nd ed. Chapman and Hall, Ltd., London. 1947. pp. 263, 271.
8. ELEK, A. and HILL, D. W. J. Am. Chem. Soc. **55**, 3479 (1933).
9. FREUDENBERG, K. and DIETRICH, G. Ann. **563**, 146 (1949).
10. HEAD, F. S. H. J. Textile Inst. **43**, T 1 (1952).
11. HEDDLE, W. J. and PERCIVAL, E. G. V. J. Chem. Soc. 1690 (1938).
12. HERMANS, P. A. Physics and chemistry of cellulose fibres. Elsevier Publishing Co., Inc., New York. 1944.
13. HEUSER, E. The chemistry of cellulose. John Wiley & Sons, Inc., New York. 1944.
14. HEUSER, E. and SCHUSTER, M. Cellulosechemie, **7**, 17 (1926).
15. HIRST, E. L., HOUGH, L., and JONES, J. K. N. J. Chem. Soc. 928 (1949).
16. HIRST, E. L. and JONES, J. K. N. J. Chem. Soc. 1659 (1949).
17. HUSBAND, R. M., LOGAN, C. D., and PURVES, C. B. Can. J. Chem. **33**, 68 (1955).
18. JACKSON, D. T. and PARSONS, J. L. Ind. Eng. Chem. Anal. Ed. **9**, 14 (1937).
19. KUNZ, A. and HUDSON, C. S. J. Am. Chem. Soc. **48**, 1978 (1926).
20. KURIYAMA, S., MIHARA, K., and UEDA, T. J. Chem. Soc. Japan, Ind. Chem. Sect. **57**, 855 (1954); Chem. Abstr. **49**, 11272 (1955).
21. KURIYAMA, S., MIHARA, K., UEDA, T. and YAMADA, S. J. Chem. Soc. Japan, Ind. Chem. Sect. **58**, 110 (1955); Chem. Abstr. **49**, 14317 (1955).
22. LAUER, K. Makromol. Chem. **5**, 287 (1951).
23. LAUER, K., JAKS, R., and SKARK, L. Kolloid-Z. **110**, 26 (1945).
24. LIESER, T. Ann. **464**, 43 (1928).
25. LIESER, T. Ann. **470**, 104 (1929).
26. LIESER, T. Ann. **483**, 132 (1940).
27. LIESER, T. and LECKZYCK, E. Ann. **519**, 279 (1935).
28. LIESER, T. and LECKZYCK, E. Ann. **522**, 56 (1936).
29. LILIENFELD, L. U.S. Patent No. 1,680,224 (Aug. 7, 1928); Chem. Abstr. **22**, 3777 (1928).
30. MATTHES, A. Faserforsch. u. Textiltech. **3**, 127 (1952); Chem. Abstr. **47**, 6661 (1953).
31. NOGUCHI, T. J. Soc. Textile Cellulose Ind. (Japan), **6**, 215, 217, 312, 314, 379, 381, 444 (1950); Chem. Abstr. **46**, 5834 (1952).
32. OTT, E. and SPURLIN, H. M. Cellulose and cellulose derivatives. Vol. II. 2nd ed. Interscience Publishers, Inc., New York. 1954. Chap. IXF by E. Kline.
33. RASSOW, B., VOERSTER, T., and WOLF, L. Papierfabr. Special Number, **28**, 83 (1930).
34. REBENFELD, L. and PACSU, E. Textile Research J. **24**, 941 (1954).
35. REEVES, R. E., ARMSTRONG, A. C., BLOUIN, F. A., and MAZZENO, L. W. Textile Research J. **25**, 257 (1955).
36. SANYAL, A. K. and PURVES, C. B. Can. J. Chem. **34**, 426 (1956).
37. SCHIRLE, C. Bull. inst. textile France, **41**, 23, 39, 43 (1953); Chem. Abstr. **48**, 14219 (1954).
38. SCHIRLE, C. and MEYBECK, J. Compt. rend. **232**, 526, 732, 1219 (1951).
39. SCHMIDT, E. and BRAUNSDORF, K. Ber. **55**, 1529 (1922).
40. SHAFFER, P. A. and SOMOGYI, M. J. Biol. Chem. **100**, 695 (1933).
41. SITCH, D. A. J. Textile Inst. **44**, T 407 (1953).
42. SOCIÉTÉ D'ÉLECTROCHIMIE, D'ÉLECTROMÉTALLURGIE ET DES ACIÉRIES ÉLECTRIQUES D'USINE. French Patent No. 982,165 (June 7, 1951); Chem. Abstr. **48**, 5499 (1954).
43. TARADOIRE, F. Bull. soc. chim. France, **8**, 860 (1941).
44. VINCENT, D. L. and PURVES, C. B. Can. J. Chem. **34**, 1302 (1956).
45. VINCENT, G. P. Chem. Eng. News, **21**, 1176 (1943).
46. WOLFROM, M. L. and EL-TARABOULSI, M. A. J. Am. Chem. Soc. **76**, 2216 (1954).
47. WOLFROM, M. L. and EL-TARABOULSI, M. A. J. Am. Chem. Soc. **75**, 5350 (1953).

THE STRUCTURE OF LINSEED MUCILAGE. PART I[1]

A. J. ERSKINE[2] AND J. K. N. JONES

ABSTRACT

The neutral polysaccharide component of linseed mucilage has been isolated and examined. On acidic hydrolysis it furnished mainly D-xylose and L-arabinose. Periodate oxidation experiments showed that the polysaccharide is of the branched chain type. Methylation experiments have confirmed this result and have given additional information on the structure of the polysaccharide.

Linseed mucilage is a mixture of polysaccharides obtained when the seeds of flax (*Linum usitatissimum*) are treated with cold water. Early workers (11, 17) showed that hydrolysis of the mucilage with dilute acid furnished a complex mixture of sugars amongst which the neutral components D-glucose, L-galactose, D-xylose, and L-arabinose were detected. The acidic fraction, which was more resistant to hydrolysis, was shown by Anderson and Crowder (3) to be a disaccharide composed of D-galacturonic acid and L-rhamnose residues. The structure of this substance was later (19) proved to be 2-*O*-D-galacturonosyl-L-rhamnose, an aldobiouronic acid which has since been isolated from several other sources (e.g. 9, 16). Several neutral disaccharides have now been detected in a partial hydrolyzate of the mucilage. From the mixture a crystalline disaccharide has been isolated and identified as 4-*O*-β-D-xylosyl-D-xylose (xylobiose).

Bailey (5) showed that linseed mucilage was not a homogeneous polysaccharide, since it was possible to precipitate fractions of different composition by addition of barium hydroxide to solutions of the mucilage. This observation was confirmed when it was shown subsequently that addition of copper acetate solutions to a solution of the mucilage gave fractions which contained differing proportions of sugar residues (7). Using a modification (8) of this fractionation procedure a polysaccharide was obtained which contained only a trace of uronic acid and in which D-xylose and L-arabinose residues were concentrated. At least three and perhaps four polysaccharides were present in the mucilage in addition to this neutral polymer. The chemistry of this neutral material has been examined in some detail. It rotates the plane of polarized light to the left whereas the other polysaccharide components have positive optical rotations. On hydrolysis it yields mainly D-xylose (*ca.* 70%) and L-arabinose (*ca.* 25%) together with traces of glucose and galactose. For this reason we shall refer to it as linseed pentosan. The glucose which is present in the pentosan probably arises from the presence of a contaminating polysaccharide, since acetylation followed by fractionation of the acetate leads to the isolation of a polysaccharide in the hydrolyzate of which no glucose can be detected. L-Rhamnose and L-fucose (7), which were found in the original mucilage, were evidently present in the other polysaccharide components. Graded acidic hydrolysis of the purified pentosan gave two disaccharides provisionally identified as *xylobiose* and a *xylosido arabinose* in which a D-xylose residue is linked by an alpha glycosidic linkage to C_5 of the L-arabinose component. The beta-linked isomer has been isolated from cholla gum (4). The rate of hydrolysis of the arabinose residues indicated that some of them were probably in the pyranose form.

Periodate oxidation of the pentosan showed that the polysaccharide was of the branched

[1]*Manuscript received June 14, 1957.*
Contribution from the Department of Chemistry, Queen's University, Kingston, Ontario, Canada. An abstract of this work was presented at the Miami meeting of the American Chemical Society, April, 1957.
[2]*Present address: National Research Council, Halifax, Nova Scotia.*

chain type since formic acid was produced (0.4 mole per pentose residue). This production of formic acid requires the consumption of 0.8 mole of periodate. Since *ca.* 1.2 moles of metaperiodate was reduced per mole of pentose ($C_5H_8O_4$), it is evident that for every end group oxidized one other sugar was also oxidized. The periodate-oxidized polymer produced xylose and arabinose on hydrolysis, which indicated that some of the sugars did not possess alpha glycol groups. Partial hydrolysis of the linseed pentosan resulted in the preferential removal of L-arabinose residues and the formation of a degraded polysaccharide which had a more positive optical rotation. Periodate oxidation of the degraded polysaccharide (cf. Tables I, II, and III) resulted in an uptake of periodate and a formation of formic acid closely similar to those produced when the undegraded polymer is oxidized. These results suggest that the initial stages of hydrolysis of the pentosan result in the elimination of L-arabofuranose residues which had been attached to D-xylopyranose groups in such a manner that the xylose residues were protected from oxidation by periodate. When the arabinose residues were eliminated a new alpha glycol grouping became exposed and the xylose residues then became susceptible to oxidation by periodate but without the formation of formic acid. These oxidation results also suggest that D-xylopyranose end groups are present in the polysaccharide and that the proportion of these end groups is not greatly increased on elimination of some of the L-arabofuranose groups. This may be explained by the elimination of a small amount of the xylose end groups as xylosidoarabinose and by assuming that L-arabofuranose groups are not attached to D-xylopyranose end groups but to a main chain of beta-1,4-linked D-xylopyranose residues. The position of the L-arabopyranose residues is unknown.

Methylation of the polysaccharide proceeded best via the acetate and gave a derivative with a negative rotation (−70°, $CHCl_3$). Hydrolysis of this product with aqueous formic acid yielded a complex mixture of sugars which was separated by chromatography. The following sugars were detected: 2,3,4-tri-*O*-methyl-, 2,3-di-*O*-methyl-, 3-*O*-methyl-D-xylose, and D-xylose. 2,3-Di-*O*-methyl-L-arabinose and 2,4-di-*O*-methyl-L-arabinose were also identified. The presence of 2,3,4,6-tetra-*O*-methyl-(D?)-galactose also was indicated. It is of interest that the L-isomer of galactose has been found in linseed mucilage (2). The optical rotation of the methylated galactose indicated that it was composed mostly of the D-form. The isolation of 2,4-di-*O*-methyl-L-arabinose proves that L-arabopyranose residues were present in the polysaccharide, which differs therefore from the type of xylan encountered in wood (18) and in cereal flours (10). It will not be possible to put forward a unique structure for the linseed pentosan until more information, qualitative and quantitative, has been obtained. However, the evidence at present available indicates that the polysaccharide is probably composed of a main chain of beta-linked D-xylopyranosyl residues to which are attached at the 2-position side chains of 1,5- or 1,3-linked xylopyranosido-arabinose. It therefore resembles neutral polysaccharides which have been isolated from *plantago* seeds (16). It is clear that much further work will be required before a structure can be advanced for this neutral polysaccharide component of linseed mucilage.

EXPERIMENTAL

Methods

The following solvent systems (v/v) were used to separate sugars on paper chromatograms: (A) ethyl acetate:acetic acid:formic acid:water—18:3:1:4; (B) *n*-butanol:pyridine:water—10:3:3; (C) *n*-butanol:ethanol:water:ammonia—40:10:49:1 (top layer).

Chromatograms were irrigated for 20 to 30 hours in solvent A, for 40 to 80 hours in solvent B, and for 12 to 20 hours in solvent C. Solvent C was used to separate methylated sugars only. For chromatographic work using cellulose columns the two solvent systems used were: (D) *n*-butanol:water—20:1 (half saturated) and (E) petroleum ether (b.p. range 100–120° C.):*n*-butanol—80:20 containing water (2 ml. per liter). The latter mixture was used to separate methylated sugars only. Sugars were detected after paper chromatograms had been sprayed with a solution of *p*-anisidine hydrochloride in *n*-butanol and then heated (15).

Solutions were evaporated under reduced pressure and at *ca.* 40° C. All optical rotations are in aqueous solution at 20±2° C.

Preparation and Fractionation of Linseed Mucilage

Linseed (500 g.) was stirred in water (1 liter) for 1–2 minutes and the liquid was immediately decanted through a Büchner funnel (without a filter paper). The seeds were washed on the filter with water (1 liter) and were stirred in a further quantity of water (5 liters) for 3 hours. The mucilaginous solution was freed from seeds and debris by filtration, and copper acetate solution (7%; 135 ml.) was added. The precipitate (I) was separated by centrifugation and other precipitates (II–IV) were obtained by adding successively (1) copper acetate solution (200 ml.) and ethanol (975 ml.), (2) ethanol (300 ml.), and (3) an excess of ethanol. The copper complexes were decomposed by dissolution in *N* hydrochloric acid (500 ml.) and the polysaccharides were precipitated by the addition of ethanol. The products were then redissolved in water and reprecipitated (ethanol) to yield fractions free from chloride and copper ions. The last fraction contained very little uronic acid (naphtharesorcinol test) and will be referred to as the linseed mucilage pentosan. It had $[\alpha]_D$ −50°±3° (*c*, 1.04 in 0.03 *N* NaOH). Found: equiv. wt. 24,900.

Hydrolysis of the Neutral Polysaccharide

The pentosan (0.222 g.) was dissolved in sulphuric acid (*N*, 20 ml.), and the solution was heated at 95° C. The following changes in optical rotation were observed: $[\alpha]_D$ −51° (initial value), +36° (5 hours), +34° (9.5 hours, constant value). The solution was neutralized ($BaCO_3$), filtered, and concentrated to a sirup, which was fractionated by chromatography on sheets of Whatman 3MM paper by use of solvent B. Sugars with chromatographic mobilities identical with those of xylose, arabinose, glucose, and galactose were detected. The sugars were isolated and examined. The fastest moving fraction was identified as D-xylose. It had m.p. 151–153° and $[\alpha]_D$ +37° (10 minutes), +19° (equilibrium value). The second pentose was L-arabinose, with m.p. 152–153° and $[\alpha]_D$ +145° (3 minutes), +94° (6 hours, constant value). The third and fourth components were present in very small amount. They had $[\alpha]_D$ +20° and +7° respectively and could neither be induced to crystallize nor to furnish crystalline derivatives. Quantitative determinations of the mixture of sugars by the method of Hirst and Jones (13) showed that the sugars were present in the approximate ratios 14:8:1:1.

Periodate Oxidation of Linseed Pentosan

The polysaccharide (0.129 g.) was dissolved in water (25 ml.), and sodium metaperiodate solution (0.25 *M*, 5 ml.) was added. The changes in optical rotation of the solution, yield of formic acid, and uptake of periodate of the solution were followed. The results are collected in Table I. After 54 and 288 hours samples of the oxidized polysaccharide were isolated and hydrolyzed, and the sugars separated and detected on the chromato-

TABLE I

Time (hr.)	α_{obs}°	Per $C_5H_8O_4$	
		Mole of formic acid	Mole of IO_4' consumed
0.02	−0.18	—	—
1.0	−0.24	—	—
2.25	−0.22	0.28	0.39
6.25	−0.21	0.34	0.63
22.5	−0.18	0.37	0.84
33.0	−0.18	0.35	0.87
142.0	—	0.40	1.16
216.0	—	0.43	1.10

gram. Xylose, arabinose, and glucose were detected in the approximate ratios of 9:4:1 and of 10:2:1 respectively.

Periodate Oxidation of Degraded Pentosan

The linseed pentosan (0.7 g.) was dissolved in sulphuric acid (*N*, 63 ml.) and the solution was heated at 60° C. for 1.3 hours; $[\alpha]_D$ −44° (5 minutes), −9° (77 minutes). The solution was neutralized ($BaCO_3$), filtered, and concentrated to a small volume. The degraded polysaccharide was precipitated by the addition of this solution to ethanol (5 volumes). The precipitate was washed several times with ethanol to remove reducing sugars. The product (0.23 g.) gave sugars which had chromatographic mobilities indistinguishable from those of xylose, arabinose, glucose, and galactose in the approximate proportions of 20:5:2:1. A sample of this degraded polysaccharide (0.113 g.) was dissolved in water (25 ml.), and sodium metaperiodate solution (0.2 *M*, 5 ml.) was added. The progress of the oxidation was followed by measurement of the optical rotation, the formic acid production, and the periodate consumption. The results are collected in Table II. In a second experiment the pentosan (0.83 g.) was hydrolyzed with sulphuric

TABLE II

Time (hr.)	α_{obs}°	Per $C_5H_8O_4$	
		Mole of formic acid	Mole of IO_4' consumed
0.03	−0.22	—	—
0.75	−0.17	0.21	0.52
2.2	−0.12	0.27	0.72
4.7	−0.10	0.32	0.78
9.5	−0.03	0.34	0.84
22.5	+0.01	0.36	0.96
45.25	+0.04	0.37	0.93

acid (*N*/40) for 12 hours at 75°. The degraded polysaccharide (0.33 g.) was isolated as described above and had $[\alpha]_D$ −42°. On hydrolysis it gave xylose, arabinose, glucose, and galactose in the approximate proportions 20:4:2:1.

A sample (0.133 g.) of the polysaccharide was oxidized in water (20 ml.) and sodium metaperiodate solution (5 ml.). The results are collected in Table III. A sample of the degraded polysaccharide was isolated after 12 days' oxidation. On hydrolysis it gave xylose, arabinose, and glucose in the approximate proportions of 10:2:1.

Graded Hydrolysis of Linseed Pentosan

The linseed pentosan (5.74 g.) was dissolved in sulphuric acid (0.1 *N*, 100 ml.), the

TABLE III

Time (hr.)	α_{obs}°	Per $C_5H_8O_4$	
		Mole of formic acid	Mole of IO_4' consumed
0.03	−0.22	—	—
0.3	−0.24	0.16	0.39
1.9	−0.19	0.25	0.50
4.6	−0.15	—	0.65
10.0	−0.10	0.33	0.68
30.5	−0.06	0.30	0.81
47.9	−0.03	0.30	0.71
77.0	—	0.30	0.81
142.0	—	0.33	0.92
216.0	—	0.30	0.81

solution was heated on the water bath, and the change in optical rotation determined; $[\alpha]_D$ −45° (15 minutes), −5° (3.5 hours). At intervals samples were withdrawn and examined chromatographically. The following sugars were detected: xylose and arabinose in a ratio of 2:1 approximately. Oligosaccharides with R_{gal} values of 1.3, 1.0, 0.7, and 0.2 (solvent B) appeared at 0.5, 1.1, and 1 hour; that with R_{gal} 1.3 was much the most intense. After 3.5 hours the solution was neutralized ($BaCO_3$), filtered, and concentrated. The concentrate was poured into ethanol and the precipitated degraded polysaccharide was recovered, washed well with ethanol, and dried. Yield: 3.13 g. (55% of the starting material), $[\alpha]_D$ −26°. On hydrolysis it yielded xylose, arabinose, and galactose in the approximate proportions 20:2:1. The filtrate and washings were concentrated to a sirup (2.12 g.), chromatographic examination of which revealed the presence of xylose, arabinose, and an oligosaccharide with R_{gal} 1.3 in the approximate ratio 1:1:1 together with much smaller amounts of at least four other oligosaccharides. The sirup was fractionated on a charcoal–celite column (20) and seven oligosaccharides were detected and separated. These had the R_{gal} values and specific rotations listed in Table IV below.

TABLE IV

	Oligosaccharide						
	1	2	3	4	5	6	7
R_{gal} values: solvent A	1.1	0.9	0.7	0.5	0.4	0.3	—
solvent B	1.3	1.0	0.7	0.5	0.4	0.3	0.2
solvent C	1.2	0.9	0.8	0.5	—	—	—
$[\alpha]_D$	+74°	+138°	—	—	+74°	+99°	−4°

Examination of Oligosaccharide 1

A sample of the major disaccharide component, 1, was hydrolyzed and the products separated chromatographically. Xylose and arabinose in the proportions 1:1 were the only sugars detected. A sample (20 mg.) of the disaccharide was oxidized with bromine water (3 ml.) for 2 days, after which the solution was non-reducing to Fehling's reagents and the disaccharide could not be detected chromatographically (*p*-anisidine spray). When this non-reducing solution was heated with dilute sulphuric acid, xylose was the only sugar produced (separated and detected chromatographically).

A sample of the disaccharide (26 mg.) was dissolved in water (10 ml.) and oxidized

with sodium metaperiodate solution (0.2 *M*, 2.6 ml.) in the dark. The yields of formic acid and uptake of periodate were determined. Found: 0.35 hour, 2.44, 3.64; 1.1 hours, 2.98, 3.94; 1.8 hours, 2.8, 4.04; 3.35 hours, 3.22, 4.30; 9.1 hours, 3.29, 4.41; and 54 hours, 3.78, 4.63 moles of formic acid produced and of IO_4' reduced per mole of disaccharide. A 5-*O*-pentopyranosylpentose requires the production of 4 moles of formic acid and the consumption of 5 moles of periodate.

Attempted Enzymic Degradation of the Pentosan

The pentosan (0.058 g.) was dissolved in zinc sulphate solution (0.0125 *M*, 3 ml.) and a minute amount (*ca.* 0.1 mg.) of *Myrothecium* cellulase (6) was added. The solution was incubated at 35° C. for 60 hours and samples were removed for chromatographic examination every 5 hours. No reducing sugars were detected.

Acetylation of the Pentosan

The pentosan (8 g.) was swollen in *N*,*N*-dimethylformamide (90 ml.) during 6 hours. Pyridine (90 ml.) was then added and the slurry was shaken for a further 30 minutes. Acetic anhydride (32 ml.) was added in four equal portions at one-hour intervals with shaking, which was continued for a further 38 hours. The solution was diluted with pyridine (80 ml.) and poured with stirring into ice water (2 liters). The solid was collected, washed well with water, and dried over calcium chloride. Yield: 12.4 g. (95%) of a white powder, $[\alpha]_D$ −46° (*c*, 1.3 in chloroform).

A sample of the product was fractionated by extraction treatment in a Soxhlet extractor with solutions containing successively greater proportions of chloroform in petroleum ether (b.p. range 35–60° C.) as follows:

Ratio—petroleum ether/chloroform	Wt. (g.)	$[\alpha]_D$
(1) 67/33	—	—
(2) 60/40	0.042	−101°
(3) 50/50	0.662	−48°
(4) 40/60	0.122	−35°

The remainder of the material was incompletely acetylated.

A portion of fraction 4 (acetyl content, 35.5%) was deacetylated and the recovered polysaccharide was hydrolyzed. Paper chromatographic examination of the hydrolyzate showed the presence of xylose, arabinose, and galactose in the approximate ratio 20:8:1.

Methylation of the Pentosan

The polysaccharide acetate (14.5 g.) was dissolved in acetone (200 ml.) at 55° C. and methylation was commenced by the dropwise addition, with stirring, of sodium hydroxide solution (30%, 350 ml.) and dimethyl sulphate (150 ml.). The reagents were added in 10 equal amounts at 10-minute intervals. The partially methylated polysaccharide separated after 3 hours. It was recovered and remethylated as described above. Yield: 6.64 g. (66%). Found: OMe, 36.3%. In a second experiment a further quantity of methylated material was prepared. The two products were combined and fractionated by dissolution in a series of mixtures of petroleum ether (b.p. 40°–60° C.) and chloroform as follows:

Petroleum ether/chloroform ratio	Wt. (g.)	$[\alpha]_D$	%OMe
90/10	0.003	—	—
80/20	0.558	−73°	—
70/30	8.496	−75°	37.9; 38.2
60/40	Trace	—	—

Hydrolysis of the Methylated Pentosan

The methylated polysaccharide (4.5 g.) was dissolved in aqueous formic acid (50%, 400 ml.) and the solution was heated under reflux at 90° C. until the optimal rotation reached a constant value; $[\alpha]_D$ −82° (initial value), −9° (30 minutes), +17° (65 minutes), +32° (185 minutes, constant value). The solution was evaporated to dryness under reduced pressure and water was added to the sirup and then distilled off to remove the last traces of formic acid. In order to hydrolyze formyl esters the sirup was heated with *N* sulphuric acid at 90° for 8 hours. The cooled solution was neutralized ($BaCO_3$), filtered, and evaporated to a sirup. Paper chromatographic examination of the sirup indicated the presence of at least seven components whose R_g values were as follows: 0.95, 0.87, 0.82, 0.72, 0.64, 0.50, and 0.26 in solvent C. These rates of movement corresponded to those of 2,3,4-tri-*O*-methyl-D-xylose (0.95), 2,3,4,6-tetra-*O*-methyl-D-galactose (0.87), 2,3-di-*O*-methyl-D-xylose (0.82), 2,3-di-*O*-methyl-L-arabinose (0.72), 2,4-di-*O*-methyl-L-arabinose (0.64), a mono-*O*-methyl-D-xylose (0.5), and D-xylose (0.24) respectively. The proportions of these sugars were estimated by the alkaline iodine method of Hirst, Hough, and Jones (12) and by a gravimetric procedure in which small portions (*ca.* 100 mg.) of the sugars were separated on sheets on Whatman No. 1 filter paper, the fractions extracted from the paper, and the sirups dried and weighed on a microbalance. The proportions of sugars found by the two methods were 15:2:19:10:1:2:9 and 13:1:12:6:1:2:9. Because it is very difficult to separate completely such a complex mixture these results are approximate only.

Large Scale Separation of the Methylated Sugars

The sirup (4.4 g.) from 4.5 g. of methylated polysaccharide was placed on the top of a cellulose column (30×4 cm.) with the aid of a little cellulose powder and fractionated by the procedure of Hough, Jones, and Wadman (14); solvent E was allowed to flow through the column. The separation of the components was followed chromatographically and, as far as possible, fractions of eluant were collected which contained one sugar derivative only. When a fraction contained several sugars it was refractionated. In this way seven major components (A–G) were isolated and identified. Owing to the losses incurred in fractionation and refractionation the total recovery of chromatographically pure sugars was 66%.

Sugar A (0.81 g.) was the fastest moving sugar. In solvents A, B, and C, it had mobilities identical with those of authentic 2,3,4-tri-*O*-methyl-D-xylose. The sirup crystallized and, on recrystallization from ether, had m.p. 87–88.5° C., not depressed on admixture with an authentic specimen; $[\alpha]_D$ +52° (5 minutes), +17° (constant value; *c*, 2.83). Found: OMe, 47.3%.

The second fraction, B, (0.014 g.) moved on the chromatogram at the same rate as 2,3,4,6-tetra-*O*-methyl-D-galactose. It had $[\alpha]_D$ +38° (*c*, 0.7). When it was heated with aniline no crystalline *N*-phenyl glycosylamine was obtained, and the sugar remains unidentified.

Fraction C (0.746 g.) was indistinguishable from 2,3-di-*O*-methyl-D-xylose. It gave the same color reactions with the *p*-anisidine hydrochloride spray (15), moved at the same rate as an authentic specimen on chromatograms, and had $[\alpha]_D$ +26° (*c*, 2.75). When a sample (0.118 g.) was heated with aniline (0.065 g.) in ethanol (6.5 ml.) for 6 hours, crystalline *N*-phenyl-2,3-di-*O*-methyl-D-xylosylamine resulted. It had m.p. 142–143° C., not depressed on admixture with an authentic specimen, $[\alpha]_D$ +185° → +84° (*c*, 0.36 in ethyl acetate), and moved on chromatograms at the same rate as an authentic specimen of the xylosylamine derivative.

Fraction D (0.252 g.) was a sirup and, from its high value of optical relation, +95° (*c*, 2.16) was judged to be a derivative of L-arabopyranose. A sample (0.096 g.), on oxidation with bromine water, gave 2,3-di-*O*-methyl-L-arabofuranolactone (0.042 g.), $[\alpha]_D$ −38° (5 minutes) → −36° (3 days) (*c*, 2.12). On reaction with ammonia in alcohol the lactone was converted to the well-characterized crystalline amine of 2,3-di-*O*-methyl-L-arabonic acid, on 92% yield. It had m.p. and mixed m.p. 157–158° C., and $[\alpha]_D$ +16° (*c*, 0.56). Found: OMe, 33.2%. A sample of the next *fraction*, *E*, (0.048 g.) moved at a rate very similar to that of 3,4-di-*O*-methyl-L-arabinose. It had $[\alpha]_D$ +68° (*c*, 1.86). The sugar was unaffected by sodium metaperiodate, a reagent diagnostic for α-glycols, before or after its reduction with sodium borohydride. The substance was therefore probably the 2,4-di-*O*-methyl isomer with which it was chromatographically similar. It was heated with alcoholic aniline when the *N*-phenyl glycosylamine of 2,4-di-*O*-methyl-L-arabinose separated, which had m.p. and mixed m.p. 141–142° (after recrystallization from ether – petroleum ether, b.p. 35–60° C.). Owing to the small amount of material available the identification of this fraction as the 2,4-di-*O*-methyl isomer of L-arabinose is given with reserve. *Fraction F* (0.119 g.) moved at the rate of a mono-*O*-methyl-D-xylose. Paper chromatography did not differentiate clearly between the isomers but the technique of paper electrophoresis showed conclusively that this fraction was 3-*O*-methyl-D-xylose. It had $[\alpha]_D$ +18° (*c*, 4.96) and on oxidation with bromine water gave the crystalline lactone of 3-*O*-methyl-D-xylonic acid, m.p. 95–96° C. and $[\alpha]_D$ +73° (5 minutes) → +41° (10 days; *c*, 0.54). Found: OMe, 19.5%. A sample of the last *fraction*, *G*, (0.30 g.) corresponded in color reactions and chromatographic mobility to D-xylose. It had m.p. 149–151° C. and $[\alpha]_D$ +30° (20 minutes) → +18° (160 minutes, constant value; *c*, 2.77).

The Graded Hydrolysis of Linseed Mucilage

Linseed mucilage (50 g.) was dissolved in 0.5 *N* sulphuric acid (500 ml.) and the solution was boiled under reflux for 8 hours. It was cooled, filtered, and passed down columns of Amberlite resin 1R120(H) and 1R4B(OH) to remove ash and acidic material of low molecular weight. The acidic effluent was neutralized ($BaCO_3$), filtered, and concentrated to a sirup which was poured into ethanol. The barium salts were collected and the filtrate was concentrated to a sirup (*ca.* 14.2 g.). The neutral sugars were then fractionated on a charcoal–celite column (20) by gradient elution (1). Monosaccharides were discarded and the disaccharide fractions were collected and examined. Samples of the four major fractions moved on chromatograms at the rates (R_{gal}) given in Table V.

TABLE V

Solvent	A	B	C
Sugar *a*	0.70	0.67	0.64
Sugar *b*	1.09	1.36	1.17
Sugar *c*	0.86	0.98	0.91
Sugar *d*	0.17	0.17	0.20

Sugar *a* was a major component. After tedious refractionation it was obtained as a crystalline solid, m.p. 186–187°, not depressed on admixture with authentic 4-β-*O*-D-xylosido-D-xylose (xylobiose), $[\alpha]_D$ −30° → −20° (*c*, 0.2). When a solution of it was heated with phenylhydrazine acetate, phenylosazone was produced with m.p. 216–218°. This substance did not depress the melting point of authentic xylobiosazone and their X-ray powder diffraction photographs were indistinguishable.

ACKNOWLEDGMENTS

The authors are indebted to the National Research Council for grants and for the award of scholarships (to A. J. E.) which made this work possible.

REFERENCES

1. ALM, R. S., WILLIAMS, R. J. P., and TISELIUS, A. Acta Chem. Scand. **6**, 826 (1952).
2. ANDERSON, E. J. Biol. Chem. **100**, 249 (1933).
3. ANDERSON, E. and CROWDER, J. A. J. Am. Chem. Soc. **52**, 3711 (1930).
4. ANDREWS, P., BALL, D. H., and JONES, J. K. N. J. Chem. Soc. 4090 (1953).
5. BAILEY, K. Biochem. J. **29**, 2477 (1935).
6. BISHOP, C. T. and WHITAKER, D. R. Chem. & Ind. **11**, 119 (1955).
7. EASTERBY, D. G. and JONES, J. K. N. Nature, **165**, 614 (1950).
8. ERSKINE, A. J. and JONES, J. K. N. Can. J. Chem. **34**, 821 (1956).
9. GILL, R. E., HIRST, E. L., and JONES, J. K. N. J. Chem. Soc. 1469 (1939).
10. GILLES, K. A. Dissertation Abstr. **14**, 453 (1954).
11. HILGER, A. Ber. **36**, 3197 (1903).
12. HIRST, E. L., HOUGH, L., and JONES, J. K. N. J. Chem. Soc. 928 (1949).
13. HIRST, E. L. and JONES, J. K. N. J. Chem. Soc. 1659 (1949).
14. HOUGH, L., JONES, J. K. N., and WADMAN, W. H. J. Chem. Soc. 2511 (1949).
15. HOUGH, L., JONES, J. K. N., and WADMAN, W. H. J. Chem. Soc. 1702 (1950).
16. LAIDLAW, R. A. and PERCIVAL, E. G. V. J. Chem. Soc. 1600 (1949).
17. NEVILLE, H. A. D. J. Agr. Sci. **5**, 11, 115 (1913).
18. SAARNIO, J., WHATHEN, K., and GUSTAFSSON, C. Acta Chem. Scand. **8**, 825 (1954).
19. TIPSON, R. S., CHRISTMAN, C. C., and LEVENE, P. A. J. Biol. Chem. **128**, 609 (1939).
20. WHISTLER, R. L. and DURSO, D. F. J. Am. Chem. Soc. **72**, 677 (1950).

THE VIBRATIONAL SPECTRA OF PYRIDINE, PYRIDINE-4-*d*, PYRIDINE-2,6-d_2, AND PYRIDINE-3,5-d_2[1]

J. K. WILMSHURST[2] AND H. J. BERNSTEIN

ABSTRACT

The infrared spectra of pyridine and pyridine-4-*d* in the vapor state and of pyridine-2,6-d_2 and pyridine-3,5-d_2 in the liquid and vapor states have been obtained. The Raman spectra of pyridine-4-*d*, pyridine-2,6-d_2, and pyridine-3,5-d_2 as liquids have also been obtained together with depolarization ratios. The vapor band contours for pyridine support the assignment of Corrsin, Fax, and Lord in most part in preference to the assignment of McCullough and co-workers but it was found necessary to reassign the b_2 frequencies to give agreement between calculated and observed thermodynamic functions. The infrared and Raman data on pyridine-4-*d* are in agreement with the reported assignment for the a_1, a_2, and b_1 modes but it was found necessary to reassign the b_2 frequencies consistent with the present assignment in pyridine. A complete vibrational assignment for pyridine-2,6-d_2 and pyridine-3,5-d_2 has been made consistent with the present assignment in pyridine.

The infrared (3, 6) and Raman (3, 5) spectra of liquid pyridine have been studied by numerous workers but only one study of the infrared spectrum of pyridine vapor has been reported (6) and in that case the resolution was not sufficient to obtain band contours. From the infrared and Raman spectra of pyridine and pyridine-d_5, Corrsin, Fax, and Lord (CFL) were able to make a complete assignment (3) of all the fundamentals, while Anderson *et al.* (1), using this assignment, could correlate the observed infrared spectra by the liquid 2,3- and 4-monodeuteropyridines. Recently a comparison of the experimental thermodynamic functions of pyridine with those calculated statistically from the observed vibrational frequencies has led McCullough *et al.* (7) to modify the assignment for pyridine and its deuterium derivatives.

Since the assignment of McCullough *et al.* (7) depends essentially on the interchange of an a_1 and b_2 vibration in the CFL assignment (3) and since in pyridine the b_2 vibrations should give rise to bands having a very pronounced Q branch while the a_1 modes give rise to bands with a much less prominent Q branch, it appeared profitable to study the vapor spectrum of pyridine. Accordingly, the infrared spectrum of pyridine vapor was reinvestigated, and the band contours were assumed to be unaffected by Coriolis interactions. These contours were not consistent with the assignment of McCullough *et al.*, and supported in most part the assignment of CFL, although it was found necessary to reassign the type b_2 vibrations to give agreement between calculated and observed (7) thermodynamic functions.

The Raman spectrum of pyridine-4-*d* as a liquid and the infrared spectrum of its vapor were also obtained and the polarization and band contour data agreed with the assignment of Anderson *et al.* (1) for the a_1, a_2, and b_1 vibrations, but the b_2 vibrations were reassigned to agree with the present assignment in pyridine (see below).

The Raman spectra of liquid pyridine-2,6-d_2 and pyridine-3,5-d_2 and the infrared spectra of their vapors and their solutions in CS_2 and CCl_4 were also obtained and a vibrational assignment made consistent with the present assignment for pyridine.

EXPERIMENTAL

The Raman spectra of the deuteropyridines* were obtained using a White Raman

[1]*Manuscript received June 24, 1957.*
Contribution from the Division of Pure Chemistry, National Research Council, Ottawa, Canada.
Issued as N.R.C. No. 4481.
[2]*National Research Council Postdoctorate Fellow 1955–57.*
**All the deuterium-substituted pyridines were made available through the courtesy of Dr. L. Leitch of these laboratories.*

grating spectrometer (8), depolarization ratios being measured by the method of Edsall and Wilson (4). The spectra are shown in Fig. 3.

The infrared spectra were measured on a Perkin Elmer model 12C double pass spectrometer equipped with LiF, CaF_2, NaCl, KBr, and CsBr optics. The spectra of the pure

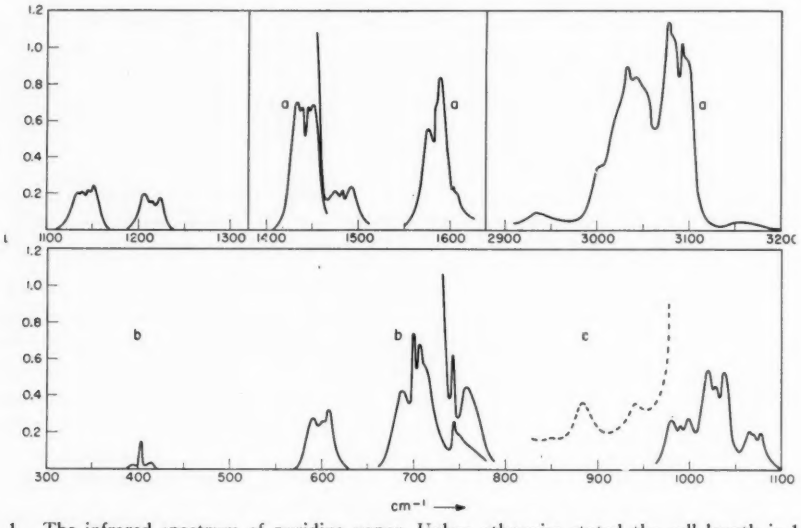

FIG. 1. The infrared spectrum of pyridine vapor. Unless otherwise stated the cell length is 1 meter and the pressure is ~14 mm.

a = 1 meter cell; pressure ~7mm.
b = 10 cm. cell; pressure ~14 mm.
c = liquid in a 0.2 mm. cell.

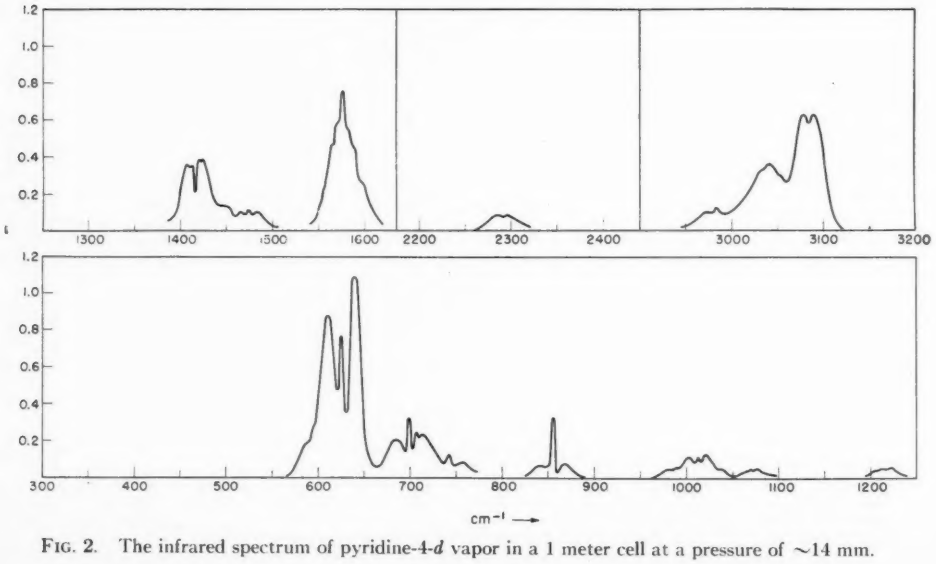

FIG. 2. The infrared spectrum of pyridine-4-*d* vapor in a 1 meter cell at a pressure of ~14 mm.

liquids gave some extremely intense bands and it was necessary to study the liquids as dilute solutions of 20 mg./cc. in CCl_4 for the region 2–7μ, and 20 mg./cc. in CS_2 for the 7–25 μ region, a 1 mm. cell being used. The spectra of the 2,6-d_2 and 3,5-d_2 pyridines are shown in Fig. 4. The vapor spectra were obtained using a 1 meter cell for the 2–25 μ region and a 10 cm. cell for the CsBr region. Before obtaining a spectrum, the gas handling equipment was thoroughly cleaned, all stopcock grease changed, and the whole line and cell pumped for at least 16 hours to minimize any contamination of the deuterium compounds. The vapor spectrum of pyridine is shown in Fig. 1, that of pyridine-4-*d* in Fig. 2, and the spectra of the 2,6-d_2 and 3,5-d_2 pyridines in Fig. 5. The observed spectra of the 2,6-d_2 and 3,5-d_2 pyridines are given in Tables V and VI respectively together with the vibrational assignments.

DISCUSSION

Pyridine, pyridine-4-*d*, pyridine-2,6-d_2, and pyridine-3,5-d_2 all belong to the point group C_{2v} and the fundamentals divide up as $10a_1$ (I.R., p) + $9b_1$ (I.R., dp) + $3a_2$ (R., dp) + $5b_2$ (I.R., dp) where I.R. and R. denote infrared active and Raman active vibrations respectively and p and dp refer to polarized and depolarized Raman bands.

In pyridine and pyridine-4-*d* the least axis of inertia coincides with the figure axis* and hence the a_1 type vibrations should give rise to type *A* bands, the b_1 type to type *B* bands, and the b_2 type to type *C* bands in the infrared. In the 2,6- and 3,5-dideutero-pyridines, however, the intermediate moment of inertia coincides with the figure axis* and in this case the type a_1 vibrations should give rise to *B* type bands, the type b_1 to *A* type bands, and the type b_2 to *C* type bands in the infrared. In all cases the *C* type bands have a weak *Q* branch, and the *B* type bands have two weak *Q* maxima.

The spectra are best discussed separately.

Pyridine

To make the calculated statistical thermodynamic functions for pyridine agree with the experimental data, McCullough *et al.* (7) found it necessary to replace in the CFL assignment (3) the fundamental at 749 cm.$^{-1}$ by a fundamental at 981 cm.$^{-1}$. This band at 749 cm.$^{-1}$ then had to be explained as a combination tone and from its intensity was necessarily regarded to be in Fermi resonance with the other fundamental at 703 cm.$^{-1}$. Thus it could only be a summation tone, and, since the lowest fundamental is at 374 cm.$^{-1}$, it must be the overtone of this frequency and, therefore, necessarily of type A_1. Hence the fundamental at 703 cm.$^{-1}$ must be a type a_1 fundamental and was assigned to ν_{6a} by McCullough *et al.* (7). The fundamental at 605 cm.$^{-1}$ assigned by CFL to ν_{6a} was then assigned as a type b_2 mode. From the vapor spectrum of pyridine (Fig. 1) it can be readily seen that the band at 605 cm.$^{-1}$ has an *A* type band contour and therefore belongs to the a_1 species consistent with the assignment of CFL. Further the bands around 700 cm.$^{-1}$ all have predominant *Q* branches typical of type *C* bands and must belong to the b_2

**Assuming the dimensions determined from the microwave spectra (2) the moments of inertia of the isotopic pyridines (in g. cm.^{2}) were calculated to be:*

	Pyridine	Pyridine-4-*d*	Pyridine-2,6-d_2	Pyridine-3,5-d_2
I_A	138.97 $\times 10^{-40}$	138.97 $\times 10^{-40}$	152.80 $\times 10^{-40}$	154.18 $\times 10^{-40}$
I_B	144.58	154.84	149.28	149.30
I_C	283.55	293.81	302.08	303.48

where I_A is the moment of inertia about the figure axis (N–C_4 direction), I_B is the moment of inertia about an axis in the plane of the molecule perpendicular to the figure axis, and I_C is the moment of inertia about an axis perpendicular to the plane of the molecule.

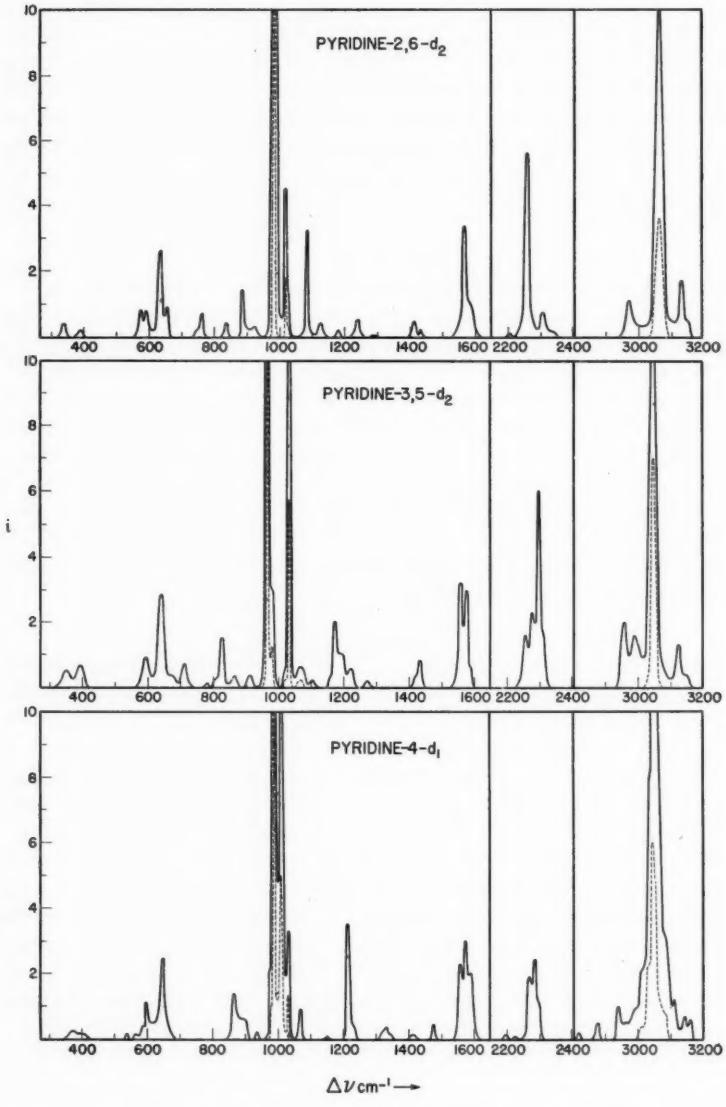

FIG. 3. The Raman spectra of liquid pyridine-4-*d*, pyridine-2,6-d_2, and pyridine-3,5-d_2.
——— Instrument gain 25%; slit ~7½ cm.$^{-1}$.
– – – – – Instrument gain 20%; slit ~5 cm.$^{-1}$.

species. Thus the present data definitely rule out the assignment of McCullough *et al.* for ν_{6a} and ν_{11}.

The vapor data reported here for pyridine are consistent with the CFL assignment for the a_1 and b_1 modes and it is considered unlikely that the CFL assignment for the a_1, a_2, and b_1 modes could be seriously in error. Thus it only remains to establish the type b_2 assignment. Instead of two bands around 700 cm.$^{-1}$ as observed by CFL we have in fact obtained three bands at 700, 707, and 749 cm.$^{-1}$ all of such intensity as to indicate that they could be taken as fundamentals. No summation tone around 700 cm.$^{-1}$ belonging to the b_2 species is possible, and, hence, a band cannot be interpreted in this way. If each of

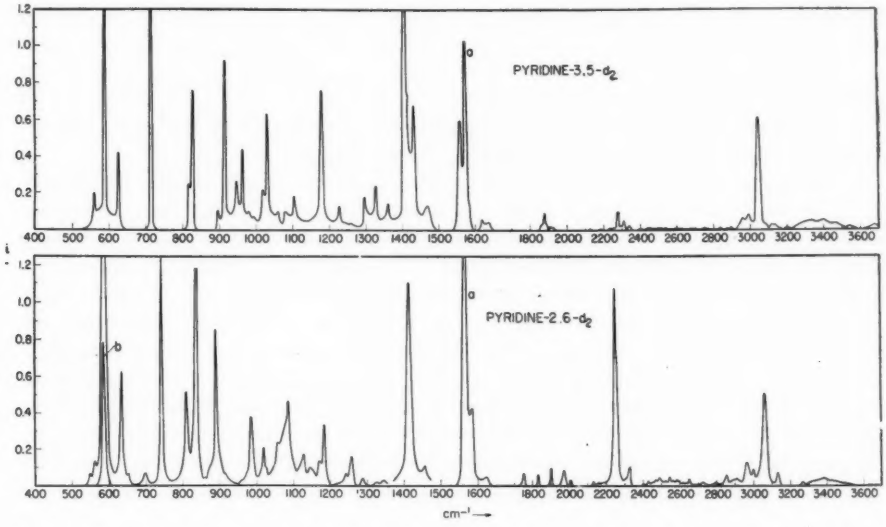

FIG. 4. The infrared spectra of pyridine-2,6-d_2 and pyridine-3,5-d_2 as solutions of 20 mg./cc. CCl_4 (1400–3700 cm.$^{-1}$) and 20 mg./cc. CS_2 (400–1400 cm.$^{-1}$). Cell thickness = 1 mm.
a = 200 mg./cc. CCL_4; cell thickness = 0.1 mm.
b = 5 mg./cc. CS_2; cell thickness = 1 mm.

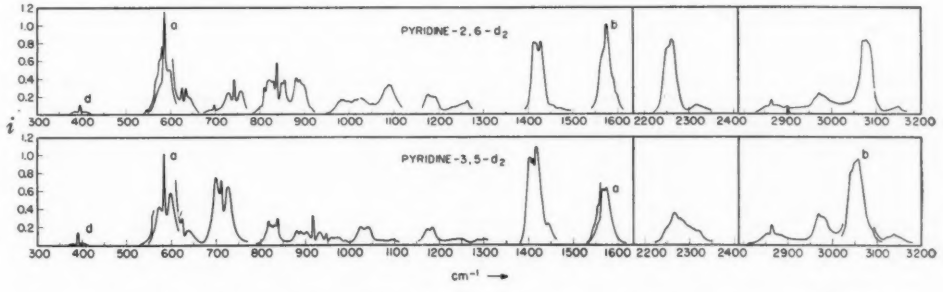

FIG. 5. The infrared spectra of pyridine-2,6-d_2 and pyridine-3,5-d_2 vapors. Unless otherwise stated the cell length is 1 meter and the vapor pressure is ~14 mm.
a = 1 meter cell; pressure ~5 mm.
b = 1 meter cell; pressure ~7 mm.
d = 10 cm. cell; pressure ~14 mm.

these three bands is considered as a fundamental a consistent assignment with pyridine-d_5 is possible by assigning one of them to ν_4 instead of the weak band at ~675 assigned by CFL to this mode and then lowering ν_5 from 942 in CFL's assignment to 886 cm.$^{-1}$. The two bands at ~675 and 942 cm.$^{-1}$ are then assigned as $\nu_{18a}-\nu_{16b}$ = 663 cm.$^{-1}$ and $\nu_{8a}-\nu_{6b}$ = 938 cm.$^{-1}$ respectively. Five type b_2 vibrations with expected *C* type contours have been observed for both pyridine-2,6-d_2 and pyridine-3,5-d_2. From the observed spectra alone, the type b_2 bands at 700 cm.$^{-1}$ and 886 cm.$^{-1}$ suggested above for pyridine fit into a correlation pattern, with the type b_2 bands of the dideuterated pyridines. However, this assignment, indicated purely on the basis of spectroscopic data, is not consistent with the experimental thermodynamic properties (7) which have been determined very accurately (to within ±0.2%). Calculation of the entropy and heat capacity of pyridine using the above assignment lead to values about 0.5% and 2% too high respectively. This large error between calculated and observed heat capacity values is well outside the experimental error and though spectroscopically the above assignment for the b_2 vibrations is consistent between the deuterated molecules it appears necessary to look for an alternative assignment consistent with the thermodynamic data.

McCullough *et al.* (7) have shown that the replacement of one frequency around 700 cm.$^{-1}$ by one around 900 cm.$^{-1}$ in the CFL assignment will bring the calculated and observed thermodynamic functions into line. As mentioned above it seems unlikely that the a_1, a_2, and b_1 frequencies are seriously in error and, hence, this change must occur in the b_2 species. This can be done by replacing the band at 707 cm.$^{-1}$ in the assignment discussed above for the type b_2 modes by one at 942 cm.$^{-1}$. This strong *C* type band at 707 cm.$^{-1}$ can then be explained as the difference tone $\nu_{18b}-\nu_{16a}$ = 711 cm.$^{-1}$ (B_2), the high intensity possibly arising from the relatively high population of the low vibrational level at 374 cm.$^{-1}$. This assignment (Table I) now gives agreement between calculated and observed thermodynamic functions within the experimental error (Table II).

The Teller–Redlich product ratio between pyridine and pyridine-d_5 is now adjusted by replacing the b_2 frequency in pyridine-d_5 at 625 cm.$^{-1}$ (coincident with ν_{6b}) by the

TABLE I

FUNDAMENTAL FREQUENCIES FOR PYRIDINE AND PYRIDINE-d_5

Frequency	Pyridine CFL	Pyridine McCullough *et al.*	Pyridine Present	Pyridine-d_5	Product ratio Calc.	Product ratio Obs.
a_1						
1	992	992	992(*A*)	962		
2	3054	3055	3054	2293		
6*a*	605	720	605(*A*)	582		
8*a*	1580	1583	1583	1530		
9*a*	1218	1218	1218(*A*)	886	0.182	0.186
12	1029	1030	1030(*A*)	1006		
13	(3054)	(3055)	(3054)	2270		
18*a*	1068	1068	1068(*A*)	823		
19*a*	1482	1483	1482(*A*)	1340		
20*a*	3036	3035	3036	2254		
b_1						
3	(1217)	1200	(1218)	908		
6*b*	652	653	652	625		
7*b*	(3054)	3055	(3036)	2285		
8*b*	1572	1571	1572	1542		
b_1 (*continued*)						
14	1375	1377	1375	1322	0.197	0.202
15	1148	1146	1148(*B*)	(887)		
18*b*	(1068)	1085	1085*	833		
19*b*	1439	1440	1439(B)	1301		
20*b*	3083	3080	3083(*B*)	(2293)		
a_2						
10*a*	886	885	886	690		
16*a*	374	374	374	329	0.543	0.556
17*a*	981	(1030)	981	798		
b_2						
4	675	675	749(*C*)	567		
5	942	981	942	823		
10*b*	749	940	886	762	0.391	0.395
11	703	605	700(*C*)	530		
16*b*	405	405	405(*C*)	371		

**Unpublished data from Chemical Research Laboratory, Teddington, Middlesex, England (quoted by McCullough et al. (7)).*

TABLE II

OBSERVED AND CALCULATED MOLAL THERMODYNAMIC PROPERTIES OF PYRIDINE IN THE IDEAL GASEOUS STATE

T,° K.	Obs.[a]	Calc.
	Entropy $S°$, cal. deg.$^{-1}$	
346.65	70.65	70.65
366.11	71.86	71.90
388.40	73.27	73.31
	Heat capacity $C_p°$, cal. deg.$^{-1}$	
374.20	23.79	23.89
397.20	25.23	25.34
420.20	26.65	26.76
450.20	28.43	28.50
500.20	31.12	31.22

[a] = *Reported by McCullough et al. (7).*

frequency at 823 cm.$^{-1}$ (coincident with ν_{18a}). The assignment for pyridine and pyridine-d_5 is given in Table I together with the product rule ratios.

Pyridine-4-d

The 4-chloropyridine used in the preparation of 4-deuteropyridine unfortunately contained about 10% pyridine as an impurity and, thus, the strong Raman band of pyridine at 1029 cm.$^{-1}$ and the strong infrared bands of pyridine around 700 cm.$^{-1}$ occur weakly in the spectra of pyridine-4-*d*.

The Raman polarization data (Table III) and infrared band contours (Fig. 2) confirm the assignment of Anderson *et al.* (1) for the a_1, a_2, and b_1 vibrations. The band at 862 cm.$^{-1}$, assigned by them to the b_1 mode ν_{18b}, was observed here to have a *C* type contour and is assigned to the b_2 vibration ν_5, ν_{18b} then being considered to be coincident with ν_5. To be consistent with the present assignment in pyridine, a b_2 type band assigned by them to a doubtful band around 660–670 cm.$^{-1}$ is replaced here by a band at 862 cm.$^{-1}$

TABLE III

RAMAN BANDS AND POLARIZATION DATA FOR PYRIDINE-4-*d*

373 (0) p?	$\nu_{16a}(a_2)$	1476 (0) p	$\nu_{19a}(a_1)$
~407 (0) dp	$\nu_{12}-\nu_{6a} = 413\ (A_1)$	1559 (1) dp	$\nu_{8b}(b_1)$
538 (0)	$\nu_{9a}-\nu_4 = \sim 545(B_2)$	1575 (1) p or dp	$\nu_{8a}\ (a_1)$
565 (0)	$\nu_{9a}-\nu_{6b} = 567(A_1)$	1590 (1) p or dp	$\nu_1+\nu_{6a} = 1586(A_1)$*
584 (0) p?	$\nu_{19b}-\nu_{15} = 579(A_1)$	2197 (0)	$\nu_1+\nu_{9a} = 2204(A_1)$
597 (0) p	$\nu_{6a}(a_1)$	2226 (0)	$\nu_{9a}+\nu_{12} = 2230(A_1)$*
648 (1) dp	$\nu_{6b}(b_1)$	2270 (1) p	$\nu_{9a}+\nu_{18a} = 2283(A_1)$*,†
866 (1) dp	$\nu_5(b_2)$	2287 (1) p	$\nu_{13}(\ _1)$
889 (0) dp	$\nu_{10a}(a_2)$	2299 (1) p?	$\nu_3+\nu_{18b} = 2301(A_1)$
936 (0) p	$\nu_{8b}-\nu_{11} = 934(A_2)$	2822 (0) p	$2\times\nu_{19b} = 2826(A_1)$
979 (1) p	$\nu_{17a}(a_2)$	2879 (0)	$\nu_{19a}+\nu_{19b} = 2889(B_1)$*
990 (10) p	$\nu_1\ (a_1)$	2942 (0) p	$2\times\nu_{19a} = 2952(A_1)$*
1010 (5) p	$\nu_{12}\ (a_1)$	2966 (0)	$\nu_{8b}+\nu_{19b} = 2972(A_1)$*
1032 (1) p	Pyridine	2991 (0)	$\nu_{8a}+\nu_{19b} = 2988(B_1)$*
1070 (0) p	$\nu_{18a}(a_1)$	3012 (1) p	$\nu_{20a}(a_1)$
1150 (0)	?	3035 (2)	$\nu_{7b}(b_1)$
1215 (2) p or dp	$\nu_{9a}(a_1)$; $\nu_3(b_1)$	3045 (6) p	$\nu_2(a_1)$
1232 (0) dp?	$\nu_{8a}+\nu_{6b} = 1245(B_1)$*,†	3055 (1) p	$\nu_{8a}+\nu_{19a} = 3051(A_1)$
~1320 (0)	?	3081 (0) dp?	$2\nu_{9a}+6b = 3078(B_1)$
1332 (0) dp	$\nu_{6a}+\nu_{10b} = 1340(B_2)$	3112 (0) p	$2\times\nu_{8b} = 3118(A_1)$
~1345 (0)	$\nu_{14}(b_1)$	3145 (0)	$2\times\nu_{8a} = 3150(A_1)$*
1413 (0)	$\nu_{19b}(b_1)$	3161 (0) p	$\nu_{10a}+\nu_{13} = 3176\ A(_2)$

**Raman band has corresponding infrared band. The assignment is that of Anderson et al. (1) unless otherwise indicated.*

†*Not the assignment of Anderson et al. (1).*

coincident with another b_2 mode ν_5 and with the b_1 mode ν_{15}. The assignment is given in Table IV together with the product rule ratios.

Pyridine-2,6-d_2

In the assignment for both 2,6- and 3,5-dideuteropyridine, the criteria defined by Anderson *et al.* (1), in addition to the polarization and band contour data, will be adhered to—namely (*a*) the frequency must lie in between the corresponding frequencies for 'light' and 'heavy' pyridine; (*b*) the intensity of the line must be compatible with the intensity of the corresponding line in the isotopic pyridines; (*c*) if the "parent" normal vibration is a "carbon" vibration, the normal vibration frequency of the dideuterospecies must lie close to the corresponding pyridine frequency; if it is a "hydrogen" vibration it must be chosen in a way consistent with the corresponding choice made in the case of the partly deuterated benzenes; (*d*) if the line in question cannot possibly be interpreted as a combination or overtone it must be one of the normal vibrations of the molecule; (*e*) any complete set of normal vibration frequencies chosen must obey the Teller–Redlich product rule.

TABLE IV

FUNDAMENTAL FREQUENCIES FOR PYRIDINE-4-*d*

		Pyridine-4-*d*		Product ratios	
Frequency	Pyridine	Anderson *et al.*	Present	Calc.	Obs.
a_1					
1	992	989	989(*A*,p)[a]		
2	3054	3033	3045(*A*,p)[a]		
6*a*	605	597	597(—,p)		
8*a*	1583	1575	1575(—,p?)		
9*a*	1218	1215	1215(*A*,p?)	0.712	0.706
12	1030	1015	1010(*A*,p)[a]		
13	3054	2285	2287(*A*,p)[a]		
18*a*	1068	1068	1068(*A*,p)		
19*a*	1482	1476	1476(*A*,p)		
20*a*	3036	3019	3012(—,p)[a]		
b_1					
3	1218	(1215)	(1215)		
6*b*	652	~ 645	648[a]		
7*b*	3036	3069	3035[a]		
8*b*	1572	1559	1559		
b_1 (*continued*)					
14	1375	1347	1347	0.724	0.718
15	1148	862	(862)		
18*b*	1085	1086	1086		
19*b*	1439	1413	1413(*B*)		
20*b*	3083	3069	3069(*B*)		
a_2					
10*a*	886	~ 890	889[a]		
16*a*	374	~ 365	373[a]	1.000	0.999
17*a*	981	968	979[a]		
b_2					
4	749	660–670	743		
5	942	834	862(*C*)		
10*b*	886	743	(862)	0.736	0.743
11	700	633	625(*C*)		
16*b*	405	~ 383	381(*C*)		

[a] = *Raman values.*
( ) = *Frequency used twice.*

In 2,6-dideuteropyridine the polarized Raman bands at 3065, 2260, 1087, 1019, 986, and 889 cm.$^{-1}$ can be assigned with reasonable certainty to the a_1 species consistent with criteria *a*, *b*, and *c*. The remaining a_1 vibrations ν_{6a}, ν_{8a}, ν_{19a}, and ν_{20a} were also chosen according to these criteria. The b_1 modes were assigned according to the criteria *a*, *b*, and *c* using criterion *e* as a final check.

There should be five type b_2 vibrations and in the spectrum five *C* type bands are observed at 839, 743, 699, 586, and 397 cm.$^{-1}$. These bands are consistent with the "spectroscopic" assignment in pyridine mentioned above, but to obtain agreement with the present assignment in pyridine dictated by the thermodynamic data one band around 700 cm.$^{-1}$ must be assigned as a difference tone of species B_2 and replaced by a band around 900 cm.$^{-1}$. The weak type *C* band at 699 cm.$^{-1}$ is assigned to the difference tone $\nu_{18a}-\nu_{16b}$ = 690 cm.$^{-1}$ (B_2) and is replaced by a band at 889, coincident with ν_{9a} and

TABLE V

INFRARED AND RAMAN SPECTRUM OF PYRIDINE-2,6-d_2

Infrared		Raman,	
Liquid	Vapor	liquid	Assignment
		340 (0) dp	a_2 Fundamental
	386		
	397 C	393 (0) dp	b_2 Fundamental
	410		
550 w	548		1568−1019 = 549 (B_1)
563 w			1457−889 = 568 (A_1)
	~566		
	~576 A?	578(0) p?	a_1 Fundamental
585 vs	586		
	598 C		b_2 Fundamental
		594(0) dp	1586−986 = 600 (A_1)
	626		
635 m	635 B??	639 (1) dp	b_1 Fundamental
	~642		
655 w		658 (0) dp	1415−765 = 650 (B_2)
	690		
699 w	699 C		1087−397 = 690 (B_2)
	707		
	731		
742 s	743 C	749 (0)	b_2 Fundamental
	757		
		765 (0) dp	a_2 Fundamental
	802		
809 m	811 C		1568−765 = 803 (B_2)
	822		
~828 wm	832		839+397−397 = 839 (B_2)
837 s	839 C	840 (0) dp	b_2 Fundamental
860 w	849 ?		b_1 Fundamental
	856		
	882		
	890		
889 s	~894 B	889 (1) p	$a_1 + b_2$ Fundamental
	~899		
~902? w			340+598 = 918 (A_2)?
915 w	~917		340+586 = 926 (B_1)
		926 (0) p?	a_2 Fundamental
			340+635 = 975 (B_2)
961 w			397+578 = 975 (B_2)
	~977		
	983		
985 m	988 B	986 (10) p	a_1 Fundamental
	~1000		
	1014		
1019 wm	1020 B?	1019 (1) p	a_1 Fundamental
	1026		
1026 w		1030 (0) p?	397+635 = 1032 (A_2)?
1058 wm	1052		1457−397 = 1060 (B_2)
	1080		
1087 m	1088	1087 (1) p	a_1 Fundamental
	1093		
1128 wm		1129 (0) dp	b_1 Fundamental
1146 w			2×578 = 1156 (A_1)
1171 w			2×586 = 1172 (A_1)
	1177		
1184 m	1186 A	1183 (0) p?	b_1 Fundamental
	1193		
~1215 w			578+635 = 1213 (B_1)
	~1233		
1243 w	~1250	1242 (0) dp	397+839 = 1236 (A_1)
1258 wm	1264		2×635 = 1270 (A_1)
1288 w		1293 (0) dp	397+889 = 1286 (B_2)
1325 w			586+743 = 1329 (A_1)
1345 w			b_1 Fundamental

Infrared		Raman,	
Liquid	Vapor	liquid	Assignment
	1414		
1415 vs	~1420 A	1415 (0) p?	b_1 Fundamental
	1429		
		1434 (0)	578+860 = 1438 (B_1)
1457 wm	~1458 B		a_1 Fundamental
	1471		
1568 vs	~1564	1568 (2) dp	b_1 Fundamental
	1577		
	1591		
1586 ms	1598 B	1586 (0) p?	a_1 Fundamental
1625 w			743+889 = 1632 (B_2)
1754 w			743+1019 = 1762 (B_2)
1833 w			860+986 = 1846 (B_1)
1903 wm			889+1019 = 1908 (A_1)
1973 wm			397+1586 = 1983 (B_2)
2009 w			889+1128 = 2017 (B_1)
2133 w			1019+1128 = 2147 (B_1)
2161 w			2×1087 = 2174 (A_1)
2179 w			765+1415 = 2180 (B_2)
2189 w			743+1457 = 2200 (B_2)
		2206 (0)	
	2253		
2252 vs	2264 B?		b_1 Fundamental
~2258 s		2260 (3) p	a_1 Fundamental
~2307 w	2318	2309 (0) p	1128+1184 = 2312 (A_1)
2330 wm		2340 (0)	889+1457 = 2346
2403 w			839+1586 = 2425 (B_2)
2431 w			986+1457 = 2443 (A_1)
2455 w			889+1586 = 2475 (A_1)
2471 w			1019+1457 = 2476 (A_1)
2490 w			1087+1415 = 2502 (B_1)
2525 w			1184+1345 = 2529 (A_1)
2546 w			986+1568 = 2554 (B_1)
2563 w			986+1586 = 2572 (A_1)
2585 w			1019+1568 = 2587 (B_1)
2598 w			1019+1586 = 2605 (A_1)
2620 w			1184+1457 = 2641 (B_1)
2640 w			1087+1568 = 2655 (B_1)
2653 w			1087+1586 = 2673 (A_1)
2726 w			1568+1184 = 2752 (A_1)
2797 w			1345+1457 = 2802 (B_1)
	2857		
2856 w	2866 A		1415+1457 = 2872 (B_1)
	2879		
~2895 w	2901		1345+1568 = 2913 (A_1)
2914 w			1345+1586 = 2931 (B_1)
	~2964		
2967 wm	2972	2973 (1) p	1415+1568 = 2983 (A_1)
	~2981		
3002 wm			a_1 Fundamental
	3072		
3067 ms	3079 A	3065 (4) p	a_1 Fundamental
	3086		b_1 Fundamental
3134 wm	3140 B	3134 (1) p	2260+889 = 3149 (A_1)
	3150		
		3152 (0) p?	1568+1586 = 3154 (B_1)
3269 w			1019+2260 = 3279 (A_1)
~3325 w			1087+2252 = 3339 (B_1)
3386 w			340+3067 = 3407 (B_2)
3429 w			1184+2252 = 3436 (A_1)
~3450 w			397+3065 = 3462 (B_2)

TABLE VI

INFRARED AND RAMAN SPECTRUM OF PYRIDINE-3,5-d_2

Infrared		Raman,	
Liquid	Vapor	liquid	Assignment
		352 (0)	a_2 Fundamental
	380		
	391 C	394 (0)	b_2 Fundamental
	402		
559	558		1589 − 1029 = 560 (B_1)
	574		
587	585 C		b_2 Fundamental
	599		
		596 (0)	a_1 Fundamental
	—		
626	625 C		1411 − 784 = 627 (B_2)
	639		
		642 (1)	b_1 Fundamental
		~675 (0)	1029 − 352 = 677 (A_2)
	700		
714	713 C	715 (0)	b_2 Fundamental
	727		
		784 (0)	a_2 Fundamental
818		~812 (0)	1411 − 596 = 815 (B_1)
	818		
	824		
828	832 B	829 (1)	a_1 Fundamental
	849		
		867 (0)	a_2 Fundamental
	882		
897	889		b_2 Fundamental
	903		
917	918 C	915 (0)	b_2 Fundamental
	932		
948	947		
	960 A		b_1 Fundamental
967	974 B	967 (10)	a_1 Fundamental
981		980 (1)	394 + 587 = 981 (A_1)
994	991		352 + 642 = 994 (B_2)
1020		1020 (0)	391 + 643 = 1034 (A_2)?
	1023		
	1029		
1029	1036 B	1034 (6)	a_1 Fundamental
	1041		
1060			1411 − 352 = 1059 (B_2)
1081		1070 (0)	b_1 Fundamental
1105		1104 (0)	b_1 Fundamental
		1161 (0)	2×585 = 1170 (A_1)
	1174		
1179	1186 B	1174 (1)	a_1 Fundamental
		1198 (0)	2×596 = 1192 (A_1)
1227	~1229	1223 (0)	596 + 642 = 1238 (B_1)
1244	~1247		352 + 897 = 1249 (B_1)
1260			352 + 918 = 1270 (B_1)
		1275 (0)	2×642 = 1284 (A_1)
	1287		
1297	1301 B?		391 + 918 = 1309 (A_1)
1328			b_1 Fundamental
1362			391 + 967 = 1358 (B_2)
	1404		
1411	1411 A		b_1 Fundamental
	1418		
~1418		1422 (0)	2×713 = 1426 (A_1)
	~1436		
1436	1440 B	1435 (0)	a_1 Fundamental
	1444		
1470			642 + 828 = 1470 (B_1)

Infrared		Raman,	
Liquid	Vapor	liquid	Assignment
1561	~1545 B	1560 (1)	596 + 967 = 1563 (A_1)
	~1556		
	1567		
1576	1575 B	1577 (1)	a_1 Fundamental
~1586		1589 (0)	b_1 Fundamental
1618			713 + 918 = 1631 (A_1)
1638			2×828 = 1656 (A_1)
1862 w			784 + 1081 = 1865 (B_2)
1872 wm			918 + 967 = 1885 (B_2)
1889 w			2×947 = 1894 (A_1)
1914 w			596 + 1328 = 1924 (B_1)
1925 w			352 + 1589 = 2941 (B_2)
2129 w			1029 + 1105 = 2134 (B_1)
2186 w			784 + 1411 = 2195 (B_2)
2234 w			828 + 1411 = 2239 (B_1)
2256 w	~2253	2258 (1) p	828 + 1436 = 2264 (A_1)
	2267		
2281 wm	2281 A	2277 (1) dp	b_1 Fundamental
	2287		
2295 w		2297 (3) p	a_1 Fundamental
	~2300		
2310 w	2311	2314 (1) p?	2×642 + 1029 = 2313 (A_1)
	2319		
2337 w			918 + 1436 = 2354 (B_2)
2401 w			828 + 1577 = 2405 (A_1)
2448 w			1029 + 1436 = 2465 (A_1)
2492 w			918 + 1577 = 2495 (B_2)
2519 w			1081 + 1436 = 2517 (B_1)
2541 w			967 + 1577 = 2544 (A_1)
2603 w			1179 + 1436 = 2615 (A_1)
2626 w			352 + 2281 = 2633 (B_2)
2651 w			1081 + 1577 = 2658 (B_1)
2683 w			1105 + 1577 = 2682 (B_1)
2747 w			1328 + 1436 = 2764 (B_1)
2836 w			1411 + 1436 = 2847 (B_1)
	2856		
2875	2865 C		585 + 2297 = 2882 (B_2)
	~2880		
2894 w			1328 + 1577 = 2905 (B_1)
2959 w		2961 (1) p	?
2994 wm	2971 B	2986 (1) p	1411 + 1589 = 3000 (A_1)
	2980	3000 (1) p	a_1 Fundamental
		3047 (7) p	a_1 Fundamental
	~3044		
3049 s	3053 ?		b_1 Fundamental
	3059		
3084 w	~3086		828 + 2281 = 3109 (B_1)
3123 w		3126 (1) p	828 + 2297 = 3125 (A_1)
	~3128		867 + 2281 = 3148 (B_2)
3136 w	3138 C	3151 (0)	1577 + 1589 = 3166 (B_1)
	3150		
3203 w			918 + 2297 = 3215 (B_2)
3344 w			1081 + 2281 = 3362 (A_1)
3400 w			391 + 3047 = 3438 (B_2)
3464 w			1179 + 2297 = 3476 (A_1)
3539 w			2×642 + 2281 = 3565 (B_1)
3681 w			642 + 3049 = 3691 (A_1)

consistent with the present assignment in pyridine (criterion *e*). Raman bands at 926, 765, and 340 cm.$^{-1}$ not having infrared counterparts were taken as a_2 fundamentals consistent with criteria *a*, *b*, *c*, and *e*.

The complete assignment is given in Table V and the fundamentals are listed in Table VII together with the fundamentals for pyridine and the product rule ratios.

Pyridine-3,5-d_2

The polarized bands at 3047 (overlapped by Hg 5025.6 Å), 2297, 1436, 1179, 1029, and 967 cm.$^{-1}$ can be assigned with reasonable certainty as a_1 modes. The remaining a_1 vibrations ν_{6a}, ν_{8a}, ν_{18a}, and ν_{20a} are assigned according to criteria *a*, *b*, and *c*. Criterion *e* is then used as a final check. Likewise the b_1 modes were chosen consistent with criteria *a*, *b*, and *c* again using *e* as a final check.

There should be five type b_2 modes in pyridine-3,5-d_2, and five bands with *C* type

TABLE VII

FUNDAMENTAL FREQUENCIES FOR PYRIDINE-2,6-d_2 AND PYRIDINE-3,5 d_2

Frequency	Pyridine	Pyridine-2,6-d_2	Pyridine-3,5-d_2
a_1			
1	992	986	967
2	3054	3065	2297
6*a*	605	578	596
8*a*	1583	1586	1577
9*a*	1218	889	1179
12	1030	1019	1029
13	3054	2260	3047
18*a*	1068	1087	828
19*a*	1482	1457	1436
20*a*	3036	3002	3000
	Product ratio	Calc. 0.507	Calc. 0.507
		Obs. 0.506	Obs. 0.512
b_1			
3	1218	1184	947
6*b*	652	635	642
7*b*	3036	2252	3049
8*b*	1572	1568	1589
14	1375	1345	1328
15	1148	1128	1105
b_1 (*continued*)			
18*b*	1068	860	1081
19*b*	1439	1415	1411
20*b*	3083	3067	2281
	Product ratio	Calc. 0.523	Calc. 0.524
		Obs. 0.526	Obs. 0.527
a_2			
10*a*	886	765	867
16*a*	374	340	352
17*a*	981	926	784
	Product ratio	Calc. 0.742	Calc. 0.745
		Obs. 0.741	Obs. 0.736
b_2			
4	749	743	713
5	942	(889)	918
10*b*	886	839	897
11	700	586	585
16*b*	405	397	391
	Product ratio	Calc. 0.728	Calc. 0.728
		Obs. 0.728	Obs. 0.758

( ) = *Frequency used twice.*

contours are observed at 918, 713, 625, 585, and 391 cm.$^{-1}$. As with pyridine-2,6-d_2 these five bands are consistent with the "spectroscopic" assignment in pyridine mentioned previously, but to obtain agreement with the present assignment in pyridine based on the thermodynamic data one band around 600 ↔ 700 cm.$^{-1}$ must be assigned as a difference tone of species B_2 and replaced by a band around 800 ↔ 900 cm.$^{-1}$.

The medium type *C* band at 713 cm.$^{-1}$ cannot be explained satisfactorily as a difference tone and must therefore be a fundamental. The medium type *C* band at 625 cm.$^{-1}$ can be assigned as the difference tone $\nu_{19b}-\nu_{17a}$ = 627 cm.$^{-1}$ (B_2) but criterion *e* then necessitates replacing this frequency by another around 860 cm.$^{-1}$. Only two bands are observed in the infrared in this region, 828 cm.$^{-1}$ (ν_{18a}), which gives a product rule ratio much too low, and 897, which gives a product rule ratio much too high. The latter frequency is taken as the b_2 fundamental here, the disagreement with the product rule ratio being considered to arise from the effect of Coriolis coupling (between the a_2 and b_2 species) on the bands, in which case the observed *Q* maximum is not necessarily a good estimate of the band center.

The Raman bands at 867, 784, and 352 cm.$^{-1}$ not having infrared counterparts were taken as a_2 fundamentals consistent with criteria *a*, *b*, *c*, and *e*. The complete assignment is given in Table VI and the fundamentals are listed in Table VII together with those for pyridine and the product ratios.

In a communication* McCullough *et al.* state that they are in agreement with our assignment for pyridine but in order to get best agreement between the observed and calculated thermodynamic properties of pyridine, they feel that the b_2 frequency at 886 cm.$^{-1}$ in our assignment should be replaced by one at 981 cm.$^{-1}$. The corresponding changes in b_2 frequency in the other deuterated pyridines suggested by them are: 823 cm.$^{-1}$ replaced by 908 cm.$^{-1}$ in pyridine-d_5; 862 cm.$^{-1}$ replaced by 962 cm.$^{-1}$ in pyridine-d_4; 897 cm.$^{-1}$ replaced by 947 cm.$^{-1}$ in pyridine-3,5-d_2; and 889 cm.$^{-1}$ replaced by 986 cm.$^{-1}$ in pyridine-2,6-d_2. Since there are no compelling spectroscopic arguments enabling a distinction to be made between the above choices, we agree with them that their suggested modification seems preferable.

ACKNOWLEDGMENTS

We are greatly indebted to Drs. McCullough, Douslin, Messerly, Hossenlopp, Kincheloe, and Waddington for allowing us to see their manuscript before publication, and for an exchange of correspondence which was helpful in arriving at a "best" assignment for pyridine.

REFERENCES

1. Anderson, F. A., Bäk, B., Brodersen, S., and Andersen, J. R. J. Chem. Phys. **23,** 1047 (1955).
2. Bäk, B., Hansen, L., and Andersen, J. R. J. Chem. Phys. **22,** 2013 (1954).
3. Corrsin, L., Fax, B. J., and Lord, R. C. J. Chem. Phys. **21,** 1170 (1953).
4. Edsall, J. T. and Wilson, E. B., Jr. J. Chem. Phys. **6,** 124 (1938).
5. Herz, E., Kahovec, L., and Kohlrausch, K. W. F. Z. physik. Chem. B, **53,** 124 (1943) and references cited therein.
6. Kline, C. H. and Turkevich, J. J. Chem. Phys. **12,** 300 (1944). (A summary of I.R. work previous to this is included in their Table 1.)
7. McCullough, J. P., Douslin, D. R., Messerly, J. F., Hossenlopp, I. A., Kincheloe, T. C., and Waddington, G. Private communication.
8. White, J. U., Alpert, N., and DeBell, A. G. J. Opt. Soc. Am. **45,** 154 (1955).

J. P. McCullough, May 27, 1957.

INFRARED SPECTRUM OF THE H_3O^+ ION IN AQUEOUS SOLUTIONS[1]

MICHAEL FALK[2] AND PAUL A. GIGUÈRE

ABSTRACT

The absorption spectra at 25° C. of aqueous solutions of mineral acids (HCl, HBr, HNO_3, $HClO_4$, H_2SO_4, H_3PO_4) and of some of their acid salts in various concentrations were measured in the infrared from 2 to 25 μ. In all cases three broad bands were present at 1205, 1750, and 2900 cm.$^{-1}$ arising from the H_3O^+ ion. Cooling the samples, and even supercooling them down to liquid air temperature, produced no major changes in the spectra. The bands of the D_3O^+ ion were also found at 960, 1400, and 2170 cm.$^{-1}$ in solutions of DCl in heavy water. Thus, the existence of discrete hydronium ions in the liquid state, with average life longer than 10^{-13} second, is confirmed. Infrared spectra provide a means of estimating the extent of ionization of strong acids in solution.

Following identification by nuclear magnetic resonance of real H_3O^+ ions in crystalline hydrates of strong acids (12, 21) some investigators have succeeded in measuring the vibrational frequencies of that ion in the solid state, both in infrared (1, 6, 7) and in Raman (15, 26). In liquid solutions, however, previous attempts to detect it spectroscopically have apparently failed* (1, 3, 8, 14, 16, 23); so much so that various explanations have been put forward to account for the lack of absorption spectrum, mostly on the basis of too short a lifetime (5, 24, 25, 28). In view of the conclusive results on the effective existence of the H_3O^+ ion from the recent extensive conductivity measurements of Conway, Bockris, and Linton (4) a renewed effort in that direction was deemed worth while. A few trial runs with a concentrated solution of hydrochloric acid immediately revealed strong and rather broad infrared bands at about 1205, 1750, and 2900 cm.$^{-1}$, in good agreement with the known bands of the hydronium ion in crystalline acid hydrates. Then the assignment was proved to be correct by the fact that these bands were present in solutions of other strong acids, and with intensities roughly proportional to the "hydrogen ion" concentration.

EXPERIMENTAL

Optical silver chloride was the only satisfactory material to confine the thin films of corrosive acid solutions. The disks were polished by grinding carefully against a large file. Films of liquid with thicknesses of the order of 10 microns, and fairly reproducible, were obtained merely by squeezing a drop of the acid solution between two freshly-ground plates. For the shorter wave-length region thicker films were secured by means of polythene gaskets. The spectra were recorded with a Perkin-Elmer spectrometer, Model 12 C, interchanging the prisms (LiF, CaF_2, NaCl, and CsBr) led to the optimum definition in each region. The deuterium chloride was prepared by the reaction of potassium chloride with *d*-phosphoric acid made from very dry phosphorus pentoxide and heavy water.

[1]*Manuscript received June 26, 1957.*
Contribution from the Department of Chemistry, Laval University, Quebec, Que.
[2]*Holder of a Cominco Fellowship.*
**However, in a discussion Bethell and Sheppard (Ref. 1, p. C 118) mentioned, without further details, that they had studied the system* $HClO_4 . H_2O$ *in the liquid state and found the spectrum of* H_3O^+*, as in the crystalline solid.*

RESULTS

The first tracing, A in Fig. 1, shows part of the absorption spectrum of liquid water with maxima at 710±25 (ν_R), 1640±5 (ν_2), 2120±15 ($\nu_2+\nu_R$), and 3400±10 cm.$^{-1}$ (ν_3). In liquid heavy water (Fig. 2) the corresponding bands are at 530, 1205, 1620, and 2500 cm.$^{-1}$. The weak band at 1460 cm.$^{-1}$ is due to HDO from a few per cent of ordinary water in our sample of heavy water. All the spectra in these and the following figures are composite tracings from a number of different runs, each covering only a portion of the whole range. Because of the time delay in changing prisms it was not always possible to scan the various regions with the same sample. Although an effort was made to work with films of nearly the same thickness the relative intensities of the various bands should not be compared too rigorously.

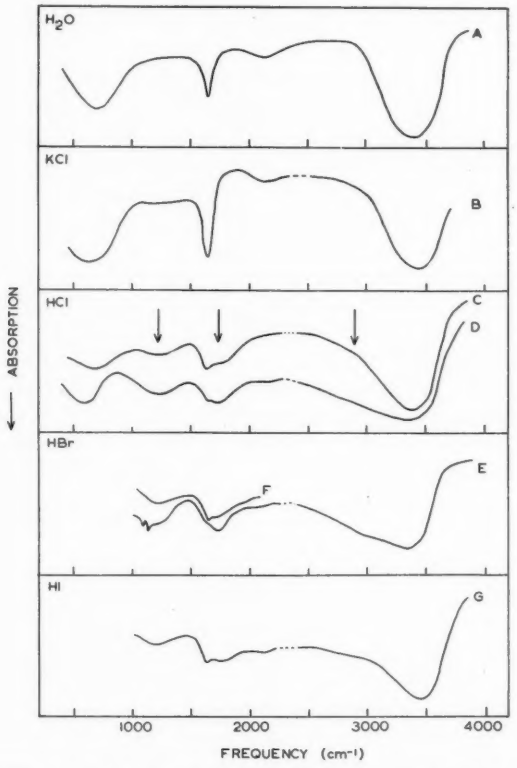

FIG. 1. Infrared absorption of thin films (5 to 10 microns) of water (A) and aqueous solutions:
B. 8 mole % KCl D. 22 mole % HCl F. 16 mole % HBr
C. 11 mole % HCl E. 30 mole % HBr G. 11 mole % HI

Dissolving a salt such as KCl in water (curve B, Fig. 1) has little effect on the infrared spectrum; only a shift of the ν_R band towards lower frequencies is noticeable. Similar shifts of ν_R occur in acid solutions: to 625 cm.$^{-1}$ in a 11 mole % solution of HCl and to 605 cm.$^{-1}$ in a 22% solution (curves C and D). In contrast, the frequencies of the two H_2O fundamentals, ν_2 and ν_3, remain practically the same in acid solutions. The

spectra of the various solutions of hydracids investigated show no indication of any undissociated hydrogen halide molecules, as could be expected in view of the moderate concentrations used.* Therefore, extra absorption in the three regions around 1205, 1750, and 2900 cm.$^{-1}$, all increasing in intensity with the acid concentration, must belong to the H_3O^+ ion. In the deuterium compounds the corresponding bands at 960, 1400, and 2170 cm.$^{-1}$ show the expected isotope shift. These frequencies are in fair

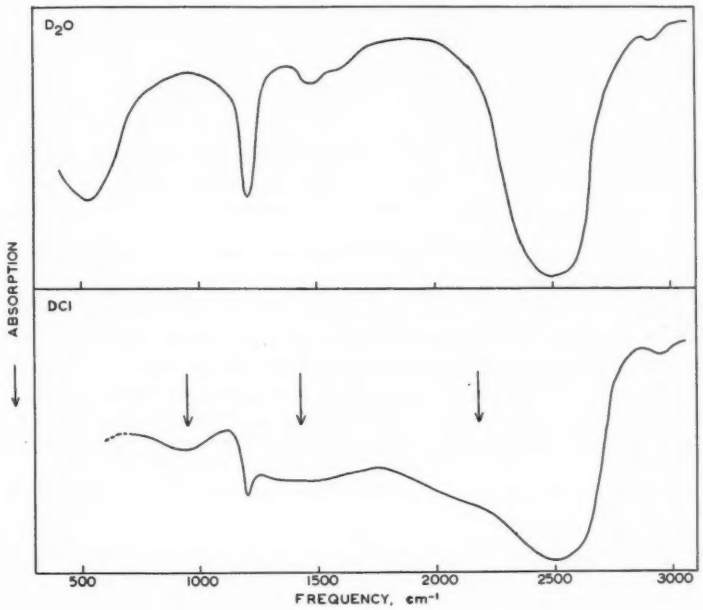

FIG. 2. Infrared spectra of liquid heavy water and of a 14 mole % solution of deuterium chloride.

agreement with the values reported for the ion in crystalline monohydrates (Table I) and may similarly be interpreted in terms of a symmetric pyramidal structure of the hydronium ion.

The broad band with maximum at 1205 cm.$^{-1}$ stands out clearly between the strong ν_R and ν_2 bands of water. By analogy with the 1069 cm.$^{-1}$ band of solid NH_3 (18) it is assigned to the ν_2 (A_1) symmetric bending mode of H_3O^+. The second band, arising from the doubly degenerate ν_4 (E) asymmetric bending, appears in dilute acid solutions as a shoulder on the high-frequency side of the ν_2 band of water. At higher concentrations a definite maximum becomes visible at 1720–1730 cm.$^{-1}$. After correction for the absorption due to water, the center of that band is estimated at 1750 ± 15 cm.$^{-1}$ (ν_4 = 1650 cm.$^{-1}$ in condensed NH_3). Existence of a band of the ion distinct from the ν_2 band of water in that region had been controversial in the case of the solid acid hydrates: cf. discussion of paper (1). To settle the question we had to vary the ratio acid/water over a wide

*In the case of HCl, Ochs, Guéron, and Magat (16) have calculated that the fundamental frequency of the free molecule at 2880 cm.$^{-1}$ should be shifted to about 2610 cm.$^{-1}$ in aqueous solutions. These authors actually found a very weak band at 2630 ± 20 cm.$^{-1}$ in the Raman spectra of solutions containing about 37 mole % HCl (under pressure); our highest obtainable concentration was 22 mole % HCl.

TABLE I

VIBRATIONAL FREQUENCIES OF THE H_3O^+ AND D_3O^+ IONS IN CRYSTALS

Substance	Spectrum	Frequencies (cm.$^{-1}$) and assignments			Ref.
		ν_2	ν_4	ν_3 and ν_1	
$H_3O^+NO_3^-$	Infrared	1134	1670	2650 to 3380	(1)
$H_3O^+I^-$	Infrared	1060	1705	2635 to 3350	(7)
$H_3O^+Br^-$	Infrared	950 1060 1150	1705	2610 to 3250	(7)
$H_3O^+Cl^-$	Infrared	1060 1150	1700	2590 to 3235	(7)
$H_3O^+F^-$	Infrared	1048 1150	1705	2468 to 3150	(7)
$H_3O^+ClO_4^-$	Raman	—	1590	2400 to 3600	(15)
$H_3O^+ClO_4^-$	Raman	1175	1577	3285	(26)
$D_3O^+Cl^-$	Infrared	785	1255	2000 to 2445	(7)

range while using a CaF_2 prism for better resolution and reducing as much as possible the interference from water vapor.

The O–H stretching region extending from 3 to 4 μ appears much more confused, unfortunately. A gradual, continuous absorption extends from about 2500 cm.$^{-1}$ almost to the maximum of the ν_3 band of water. Although the absorptions of H_2O and H_3O^+ in that region cannot be rigorously separated, a rough approximation is achieved by taking the ratio of absorption of the acid solution to that of pure water, as shown in Fig. 3. The film of acid solution used for that purpose was slightly thicker than that of

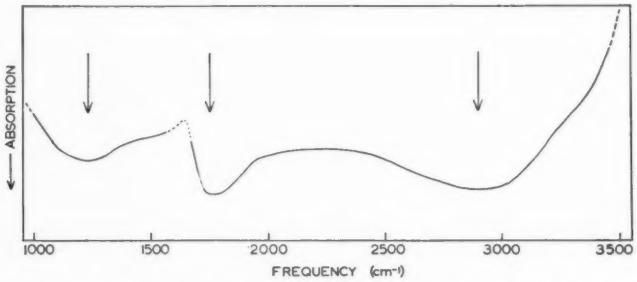

FIG. 3. Differential absorption of a 21 mole % solution of HCl minus that of pure water.

pure water in order to have nearly the same amount of water in both cases. Obviously this procedure overlooks the expected interaction of the H_2O and H_3O^+ vibrations. Nevertheless it shows definitely that extra absorption in that region is due mainly to one broad band, presumably ν_3 (E), centered around 2900±150 cm.$^{-1}$. In the deuterium compounds the presence of the corresponding band at 2170 cm.$^{-1}$ is more distinct.

Solutions of the other two hydracids studied (E, F, and G, Fig. 1) showed the same relative intensities of the various bands as those of HCl. The sharp peaks at 1110 and 1150 cm.$^{-1}$ in the spectrum of concentrated solutions of HBr must arise from an unknown impurity. Acids with polyatomic anions are less suitable for studying the spectrum of the hydronium ion because of the anion's own spectrum. In perchloric acid (Fig. 4) the situation is not too unfavorable, the only interference coming from the strong ν_3 band

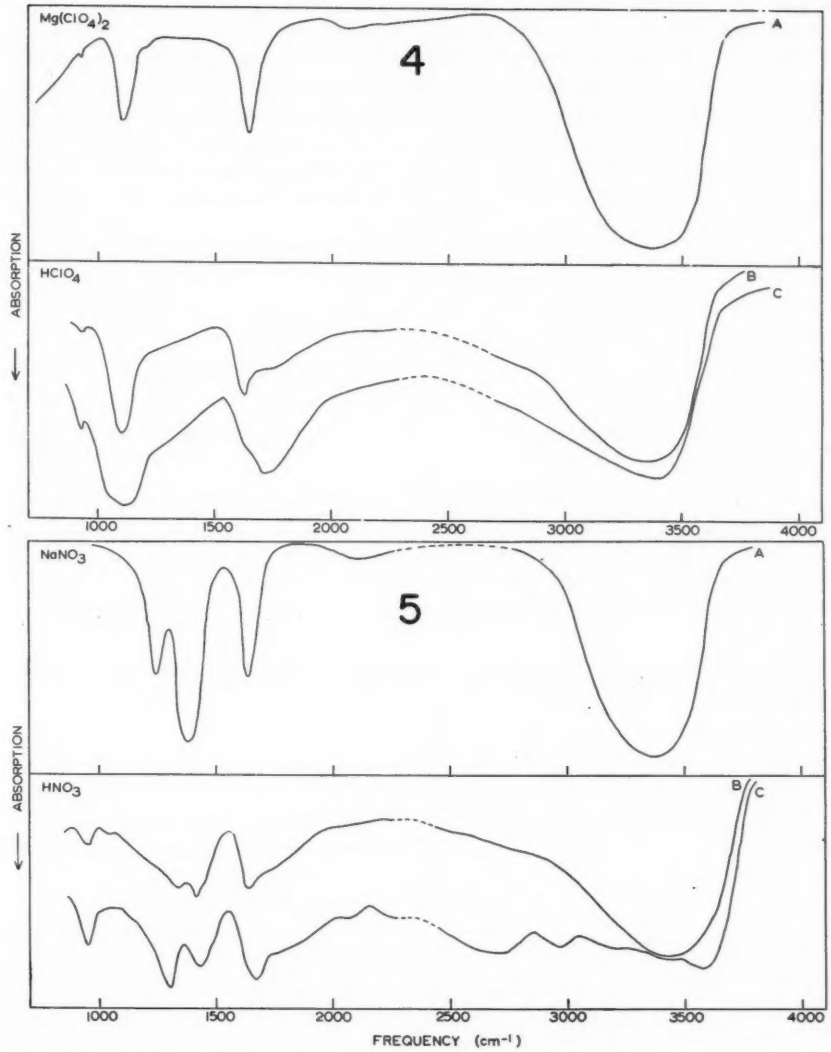

FIG. 4. Spectra of a 4 mole % solution of magnesium perchlorate (A), and of 12 (B) and 28 (C) mole % perchloric acid solutions.

FIG. 5. Infrared spectra of a 17 mole % solution of sodium nitrate (A), and of 15 (B) and 37 (C) mole % solutions of nitric acid.

of ClO_4^- at 1100 cm.$^{-1}$. In nitric acid, however, the ν_2 band of H_3O^+ is completely hidden, at all concentrations, by several strong absorption peaks of the nitrate ion in that region while the other two bands, ν_3 and ν_4, are discernible only in dilute solutions (Fig. 5 B). As the concentration is increased the absorption due to un-ionized HNO_3 molecules becomes more and more prominent (Fig. 5 C). Previous studies of the Raman spectra

(3, 19, 20) had already confirmed that in concentrated solutions HNO_3 is much less dissociated than $HClO_4$.

For polybasic acids further complication may arise from the presence of several ionic species. Yet the ν_3 and ν_4 bands of H_3O^+ are easily recognized in solutions of sulphuric (Fig. 6) and phosphoric acids (Fig. 7). These two bands become most intense in concentrated solutions of the former acid (Fig. 6 C) indicating an exceedingly high concentration of ionized species, in agreement with recent Raman investigations; for a

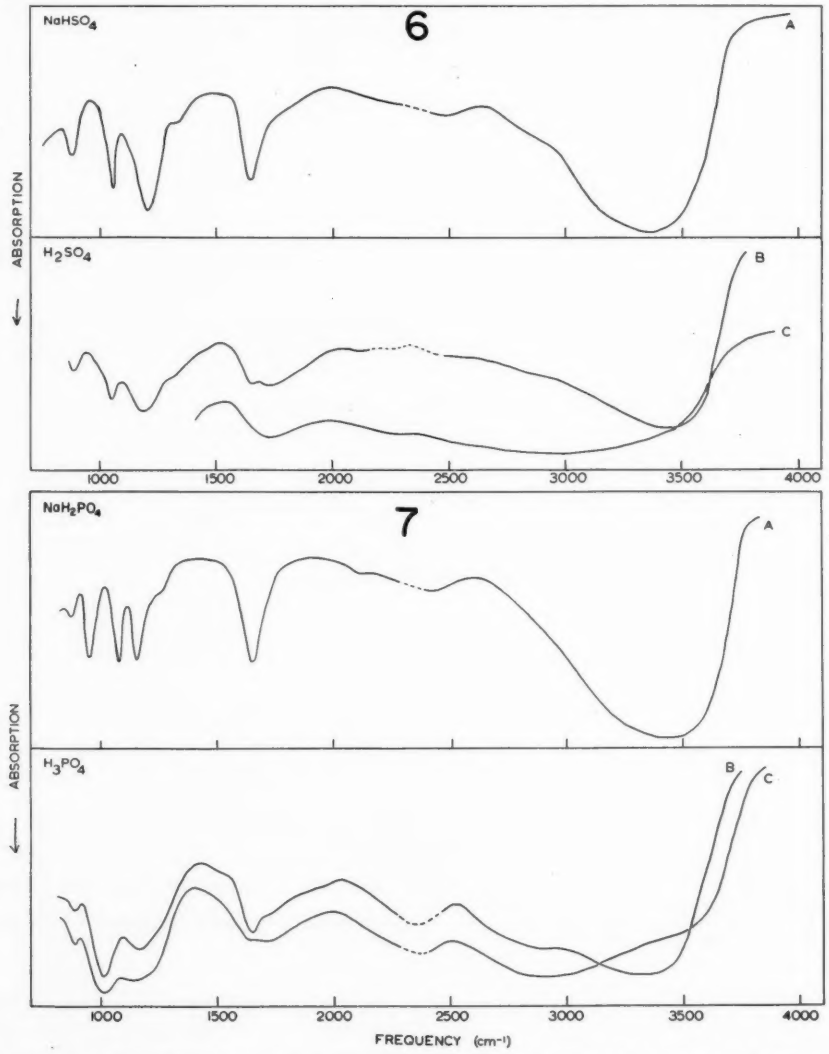

FIG. 6. Infrared spectra of a 4 mole % aqueous solution of sodium bisulphate (A), and of 24 (B) and 42 (C) mole % solutions of sulphuric acid.

FIG. 7. Infrared absorption of aqueous solution of (A) 18 mole % sodium dihydrogen phosphate, (B) 17 mole % phosphoric acid, and (C) 51 mole % of same.

review, cf. (2). On the contrary the ion bands are quite weak in solutions of H_3PO_4. Correspondingly, no H_3O^+ bands could be detected in the acid salt NaH_2PO_4 (Fig. 7 A), but they were present, if rather weak, in $NaHSO_4$ (Fig. 6 A). Lastly the H_3O^+ ion bands were missing even in fairly concentrated solutions of sulphurous, selenious, and hypophosphorous acids. All these observations are consistent with the known degrees of dissociation of these various acids.

In the overtone region, addition of acids produces no striking change in the infrared spectrum of water as may be seen in Fig. 8. The weak and very diffuse shoulder at

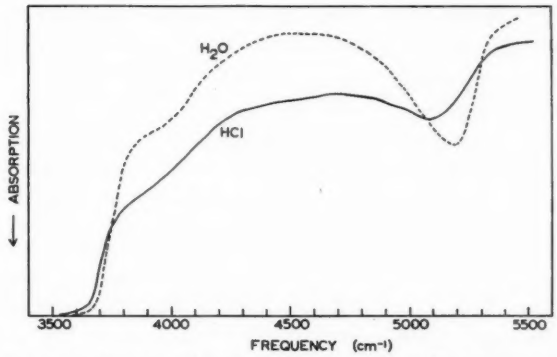

FIG. 8. Absorption spectra in the near infrared of a 40 micron thick film of pure water and a 21 mole % solution of hydrochloric acid.

3950 cm.$^{-1}$ is shifted down to about 3850 cm.$^{-1}$, confirming its assignment to the combination $\nu_3+\nu_R$. Indeed, the librational frequency in liquid water is lowered by about 100 cm.$^{-1}$ on addition of acids, as noted above. A more pronounced change appears in the overtone $2\nu_3$ at 5180 cm.$^{-1}$, resulting in deformation and displacement of the maximum towards lower frequencies, and increased over-all absorption between 4200 and 5000 cm.$^{-1}$. Similar observations on higher overtone bands had been noted in early investigations of the near infrared region (8, 23).

DISCUSSION

Existence of the H_3O^+ *Ion*

The main reason, until recently, for doubting the reality of the hydronium ion had been the negative results of all previous search for its vibrational spectrum. Application of the magnetic resonance method (12, 21) had settled the question as far as the solid state was concerned; but the case of most immediate interest to the chemist, that of aqueous acid solutions, remained unsolved. Direct inference from one physical state to the other was not warranted here because of the much greater freedom of molecules and ions in the liquid phase. Now, the present spectroscopic data cannot be reconciled with any of the various other models proposed before, such as the proton oscillating in a "cage" of strongly polarized water molecules (5), or the "hydrated proton", $H^+.(H_2O)_n$ (28), or again $H_5O_2^+$ (11). A true chemical bond between the proton and one of the adjacent water molecules must subsist long enough for the resulting species to undergo normal vibrations. Failure to observe these in the past must be ascribed to unfavorable circumstances. Thus the strong polarity of the ion implies a rather weak Raman spectrum, as pointed out elsewhere (cf. discussion of paper (1), p. C 118). So far only one

such investigation has been completely successful owing, apparently, to the use of a large single crystal (26). In aqueous solutions the situation is complicated further by the very strong and diffuse water bands almost coincident with those of the ion (except for ν_2 of the latter).

As for the infrared, the early work was confined to the overtone region on account of experimental difficulties (8, 23). The almost continuous absorption then observed was ascribed to the effect of the approaching proton on the vibrations of the water molecule (24, 25). It is now known from conductivity measurements that the proton actually spends only a short fraction of the total time in jumping from one H_2O molecule to another (4). Finally Bethell and Sheppard (1) in their infrared study of the liquid HNO_3–H_2O mixture were handicapped by the very incomplete ionization of the acid (3).

Average Lifetime of the H_3O^+ *Ion*

Because of the great mobility of the proton an individual H_3O^+ ion could not exist *permanently* as such in aqueous solution at ordinary temperature. Now, the lowest frequency reported here (960 cm.$^{-1}$ for ν_2 of D_3O^+) sets a lower limit of 3×10^{-13} seconds for the lifetime of the ion. Various estimates (cf. (4) for a list of references), based in particular on the activation energy of the proton conductance in acid solutions, have ranged from 10^{-11} to 10^{-14} seconds. The latter figure is certainly too low, since, by the uncertainty principle, it would result in almost infinite broadening of the absorption bands ($\Delta\nu$ = 1000 cm.$^{-1}$ for $\Delta t = 3\times10^{-14}$ seconds). Also, contrary to our observations, the bands should be much wider in the liquid than in the solid and should become more so with increasing temperature.

As a matter of fact the ion bands appear just as diffuse as those of water and the explanation is no doubt the same, namely hydrogen bonding. In addition to these hydrogen bonds the hydronium ion, like other cations and anions, must polarize neighboring water molecules forming the so-called hydration sphere. From dielectric measurements at radio frequencies Hasted (10) has estimated that on the average eight water molecules have their rotation blocked around each hydronium ion. Conversely the anion will deform the H_3O^+ ion as well as the water molecules. However, this effect is noticeable only in the most concentrated acid solutions or, better yet, in the crystalline hydrates. As may be gathered from Table I the O–H stretching frequencies and the librational frequency ν_R decrease with increasing electronegativity of the anion. The shift is particularly large in the case of hydrofluoric acid. Furthermore, the bending frequencies ν_2 and ν_4 of H_3O^+ are appreciably higher (by about 50 cm.$^{-1}$) in the aqueous solutions than in the corresponding crystalline monohydrates, whereas the stretching frequency appears to be lower. This indicates that the O–H . . . O bonds formed in solutions are stronger than the O–H . . . X bonds with the neighboring anions in the solid hydrates owing, possibly, to less favorable orientations in the latter case.

Structure of the H_3O^+ *Ion*

The present results confirm the pyramidal configuration, with C_{3v} symmetry, which appears the most probable for the ion by analogy with the isoelectronic NH_3 molecule (1). Theoretically the third O–H bond, equivalent to the other two by virtue of resonance, is formed by overlap of the 1*s* orbital of the proton with the remaining 2*p* orbital of the oxygen of a water molecule. It is known, from the proton affinity of water, that the hydroxyl bond energy is even greater in the ion (133 kcal.) than in water (22). Because of some sp^3 hybridization the bond angles should approach the tetrahedral value. This view is consistent with the existing data on the parameters of the H_3O^+ ion in crystalline

hydrates. From magnetic resonance study Richards and Smith (21) found the inter-hydrogen distance to be 1.72±0.02 Å at 90° K. in $H_3O^+ClO_4^-$, a value no doubt more reliable than the rough estimate (1.58 Å) of the Japanese authors (12). The O–H bond length is not so accurately known, but it must be quite close to that in ice, 1.01 Å (17), since the stretching frequencies are nearly the same in both compounds. As explained above, this parameter could vary slightly from one acid to the other depending on the electronegativity of the anion. A neutron diffraction study of the crystalline hydronium compounds would be valuable in that connection.

At any rate the above data point to a rather flat pyramid for the H_3O^+ ion, in agreement with the X-ray measurements on solid nitric acid hydrates (13). Richards and Smith have observed that on warming to 0° C. the absorption line of the ion narrowed considerably, an effect which they attributed to rapid reorientation about more than one axis in the solid. Considering the above structure, it is conceivable that some double minimum inversion occurs as in the NH_3 molecule.

The 3 μ Region

Of the two stretching vibrations of the pyramidal H_3O^+ ion the totally symmetric mode, ν_1 (A_1), should be much weaker in infrared than ν_3 (E), the asymmetric one. Therefore it is logical to assume that the latter is responsible for most of the absorption at 2900 cm.$^{-1}$. In the infrared spectra of the crystalline acid hydrates Ferriso and Hornig (6, 7) found two equally intense bands at 3250 and 2600 cm.$^{-1}$ which they assigned tentatively to ν_1 and ν_3 of the ion respectively. However, this assignment is questionable both on account of the equal intensities and the rather large frequency difference.* The infrared spectra of the crystalline hydrates of ammonia measured in the same laboratory (27) show no trace of absorption around 2600 cm.$^{-1}$. As pointed out by Taylor and Vidale (26) ν_1 should have nearly the same frequency as ν_3, probably a little lower; hence their assignment of the Raman band at 3285 cm.$^{-1}$ to ν_1 of H_3O^+. Application of the Teller-Redlich rule is of no use here to distinguish between ν_1 and ν_3 because of the large uncertainty in the vibrational frequencies of H_3O^+ and D_3O^+.

In several cases we have succeeded in crystallizing thin films of acid solutions by cooling with liquid air. The spectra of such films were strikingly different from those of the supercooled films at the same temperature† mainly in the O–H stretching region. There, the 2900 cm.$^{-1}$ band was replaced by several new bands, the strongest of which at about 2750 cm.$^{-1}$ in a 20 mole % HCl solution undoubtedly corresponds to the 2600 cm.$^{-1}$ band of Ferriso and Hornig. Clearly the available data are not sufficient to decipher the spectra in that region.

In conclusion it may be noted that the infrared spectra can provide information on the degree of ionization of strong acids in concentrated solutions. While the present results on solutions of HNO_3, $HClO_4$, H_2SO_4, $NaHSO_4$, H_3PO_4, and NaH_2PO_4 allow only qualitative estimates of the hydronium ion concentration, these are found to be consistent with the available evidence from other sources. A quantitative investigation would be of particular interest in the case of hydrogen halide solutions, where the usual

**Some other features in the interpretation of these authors are open to question. Thus, the contention that there is no evidence for H_2O bands is not substantiated by their tracings. The two main bands at 3250 and 1650–1700 cm.$^{-1}$ are almost always present; the latter in particular is certainly too intense to arise only from ν_4 of H_3O^+. Their method of preparation of the samples may have led to some segregation unless they were carefully annealed. Similarly, the medium intensity band at 2100 cm.$^{-1}$ (except in H_3OF) seems too strong for the overtone $2\nu_2$ considering that this mode is entirely missing in condensed NH_3 (18). We would rather assign it to the combination $\nu_2+\nu_R$ of ice (9).*

†This confirms the observations already made in this laboratory of supercooled water films at −180° C. (9).

methods based on the determination of the anion concentration from its Raman spectrum do not apply. More accurate determinations will require exact knowledge of the thickness of the sample and correction for mutual interference of the water and acid bands.

ACKNOWLEDGMENTS

The authors are grateful to the National Research Council for financial assistance and to the Consolidated Mining and Smelting Co. for a Fellowship.

RÉSUMÉ

On a mesuré le spectre infrarouge de 2 à 25 μ de minces films de solutions aqueuses d'acides minéraux et de quelques uns de leurs sels acides. Dans tous les cas on a observé trois bandes diffuses à 1205, 1750, et 2900 cm.$^{-1}$ dues à l'ion H_3O^+. Ces bandes gardaient à peu près la même apparence dans les échantillons refroidis, et même en surfusion à la température de l'air liquide. Dans les acides deuterés les bandes de l'ion D_3O^+ apparaissent à 960, 1400 et 2170 cm.$^{-1}$. On a ainsi confirmé l'existence à l'état liquide d'ions H_3O^+ ayant une vie moyenne d'au moins 10^{-13} sec.

REFERENCES

1. Bethell, D. E. and Sheppard, N. J. chim. phys. **50**, C 72 (1953).
2. Brubaker, C. H. J. Chem. Educ. **34**, 325 (1957).
3. Chédin, J. J. chim. phys. **49**, 109 (1952).
4. Conway, B. E., Bockris, J. O. M., and Linton, H. J. Chem. Phys. **24**, 834 (1956).
5. Darmois, E. J. phys. radium, **11**, 577 (1950).
6. Ferriso, C. C. and Hornig, D. F. J. Am. Chem. Soc. **15**, 4113 (1953).
7. Ferriso, C. C. and Hornig, D. F. J. Chem. Phys. **23**, 1464 (1955).
8. Freymann, R. and Guéron, J. Bull. soc. chim. France (V), **6**, 1298 (1939).
9. Giguère, P. A. and Harvey, K. B. Can. J. Chem. **34**, 798 (1956).
10. Hasted, J. B. J. chim. phys. **50**, C 118 (1953).
11. Huggins, M. L. J. Phys. Chem. **40**, 723 (1936).
12. Kakiuchi, Y., Shono, H., Komatsu, H., and Kigoshi, K. J. Chem. Phys. **19**, 1069 (1951).
13. Luzzati, V. Acta Cryst. **6**, 157 (1953).
14. Millen, C. J. and Vaal, E. G. J. Chem. Soc. 2913 (1956).
15. Mullhaupt, J. T. and Hornig, D. F. J. Chem. Phys. **24**, 169 (1956).
16. Ochs, L., Guéron, J., and Magat, M. J. phys. radium, **1**, 85 (1940).
17. Peterson, S. W. and Lévy, H. A. Acta Cryst. **10**, 70 (1957).
18. Reding, F. P. and Hornig, D. F. J. Chem. Phys. **19**, 594 (1951).
19. Redlich, O. and Bigeleisen, J. J. Am. Chem. Soc. **65**, 1883 (1943).
20. Redlich, O., Holt, E. K., and Bigeleisen, J. J. Am. Chem. Soc. **66**, 13 (1944).
21. Richards, R. E. and Smith, J. A. S. Trans. Faraday Soc. **47**, 1261 (1951).
22. Sherman, J. Chem. Revs. **11**, 98 (1932).
23. Suhrmann, R. and Breyer, F. Z. physik. Chem. B, **23**, 193 (1933).
24. Suhrmann, R. and Wiedersich, I. Z. Elektrochem. **57**, 93 (1953).
25. Suhrmann, R. and Wiederisch, I. Z. anorg. Chem. **273**, 166 (1953).
26. Taylor, R. C. and Vidale, G. L. J. Am. Chem. Soc. **78**, 5999 (1956).
27. Waldron, R. D. and Hornig, D. F. J. Am. Chem. Soc. **75**, 6079 (1953).
28. Wicke, E., Eigen, M., and Ackermann, T. Z. physik. Chem. **1**, 342 (1954).

ARSENIDES OF THE TRANSITION METALS

II. THE NICKEL ARSENIDES[1]

R. D. HEYDING AND L. D. CALVERT

ABSTRACT

Alloys of nickel and arsenic containing up to 60% As by weight have been studied by means of room temperature and high temperature Debye–Scherrer diagrams. Three compounds have been identified: Ni_5As_2, $Ni_{12-x}As_8$ (maucherite), and NiAs (niccolite). The first of these is homogeneous from Ni_5As_2 to $Ni_{4.8}As_2$ at room temperature, and to $Ni_{4.6}As_2$ above 250° C., while the latter is homogeneous from NiAs to $Ni_{0.95}As$. Contrary to expectations the stability region of the compound $Ni_{12-x}As_8$ is very narrow, and occurs at $Ni_{11}As_8$ rather than at Ni_8As_2. Evidence is presented in support of Hansen's contention that this compound has an incongruent melting point. Alloys in the region corresponding to $Ni_{4.6}As_2$ undergo two transitions below 200° C., one of which is martensitic and produces a metastable phase, while the other is believed to result in the formation of a new compound, as yet unidentified. The diffraction patterns are discussed in some detail.

INTRODUCTION

An investigation of the X-ray powder diffraction patterns of iron and cobalt arsenides was reported recently in this journal (9). In continuation of a general investigation of the arsenides of the transition metals, diffraction patterns of the analogous nickel/arsenic alloys have been obtained and are discussed here. As in the earlier investigation, this study has been limited to those alloys containing 20–60% As by weight.

In Friedrich's phase diagram of the nickel/arsenic system, two simple eutectics are shown: the first occurs between the solid solution of As in Ni and the compound Ni_5As_2, and the second between Ni_5As_2 and the compound NiAs (4). Both compounds have congruent melting points. According to the diagram, the first exists over a considerable concentration range, while the second exhibits little or no variation in composition. The latter compound occurs naturally as the mineral niccolite.

Undoubtedly a third compound also exists corresponding to the mineral maucherite, which has been assigned the formula $Ni_{12-x}As_8$. In alloys of composition between Ni_5As_2 and NiAs, that is, in the region where this third compound should appear, Friedrich detected a solidus transition which could not be assigned a definite temperature because of supercooling effects. However, the maximum evolution of heat associated with this transition was attained for the alloy corresponding to Ni_3As_2, and he assumed that this compound was formed by the reaction of Ni_5As_2 with NiAs. Hansen has observed that if sufficient allowance were made for pronounced supercooling, Friedrich's data could be interpreted only in terms of the formation of a compound, presumably Ni_3As_2, with an incongruent melting point (5). In general, subsequent reproductions of the phase diagram have been drawn in accord with Hansen's interpretation, although Hansen does not explain the thermal arrests observed in the region between Ni_5As_2 and the eutectic at 43% As.

The structure of NiAs is well known, but there is a large variation in unit cell dimensions reported in the literature. These variations could be indicative of variable composition, a common phenomenon among compounds with the NiAs structure (14), but may be due in part to impurities. It has been shown, for example, that small amounts of antimony (8) or of cobalt (9) alter the unit cell dimensions considerably.

The situation with respect to maucherite is much less certain, in spite of single crystal

[1]*Manuscript received April 29, 1957.*
Contribution from the Division of Applied Chemistry, National Research Council, Ottawa.
Issued as N.R.C. No. 4480.

studies on the mineral by Laves (11) and, in particular, by Peacock (12). Apparently rotation and Weissenberg photographs indicate a prominent tetragonal subcell, although a larger cell, four times the volume of the subcell, is required to describe all of the observed diffraction effects. While the atom positions were not determined, both authors consider the mineral to be deficient in nickel atoms, and regard the larger unit cell to be the result of the ordering of vacancies. Hewitt's powder diffraction pattern of a synthetic mineral is in good agreement with the pattern of maucherite (8), with the rather important exception that those reflections which Peacock assumed were due to the β component in the radiation are not recorded in Hewitt's data.

Only one short reference to the diffraction pattern of Ni_5As_2 appears in the literature (6), indicating that the unit cell is hexagonal. No details were given.

In addition to the primary object of establishing powder diffraction patterns for the Ni/As alloys, we hoped to obtain some information on the following points: (*a*) the limits of homogeneity of the compound Ni_5As_2, and, if possible, some indication of the detailed structure of the compound; (*b*) the structural relationships between the compound Ni_3As_2 and the mineral maucherite, and the behavior of this compound at temperatures in and below the liquidus region of the phase diagram; and (*c*) the limits of homogeneity of the compound NiAs, and the variation in its unit cell dimensions with composition.

EXPERIMENTAL

High purity nickel sponge containing less than 0.8 p.p.m. total impurities as Fe, Cu, Si, and Mg was obtained from Johnson, Matthey & Co. The surface oxide was reduced in hydrogen at 650–700° C. immediately prior to mixing the components. Commercial 'Pure' metallic arsenic was purified by double vacuum sublimation to eliminate heavy metals and reduce the antimony content to less than 50 p.p.m.

The techniques employed in preparing and heat-treating the alloys were identical to those reported previously for the corresponding iron and cobalt alloys.[2]

Debye–Scherrer diagrams were taken in 11.46-cm. Philips room temperature cameras and a 19-cm. Unicam high temperature camera, using nickel-filtered copper radiation. The silica specimen capillaries used in the high temperature camera were attacked by liquidus phases at all concentrations. Diffraction by the products of the reaction between the silica and the liquid alloys masked the pattern of the solid alloy, making it impossible to determine with certainty the structure of the solid in two-phase liquidus–solidus regions, or in any region once a liquidus phase had been formed. The patterns of specimens removed from capillaries after pronounced attack and exposed in new capillaries were identical to the original patterns.

Some 50 alloys were prepared and studied by the usual quenching and annealing techniques. The compositions studied in the high temperature camera are denoted by arrows on the composition axis of the phase diagram, Fig. 1. The position of the liquidus–solidus phase boundary in this figure is taken directly from Friedrich.

[2]*Of the methods given in the literature for the preparation of transition metal arsenides, other than by the direct union of* As *and the metal, the procedure described by Arrivaut for the preparation of* Ni_3As_2 *is unique (1). Nickel powder was treated with a concentrated aqueous solution of* $HAsO_2$ *and* $AsCl_3$ *at about 95° C. rather than with the arsenical gases or vapors and moderate temperatures normally employed. We repeated this preparation, and found that the product was a mixture of arsenides, the major component being a function of the time the reaction had been allowed to proceed. Alloys of 45–50%* As *were formed within the first 24 hours; thereafter the reaction proceeded more slowly. Even after 2 weeks, when the major component was* NiAs, *the reaction showed no sign of approaching completion. The solid products were so finely divided that sharp diffraction patterns were obtained only after annealing at 400° C.*

RESULTS AND DISCUSSION

For convenience, the phases detected have been assigned Greek letters as shown in Fig. 1.

Alloys with 22–35.6% As. *The β Phase*, Ni_5As_2

The diffraction patterns of alloys containing 22–33.8% As indicate the presence of two phases, the α solid solution of As in Ni, and the β or Ni_5As_2 phase. Patterns of quenched and annealed samples and of samples in the high temperature camera showed no phase changes below 900° C.

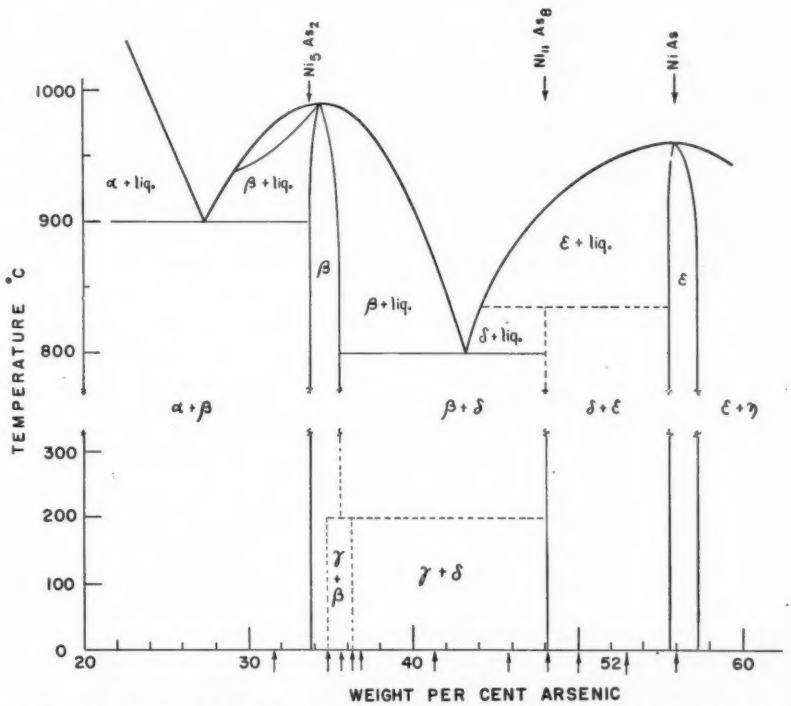

FIG. 1. The phase diagram of the Ni/As system. The liquidus/liquidus–solidus curves are taken from Friedrich (4). Modifications are based on the present investigation and are explained in the text.

Only one phase was observed in the 33.8–34.8% As region. The patterns at room temperature of alloys of any one composition were identical, regardless of the heat treatment of the specimen, and no phase change from room temperature to 900° C. could be detected in the high temperature camera. There was, however, an obvious variation in lattice dimensions with concentration, the maximum interplanar spacings occurring near 33.8% As, corresponding to Ni_5As_2. Diffraction patterns from the high temperature camera of an alloy containing 35.6% As showed only the β phase from 200°–950° C., although some irreversible reflections appeared above 900° C. as a result of reactions between the capillary and the sample. The interplanar distances for

this alloy were found to be greater than the spacings in the 34.8% alloy at the same temperatures, but identical to alloys in which the δ phase could be detected. Hence, above 200° C. the range in homogeneity of the β phase is estimated to be 33.8–35.6% As, in good agreement with Friedrich's values of 33.5–35.7% As.

There is no similarity in the diffraction pattern of this phase and the patterns of any of the phosphides or arsenides of the transition metals at comparable atom ratios: e.g., Ni_2P, Ni_3P, Co_2P, and Fe_2As. The pattern was indexed on a hexagonal unit cell with dimensions very similar to those reported by Hellner (6). By analyzing the pattern in the manner described by Henry, Lipson, and Wooster (7), the constant for the hexagonal a axes was obtained almost immediately, while the constant for c was selected to correspond to the minimum dimension which permitted all of the reflections to be indexed. The unit cell dimensions at 33.8% As are a = 6.83 Å, and c = 12.60 Å, and at 34.8% As, 6.82 and 12.50 Å, as compared to Hellner's values, 6.80 and 12.48 Å. The density of the stoichiometric compound Ni_5As_2 was 8.61 g./cc., corresponding to 6 molecules per unit cell. The contraction of the lattice with increasing As concentration indicates that the variable composition of this compound may be the result of the formation of vacant Ni sites. Difficulty was encountered in indexing the pattern of the stoichiometric compound at very high orders owing to overlap of reflections. Accordingly the intensities, interplanar spacings, and indices of the major reflections of the alloy corresponding to $Ni_{5-0.23}As_2$ were chosen to represent this phase, and are recorded in Table I.

TABLE I

POWDER DIFFRACTION PATTERN OF $Ni_{5-0.23}As_2$

(Hexagonal or trigonal aspect symbol P–c–;
a = 6.815±0.003 Å, c = 12.498±0.007 Å; ρ_{calc} = 8.50 g./cc., ρ_{obs} = 8.55 g./cc.;
Ni-filtered Cu radiation, $\lambda\alpha_1$ = 1.5405 Å; camera diameter, 11.46 cm.; cutoff 20 Å; Temp. 24° C.)

I_{obs}	hk^*l	d_{obs}	d_{calc}	d_{obs}	hk^*l	d_{obs}	d_{calc}
25	11*1	3.28	3.29	40	41*5	1.142	1.145
25	00*4	3.10	3.12	40	33*0 32*6	1.134	1.136 1.135
40	11*2	2.97	2.99				
20	10*4	2.75	2.76	60B	33*3 41*6	1.094	1.096 1.095
20	20*2	2.66	2.67	30	33*4	1.066	1.068
30	11*4	2.29	2.30	50	30*10	1.054	1.054
55	21*1	2.19	2.20	20	22*10	1.007	1.008
60	20*4	2.14	2.15	30	20*12	0.9816	0.9822
100	11*5	2.01	2.02	20	50*8	0.9418	0.9418
100	21*3 10*6	1.96	1.97 1.96	20	41*10	0.8966	0.8969
40	21*4	1.81	1.81	20	52*5 21*13	0.8834	0.8839 0.8832
50	11*6	1.77	1.78	20	52*6	0.8606	0.8607
35	30*4 21*5	1.66	1.66	25B	70*4 53*4 30*14	0.8134	0.8141 0.8130
50	22*5	1.403	1.407				
40	22*6	1.316	1.319	20	41*12	0.8099	0.8099
20	31*6	1.284	1.286	20	44*6	0.7885	0.7886
30	21*8 41*1	1.279	1.280 1.281	20	53*6 70*6	0.7816	0.7816
50	32*4	1.239	1.242				
55	11*10	1.171	1.173				

Inspection of the indices shows that there are no restrictions on reflections from *hkl* or *hhl* planes, but for reflections from *h*0*l* planes, $l = 2n$. Hence the space group symbol is of the form $P\text{–}c\text{–}$, for which there are five possibilities: the trigonal space groups $P3c1$ and $P\bar{3}c1$, and the hexagonal space groups $P6_3cm$, $P\bar{6}c2$, and $P6_3/mcm$. Unfortunately, no further selection can be made immediately. Theoretically, positions could be found for the 30 Ni atoms and the 12 As atoms required by the unit cell in all five space groups. Examples of only two of these groups have been observed in intermetallic systems; two A_2B compounds have the triagonal $P\bar{3}c1$ structure, and three A_5B_3 compounds have the hexagonal $P6_3/mcm$ structure (3). There does not appear to be any similarity between these structures and the structure of Ni_5As_2.

Alloys with 34.8–43% As. *The β′ and γ Phases*

High temperature diffraction patterns at 200° to 800° C. of alloys with 36.3 to 41.3% As showed the presence of the β (Ni_5As_2) phase and the δ($Ni_{12-x}As_8$) phase, as one would predict on consideration of Hansen's diagram. At temperatures below 200° C., however, one of two new patterns was also obtained, depending on the temperature program. Similar patterns were obtained for alloys which contained 34.6% As, and which were therefore within the homogeneous β field above 200° C. In this whole region of 34.8 to 43% As, the room temperature diffraction patterns were remarkably dependent on the history of each specimen, the relative intensities of the β pattern and the two new patterns being a function of the heat treatment given to the sample.

For the purpose of this discussion, these two patterns will be referred to as the β′ and the γ patterns, representing the β′ and γ phases respectively. It should be noted that since the patterns of the β′ and β phases are quite similar at low orders, and since the majority of photographs containing the β′ phase were diffuse at high orders, it has been necessary to base the estimates of the relative concentration of this phase on the intensities of two or three lines at rather low orders. In addition, it is to be understood that although reference may not be made to the diffraction pattern of the δ phase, this phase was detected in all alloys containing over 36.8% As.

The β′ pattern was obtained for all alloys quenched from the melt or from 700° C., with no reflections due to the β phase visible at high orders. Alloys quenched from 400° C. also exhibited this pattern, but with a reduction in intensity of the lines characteristic of this phase. By cooling the specimens from 400° C. to room temperature over a period of 2 to 3 days, the intensities were reduced to one hundredth of the intensities of the reflections from quenched samples. A series of specimens of alloys in this concentration range, chosen at random with respect to their previous heat treatment, were annealed at 170° C. for 9 days, and a second series at 78° C. for 12 days. Both series were cooled slowly to room temperature. The diffraction pattern contained no β′ reflections, but consisted of the β and γ patterns, the intensity of the latter pattern ranging from weak to moderately strong.

On heating alloys containing the β′ phase to 50° C. in the high temperature camera, the β′ pattern was replaced by the γ pattern within 24 to 48 hours depending on the concentration of the β′ phase originally present. The β′ and γ phases appeared to be related in that the greater the intensities of the β′ pattern in the room temperature photographs, the more intense the γ pattern at 50° C. Once formed, the γ phase was retained on heating and on cooling to any temperature between 14° and 200° C., but with no appreciable variation in intensity with time. By cooling the camera from 200° C. to room temperature as rapidly as possible, traces of the β′ phase appeared. Between 200° and 240° C. the

γ pattern disappeared, and patterns of the β phase with precise high order reflections were obtained. Rapid cooling from 250° to 80° C. resulted in the formation of traces of the γ phase, and from 250° to 14° C., traces of the β' phase.

Apparently two distinct phase changes occur in alloys in this concentration range. The first of these, the change of the β phase to the β' phase, is a function of the degree of thermal shock to which the alloy has been subjected, and is clearly a diffusionless, i.e. martensitic, transformation. It has been mentioned that the diffraction pattern of the β' phase is very similar to the pattern of the β phase. It can be indexed with reference to a hexagonal unit cell similar in dimensions to the unit cell of Ni_5As_2, as shown in Table II. Aside from the doubling of reflections and the dissimilarity at high orders arising from the variation in dimensions, the important feature in the β' pattern is the appearance of reflections from $h0l$ planes for which l is odd. Hence it appears that the glide occurring in the Ni_5As_2 crystal during this transformation produces a crystal of different space group within the same crystal system. The β' phase is metastable, and is not observed in alloys annealed below 200° C.

TABLE II

LOW ORDER DIFFRACTION PATTERN OF THE Ni/As β' PHASE

(Hexagonal aspect symbol $P---$;
$a = 6.70 \pm 0.05$ Å; $c = 12.41 \pm 0.07$ Å;
Ni-filtered Cu radiation, $\lambda_{\alpha_1} = 1.5405$ Å;
Camera diameter, 11.46 cm.; cutoff 20 Å; Temp. 24° C.)

I_{obs}	$I_{Ni_5As_2}$†	$hk*l$	d_{obs}	d_{calc}	I_{obs}	$I_{Ni_5As_2}$†	$hk*l$	d_{obs}	d_{calc}
15	25	11*1	3.22	3.24	100	100	11*5	1.998	1.996
10	25	00*4	3.09	3.11	80	100	10*6	1.953	1.951
25	40	11*2	2.95	2.95	90		21*3	1.933	1.938
10	—	20*1	2.82	2.83	5	—	30*1	1.912	1.916
15	20	10*4	2.73	2.74	30B	40	21*4	1.795	1.792
20	20	20*2	2.62	2.63	60	50	11*6	1.763	1.767
30	30	11*4	2.28	2.28	5	5	20*6	1.691	1.686
30	55	31*1	2.17	2.16	5		22*0	1.672	1.675
40	60	20*4	2.12	2.12	15	15	22*1	1.659	1.661
25	10	21*2	2.07	2.07	15	35	30*4	1.642	1.642
							21*5		1.645

†*Intensity of reflection from same plane in* Ni_5As_2.

The second transformation, resulting in the formation of the γ phase, occurs between 100° and 200° C. The maximum concentration of this phase, estimated by diffraction intensities, did not exceed 50% even after the most extended annealing periods. Since equilibrium was not attained, the composition of this phase is not known with any certainty. There were indications, however, that the composition is close to the arsenic-rich limit of the β phase, and may lie within the high temperature β phase limits. Patterns of all alloys containing more than 36.8% As contained elements of the δ phase, which did not alter appreciably in intensity with heat treatment, while the greatest concentrations of the γ phase were obtained for alloys in which no δ phase could be detected, that is, alloys containing less than 36.5% As.

It appears that the compound $Ni_{5-x}As_2$, with x between 0.23 and 0.27, forms a new compound below 200° C. either by a direct transition or by the formation of an intermediate martensitic phase, depending upon the rate of cooling. The conversion of the martensitic phase to the new compound is the more rapid of the two transformations. The diffraction pattern of this compound was observed only in the presence of the β

pattern, both being very diffuse. The principal lines of the pattern recorded in Table III were obtained by subtracting all lines of the β pattern with the exception of two obviously superimposed reflections. The results of the calculations commonly employed in indexing powder diagrams were not conclusive, and the unit cell is as yet unknown.

TABLE III

DIFFRACTION PATTERN OF THE Ni/As γ PHASE

(Unit cell and space group unknown;
Cu K_{α_1} radiation; λ_{α_1} = 1.5405 Å; Ni filter;
Camera diameter, 11.46 cm.; cutoff 20 Å; Temp. 24° C.)

I	*d*	*I*	*d*
3	3.18	1	2.06
10	2.90	100	1.98
1	2.67	90*B*	1.91
1	2.49	20	1.82
3	2.45	30	1.75
2	2.25	15	1.63
15	2.21	25*B*	1.38
20*B*	2.18	20*B*	1.29

Alloys with 43–53% As. The δ Phase, $Ni_{12-x}As_8$

The pattern of the β phase (with the β' or γ phases, depending on the heat treatment of the sample) was present in all room temperature diffraction patterns of alloys containing up to 47.5% As, and the pattern of the ϵ phase appeared in alloys containing 50% As. For alloys with intermediate concentrations only the δ phase was observed. The δ patterns were identical whether this phase was in equilibrium with the β phase or the ϵ phase.

In the high temperature camera, an alloy containing 45.8% As exhibited the δ pattern and elements of the β pattern at all temperatures to 790° C.[3] At 805° C. the β phase had disappeared and some melting occurred. At 830° C. the presence of considerable liquidus phase was indicated both by incomplete diffraction lines on the film, and by the appearance of the sample recovered from the camera. An alloy containing 48.1% As, exhibiting only the δ phase, also remained unaltered to 805° C. where some indication of melting was recorded. At 830° C. the δ pattern was still visible, although the sample was almost completely melted. For alloys containing both the δ and ϵ phases (50% and 53% As), no transition was observed below 830° C., but some liquidus appeared at 830°–840° C. Although the silica capillaries were attacked to a considerable extent at these temperatures, the principal lines of the ϵ pattern could still be recognized although reflections due to the δ phase were absent.

Contrary to expectations, the δ phase is homogeneous over a very short concentration range, and the composition corresponds to the stoichiometric formula $Ni_{11}As_8$. The compound Ni_3As_2, the '*ideal*' *maucherite*, did not appear, and presumably does not exist.[4]

[3] *Camera temperatures were registered by an axial thermocouple about 5 mm. from the sample. The observed thermal e.m.f. was related to actual specimen temperature in the usual manner, i.e., by determination of the lattice dimensions of a silver specimen at various e.m.f. values and hence the specimen temperature at those values. Considering the accuracy of this calibration, and the normal fluctuation in camera temperature during the exposure period, the uncertainty in specimen temperatures above 700° C. is estimated to be ±10° C.*

[4] *In his first paper (12), Peacock describes the cell content of maucherite as* $16[Ni_3As_2]-4Ni$, *to indicate a defect structure with vacant nickel positions. Presumably in the ideal compound these vacancies would be occupied. In referring to ideal maucherite as* Ni_4As_3, *Donnay and Nowacki (2) have apparently misquoted Peacock's second paper on the subject, although only a brief abstract of this paper has appeared in print (13). Wyckoff's description of the mineral heazlewoodite as* Ni_3As_2, *rather than* Ni_3S_2, *is a simple typographical error (15).*

The data obtained from the high temperature camera, indicating the formation of a liquidus at 800° C. for $\beta+\delta$ phase alloys, and at 835° C. for $\delta+\epsilon$ phase alloys, strongly support Hansen's contention that the compound has an incongruent melting point. Additional, but less convincing, evidence in favor of this conclusion was contained in room temperature diffraction patterns of alloys from the β phase to the ϵ phase. In none of the quenched specimens were the β and ϵ phases observed in the presence of each other, as might be expected if these two phases reacted to form the δ phase. On the other hand, for alloys containing the δ and ϵ phases, the relative intensity of the ϵ phase pattern was greater for specimens quenched from temperatures above 850° C. than for specimens annealed at 700° C.

The diffraction pattern of the δ phase is identical to that of maucherite. The pattern is recorded in Table IV, in which the interplanar spacings according to Peacock (12) and to Hewitt (8) have been included for comparison. Reflections of relative intensity less than 20 have been excluded for d values below 1.2 Å. The appearance of doublets at low and intermediate orders, where only one reflection had been previously observed, is attributed to the high resolving power of the 19-cm. camera rather than to any structural difference in the specimens.

Studies of single crystals of maucherite by Laves (11) and by Peacock have shown the crystal to be tetragonal with a well-defined tetragonal *pseudocell* having a axes half the length of the a axes of the *full cell*. Evidently some ordering in the lattice produced intercalated row lines with l indeterminate in rotation photographs about [001], and intercalated layer lines in photographs about [100], which occasionally resolved into spots requiring the larger a dimension for complete indexing. Peacock has stated that the continuous reflections requiring the full cell should not and do not appear on the powder diffraction pattern, since they are indeterminate in l. This is equivalent to saying that while the degree of ordering was sufficient to appear in single crystal photographs to the extent that the number of continuous diffractions which were resolved into spots permitted a definition of the full cell, the ordering was not considered sufficient to be manifest in the powder diagram.

Three reflections in the δ phase diffraction pattern at d = 3.03, 1.89, and 1.02 Å could not be indexed with reference to the pseudocell, provided the extinctions defined by Peacock were obeyed. The first two of these are present in the maucherite diagram and, together with the reflection at d = 2.30 Å, were indexed by Peacock as reflections due to Cu K_β radiation. This was a logical assumption since unfiltered radiation was used, the indices agreed with the indices of the three strongest K_α reflections, and corresponding spots were observed in Weissenberg photographs. However, the intensities of these reflections (recorded by Peacock as w, vw, m) are not the intensities to be expected from planes whose K_α reflection intensities are essentially identical (s, s, s); and moreover, the intensities are in qualitative agreement with the intensities observed in the δ pattern with filtered radiation (15, 5, 55). While there may have been some fortuitous reflection of K_β radiation at these angles, the lines are predominantly the result of K_α radiation on the same planes in the mineral as in the δ phase.

Of the three reflections requiring the full cell for indexing, the second and third are unlike the precise reflections of the rest of the pattern in that the intensity distributions are not symmetrical, but rise sharply on the low angle side and fall off slowly on the high angle side. This 'smeared' effect is also apparent in the diffraction patterns of the mineral reproduced in Peacock's paper. Such an intensity distribution is indicative of partial ordering, presumably in this instance along the c axis, inasmuch as the indices are of the

TABLE IV

POWDER DIFFRACTION PATTERN OF THE Ni/As δ PHASE, $(Ni_{11}As_8)_4$

(Tetragonal $P4_12_12$ or $P4_32_12$;
full cell, $a = 6.868 \pm 0.004$ Å, $c = 21.80 \pm 0.02$ Å;
pseudocell, $a' = a/2$, $c' = c$; $\rho_{calc} = 8.03$, $\rho_{obs} = 7.95$;
Ni-filtered Cu radiation, $\lambda_{\alpha_1} = 1.5405$ Å;
camera diameter, 19 cm.; cutoff, 8.5 Å; Temp. 24° C.)

I_{obs}	d_{obs}	$d_{Peacock}$†	d_{Hewitt}‡	d_{calc}	$h'k'l'$ Pseudocell	hkl§ Full cell
15	3.03	3.01β		3.07	—	210
15	2.70	2.70	2.71	2.72	008	
80	2.68			2.70	105	
35	2.35	2.36	2.39	2.37	112	
5	2.30	2.24β		2.31	107	
100	2.01	2.02	2.03	2.02	116	
20	1.97	1.98	1.97	1.98	019	
55B	1.89	1.89β		1.90	—	320, 219, 1, 0, 10
20	1.81	1.82	1.83	1.82	0, 0, 12	
90	1.71	1.72	1.73	1.72	200	
2	1.69			1.70	202	
30	1.62	1.62	1.63	1.62	1, 1, 10	
2	1.52			1.52	211	
25	1.50	1.51	1.51	1.51	0, 1, 13	
40	1.487	1.447	1.48	1.453	1, 1, 12	
20	1.447			1.452	028	
20	1.361	1.362	1.45	1.363	0, 0, 16	
5	1.345			1.348	0, 2, 10	
5	1.338			1.340	0, 1, 15	
15	1.294	1.297		1.296	219	
18	1.244	1.243		1.247	0, 2, 12	
70	1.212	1.211	1.21	1.214	220	
50	1.131	1.131	1.13	1.133	1, 2, 13	
60	1.107	1.104		1.109	228	
20	1.083	1.081	1.08	1.084	1, 1, 18	
20	1.079			1.081	312	
40	1.067	1.065	1.07	1.068	0, 2, 16	
35	1.039	1.042	1.04	1.041	316	631
20B	1.022			1.022	—	3, 2, 18
25	0.9709	0.970	0.970	0.9722	1, 3, 10	
20	0.9433	0.942		0.9455	0, 3, 13	
20	0.9290	0.927		0.9305	235	
25	0.9067	0.904		0.9066	2, 2, 16	
20	0.8584	0.858		0.8584	400	
40	0.8276	0.827		0.8283	3, 2, 13	
50	0.8185	0.817		0.8190	408	
20	0.8110	0.807		0.8115	3, 0, 19	
20	0.8091			0.8093	6, 2, 18	
25	0.8072			0.8072	332	
30	0.8033	0.802		0.8031	2, 0, 24	
20	0.7989			0.7989	4, 0, 10	

†*For the mineral maucherite, after Peacock (12). Values marked β are recalculated from d values given by Peacock for* Cu K_β *radiation.* $a = 6.844$ Å, $c = 21.83$ Å.
‡*After Hewitt (8).*
§$(hkl) = (2h'2k'l')$.

form (*hkl*). The first reflection requiring the full cell is sharper, but is a reflection from a plane parallel to the *c* axis. It is evident that considerable ordering was obtained not only in alloys of the δ phase, but also in the mineral used in the powder diffraction studies. The fact that Hewitt did not record any of these lines is probably a result of conformation with Peacock's notation in the identification of this phase, rather than the result of complete disordering in his specimens. Complete ordering or disordering was not

observed in any of our alloys. The ordering phenomenon in maucherite has been discussed recently by Jagodzinski and Laves (10).

In Table IV, the indices assigned to the reflections with respect to the pseudocell were selected on the basis of the agreement obtained between observed and calculated values of $\sin^2\theta$, within the limitations of the systematic extinctions defined by the single crystal data. Although these indices agree with those accepted by Peacock, there is some uncertainty because of the large number of possible reflections. As Peacock remarked, the most that can be said is that the identification is probably correct for the great majority of the lines. However, the necessity of referring to the full cell to index three of the reflections increases the uncertainty in the indices based on the pseudocell, since it is possible that some of these reflections are also the result of ordering in the lattice. The number of permitted reflections from the larger cell is about four times greater than from the pseudocell, and any attempt to assign indices without prior knowledge of atom positions would be completely unjustified.

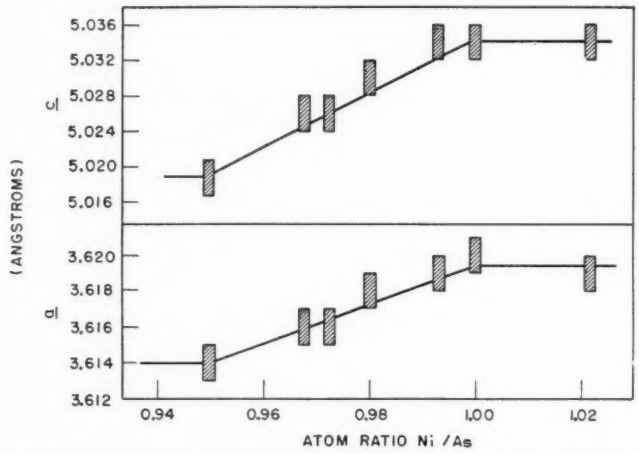

FIG. 2. Variation in the lattice parameters of hexagonal NiAs with composition.

Alloys with 53–60% As. *The* ϵ *Phase*, NiAs

The δ and ϵ phase patterns were present in alloys with 53–55.5% As, and the ϵ and η patterns [5] in alloys containing over 58% As. Within the 55.5–58% As region the phase,

TABLE V

VARIATION IN UNIT CELL DIMENSIONS OF NiAs (IN Å) WITH TEMPERATURE (IN ° C.)

	15°	294°	512°	612°	776°	798°
a	3.618	3.630	3.642	3.649	3.659	3.660
c	5.032	5.054	5.076	5.088	5.108	5.112

i.e., the compound NiAs, was homogeneous with evident variation in the lattice dimensions of the unit cell. No transformations were observed in the diffraction patterns of an alloy containing 56% As at temperatures to 800° C.

[5] *The pattern of the* η *phase is identical to the pattern of the mineral rammelsbergite* $NiAs_2$.

To estimate the range of variable composition of NiAs, several alloys were prepared in the 55–58% As region, and the unit cell dimensions determined as accurately as possible on specimens quenched from 700° C. The results are shown graphically in Fig. 2. The limiting values of the cell dimensions were obtained from photographs in which either the δ or the η patterns were present. Apparently the deficiency in Ni does not exceed 5%. There is some indication that metalloid deficiencies may also occur, but the apparent contraction for Ni/As ratios greater than one is of the same order of magnitude as the uncertainty in cell dimensions. The dimensions of the lattice with all atom sites occupied are $a = 3.619 \pm 0.002$ Å and $c = 5.034 \pm 0.002$ Å, while the minimum dimensions corresponding to the maximum number of vacancies are 3.614 and 5.020 Å. Cell dimensions reported for niccolite are generally less than these values, although the dimensions of two synthetic specimens were apparently somewhat larger (8, 14).

The variation in unit cell dimensions of the stoichiometric compound with temperature is given in Table V. The approximate mean linear coefficient of expansion between 0° and 800° C. along the a axis is 15×10^{-6} deg.$^{-1}$ and along the c axis 20×10^{-6} deg.$^{-1}$. These coefficients are considerably smaller than the coefficients obtained for the iron and cobalt analogues, FeAs and CoAs (9).

ACKNOWLEDGMENTS

We wish to express our thanks to Mrs M. Beck, who obtained and measured the great majority of the diffraction patterns, and to Dr. W. G. Henry, who assisted greatly in the preparation of alloys in his chill casting apparatus.

ERRATUM

On page 454 and in Table V of the first paper in this series (9) the space group symbol for CoAs is erroneously given as *Pnma*. For the setting chosen this should read *Pmcn*.

REFERENCES

1. Arrivaut, G. Compt. rend. **192**, 1238 (1931).
2. Donnay, J. D. H. and Nowacki, W. Crystal data. Memoir 60. The Geological Society of America. 1954. p. 52.
3. Donnay, J. D. H. and Nowacki, W. Crystal data. Memoir 60. The Geological Society of America. 1954. pp. 54 ff., 420 ff.
4. Friedrich, K. and Benningson, F. Metallurgie, **7**, 200 (1907).
5. Hansen, M. Der Aufbau der Zweistofflegierungen. Edwards Bros. Inc., Ann Arbor, Mich. 1937. pp. 187 ff.
6. Hellner, E. Fortschr. Mineral. **29–30**, 59 (1951).
7. Henry, N. F. M., Lipson, H., and Wooster, W. A. The interpretation of X-ray diffraction photographs. McMillan & Co., Ltd., London. 1951. pp. 181 ff.
8. Hewitt, D. F. Econ. Geol. **43**, 408 (1948).
9. Heyding, R. D. and Calvert, L. D. Can. J. Chem. **35**, 449 (1957).
10. Jagodzinski, H. and Laves, F. Schweiz. mineral. petrog. Mitt. **28**, 456 (1948).
11. Laves, F. Z. Krist., Abt. A, **90**, 279 (1935).
12. Peacock, M. A. Mineral. Mag. **25**, 557 (1940).
13. Peacock, M. A. Am. Mineralogist, **27**, 229 (1942).
14. Wyckoff, R. W. G. Crystal structures. Vol. I. Interscience Publishers, Inc., New York. 1948. Chap. III, text p. 28.
15. Wyckoff, R. W. G. Crystal structures. Vol. I. Interscience Publishers, Inc., New York. 1948. Chap. V, table p. 13*a*.

THE GAS PHASE REACTION OF METHYL RADICALS WITH HEXAFLUOROACETONE[1]

G. O. PRITCHARD[2] AND E. W. R. STEACIE

ABSTRACT

The photolytic and thermal decomposition of azomethane in the presence of hexafluoroacetone produces small amounts of fluorinated products, mainly fluoroform. The mechanism of this and related reactions is discussed. It is concluded that the proposed reaction

$$CH_3 + CF_3COCF_3 \rightarrow CH_3COCF_3 + CF_3$$

has an activation energy of about 6 kcal./mole, with a steric factor of about 10^{-5}.

INTRODUCTION

In the gas phase photolysis of trifluoroacetone, at high temperatures and low intensities, Sieger and Calvert (9) found that ethane must be formed predominantly by some reaction other than

$$CH_3 + CH_3 \rightarrow C_2H_6.$$

They suggested that the high ethane yield may result either through the addition of methyl radicals to the carbonyl double bond,

$$CH_3 + CF_3COCH_3 \rightarrow CF_3CO(CH_3)_2, \qquad [I]$$

followed by

$$CF_3CO(CH_3)_2 \rightarrow C_2H_6 + CF_3CO,$$

or by the direct abstraction reaction,

$$CH_3 + CH_3COCF_3 \rightarrow C_2H_6 + CF_3CO. \qquad [II]$$

The authors pointed out that confirmation of reactions of the type [I] and [II] is scant, although they suggest that the results of the photolysis of biacetyl at high temperatures can be interpreted as the addition of a methyl radical to a carbonyl double bond:

$$CH_3 + (CH_3CO)_2 \leftrightharpoons (CH_3)_2COCOCH_3,$$

$$(CH_3)_2COCOCH_3 \rightarrow CH_3COCH_3 + CH_3CO.$$

The direct abstraction of a radical from a molecule has been cited in the photolysis of $(CH_3)_2Hg$,

$$CH_3 + (CH_3)_2Hg \rightarrow C_2H_6 + CH_3Hg,$$

although it is only important above 200° C.

Also, Sieger and Calvert found, at high temperatures, the chain formation of CH_3-containing molecules (four CH_3 per quantum at 350° C.), and a marked deficiency in CF_3-containing species in the gaseous products. They suggest that CF_3 radicals generate CH_3 radicals via

$$CF_3 + CF_3COCH_3 \leftrightharpoons (CF_3)_2COCH_3,$$

$$(CF_3)_2COCH_3 \rightarrow CH_3 + CF_3COCF_3.$$

Analytical difficulties prevented analysis for the expected CF_3COCF_3.

[1]*Manuscript received June 20, 1957.*
Contribution from the Division of Pure Chemistry, National Research Council, Ottawa, Canada. Issued as N.R.C. No. 4476.
[2]*National Research Council of Canada Postdoctorate Fellow, 1955–57.*

In view of this work it seemed of interest to investigate further the possibility of the occurrence of these types of reaction in the gas phase. The most convenient way of doing this appeared to be the photolytic or thermal decomposition of azomethane in the presence of hexafluoroacetone, followed by analysis for any CF_3-containing products, which would be formed if the reactions

$$CH_3 + CF_3COCF_3 \rightarrow CH_3COCF_3 + CF_3 \qquad [I]$$

and

$$CH_3 + CF_3COCF_3 \rightarrow CH_3CF_3 + CF_3CO \qquad [II]$$

took place.

EXPERIMENTAL

The apparatus consisted of a quartz reaction vessel (10 cm. long, 5 cm. diam.), which had a volume of 174 ml., mounted in an aluminum block furnace, the temperature of which could be controlled to $\pm 1°$ C. The quartz cell was connected to the rest of the vacuum system through a mercury cutoff. The gas analysis line consisted of the standard arrangement of temperature-controlled traps, a mercury diffusion pump, and a combined Toepler and gas burette.

Pure, thoroughly dry samples of hexafluoroacetone and azomethane were supplied by Dr. L. C. Leitch of these laboratories. Between 40 and 100 mm. of ketone and 100 to 200 mm. of azomethane were admitted to the reaction vessel, thoroughly mixed with a Toepler-type pump, and then irradiated for a known time. The resulting gases were pumped off and analyzed, cuts being taken at appropriate temperatures.

The light source was a B.T.H. high-pressure mercury lamp (type ME/D, 250 watts) operated on 220 v. d-c. The beam was collimated by a single quartz lens and a stop, the reaction cell being fully illuminated. The 3660 Å line was isolated using the appropriate filters (5). At this wavelength only the azomethane was photolyzed.

RESULTS

Under these conditions, the photolysis of mixtures of CF_3COCF_3 and $CH_3N_2CH_3$ at 200° C. produced small amounts of CF_3H. This was identified by the CF_2H^+ (51) ion in the mass spectrometer. The amount of CF_3H formed was of the same order of magnitude as the amount of C_2H_6 produced. Below 200° C. the quantity of CF_3H formed decreased, and also some other CF_3-containing compound was identified in the mass spectrum of the products. (The ratio of the CF_3^+ (69) to the CF_2H^+ (51) peak was too great for pure CF_3H. This was thought to be due to the formation of CF_3CH_3 at the lower temperatures.) The thermal decomposition of azomethane in the presence of hexafluoroacetone at 300° C. resulted in the production of relatively large quantities of fluoroform. Blank runs carried out with the ketone alone, under the above conditions, did not yield any detectable amounts of CF_3-containing products.

In all the experiments, the main gaseous products were nitrogen and methane. These were pumped off at −210° C. The next fraction was collected at −150° to −155° C. This contained the CF_3H and C_2H_6, some CO_2, and, in some cases, traces of CF_3CH_3. The percentage decomposition of the azomethane in runs 1 to 8 (Table I) was less than 5%, so that steady state conditions could be assumed. In the experiment at the highest temperature, 245° C., the thermal decomposition of azomethane was only 0.3% in 5 minutes (7).

Table I (runs 1 to 8) brings out several points helpful in the elucidation of a reaction

TABLE I

Run	Temp., °C.	Time, min.	Conc., mole/cc.×10⁶		Products, mole/cc.							$k_1/k_2^{\frac{1}{2}}$, (mole/cc.)$^{-\frac{1}{2}}$sec.$^{-\frac{1}{2}}$	Remarks
			CF_3COCF_3	$CH_3N_2CH_3$	$CF_2H\times10^9$	$C_2H_6\times10^9$	CF_3CH_3	$CO_2\times10^9$	$CH_4\times10^8$	$N_2\times10^7$	$CO\times10^9$		
1	163.0	5	2.28	4.78	1.90	20.6	1.30×10^{-9}	2.0			None	0.562	
2	183.0	5	1.31	5.24	1.57	13.4	None	0.7				0.599	
3	183.0	5	2.25	3.87	2.69	8.21	1.35×10^{-9}	1.5	2.24	1.45		1.15	
4	205.0	5	1.96	2.76	3.37	9.13	6.63×10^{-10}	1.7	2.35	1.29		1.24	
5	207.0	5	1.64	7.22	3.23	10.3	None	0.8				1.12	
6	220.0	5	2.74	6.01	3.89	6.69	None	2.0	5.60	2.17		1.00	
7	228.0	5	2.25	3.89	5.05	8.47	None	2.2				1.46	
8	245.0	5	2.54	4.66	7.06	9.54	7.63×10^{-11}	2.5			None	1.66	
9	139.0	30	1.65	3.36	2.15	87.8	5.40×10^{-10}	1.6				0.130	
10	175.0	30	2.27	2.65	16.4	49.1	None	5.0	12.1	8.00		0.766	
11	230.0	30	1.92	2.92	34.6	23.9	None	10.0	25.6	9.64	8.0	2.82	
12	181.0	100.5	2.28	5.34	0.936	1.14	None	0.6				0.517	5% Neutral density filter
13	205.5	17	5.81	10.0	1.47	3.75	None	50				0.129	30% Neutral density filter
14	236.5	339	6.35	9.85	5.12	2.35	None	100				0.117	Thermal dark reaction
15	264.5	30	2.15	4.50	8.86	1.53	None	8.0			1.0	2.49	Thermal dark reaction

mechanism. Runs 9, 10, and 11 are not considered reliable, owing to the fact that more than 30% of the azomethane was decomposed in these experiments, and also to a more serious factor which will be discussed later.

(1) The N_2+CH_4 mixtures obtained in runs 1 and 8 were analyzed for CO in a CuO furnace maintained at 250° C. and none was found. The mixtures analyzed should have contained more than 1% CO (based on $CO \geq \frac{1}{2}CF_3H$ formed) if CF_3 radicals were produced by photolysis of the ketone, which would have been easily detected.

(2) No C_2F_6 was detected in the products.

(3) The CO_2 found probably arises from a residual 0.5% impurity in the hexafluoroacetone, detected in the mass spectrometer.

(4) Below 150° C. only traces of CF_3-containing products were found in the large amounts of ethane obtained; at room temperature no CF_3-products were obtained at all.

(5) The column headed CF_3CH_3 requires some justification. In the runs at lower temperatures the CF_3^+ (69) peak in the mass spectrum of the products indicated the presence of some CF_3-containing compound other than CF_3H (calculated from the CF_2H^+ (51) peak). Absence of the characteristic CF_3CO^+ (97) and $C_2F_5CO^+$ (147) peaks indicated that this was not due to carry-over of CF_3COCF_3 in the low-temperature distillation. There was usually close agreement between the measured pressure of the gaseous mixture (CF_3H, C_2H_6, and CO_2) admitted to the ionization chamber of the mass spectrometer and the total pressure of these gases calculated from the ion-peak heights except in cases where the CF_3^+ (69) appeared too large compared to the CF_2H^+ (51). Here the calculated total pressure was found to be less than the measured pressure. It seemed justified to assume this "extra" gas was CF_3CH_3. If large quantities of CF_3CH_3 were formed, the distillation technique employed would not have separated all the gas from the residual mixture, but the significant fact is that, using exactly identical analytical procedure in each experiment, the amounts of CF_3CH_3 formed decreased with increasing temperature.

DISCUSSION

In the system we have $CH_3N_2CH_3 + h\nu \rightarrow 2CH_3 + N_2$. The formation of fluoroform, which presumably can only arise from the reaction

$$CF_3 + CH_3N_2CH_3 \rightarrow CF_3H + CH_2N_2CH_3,$$

means some mechanism must be found involving CF_3 radicals. The preceding evidence shows that they are not formed in a primary step, but are generated when CH_3 radicals are present in the system.

The proposed gas phase reaction step is addition of a CH_3 radical to the carbonyl double bond:

$$CH_3 + CF_3COCF_3 \leftrightharpoons CF_3CH_3COCF_3.$$

This may or may not be reversible.

Possible modes of decomposition of the species $CF_3CH_3COCF_3$ are

$$CF_3CH_3COCF_3 \rightarrow CH_3COCF_3 + CF_3, \qquad [I]$$

$$\rightarrow CF_3CH_3 + CF_3CO, \qquad [I']$$

$$\rightarrow C_2F_6 + CH_3CO. \qquad [I'']$$

Also the direct abstraction

$$CH_3 + CF_3COCF_3 \rightarrow CH_3CF_3 + CF_3CO \qquad [II]$$

has to be considered.

Reaction [I″] can be discarded, as no C_2F_6 was formed. The products of [I′] and [II] are identical, so these reactions can be considered together.

As both modes of formation of CF_3CH_3 require a positive activation energy, the amounts formed should increase with temperature. Also the CF_3CO radical would decompose spontaneously (3), giving CO and $CF_3CH_3 \geqslant CF_3H$ formed. None of these conditions was found to hold. The CF_3CH_3 yields were small and decreased with temperature. As noted previously, analysis of the non-condensable products from runs 1 and 8 indicated no detectable CO. According to reactions [I′] and [II] the amount of CO $\geqslant$ the amount of CF_3H formed, so that the mixtures analyzed would have contained more than 2% CO.

The data suggest a purely CF_3 radical mechanism to account for the CF_3-containing products, e.g. reaction [I]. This is consistent with no CO formation and the fact that CF_3H formation increases, so that CF_3CH_3 formation decreases with increasing temperature, assuming the CF_3–CH_3 radical recombination reaction has approximately zero activation energy. On this basis, very little CF_3CH_3 would be found in any case. At 200° C. and above, $R_{CH_4} > R_{C_2H_6}$, and it is now well established (2, 8) that H-atom abstraction reactions by CF_3 radicals are very much faster than those involving CH_3 radicals from the same H-containing compound, so that $R_{CF_3H} \gg R_{CF_3CH_3}$. The low concentration of CF_3 radicals discounts any possibility of C_2F_6 formation.

Assuming mechanism [I] to be operative, we have

$$CH_3 + CF_3COCF_3 \underset{k_r}{\overset{k_f}{\rightleftharpoons}} CF_3CH_3COCF_3 \xrightarrow{k_I} CF_3 + CH_3COCF_3. \qquad [I]$$

If all the CF_3 radicals end up as CF_3R, then if $CF_3CH_3COCF_3$ reaches a steady state,

$$R_{CF_3R} = k_f[CH_3]\,[CF_3COCF_3]/(1+k_r/k_I).$$

Assuming that the back reaction is unimportant, i.e. $k_r = 0$, (or alternatively, regarding the species $CH_3CO(CF_3)_2$ as a transition state complex), and that all the CF_3 radicals abstract a hydrogen atom

$$CF_3 + CH_3N_2CH_3 \xrightarrow{k_1} CF_3H + CH_2N_2CH_3, \qquad [1]$$

we can write

$$R_{CF_3COCH_3} = R_{CF_3H} = k_I\,[CH_3]\,[CF_3COCF_3],$$

where k_I is the rate constant for the over-all reaction

$$CH_3 + CF_3COCF_3 \xrightarrow{k_I} CF_3 + CH_3COCF_3. \qquad [I]$$

If ethane is formed only in

$$CH_3 + CH_3 \rightarrow C_2H_6, \qquad [2]$$

under steady-state conditions we have

$$R_{CF_3H}/R^{\frac{1}{2}}_{C_2H_6} = k_I/k_2^{\frac{1}{2}}[CF_3COCF_3].$$

Considering the other possible fates of the CF_3 radicals:

$$CF_3 + CH_3 \xrightarrow{k_3} CF_3CH_3, \qquad [3]$$

$$CF_3 + CH_3N_2CH_3 \rightarrow CH_3CF_2N_2CH_3, \qquad [4]$$

and

$$CF_3 + CF_3 \xrightarrow{k_5} C_2F_6, \qquad [5]$$

so that

$$R_{CF_3COCH_3} \equiv R_{CF_3H}+R_{CF_3CH_3}+R_{CH_3CF_2N_2CH_3}+R_{C_2F_6},$$

R_{CF_3H} is measured, $R_{CF_3CH_3}$ is estimated or is assumed zero, $R_{C_2F_6} = 0$, $R_{CH_3CF_2N_2CH_3} = k_4R_{CF_3H}/k_1$, and

$$\{R_{CF_3H}(1+k_4/k_1)+R_{CF_3CH_3}\}/R^{\frac{1}{2}}_{C_2H_6} = (k_1/k_2^{\frac{1}{2}})\ [CF_3COCF_3].$$

We can estimate k_4/k_1 as follows. (It is assumed that all the species formed in [4] are saturated by the excess of methyl radicals.) Jones and Steacie (4) have measured the rates of the reactions

$$CH_3 + CH_3N_2CH_3 \xrightarrow{k_6} CH_4 + CH_2N_2CH_3 \qquad [6]$$

and

$$CH_3 + CH_3N_2CH_3 \xrightarrow{k_7} (CH_3)_2N_2CH_3 \qquad [7]$$

obtaining

$$k_6/k_2^{\frac{1}{2}} = 2\times10^4e^{-7600/RT} \quad \text{and } k_7/k_2^{\frac{1}{2}} = 5\times10^3\ e^{-6300/RT}(\text{mole/cc.})^{-\frac{1}{2}}\text{sec.}^{-\frac{1}{2}}.$$

It has been shown (2) for a number of H-abstraction reactions that CF_3 radicals have an activation energy of about 3 kcal. less than and a steric factor of 10 times that of CH_3 radicals. If this is true here also, we may write approximately, knowing $k_2 \approx k_5$ (1),

$$k_1/k_5^{\frac{1}{2}} = 2\times10^5\ e^{-4500/RT}(\text{mole/cc.})^{-\frac{1}{2}}\text{sec.}^{-\frac{1}{2}}.$$

Also the rate of the reaction

$$CF_3 + CF_3N_2CF_3 \rightarrow (CF_3)_2N_2CF_3 \qquad [8]$$

has been measured (8); $k_8/k_5^{\frac{1}{2}} = 3.0\times10^3e^{-3500/RT}(\text{mole/cc.})^{-\frac{1}{2}}\text{sec.}^{-\frac{1}{2}}$. From the rate expressions for reactions [7] and [8], it would seem probable that for reaction [4],

$$CF_3 + CH_3N_2CH_3 \rightarrow CH_3CF_2N_2CH_3, \qquad [4]$$

we can write $k_4/k_5^{\frac{1}{2}} \sim 10^3e^{-3500/RT}(\text{mole/cc.})^{-\frac{1}{2}}\text{sec.}^{-\frac{1}{2}}$.

So k_4/k_1 approximately equals $10^3e^{-3500/RT}/10^5e^{-4500/RT}$, i.e. about 10^{-2} at 500° A., which is only a correction of 1% to R_{CF_3H}. This is very approximate, but even if the steric factor in reaction [4] was assumed to be a power of 10 greater, this is still only a 10% correction, so it has been assumed that $R_{CH_3CF_2N_2CH_3} = 0$.

In Fig. 1, $k_1/k_2^{\frac{1}{2}} = (R_{CF_3H}+R_{CF_3CH_3})/R^{\frac{1}{2}}_{C_2H_6}\ [CF_3COCF_3]\ (\text{mole/cc.})^{-\frac{1}{2}}\text{sec.}^{-\frac{1}{2}}$ is plotted

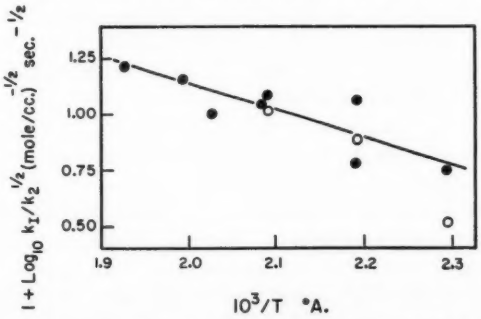

FIG. 1. Arrhenius plot for the reaction $CH_3 + CF_3COCF_3 \rightarrow CH_3COCF_3 + CF_3$. The open circles represent runs 1, 3, and 4 without the CF_3CH_3 correction.

versus the reciprocal of the absolute temperature. The curve drawn gives $E_1-\frac{1}{2}E_2 = 5.7\pm1.5$ kcal./mole and $A_1/A_2^{\frac{1}{2}} = 4\times10^2$ (mole/cc.)$^{-\frac{1}{2}}$sec.$^{-\frac{1}{2}}$, where E and A are the parameters of the Arrhenius equation. There is considerable scatter in Fig. 1, but knowing that $E_2 = 0$ and $A_2 = 5\times10^{13}$ (mole/cc.)$^{-1}$sec.$^{-1}$, it appears that the reaction

$$CH_3 + CF_3COCF_3 \rightarrow CH_3COCF_3 + CF_3$$

has a low activation energy, about 6 kcal./mole, and a very low steric factor, about 10^{-5}.

The above treatment is rather complex and may be somewhat arbitrary. However, the mere qualitative fact that CF_3H is formed at all essentially establishes the mechanism, and it seems impossible to explain it in any other way.

FURTHER EXPERIMENTS

If the preceding kinetic interpretation is correct, reduction in the steady-state methyl radical concentration would lead to an increase in the production of CF_3H over C_2H_6 and CF_3CH_3 without altering the $k_1/k_2^{\frac{1}{2}}$ ratios. This was investigated by putting neutral density filters into the light beam to reduce the intensity of the light, and also, above 200° C., the same effect was attained by very slow thermal decomposition of the azomethane. Conditions were chosen so that about 5% of the azomethane was decomposed. The results of these experiments are recorded in Table I, runs 12 to 15. No consistency was found in the rate constants, and in some cases large amounts of CO_2 and some CO were found in the reaction products.

The large quantities of CO_2 obtained in these experiments, especially runs 13 and 14, are difficult to account for. No SiF_4 was detected in the products, so that it is unlikely that the CO_2 is formed owing to reaction of the CF_3 radicals with the walls of the reaction vessel. A possible reaction sequence is:

$$2CF_3 + 3H_2O \rightarrow 6HF + CO + CO_2,$$

$$\tfrac{3}{2}SiO_2 + 6HF \rightarrow \tfrac{3}{2}SiF_4 + 3H_2O,$$

but in any case all the reactants were carefully dried before use.

Low-temperature fractionation of samples of the ketone (identical to the procedure followed in the analysis of a run) yielded quantities of CO_2 of the order of magnitude of those obtained in runs 1 to 8, owing to a slight residual impurity of CO_2 in the CF_3COCF_3 used.

Another disturbing factor was that the pressure in the cell dropped during the reaction, and analysis of the products indicated a loss of CF_3COCF_3 and $CH_3N_2CH_3$.

Further investigation showed that when about equal amounts of CF_3COCF_3 and $CH_3N_2CH_3$ (about 10 cm. of each in 200 ml.) were mixed in a sealed glass bulb at room temperature, the pressure dropped steadily. No noticeable change occurred in the first 10 minutes, but after 30 minutes the pressure had dropped by 1%, after 3 hours by 5%, and after 48 hours most of the gases seemed to have disappeared. This reaction occurred in the complete absence of light. Analysis indicated that no non-condensables, C_2H_6, C_2F_6, or CF_3H, were formed, i.e. the reaction was not free radical. A colorless liquid was left in the bulb together with small amounts of $CH_3N_2CH_3$ and/or CF_3COCF_3, which were pumped off. The mass spectrum of the liquid was complex; it contained peaks characteristic of azomethane and hexafluoroacetone with many intermediates, but no parent peaks for either of these compounds were observed. Two small ion peaks were also observed at about 20 mass units above 200.

Microanalysis of the liquid gave %C = 26.97, %H = 2.91, and %N = 12.71. Infrared

spectroscopy of the pure liquid and in CS_2 solution indicated the absence of a >C=O band at 1800 cm.$^{-1}$, but a well-defined band was obtained at 3400 cm.$^{-1}$, typical of an —OH group. Other principal bands were at 990 and 1020; 1183, 1218, 1240, and 1269 (C—F vibrations); 1325 and 1385; 1495 and 1618 (pure liquid phase only); and 2800 to 3000 cm.$^{-1}$ (C—H vibrations). This evidence appears to be consistent with the compound $(CF_3)_2CCH_2\begin{matrix}OH\\ \diagup\\ \diagdown\\ N_2CH_3\end{matrix}$, which has a molecular weight of 224, and %C = 26.8, %H = 2.68, and %N = 12.5.

Owing to this reaction and any possible consequences of it (e.g., breakdown of the compound formed may result in the production of water in the system and consequent CO_2 formation) it is thought that data from any but the shortest runs are invalidated; hence runs 9 to 15 will not be considered further. No such reaction was found to occur between CH_3COCH_3 and $CH_3N_2CH_3$.

Attempts were also made to look for CF_3COCH_3 in the reaction products of some of the runs. Fractions were collected at −110° C. and rapidly analyzed on the mass spectrometer (before reaction between the CF_3COCF_3 and $CH_3N_2CH_3$ occurred). The parent peak of CF_3COCH_3 is negligible, but the ratio of CF_3^+ (69) to CF_2^+ (50) to CH_3CO^+ (43) was found to be 11.4 to 1.0 to 31.7. In the best attempt, after allowance for the contribution of the azomethane and hexafluoroacetone (over 95% of the mixture), estimated from the $CH_3N_2CH_3^+$ (58) and $C_2F_5CO^+$ (147) ions, the ratio of the peak heights for these mass numbers was 10.3 to 1.0 to 39.7. As the correction was very large, this is in no way conclusive.

As further pursuance of exact data did not seem justified, a few qualitative experiments with other compounds were carried out.

Above 250° C., the thermal decomposition of azomethane in the presence of trifluoroacetone produced some CF_3H. However, no CD_3H or CD_4 was found in similar experiments using d_6-acetone.

Recently, in these laboratories (6), the reaction

$$CN + CH_3CN \rightarrow CH_3 + (CN)_2$$

has been proposed in the photolysis of CH_3CN to account for some of the methane formed. This was verified by photolyzing $(CN)_2CO$ in the presence of CH_3CN. Some CH_4 was present in the reaction products.

We have found that if CF_3COCF_3 is photolyzed at 300° C. in the presence of CH_3CN (CH_3CN does not absorb at the wavelength used, 3130 Å), some CH_4 is obtained. Also CF_3H was identified in the products of the reaction of the thermal decomposition of of azomethane in the presence of CF_3CN at 300° C.

These reactions could occur by radical addition to the C≡N triple bond: $CX_3 + CY_3CN \leftrightharpoons CX_3CY_3CN \rightarrow CY_3 + CX_3CN$.

CONCLUSION

Smith and Calvert (10) have attempted to verify the reaction

$$CF_3 + CH_3COCF_3 \rightarrow CH_3 + CF_3COCF_3$$

by photolyzing mixtures of trifluoroacetophenone and trifluoroacetone. The system is complicated, but they find indirect evidence that CF_3 radicals regenerate CH_3 radicals by interaction with CH_3COCF_3. In further work on the photolysis of trifluoroacetone

alone, they find a relatively large quantum yield of CF_3CH_3 at 348° C., suggesting that the reaction

$$CF_3 + CH_3COCF_3 \rightarrow CF_3CH_3 + COCF_3 \qquad [II]$$

may become important at very high temperatures. In the earlier work (9), at lower temperatures, a decrease in the quantum yield of CF_3CH_3 with temperature was found, which suggested that reaction [II] was unimportant. This, together with the present work, indicates that the other type [II] reaction

$$CH_3 + CH_3COCF_3 \rightarrow C_2H_6 + COCF_3$$

proposed as a chain step in the photolysis is unimportant, at least up to 300° C., although this type of reaction is needed to explain the high quantum yields of CO obtained at 350° C.

Smith and Calvert made careful analysis for CF_3COCF_3 but failed to find any. They point out that there is no alternative mechanism to

$$CF_3 + CH_3COCF_3 \rightleftharpoons CH_3CO(CF_3)_2 \rightarrow CH_3 + CF_3COCF_3$$

and conclude that the generation of CH_3 from CF_3 radicals probably occurs by some other undefined heterogeneous path:

$$CF_3 + CH_3COCF_3 \rightarrow X \rightarrow CH_3 + \text{non-volatile products.}$$

The mechanism of the photolysis of trifluoroacetone at high temperatures appears to be very complicated, but we may conclude from the simpler systems studied in this work that the gas phase regeneration of radicals does occur, probably through addition to carbonyl double or cyano triple bonds.

ACKNOWLEDGMENTS

The authors wish to thank Mrs. K. O. Kutschke and Miss B. Thornton for the mass spectrometric analyses, Mr. R. Lauzon for the infrared analysis, and Mr. R. Séguin for the microanalysis.

REFERENCES

1. Ayscough, P. B. J. Chem. Phys. **24,** 944 (1956).
2. Ayscough, P. B. and Steacie, E. W. R. Can. J. Chem. **34,** 103 (1956).
3. Ayscough, P. B. and Steacie, E. W. R. Proc. Roy. Soc. A, **234,** 476 (1956).
4. Jones, M. H. and Steacie, E. W. R. J. Chem. Phys. **21,** 1018 (1953).
5. Kasha, M. J. Opt. Soc. Am. **38,** 929 (1948).
6. McElcheran, D. E. and Steacie, E. W. R. In press.
7. Page, M., Pritchard, H. O., and Trotman-Dickenson, A. F. J. Chem. Soc. 3878 (1953).
8. Pritchard, G. O., Pritchard, H. O., Schiff, H. I., and Trotman-Dickenson, A. F. Trans. Faraday Soc. **52,** 849 (1956).
9. Sieger, R. A. and Calvert, J. G. J. Am. Chem. Soc. **76,** 5197 (1954).
10. Smith, R. M. and Calvert, J. G. J. Am. Chem. Soc. **78,** 2345 (1956).

POLAROGRAPHY OF URANIUM

III. URANIUM(VI) IN FLUORIDE MEDIA[1]

DAVID J. MCEWEN[2] AND THOMAS DE VRIES

ABSTRACT

The uranium(VI) and (V) polarographic waves were studied in chloride and perchlorate supporting electrolytes of 0.1 *M* to almost neutral acidities and containing 0 to 100 fold excess of fluoride. The concentrations of the uranium(VI)–fluoride species ($UO_2F_n^{+2-n}$, $n = 1 - 4$) were calculated and it is shown that the first two species, UO_2F^+ and UO_2F_2, are either reduced reversibly at the D.M.E., or dissociate rapidly to the uncomplexed ion, UO_2^{++}, which is known to reduce reversibly. The $UO_2F_4^{=}$ species, and possibly also $UO_2F_3^-$, is reduced irreversibly, and the rate constant of the electron transfer process, $k_f°$, and the transfer coefficient, α, were calculated by two methods. The electrode reaction is proposed as $UO_2F_n^{+2-n} + e^- = UO_2^+ + nF^-$. The rate of disproportionation of uranium(V) was found to depend upon the F/U ratio, and the rate constants for the reaction were calculated.

INTRODUCTION

In experiments leading to the development of an amperometric method for the determination of fluoride with uranium(IV),* the effects of the presence of fluoride on the cathodic waves of uranium(VI) and (V) were also studied. The only previous studies of the effect of fluoride on the polarography of uranium(VI) have been made by Furman and Haight (5). These authors studied the uranium(VI) wave using supporting electrolytes of sodium fluoride and hydrofluoric acid, and were interested only in the ability of fluoride-containing electrolytes to remove interfering waves in the polarographic determination of uranium.

The polarography of uranium has been studied quite extensively,† and in non-complexing media it is well established that the reduction of uranium(VI) gives three waves, i.e., U(VI) to (V), U(V) to (IV), and U(IV) to (III). In moderately acidic solutions the second and third waves merge to form a composite wave. Because fluoride ions complex with uranium(VI) and more strongly with uranium(IV), the effect on the polarography of uranium(VI) is twofold: (1) the reduction of the uranium(VI)–fluoride complexes at comparatively high concentrations of fluoride becomes irreversible, and (2) in weakly to moderately acidic solutions the depolarization product, uranium(V), disproportionates rapidly in the presence of fluoride to uranium(VI) and (IV), thus regenerating the depolarizer and increasing the limiting current of the electrode process.

The early workers on the polarography of uranium noticed that high acidity and the presence of certain complexing agents greatly increased the height of the uranium(VI) wave. Herasymenko (9) correctly identified the increase of the limiting current of uranyl solutions of high acidity with the disproportionation of uranium(V) at the electrode surface. Kern and Orlemann (11) and Heal and Thomas (8) made direct measurements of the kinetics of the disproportionation of uranium(V) in perchloric and sulphuric acid solutions, respectively. These authors found that the rate of the disproportionation is

[1]*Manuscript received May 21, 1957.*

Contribution from the Department of Chemistry, Purdue University, Lafayette, Indiana. Abstracted from a portion of the Ph.D. thesis of David J. McEwen, Purdue University, 1957. This work was financially supported in part by the Purdue Research Foundation, for which acknowledgment is gratefully made. Parts I and II are to be published.

[2]*Present address: Canadian Industries Limited, Central Research Laboratory, McMasterville, Quebec.*

**Part I of this series, to be published.*

†For a review of many of the important studies on the polarography of uranium, see References 12 and 24b.

first order with respect to the hydrogen ion concentration, and second order with respect to the uranium(V) concentration, so that

$$-d\,\mathrm{U(V)}/dt = k[\mathrm{H^+}][\mathrm{UO_2^+}]^2. \qquad [1]$$

Kern and Orlemann proposed that the disproportionation reaction can be written as

$$\mathrm{UO_2^+ + H^+ = UO_2H^{++}}, \qquad [2a]$$

$$\mathrm{UO_2H^{++} + UO_2^+ = UO_2^{++} + UOOH^+}, \qquad [2b]$$

$$\mathrm{UOOH^+ \rightarrow} \text{ stable U(IV) species}, \qquad [2c]$$

where equation [2*b*] is believed to represent the rate-determining step of the disproportionation reaction.

In this paper the effects of fluoride on the potential and current of the uranium(VI) and (V) waves will be discussed. Concentrations of the uranium(VI)–fluoride species have been calculated and the results are explained on the basis of recently-advanced theories on irreversible and reaction-controlled processes. The rate of disproportionation of uranium(V) could not be measured directly in the presence of fluoride, but it was measured at the D.M.E.

EXPERIMENTAL

The reagents, apparatus, and technics for the experimental work have been described.* With an uncorrected mercury column height of 50 cm., an 8.6-cm. length of marine barometer tubing used as the dropping mercury electrode (D.M.E.) gave m and t values of 1.350 mg./second and 5.60 seconds/drop respectively ($m^{2/3}t^{1/6} = 1.63$ mg.$^{2/3}$sec.$^{-1/2}$) at -0.5 volt vs. S.C.E. The half-wave potential values were not corrected for the ohmic drop in the cell circuit, since the resistance of the circuit averaged 600 ohms and the currents seldom exceeded 3 μa. Except where otherwise indicated, condenser damping was not used in the cell circuit, so that maximum limiting currents were measured and are designated by the symbol i_L. It was found that when condenser damping was used, the ratio of average to maximum current was only 0.82, as compared to the theoretical value of 0.857 predicted by the Ilkovic equation.

Triton X-100 (Rohm and Haas trade name for iso-octyl phenoxy polyethoxy ethanol) was used as maximum suppressor. Less than 0.002% of this suppressor should be used, since it was found that 0.002% had a slight effect and 0.003% a marked effect on the characteristics of the uranium(VI) wave.

Uranium(VI) perchlorate and chloride were prepared by twice evaporating a solution of uranyl acetate dihydrate with the corresponding acids. These solutions were standardized by reduction in a 90% cadmium–amalgam reductor and titrating the reduced solution with potassium dichromate (24*a*).

PROLEGOMENA OF THE THEORY OF IRREVERSIBLE AND REACTION-CONTROLLED ELECTRODE PROCESSES

Among the first attempts to solve the problem of irreversible and reaction-controlled electrode reactions at the dropping mercury electrode are those which use the concept of the Nernst diffusion layer for the diffusion process taking place in the region very close to the mercury surface, or those which adapt with approximations the more rigorously derived relationships for linear diffusion to the case of diffusion to an expanding spherical surface. These methods, both of which are approximations, have been recently

*Part I of this series, to be published.

reviewed (4) and will not be mentioned further here. More recently, Koutecky and co-workers in a series of papers have solved several problems dealing with electrode reactions at the D.M.E. (2, 13–15, 25), and electrode processes preceded (16, 19) and followed (17) by chemical reactions. As a special case of this last type of electrode process, Koutecky and Koryta (18) have also discussed the disproportionation of the depolarizer product at the electrode surface.

Matsuda and Ayabe have derived general equations for the reduction of simple (21) and complex (22) metal ions at the D.M.E. By introducing the appropriate transformations, these general equations can be simplified for the case of reversible or irreversible electrode reactions.

1. Equations and Calculations for Slow Electrode Reactions (Irreversible) at the Dropping Mercury Electrode

The case of electrode reactions at the D.M.E. controlled by the kinetics of the electron transfer was first treated rigorously by Koutecky (13), who solved the problem by treating it as an equivalent problem of diffusion to an expanding plane surface, i.e., the curvature of the expanding spherical surface was neglected. The equation for this equivalent problem is expressed by the inclusion of the term (10) $2x/3t \cdot \partial C/\partial x$ in the equation for Fick's second law of diffusion to a plane surface. The mathematical solution of the problem is given by Koutecky in the form

$$i_L/i_d = F(\chi) \qquad [3]$$

for which

$$\chi = (k_f/D_a^{1/2}+k_b/D_b^{1/2})(12t/7)^{1/2}. \qquad [4]$$

i_L is the maximum limiting current, i_d is the maximum diffusion current, t is the drop time, k_f and k_b are the forward and reverse rate constants of the electron transfer reaction, D_a and D_b are the diffusion coefficients of the depolarizer and depolarizer product, respectively. For assigned values of χ, Koutecky has calculated corresponding values of $F(\chi)$. Later Weber and Koutecky (25) extended the calculated values of $F(\chi)$ and included values of $\overline{F(\chi)}$, i.e., values for the ratio of the average currents.

Since, as has been mentioned, in his original calculations (13) Koutecky neglected the curvature of the dropping mercury electrode, Koutecky and Cizek (14) have recently calculated correction factors which when applied to Koutecky's original calculations give values of the kinetic currents corrected for spherical diffusion. Thus equation [3] becomes

$$i_L/i_d = F(\chi)-\xi H_c(\chi) \qquad [3a]$$

for which

$$\xi = 50.4\, D^{1/2}t^{1/6}m^{-1/3} \qquad [5]$$

and $H_c(\chi)$ is the correction factor for maximum currents. In equation [5] D is the diffusion coefficient of the depolarizer in cm.^{2}/second, t is the drop time in seconds, and m is the rate of flow of mercury in mg./second.

Since it will be assumed in the analysis of the irreversible waves in the present work that the value of k_b is small compared to the value of k_f, χ (equation 4) can now be expressed by

$$\chi = k_f(12t/7D)^{1/2}. \qquad [4a]$$

The rate constant k_f for the forward reaction of a cathodic process varies with the electrode potential E according to the equation (6)

$$k_f = k_f^\circ \exp(-\alpha n_a FE/RT) \qquad [6]$$

in which α is the transfer coefficient, n_α is the number of electrons involved in the activation step of the reduction process, and k_f° is the rate constant of the electron transfer reaction at 0 volt (N.H.E.), and the remaining symbols have their usual meaning. Application of equations [3*a*], [4*a*], and [6] to the analysis of irreversible waves will be discussed in Section 5.

2. Equations and Calculations for Determining the Rate of Disproportionation of the Depolarizer Product at the Surface of the Dropping Mercury Electrode

Orlemann and Kern (23) first attempted the measurement of the disproportionation rate of uranium(V) at the D.M.E. They solved the problem of the increased currents due to the regeneration of uranium(VI) by multiplying the equation for linear diffusion, derived on the basis of the concept of reaction volume, by the factor $(7/3)^{1/2}$ in order to convert the equation to the case of diffusion to the D.M.E. However, their results, as compared to direct measurements of the disproportionation rate (11), were low by factors of 1.3 to 4.0, and this discrepancy is probably due to the approximations used in their derivations. Later Koutecky and Koryta (18) derived the equations for the problem of disproportionation of the depolarizer product at the D.M.E. by using the same assumptions as used in earlier papers (13, 17). Their experimental results for the rate of disproportionation of uranium(V) are in better agreement with the values determined by direct measurement (11). Koutecky and Koryta expressed the mathematical solution for this problem in the form

$$i_L/i_d = 1 + \sum_{i=1}^{\infty} C_i \xi^i \qquad [7]$$

where i_L is the maximum limiting current, i_d is the maximum diffusion current, and ξ is defined by the equation

$$\xi = 2akt \qquad [8]$$

for which a is the initial concentration of the depolarizer, k is the rate constant of the disproportionation reaction, and t is the drop time. The values of C_i have been calculated by Koutecky and Koryta for values of i from 1 to 7. From these values of C_i we have calculated values of i_L/i_d for assigned values of ξ, which are listed in Table I. A graph was drawn for these values in order to use equation [7] in the work to be given in Section 6.

TABLE I

ξ	0.5	1.0	1.5	2.0	2.5	3.0	3.5	4.0	4.5	5.0
i_L/i_d	1.0408	1.0765	1.1081	1.1362	1.1614	1.185	1.206	1.23	1.25	1.27

RESULTS

3. Effects of Fluoride on the Polarography of Uranium(VI)

The polarography of uranium(VI) in the presence of fluoride was studied in supporting electrolytes whose acidities ranged from 0.1 *M* to almost neutral. In each case, about 20 ml. of a solution containing uranium(VI) was electrolyzed without fluoride, and then successive aliquots of fluoride solution were added. For moderately acidic solutions, the uranium(VI) concentration was kept as low as possible so as to keep the hydrofluoric acid concentration small at large F/U ratios. In almost neutral unbuffered solutions, the pH varied by approximately one unit during the fluoride additions. This change of pH, however, did not seem to affect results to any marked extent.

A portion of the results obtained from these studies is listed in Table II. The calculation of the concentrations of the uranium(VI)–fluoride species will be discussed in Section 4. The symbols C_U, C_F, and C_H represent the total concentrations of uranium(VI), fluoride, and hydrogen ions, respectively. The mean ligand number, $\overline{n}_M$, is defined by equation [10].

The effects of fluoride on the polarographic waves of uranium(VI) may be roughly classed into three groups: (*a*) The limiting current of the uranium(VI) wave increases to approximately double the current obtained in the absence of fluoride without any change in the half-wave potential. (*b*) The limiting current increases to double its initial value as in case (*a*), but with a shift in the half-wave potential to more negative values. (*c*) The half-wave potential decreases to more negative values, but the limiting current increases only slightly.

Conditions of case (*a*) were obtained in 0.08 *M* hydrochloric acid. As shown in Table II A and Fig. 1 (× curve) the limiting current increases to approximately double its initial value, owing to the disproportionation of uranium(V). In Fig. 2, it can be seen that there is essentially no change in the half-wave potential of the uranium(VI) wave. The polarographic wave of solution 6, Table II A, was analyzed by plotting $\log[i/i_d - i)]$ vs. E. A slope value of 62 mv. was obtained, in good agreement with the theoretical value of 59 mv. for a reversible one-electron reduction. Therefore, it may be concluded that the UO_2F^+ and UO_2F_2 species (solution 6 contained 54% UO_2F^+ and 41% UO_2F_2) are either reduced reversibly at the D.M.E., or dissociate very rapidly to the uncomplexed (hydrated) ion, UO_2^{++}, which is known to reduce reversibly. Since Ahrland and co-workers (1) have shown that UO_2F^+ is a fairly stable species, it is quite probable that the former statement is closer to the truth.

Conditions of case (*b*) were obtained in 0.008 *M* hydrochloric acid, 0.1 *M* potassium chloride (Table II B and Figs. 1, 2, and 3, □ curve). In this supporting electrolyte, the limiting current of the U(VI) wave again increases to double its initial value. As would be expected, this increase of the limiting current of the U(VI) wave coincides with the sharp decrease of the U(V) to (III) wave shown in Fig. 3. The half-wave potential of the U(VI) wave shows only a moderate change marked by a sudden shift to more negative values at F/U ratios greater than 50. When the per cent of each uranium(VI)–fluoride species and the half-wave potential are plotted against the mean ligand number, $\overline{n}_M$, of uranium(VI) (Fig. 4), it can be seen that the sharp decrease of the half-wave potential coincides very closely with the formation of the $UO_2F_4^=$ complex. The first portion of the half-wave potential curve probably shows the effect of the $UO_2F_3^-$ complex. From these observations, plus those to be discussed in Section 5, it is proposed that the reduction at the D.M.E. of $UO_2F_3^-$ is partially reversible and $UO_2F_4^=$ is essentially irreversible.

The limiting current of the U(VI) wave increases to double its initial value in the presence of fluoride up to a pH of about 4. In Figs. 1 and 2, the supporting electrolyte for the ▽ curve was 0.006 *M* perchloric acid, and 0.1 *M* sodium perchlorate; for the ◇ curve, 0.05 *M* potassium sulphanilate,* pH 3.6, 0.1 *M* potassium chloride. In these four supporting electrolytes the rate of disproportionation is approximately the same and independent of the acid concentration up to a pH of 4. However, it can be seen that the acid concentration does affect the F/U value at which the limiting current starts to increase, owing to the formation of un-ionized hydrofluoric acid. For 0.08 *M*

**Sulphanilic acid is about the only buffering medium of pH 3 to 4 which does not appreciably complex any of the oxidation states of uranium.*

TABLE II

CONCENTRATIONS AND POLAROGRAPHIC DATA OF URANIUM(VI)–FLUORIDE SPECIES

Soln.	Concentration, mM													U(VI)–(V)		U(V)–(III)†	
	C_U	C_{F^-}	C_{H^+}	H^+	F^-	HF	HF_2^-	UO_2^{++}	UO_2F^+	UO_2F_2	$UO_2F_3^-$	$UO_2F_4^-$	$\bar{n}_M$	$-E_{\frac{1}{2}}$ (S.C.E.), volt	I_L* $(-E_{\frac{1}{2}}$ – 0.4 v.)	$-E_{\frac{1}{2}}$ (S.C.E.), volt	I_L*
A. 0.08 M hydrochloric acid, 0.1 M potassium chloride																	
1	0.205	0.063	87.5	—	—	0.057	—	.199	.006	—	—	—	0.029	0.180	1.93	0.89	
2	0.205	0.100	86.0	—	—	0.089	—	.194	.011	—	—	—	0.054	0.180	1.96	0.91	
3	0.205	0.162	83.5	—	—	0.144	—	.187	.018	—	—	—	0.088	0.183	1.98	0.97	
4	0.200	0.85	78.0	—	—	0.78	—	.130	.070	—	—	—	0.35	0.190	2.15	—	
5	0.190	2.55	74.5	—	0.039	2.41	—	.064	.113	.013	—	—	0.72	0.200	2.86	—	
6	0.186	13.9	72.8	—	0.26	13.4	—	.010	.100	.076	—	—	1.35	0.180	3.8	—	
B. 0.008 M hydrochloric acid, 0.1 M potassium chloride																	
7	0.210	0.192	8.20	8.11	0.013	0.093	—	.127	.080	.0032	—	—	0.41	0.195	1.95	0.99	2.94
8	0.202	0.616	8.76	8.37	0.053	0.39	—	.053	.128	.021	—	—	0.84	0.220	2.12	1.04	1.73
9	0.192	1.76	8.35	7.05	0.208	1.30	—	.011	.107	.067	.007	—	1.37	0.240	3.03	—	—
10	0.190	6.40	8.27	3.71	1.40	4.55	.025	—	.023	.099	.068	—	2.24	0.275	3.69	—	—
11	0.188	13.2	8.16	1.34	5.7	6.7	.15	—	—	.044	.123	.021	2.88	0.33	3.99	—	—
12	0.184	24.1	7.98	0.54	15.4	7.2	.43	—	—	.015	.115	.054	3.20	0.41	3.89	—	—
C. 0.2 M sodium perchlorate																	
13	0.510	—	—	—	—	—	—	.510	—	—	—	—	—	0.170	1.90	0.98	1.24
14	0.500	0.49	—	—	0.057	—	—	.122	.323	.055	—	—	0.87	0.235	1.98	1.01	1.88
15	0.465	2.27	—	—	1.24	—	—	—	.070	.250	.145	—	2.22	0.33	2.16	1.11	1.52
16	0.460	4.53	—	—	3.32	—	—	—	.017	.164	.255	.024	2.63	0.38	2.22	1.14	1.37
17	0.455	11.1	—	—	9.7	—	—	—	—	.067	.305	.083	3.04	0.44	2.24	1.25	1.20
18	0.435	32.0	—	—	30.5	—	—	—	—	.016	.225	.194	3.40	0.53	2.30	1.55	1.01
19	0.64	31.4	—	—	29.2	—	—	—	—	.025	.338	.277	3.39	0.52	2.28	1.55	1.03
20	0.84	30.7	—	—	28.0	—	—	—	—	.035	.453	.352	3.38	0.51	2.32	1.57	—

0.002% Triton X-100.

$I_L = i_L/C$ millimoles.

†*For 0.2 M sodium perchlorate, this column refers to the* U(V) *to* U(IV) *wave.*

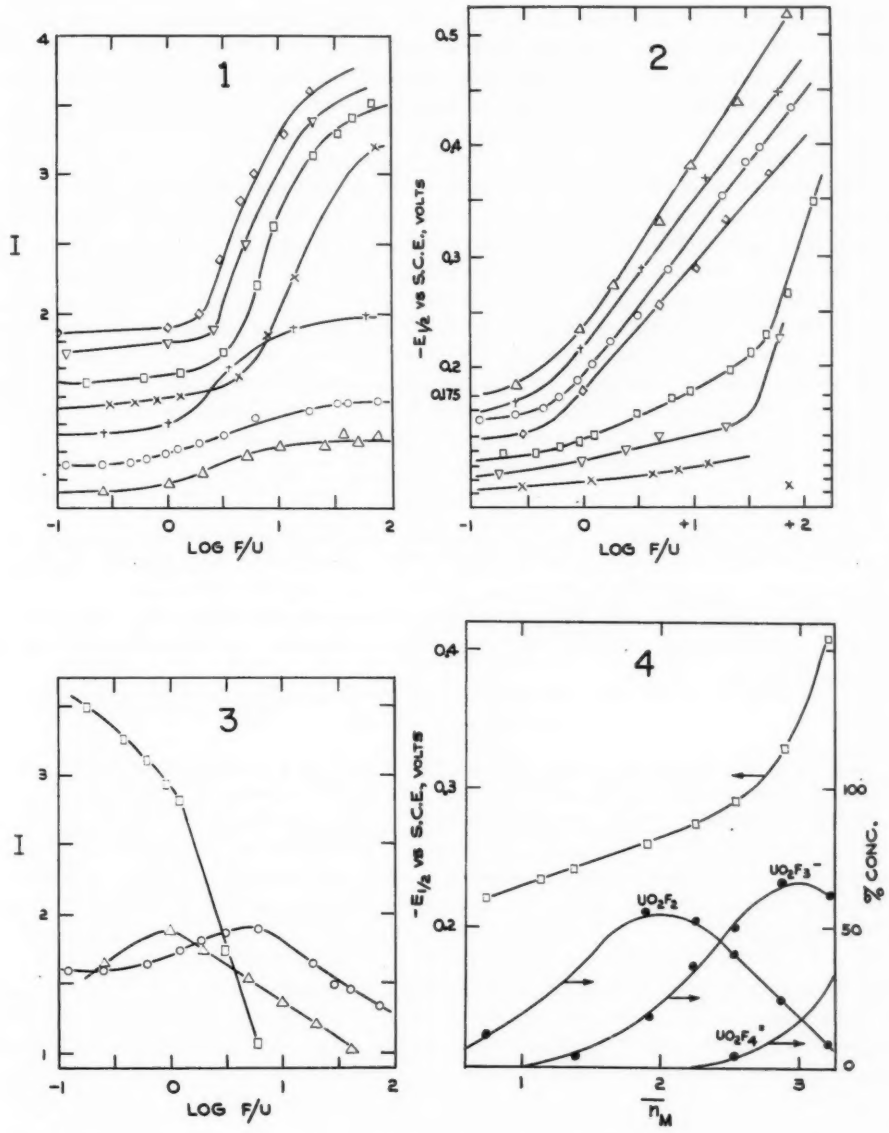

FIG. 1. Effect of fluoride on the limiting current constant of the U(VI) wave.
FIG. 2. Effect of fluoride on the $E_{\frac{1}{2}}$ of the U(VI) wave.
FIG. 3. Effect of fluoride on the limiting current constant of the U(V) cathodic wave.
FIG. 4. Change of the $E_{\frac{1}{2}}$ of the U(VI) wave with the concentration of the uranium(VI)–fluoride species in 0.008 *M* hydrochloric acid, 0.1 *M* potassium chloride.

hydrochloric acid (× curve) this F/U value is about 4; for a pH of 3.6 (◇ curve) it is about 2.

The supporting electrolyte of curve + was 0.1 *M* sodium perchlorate, pH *ca.* 4.5, in which case the limiting current increased only 50% above its initial value. At this pH there was enough acid present to allow only about half of the uranium(V) to disproportionate before diffusing back into the bulk of the solution.

Conditions of case (*c*) were obtained in 0.1 *M* potassium chloride (○ curve) or 0.2 *M* sodium perchlorate (△ curve) of pH 5 to 6. Table II C lists the data for the latter supporting electrolyte. The limiting current of the U(VI) wave increases only slightly owing to an almost total absence of hydrogen ions. The limiting current of the uranium(V) wave (Fig. 3) first increases and then decreases. Harris and Kolthoff (7) pointed out that the second wave in almost neutral media could be due to the reduction of UO_2^+ to UO_2 and UO_2OH^+ to UO_2OH. The UO_2 forms a solid or ephemeral layer on the mercury drop which hinders the reduction of uranium(V) and decreases the height of the second wave. Thus the presence of moderate amounts of fluoride would increase the current of the second wave by attacking the UO_2 layer on the mercury drop and also preventing hydrolysis of the uranyl ion. Larger amounts of fluoride tie up any excess of free hydrogen ions and also probably precipitate uranium(IV)–fluoride complexes on the mercury drop to again decrease the current of the second wave.

4. Calculation of the Concentrations of the Uranium(VI)–Fluoride Species

The data of Ahrland *et al.* (1) were used in calculating the concentrations of the uranium(VI)–fluoride species listed in Table II. In determining the formation constant of each species potentiometrically, these workers measured the hydrogen ion activity with a quinhydrone electrode, but used concentrations in the remaining calculations. The formal equilibrium constant in 1 *M* sodium perchlorate for hydrofluoric acid is therefore given by

$$[HF]/a_{H^+}[F^-] = 870. \qquad [9]$$

Latimer (20) has given the value of 0.58 as the activity coefficient of 1 *m* sodium perchlorate. Assuming that the activity coefficient of HF is unity, dividing equation [9] by 0.58 gives 1490, which is exactly the value for the equilibrium constant based on activities determined by Broene and De Vries (3). Therefore, it is reasonable to assume that the activity coefficients of 1 *m* sodium perchlorate given by Latimer adequately express the activity of the fluoride in 1 *M* sodium perchlorate solutions used by Ahrland and co-workers (1).

Since 0.1 to 0.2 *M* chloride or perchlorate supporting electrolytes were used in the present work, adjustment of the formal formation constants in 1 *M* sodium perchlorate for the change in ionic strength should be made. Consequently, we multiplied the formation constants given by Ahrland *et al.* by the factors 0.72/0.58 and 0.77/0.58 to convert them to formal formation constants for 0.2 and 0.1 *M* solutions respectively. Using these latter constants, the concentrations listed in Table II were then calculated. The symbol $\overline{n}_M$ is defined by

$$\overline{n}_M = \sum_{n=1}^{N} n[UO_2F_n^{+2-n}]/C_U. \qquad [10]$$

5. Calculation of the Values for αn_a, k_s, k_f°, and $(p-q)$ for Irreversible Electrode Processes

For the polarographic waves of solutions 16–20 values of αn_a, k_s, and k_f° were calcu-

lated using the theory of Section 1, and values of αn_α, k_f°, and $(p-q)$ using the theory of Matsuda and Ayabe (22), to be discussed presently.

In applying the theory of Section 1 to each polarographic wave, a series of corresponding i_L (from which i_L/i_d values are calculated) and E (N.H.E.)* values were tabulated. Applying the data of Weber and Koutecky (25) and Koutecky and Cizek (14) to equation [3*a*], values of χ were graphically determined, from which k_f was calculated using equation [4*a*]. Log k_f values were then plotted against E as shown in Fig. 5. From

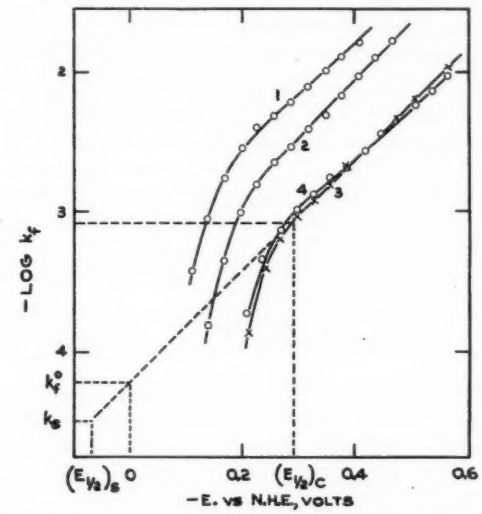

FIG. 5. Analysis of the U(VI) wave in 0.2 *M* sodium perchlorate and F/U of (1) 10, (2) 25, (3) 74, 50, (4) 37, using Koutecky's data.

TABLE III

VALUES OF αn_α, k_s, AND k_f° CALCULATED USING THE DATA OF KOUTECKY AND OF MATSUDA AND AYABE

Curve, Figs. 5 and 6	Soln., Table II	U(VI) conc., m*M*	Fluoride conc., m*M*	Koutecky			Matsuda and Ayabe		
				αn_α	k_s, cm./sec.	k_f°, cm./sec.	αn_α	k_f°, cm./sec.	$(p-q) = \frac{}{n_M}$
				0.1 *M* Potassium chloride					
–	21	0.212	8.8	0.19	$10^{-3.52}$	$10^{-3.33}$	0.21	$10^{-3.45}$	3.00
–	22	0.209	16.2	0.19	$10^{-3.75}$	$10^{-3.55}$	0.20	$10^{-3.58}$	3.21
				0.2 *M* Sodium perchlorate					
1	16	0.46	4.53	0.22	$10^{-3.54}$	$10^{-3.28}$	0.21	$10^{-3.28}$	2.63
2	17	0.455	11.1	0.25	$10^{-4.01}$	$10^{-3.71}$	0.23	$10^{-3.57}$	3.04
3	18	0.435	32.0	0.23	$10^{-4.48}$	$10^{-4.21}$	0.25	$10^{-4.20}$	3.40
	19	0.64	31.4						
4	20	0.84	30.7	0.21	$10^{-4.31}$	$10^{-4.05}$	0.22	$10^{-4.07}$	3.38

the linear portions of these curves values of αn_α were calculated using equation [6]. Extrapolating the linear portions to 0 volt and $(E_{\frac{1}{2}})_s$ (half-wave potential of UO_2^{++}) gives the values of k_f° and k_s, respectively, listed in Table III. Since the electron change in the electrode reaction is one, the value of n_α is probably also one. The values listed under αn_α would then be the values of the transfer coefficient, α.

*E (S.C.E.) = 0.24 volt (N.H.E.).

We have also listed in Table III the corresponding values for solutions 21 and 22, in order to compare the rate constants for different concentrations of uranium(VI). Solutions 17, 20, and 21 have approximately the same F/U ratio, but contain double the uranium(VI) concentration in each case. As indicated by the rate constants for these solutions, the electrode reaction became more irreversible with increasing uranium (VI) concentration, because more current is drawn during the electrode process. The curved portion of each line in Fig. 5 corresponds to the initial portion of each polarographic wave, where the current drawn during the first stage of the electrode process is small compared to the diffusion current.

For the irreversible reduction of complex ions, which may be represented as

$$MX_p^{(m-pb)+} + ae^- = MX_q^{(m-a-qb)+} + (p-q)X^{-b}, \qquad [11]$$

Matsuda and Ayabe (22) have derived the following equation for the polarographic wave:

$$E = E_{\frac{1}{2}} - (0.059/\alpha n_a) \log[i/(i_d - i)] \qquad (25^\circ \text{ C.}) \qquad [12]$$

for which

$$E_{\frac{1}{2}} = \frac{0.059}{\alpha n_a}\left\{\log f_p k_f^\circ (t/D)^{\frac{1}{2}} - 0.049 - \log(i_L/i_d) - \log\left[\sum_{n'=0}^{N} (f_x C_x)^{n'-(p-q)} \left(f_p \prod_{n=1}^{(p-q)} K_n\right) \Big/ \left(f_{n'} \prod_{n=0}^{n'} K_n\right)\right]\right\}, \qquad [13]$$

where f's represent activity coefficients, K_n are the dissociation constants of the species $UO_2F_n^{+(2-n)}$ ($K_0 = 1$), $(p-q)$ is the ligand change of the electrode process, n equals 1, 2, . . . , N, where N is the maximum number of ligands complexed by the metal ion, M, which Ahrland, *et al.* (1) have found to be 4 for uranium(VI)–fluoride complexes, and the remaining symbols are explained elsewhere in this paper. Since formal rate constants were calculated in applying the theory of Section 1, the f's will be neglected and formal rate constants also calculated from equation [13].

By plotting $\log [i/(i_d - i)]$ vs. E for the polarographic waves of solutions 16–22, the values of αn_a listed in Table III were calculated using equation [12]. Substituting into equation [13] these values of αn_a, the values of K_n (which are reciprocals of the adjusted formation constants discussed in Section 4), and known values of the other variables, values of $\log k_f^\circ$ were calculated for assigned values of $(p-q) = 1, 2, 3, 4$, and plotted against each other as shown in Fig. 6 (open figures). The minimum value of k_f° for each curve, which occurs very closely to $(p-q) = \overline{n_M}$, is listed in Table III. For comparison, the values of k_f° calculated using the data of Koutecky were plotted at $(p-q) = \overline{n_M}$ (solid figures, Fig. 6). Since these two methods gave values of k_f° which agree very closely, it appears that $(p-q) = \overline{n_M}$ and the electrode reaction may therefore be written as

$$UO_2F_n^{+(2-n)} + e = UO_2^+ + nF^-. \qquad [14]$$

This also indicates that the fluoride complexes of uranium(V), if any, are probably quite weak.

6. Rate of Disproportionation of Uranium(V)

Prior to measuring the rate of disproportionation of uranium(V) at the D.M.E., we measured the rate directly by following the decrease of the current of the uranium(V) anodic wave with time using much the same apparatus and technic described by Kern and Orlemann (11). With fluoride absent in perchlorate media, we calculated a value

for k (equation 1) of 90 l. mole^{-1} sec.$^{-1}$ at unit hydrogen ion activity and ionic strength of 0.13, in satisfactory agreement with the value of 80 l. mole^{-1} sec.$^{-1}$ reported by Kern and Orlemann.

We also attempted to measure the rate of disproportionation of uranium(V) in the presence of fluoride by a similar procedure. The uranium(V) was generated in an electrolysis cell, the current of the uranium(V) anodic wave noted, and then small amounts of fluoride were added. However, in the presence of fluoride, the uranium(V) disproportionated so fast that direct measurement of the rate was found to be impossible, even when the pH was increased to 3.5. As shown by curve +, Fig. 1, the disproportionation reaction is appreciable in the presence of fluoride even at a pH of 4.5.

Because we were unable to measure directly the kinetics of the disproportionation of uranium(V) in the presence of fluoride, we cannot therefore formulate a rate expression for the reaction. This situation makes application of the theory discussed in Section 2 difficult and somewhat risky. However, an attempt was made to correlate the data of Table II with the theory and reasonable results were obtained. As an example of the application of the theory of Section 2, I_L/I values (equal to i_L/i_d) were calculated from the data given in Table II B and plotted against F/U values (Fig. 7). ξ values were then graphically determined using the data of Table I. For supporting electrolytes of pH < 4, the I_L/I values first increase, level off, and then sharply increase again. This gives two straight lines when ξ is plotted against F/U. With a pH > 4.5, only the first increase in the I_L/I values was obtained. If we let

$$\xi = 2kt\,\mathrm{F/U}, \qquad [15]$$

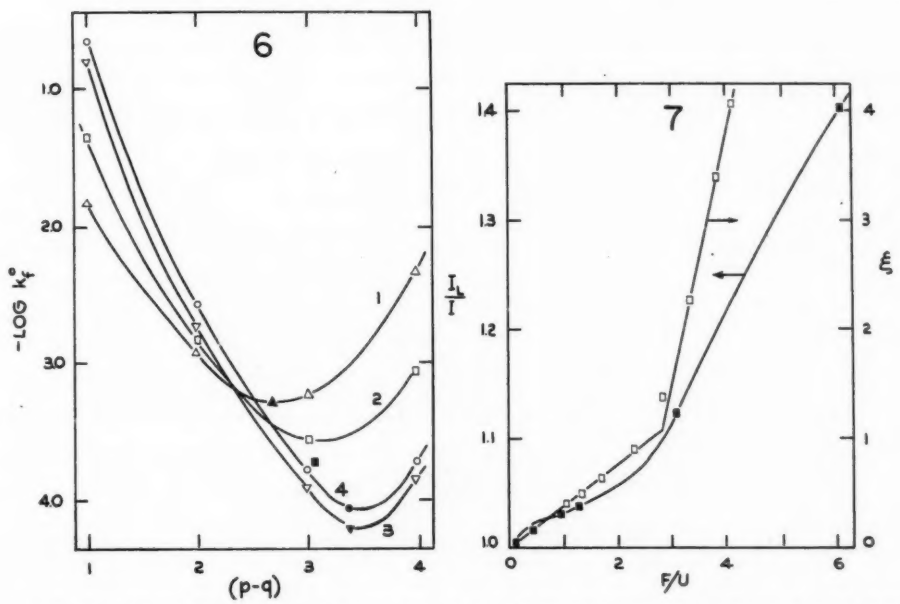

FIG. 6. Plot of log k_f° vs. the ligand change, $(p-q)$, for 0.2 M sodium perchlorate (open figures). Solid figures indicate the value of log k_f° calculated from Koutecky's data at the value of the mean ligand number, $\bar{n}_M$.

FIG. 7. Plot of I_L/I and ξ vs. F/U for 0.008 M hydrochloric acid, 0.1 M potassium chloride.

then k values can be calculated from the slopes of these lines (designated as k_1 and k_2 for the first and second linear portions). These k values for the supporting electrolytes studied in this work are listed in Table IV. Up to F/U ratios between 2 and 4, the

TABLE IV

RATE CONSTANTS FOR THE DISPROPORTIONATION OF URANIUM(V) AT THE D.M.E.

UO_2^{++}, mM	Supporting electrolyte	k_1, sec.$^{-1}$	k_2, sec.$^{-1}$
0.2	0.08 M HCl, 0.1 M KCl	—	0.10
0.2	0.008 M HCl, 0.1 M KCl	0.037	0.20
0.2	0.008 M HCl, 0.1 M KCl	0.038	0.23
0.5	0.006 M $HClO_4$, 0.1 M $NaClO_4$	0.045	0.28
0.5	0.05 M K sulphanilate, 0.1 M KCl, pH = 3.6	0.045	0.40
0.2	0.05 M K sulphanilate, 0.1 M KCl, pH = 3.9	0.067	0.13
0.5	0.1 M $NaClO_4$, pH = 4.5	0.055	0.20
0.2	0.1 M KCl	0.056	—
0.5	0.2 M $NaClO_4$	0.045	—

values of the rate constant indicated by k_1 were obtained. Above these F/U ratios, the rate of disproportionation increases several fold, as indicated by the values calculated for k_2. This is probably due to the increased stability of uranium(IV)–fluoride complexes at these higher F/U ratios. However, with the data at hand, it is impossible to formulate a mechanism for the reaction.

REFERENCES

1. AHRLAND, S., LARSSON, R., and ROSENGREN, K. Acta Chem. Scand. **10**, 705 (1956).
2. BRDICKA, R. Collection Czechoslov. Chem. Communs. **19**, S41 (1954).
3. BROENE, H. H. and DE VRIES, T. J. Am. Chem. Soc. **69**, 1644 (1947).
4. DELAHAY, P. New instrumental methods in electrochemistry. Interscience Publishers, New York. 1954.
5. FURMAN, N. H. and HAIGHT, G. P., Jr. U.S. Atomic Energy Comm. Document M-4245 (Declassification date: Nov., 1953).
6. GLASSTONE, S., LAIDLER, K., and EYRING, H. The theory of rate processes. McGraw-Hill Book Co., Inc., New York. 1941. p. 576.
7. HARRIS, W. E. and KOLTHOFF, I. M. J. Am. Chem. Soc. **69**, 446 (1947).
8. HEAL, H. G. and THOMAS, J. G. N. Trans. Faraday Soc. **45**, 11 (1949).
9. HERASYMENKO, P. Trans. Faraday Soc. **24**, 272 (1928).
10. ILKOVIC, D. J. chim. phys. **35**, 129 (1938).
11. KERN, D. M. H. and ORLEMANN, E. F. J. Am. Chem. Soc. **71**, 2102 (1949).
12. KOLTHOFF, I. M. and LINGANE, J. J. Polarography. 2nd ed. Interscience Publishers, New York. 1952. pp. 462–467.
13. KOUTECKY, J. Collection Czechloslov. Chem. Communs. **18**, 597 (1953). (For English Translation, see Document Atomic Energy Research Establ. Lib. Trans. 509 (1955).)
14. KOUTECKY, J. and CIZEK, J. Collection Czechlosov. Chem. Communs. **21**, 836 (1956).
15. KOUTECKY, J. Collection Czechoslov. Chem. Communs. **21**, 1056 (1956).
16. KOUTECKY, J. Collection Czechoslov. Chem. Communs. **19**, 857, 1045, 1093 (1954).
17. KOUTECKY, J. Collection Czechoslov. Chem. Communs. **18** 311 (1953); **20**, 116 (1955).
    KOUTECKY, J. and CIZEK, J. Collection Czechoslov. Chem. Communs. **21**, 1063 (1956).
18. KOUTECKY, J. and KORYTA, J. Collection Czechoslov. Chem. Communs. **19**, 845 (1954); **20**, 423 (1955).
19. KOUTECKY, J. Nature, **174**, 233 (1954).
20. LATIMER, W. M. The oxidation states of the elements and their potentials in aqueous solutions. 2nd ed. Prentice-Hall, Inc., New York. 1952. p. 354.
21. MATSUDA, H. and AYABE, Y. Bull. Chem. Soc. Japan, **28**, 422 (1955).
22. MATSUDA, H. and AYABE, Y. Bull. Chem. Soc. Japan, **29**, 134 (1956).
23. ORLEMANN, E. F. and KERN, D. M. H. J. Am. Chem. Soc. **75**, 3058 (1953).
24. RODDEN, C. J. (*Editor-in-Chief*). Analytical chemistry of the Manhattan project. National Nuclear Energy Series, Div. VIII. McGraw-Hill Book Co., Inc., New York. 1950. (*a*) p. 68; (*b*) pp. 596–610.
25. WEBER, J. and KOUTECKY, J. Collection Czechoslov. Chem. Communs. **20**, 980 (1955).

STIGMASTA-3,5,22-TRIENE AND DISTIGMASTERYL ETHER

R. G. LINBURG[1] AND R. H. COX[2]

In 1896, Mauthner and Suida (4) treated fused cholesterol with anhydrous copper sulphate and obtained an intramolecular dehydration product, cholesta-3,5-diene, and an intermolecular dehydration product, dicholesteryl ether. By treating stigmasterol in a similar manner, we have prepared stigmasta-3,5,22-triene and distigmasteryl ether. To the best of our knowledge, the only dehydration product of stigmasterol which has been reported previously is *i*-stigmastatriene (1).

Certain of the physical properties of stigmasterol and of the two dehydration products prepared by us are compared in the table below with those of the respective analogues (2) in the cholestane series. Optical rotation and ultraviolet absorption data readily illustrate that the intramolecular dehydration product synthesized in this study has the 3,5-diene configuration, i.e., it is stigmasta-3,5,22-triene. Evidence supporting rearrangement from the homoannular 2,4- to the heteroannular 3,5-diene system in the steroid nucleus has been discussed previously (2).

MELTING POINT, OPTICAL ROTATORY POWER, AND SOLUBILITY

	M.p., ° C.	$[\alpha]_D$	Solubility	Reference
Cholesterol	149	−39°	Soluble ethanol and benzene	3
Stigmasterol	170	−49°	Soluble ethanol and benzene	3
Dicholesteryl ether	196–199	−39°	Insoluble hot ethanol; soluble benzene	2
Distigmasteryl ether	200–204	−54°	Insoluble hot ethanol; soluble benzene	
Cholesta-3,5-diene	79–80	−90°	Soluble hot ethanol; soluble benzene	2
Stigmasta-3,5,22-triene	111–112	−109°	Soluble hot ethanol; soluble benzene	

ULTRAVIOLET ABSORPTION SPECTRUM

		λ_{max} (mμ)	ϵ_{max}	Reference
Cholesta-3,5-diene	Maxima	235	18,450	2
		229	17,300	
	Minimum	231	17,000	
	Shoulder	243	12,050	
Stigmasta-3,5,22-triene	Maxima	235	20,400	
		229	20,400	
	Minimum	231	19,500	
	Shoulder	242	13,800	

EXPERIMENTAL

Stigmasta-3,5,22-triene

An intimate mixture of 5 g. of stigmasterol and 5 g. of anhydrous copper sulphate was heated at 200° C. until all signs of frothing had ceased (about 20 minutes). The cooled reaction mixture was exhaustively extracted with benzene, the inorganic material

[1]*This note represents part of a dissertation submitted by R. G. Linburg in partial fulfillment of the requirements for the degree of Bachelor of Science in Pharmacy at the University of British Columbia, 1950.*

[2]*Present address: Vick Chemical Company, New York 17, New York.*

being removed by filtration. The benzene extract was evaporated to dryness and the residue was exhaustively extracted with hot ethanol. Concentration and cooling of the ethanolic extract yielded 2.5 g. of crude, crystalline stigmasta-3,5,22-triene, which on recrystallization from ethanol was obtained as colorless, needle-shaped crystals melting at 111–112° C.; $[\alpha]_D = -109°$; $\epsilon_{max} = 20{,}400$ at 235 mμ.

Analysis: Calc. for $C_{29}H_{46}$: C, 88.25; H, 11.75. Found: C, 88.54; H, 11.57.

Distigmasteryl Ether

The residue that remained after removal of the stigmasta-3,5,22-triene from the original benzene-soluble fraction was twice recrystallized from benzene–acetone. The 1.4 g. of colorless, crystalline distigmasteryl ether so obtained melted at 200–204° C., $[\alpha]_D = -54°$. It was relatively insoluble in ethanol, acetone, and diethyl ether, but dissolved readily in benzene.

Analysis: Calc. for $C_{58}H_{94}O$: C, 86.28; H, 11.73. Found: C, 86.47; H, 11.90.

Physical Measurements

Melting points are corrected.

Optical rotatory measurements were made at room temperature (about 25° C.), using 2% concentrations of the compounds under test in chloroform.

Ultraviolet absorption spectra were obtained with a Beckman DU spectrophotometer, using 0.001% concentrations of the compounds under test in absolute ethanol.

1. Centolella, A. P., Heyl, F. W., and Herr, M. E. J. Am. Chem. Soc. **70**, 2953 (1948).
2. Cox, R. H. and Spencer, E. Y. Can. J. Chem. **29**, 398 (1951).
3. Fieser, L. F. and Fieser, M. Natural products related to phenanthrene. 3rd ed. Reinhold Publishing Corporation, New York. 1949.
4. Mauthner, J. and Suida, W. Monatsh. **17**, 29 (1896).

Received May 27, 1957.
Faculty of Pharmacy,
University of British Columbia,
Vancouver, B.C.

CANADIAN JOURNAL OF CHEMISTRY

Notes to Contributors

Manuscripts

(i) ***General.*** Manuscripts, in English or French, should be typewritten, double spaced, on paper 8½ × 11 in. **The original and one copy are to be submitted.** Tables and captions for the figures should be placed at the end of the manuscript. Every sheet of the manuscript should be numbered.

Style, arrangement, spelling, and abbreviations should conform to the usage of this journal. Names of all simple compounds, rather than their formulas, should be used in the text. Greek letters or unusual signs should be written plainly or explained by marginal notes. Superscripts and subscripts must be legible and carefully placed.

Manuscripts and illustrations should be carefully checked before they are submitted. Authors will be charged for unnecessary deviations from the usual format and for changes made in the proof that are considered excessive or unnecessary.

(ii) ***Abstract.*** An abstract of not more than about 200 words, indicating the scope of the work and the principal findings, is required, except in Notes.

(iii) ***References.*** References should be listed **alphabetically by authors' names,** numbered, and typed after the text. The form of the citations should be that used in this journal; in references to papers in periodicals, titles should not be given and only initial page numbers are required. The names of periodicals should be abbreviated in the form given in the most recent *List of Periodicals Abstracted by Chemical Abstracts*. All citations should be checked with the original articles and each one referred to in the text by the key number.

(iv) ***Tables.*** Tables should be numbered in roman numerals and each table referred to in the text. Titles should always be given but should be brief; column headings should be brief and descriptive matter in the tables confined to a minimum. Vertical rules should be used only when they are essential. Numerous small tables should be avoided.

Illustrations

(i) ***General.*** All figures (including each figure of the plates) should be numbered consecutively from 1 up, in arabic numerals, and each figure referred to in the text. The author's name, title of the paper, and figure number should be written in the lower left corner of the sheets on which the illustrations appear. Captions should not be written on the illustrations (see Manuscripts (i)).

(ii) ***Line Drawings.*** Drawings should be carefully made with India ink on white drawing paper, blue tracing linen, or co-ordinate paper ruled in blue only; any co-ordinate lines that are to appear in the reproduction should be ruled in black ink. Paper ruled in green, yellow, or red should not be used unless it is desired to have all the co-ordinate lines show. All lines should be of sufficient thickness to reproduce well. Decimal points, periods, and stippled dots should be solid black circles large enough to be reduced if necessary. Letters and numerals should be neatly made, preferably with a stencil (**do NOT use typewriting**), and be of such size that the smallest lettering will not be less than 1 mm. high when reproduced in a cut of suitable size.

Many drawings are made too large; originals should not be more than 2 or 3 times the size of the desired reproduction. In large drawings or groups of drawings the ratio of height to width should conform to that of a journal page but the height should be adjusted to make allowance for the caption.

The original drawings and one set of clear copies (e.g. small photographs) are to be submitted.

(iii) ***Photographs.*** Prints should be made on glossy paper, with strong contrasts. They should be trimmed so that essential features only are shown and mounted carefully, with rubber cement, on white cardboard with no space or only a very small space (less than 1 mm.) between them. In mounting, full use of the space available should be made (to reduce the number of cuts required) and the ratio of height to width should approximate that of a journal page (5½ × 7¾ in.); however, allowance must be made for the captions. Photographs or groups of photographs should not be more than 2 or 3 times the size of the desired reproduction.

Photographs are to be submitted in duplicate; if they are to be reproduced in groups one set should be mounted, the duplicate set unmounted.

Reprints

A total of 50 reprints of each paper, without covers, are supplied free. Additional reprints, with or without covers, may be purchased.

Charges for reprints are based on the number of printed pages, which may be calculated approximately by multiplying by 0.5 the number of manuscript pages (double-spaced typewritten sheets, 8½ × 11 in.) and including the space occupied by illustrations. An additional charge is made for illustrations that appear as coated inserts. The cost per page is given on the reprint requisition which accompanies the galley.

Any reprints required in addition to those requested on the author's reprint requisition form must be ordered officially as soon as the paper has been accepted for publication.

Contents

Printed in Canada *by* University of Toronto Press